DEVELOPING A MONITORING PROGRAM FOR DUSKY GROUSE IN MONTANA

by

Elizabeth Ashley Leipold

A dissertation submitted in partial fulfillment
of the requirements for the degree

of

Doctor of Philosophy

in

Ecology and Environmental Sciences

MONTANA STATE UNIVERSITY
Bozeman, Montana

December 2023

ACKNOWLEDGEMENTS

I would like to thank Dr. Lance McNew for his guidance, enthusiasm, and support throughout this project. In addition, I would like to thank, Dr. Claire Gower for her support, enthusiasm, and guidance throughout this project and assistance with data collection. I would also like to thank the members of the Wildlife Habitat Ecology Lab, both past and present for their friendship and feedback. In addition, I would like to thank my committee members, Dr. Lance McNew, Dr. Claire Gower, Dr. Jay Rotella, and Dr. Katharine Banner for their feedback and insights.

I would also like to thank all of the technicians who assisted in collecting data for this project: Teagan Byorth, Lara Macon, David Forbes, Rob Francisco, Mikaela Howie, Chris Smith, Luke Johnson, Lulu McMahon, Thomas Hull, Kellan Karch, Haley Burger, and Alisha Gill. In addition, I would like to thank all the volunteers and Montana, Fish, Wildlife & Parks wildlife biologists who also assisted with data collection. I could not have done this project without the large amount of people who volunteered their time and effort for conducting surveys. I would also like to thank Cara Staab and Christian Meny and the Bird Conservancy of the Rockies for the collection of the IMBCR data used for the habitat analysis.

This project was funded by the general sale of hunting and fishing licenses in Montana and matching funds under Federal Aid in Wildlife Restoration grant W-162-R-0 from Montana, Fish, Wildlife and Parks and the Montana Agricultural Experiment Station at Montana State University.

TABLE OF CONTENTS

TABLE OF CONTENTS CONTINUED

TABLE OF CONTENTS CONTINUED

TABLE OF CONTENTS CONTINUED

LIST OF TABLES

Table Page

LIST OF TABLES CONTINUED

Table Page

LIST OF TABLES CONTINUED

Table Page

LIST OF TABLES CONTINUED

Table Page

LIST OF FIGURES

Figure Page

LIST OF FIGURES CONTINUED

Figure Page

LIST OF FIGURES CONTINUED

Figure Page

ABSTRACT

Rigorous monitoring programs for Dusky Grouse (*Dendragapus obscurus*), a game species, are lacking. Difficult-to-reach habitat and low probability of detection makes monitoring Dusky Grouse difficult. Our objectives were to 1) evaluate Dusky Grouse habitat associations and generate a state-wide map predicting Dusky Grouse habitat, 2) evaluate sampling methods and survey conditions for maximizing Dusky Grouse detection, and 3) evaluate protocols (*i.e.*, number of sites and visits) and analytical methods for producing annual unbiased and precise indices of abundance. We created our habitat model using resource selection functions, random forest, and an ensemble approach. We compared spring v. summer sampling, use of electronic playback to increase detection, effect of route type (off-trail, trail, road) on point counts, and the effect of weather, background noise, day, and time on probability of detection. We evaluated and compared four analytical methods using simulations: time-to-detection model with hierarchical distance sampling, N-mixture model, raw count (naïve) and hierarchical distance sampling model. Multiple habitat characteristics affected relative probability of Dusky Grouse use including tree height and conifer forest vegetation types. Both habitat modeling methods were highly predictive and therefore we used an ensemble (frequency histogram) approach to create a state-wide map of Dusky Grouse habitat that was used to identify appropriate sampling sites for population monitoring. Spring point-count surveys conducted with electronic playback were most effective. Surveys located along roads/trails best balanced the trade-offs between sampling effort and survey design requirements, despite limiting inferences to Dusky Grouse populations located in prime habitat along roads/trails. Detection of Dusky Grouse was highest on clear days, with little wind and background noise, with surveys occurring 9–162 minutes post-sunrise during 3–23 May. Simulation results indicated that N-mixture models where 80 sites visited four times resulted in unbiased estimates of population size with the highest precision. Transect-based distance sampling survey protocols during the spring also produced unbiased and acceptably precise (≤15% CV) estimates of grouse density when ≥35 transects of ≥2.6-km length were surveyed per area of inference (*e.g.*, administrative region). Our results provide baseline information necessary for the development of a state-wide monitoring program for Montana.

INTRODUCTION

Accurate and precise estimates of abundance and population trends are necessary for effective conservation and management of our wildlife resources, particularly game species (Aebischer and Baines 2008, Joseph et al. 2009, Jakob et al. 2014, Weiser et al. 2019, Neubauer and Sikora 2020). It is challenging to effectively manage species and populations without rigorous monitoring programs. Knowledge gaps that limit our understanding of population trends and species distributions restrict our understanding of a species' current status as well as its response to threats and environmental changes (Guisan et al. 2006, Sillett et al. 2012, Sofaer et al. 2019). Population monitoring of game species provides managers with information to evaluate the effect of management actions, set harvest regulations (*e.g.*, bag limits, season lengths), and forecast numbers for hunting seasons for the public (Aebischer and Baines 2008, Sands and Pope 2010, Powell et al. 2011, Franceschi et al. 2014). Long-term monitoring may be financially costly and require high observer effort, highlighting the necessity of well-planned surveys and programs to achieve management goals while operating with limited resources (Weiser et al. 2019, Anderson and Stiedl 2019).

Dusky Grouse (*Dendragapus obscurus*) are an under-monitored upland game species that inhabit open coniferous forests of the western mountain ranges of North America from the central Yukon to northern Arizona and New Mexico (Aldrich 1963, Zwickel and Bendell 2004). A food source for many different raptor and mammalian species, Dusky Grouse also provide economic and recreational benefits through revenue from hunting license sales and bird-watching opportunities (Pelren and Crawford 1999, Sands and Pope 2010). Although Breeding Bird Survey (BBS) data suggests most populations are stable, low detection rates make

population trend estimates uncertain (Sauer et al. 2020) and many environmental and anthropogenic forces threaten Dusky Grouse habitat and populations. Dusky Grouse populations may be negatively impacted by beetle-killed forests, wildfire, timber harvest, and climate change (Bendell and Elliot 1967, Martinka 1972, Pelren and Crawford 1999, Chan-McLeod 2003, Youtz et al. 2022). Although Dusky Grouse likely occupy much of their historical distribution, habitat loss resulting from agricultural expansion and urbanization has resulted in local extirpations (Schroeder 2006); one study suggests that Dusky Grouse populations have declined in the past 100+ years as a result of timber harvest and overhunting (DeSante and George 1994). Despite being a commonly hunted upland game species, agencies lack information on Dusky Grouse abundance, distribution, and population trends necessary for effective management.

Dusky Grouse are often managed as part of an aggregation of forest grouse species, including ruffed grouse (*Bonasa umbellus*), spruce grouse (*Falcipennis canadensis*), and Sooty Grouse (*Dendragapus fuliginosus*). Until 2006, dusky and sooty grouse were considered one species, the blue grouse (Schroeder 2006), and these grouse are still monitored as a single species in many states. The species designation change was based on mitochondrial DNA, but sooty grouse and Dusky Grouse also differ in the color of the bare neck patches visible during breeding displays and loudness of their hooting calls (Brooks 1929, Barrowclough 2004). Forest grouse hunting occurs across the entire distribution of the Dusky Grouse, but hunting statistics are often collected for all forest grouse species in aggregate. In states such as Nevada, Washington, and Oregon, hunting statistics for dusky and sooty grouse are combined (Espinosa 2018, Washington Department of Fish and Wildlife 2022, Oregon Department of Fish & Wildlife 2023). In Washington and Utah all forest grouse species are managed collectively, but

individual species statistics may be available (Bernales et al. 2017, Washington Department of Fish and Wildlife 2022). In Nevada during 2007–2017, 1,119 hunters harvested around 1,400 blue grouse annually, while in Utah from 1963–2016, an annual average of 14,000 hunters harvested 39,000 forest grouse (Bernales et al. 2017, Espinosa 2018). Some states such as Montana, Wyoming, and Colorado collect species-specific information from hunter harvest data (Gates 2019, Colorado Parks and Wildlife 2020, Montana Fish, Wildlife and Parks 2021). In Wyoming from 2009–2018 the 10-year average was 3,600 hunters per year harvesting approximately 8,400 Dusky Grouse (Gates 2019). In Colorado, annual averages were not easily accessible, but from 2019–2020, around 7,000 hunters harvested approximately 12,379 Dusky Grouse (Colorado Parks and Wildlife 2020). Until recently in Montana, Dusky Grouse statistics for the past decade were not available, but numbers for 2021–2022 show that approximately 5,600 hunters harvested 12,300 Dusky Grouse (Montana Fish, Wildlife, and Parks 2021). Even in states with species-specific hunter harvest data, population monitoring for Dusky Grouse is often non-existent beyond basic hunter harvest surveys or wing and tail collections, which provide little relevant information on population trends (Dahlgren et al. 2021, McNew et al. 2023).

Information from hunter harvest surveys and wing and tail samples have been used to estimate grouse population trends and productivity (Amman and Ryel 1963, Aebisher and Baines 2008, Sands and Pope 2010). Hunter harvest surveys consist of telephone and mail questionnaires used to estimate harvest and hunting effort under the premise that survey results could reflect changes in species abundance as well as hunting effort and harvest (Aebischer and Baines 2008, Sands and Pope 2010). Hunter harvest surveys can be biased due to hunters

unintentionally inflating success rates or giving rounded answers, providing non-random sampling information (*i.e.*, hunting may occur more in some areas than others), and non-responses from hunters that do not return surveys (Atwood 1956, Rogers 1963, Sands and Pope 2010). Productivity indices are estimated using the ratio of harvested juveniles to adult females, which is calculated from wing and tail samples (Flanders-Wanner 2004, Hagen and Loughin 2008). However, age ratios calculated from wings of hunter harvested grouse most likely yield biased estimates if uncorrected for age-specific vulnerability to hunting (Flanders-Wanner et al. 2004, Hagen and Loughin 2008, Sands and Pope 2010). Moreover, hunter harvest data does not provide information on populations prior to harvest and may be better for monitoring hunter effort than game bird population trends (Sands and Pope 2010). For Dusky Grouse, hunter harvest data may be especially limited in amount and applicability as this species often migrates higher in elevation to relatively inaccessible coniferous habitat starting in late summer (Zwickel and Bendell 2004).

Other survey methods for monitoring upland game bird populations include spring breeding season surveys and summer brood surveys (Rogers 1963, Sands and Pope 2010). For many grouse species, male courtship displays increase detection probability of males during the spring breeding season. Traditionally, biologists use hooting and drumming counts from displaying males during spring surveys to estimate density and abundance of forest grouse populations (Rogers 1963, Sands and Pope 2010). In addition, brood surveys conducted along roads in late summer are used to monitor productivity and abundance of forest grouse (Schroeder 2010). Summer brood count surveys may result in small sample sizes due to low detectability, leading to imprecise estimates which may not be representative of productivity (Sands and Pope

2010, Hansen et al. 2015). Previously in Montana, Dusky Grouse hooting surveys based on protocols for ruffed grouse drumming surveys, brood counts, hunter check stations, wing and tail samples, and harvest questionnaires were used to monitor populations of Dusky Grouse, but in recent decades few if any surveys have occurred (Rogers 1963, Newell 2016).

Statistical Methods for Unbiased Population Estimates

Even though population counts and relative abundance indices are commonly used to monitor grouse, they do not account for observation error (Rosenstock et al. 2002, Sands and Pope 2010). Imperfect detection (*i.e.*, downward-biased observation error) of individuals limits the ability of population counts or relative abundance indices to provide unbiased estimates of abundance or population trends if detection probability varies temporally or spatially (Rosenstock et al. 2002, Sands and Pope 2010). Without considering detectability, observed population trends result from variation in detection probability rather than variation in population size (Rosenstock et al. 2002, Kéry and Royle 2016). Failure to adjust grouse counts to account for detectability can result in underestimation of population densities or occupancy, downward bias in abundance and trend estimates, and imprecise understanding of spatial distribution or habitat relationships (Thomspson 2002, Kéry et al. 2005, Royle et al. 2005). Incorrect or biased inferences can lead to incorrect management recommendations, which is especially problematic for game species where abundance estimates are used to set harvest limits (Kéry and Schaub 2012, Jakob et al. 2014). There are several modeling approaches that account for imperfect detection with unmarked individuals (*i.e.*, distance sampling, time-removal models, N-mixture models), and these methods show potential for monitoring forest grouse (Buckland et al. 2001,

Farnsworth et al. 2002, Warren and Baines 2011, Amundson et al. 2014, Franceschi et al. 2014, Jakob et al. 2014, Kéry and Royle 2016, McCaffery et al. 2016).

Distance sampling models estimate the probability of detection using distance-decay functions, assuming detection probability decreases with distance from the observer (Buckland et al. 2001). Assumptions of distance sampling include: 1) individuals are distributed independently of the transects or point locations, 2) perfect detection of individuals located on the transect or at the point, 3) distances are measured accurately, 4) individuals are detected at their initial location, 5) correct identification of individuals and no double-counting, and 6) individuals are distributed uniformly in regard to distance from the transect or in regard to distance from the point, individuals are distributed according to a triangular distribution (Buckland et al. 2001, Thomas et al. 2010, Buckland et al. 2015, Sollman et al. 2015). An advantage of distance sampling is that it only requires visiting a survey site once, and hierarchical models allow us to incorporate covariates for both detection and abundance (Buckland et al. 2001, Kéry and Royle 2016). A disadvantage of distance sampling is that it requires an adequate number of detections (*e.g.*, 75–100 for point counts and 60–80 for line transects) for analysis, an appropriate distance-decay function for the data to be chosen (Buckland et al. 2001)., and detections to occur at varying distances.

Time-removal models estimate detection as a product of both availability and perceptibility. Availability is the probability that an individual produces a cue (like hooting or wing flutter) that allows it to be detected, while perceptibility is the probability that an observer detects an individual provided it produces a cue (Farnsworth et al. 2002, Amundson et al. 2014). Time-removal models break a survey into time-intervals and record the interval in which an

individual is first detected, using this to estimate detection (Farnsworth et al. 2002). More recent models, such as hierarchical distance sampling with time-removal, allow the separate estimation of availability and perceptibility with covariates on both detection components and abundance (Amundson et al. 2014, Kéry and Royle 2016). Combing hierarchical distance sampling with time-removal, a model that accounts for availability, may be especially useful for relaxing the distance sampling assumption of perfect detection at a distance of 0 (Amundson et al. 2014). Assumptions of time-removal with hierarchical distance sampling methods include those for distance sampling plus 1) availability and perceptibility are independent or the probability of one does not affect the probability of the other, 2) the survey occurs within a period of closure where there is no births, deaths, emigration, or immigration, and 3) probability an individual is present in the survey area is equal to 1 (Amundson et al. 2014). A disadvantage of hierarchical distance sampling with time removal is that with low availability, precision of abundance estimates may also be low (Amundson et al. 2014).

N-mixture models are hierarchical models that use spatially and temporally replicated counts to estimate local abundance while incorporating imperfect detection (Royle 2004). Assumptions of N-mixture models are: 1) counts occur within a period of closure, 2) no false positives where an individual is counted twice, 3) all individuals are detected independently or the detection of one individual is not affected by the probability of detecting a different individual, 4) all individuals have the same probability of detection at a site during a given survey, and 5) the distributions of abundance and probability of detection are adequately described by their chosen parametric distribution (Royle 2004, Kéry and Schaub 2012). An advantage of N-mixture models is that covariates can be modeled on both abundance and

detection (Kéry 2008). In addition, while N-mixture models perform better with higher detections and more spatial and temporal replicates, they can still perform well with sparse or patchy data that contains many zeros (Yamaura 2013, Kéry and Royle 2016, McCaffery et al. 2016). The disadvantages of N-mixture models are that they are very sensitive to assumption violations, they require repeat visits which increases travel costs and time commitment for observers, and a large number of sites may be needed when densities are low in order to obtain enough non-zero observations for reliable inferences (Royle 2004, Dénes et al. 2015, Barker et al. 2018, Duarte et al. 2018, Knape et al. 2018, Link et al. 2018).

Developing a Population Monitoring Program

There are many factors to consider when creating a population monitoring program for wildlife management. First and foremost, population monitoring methodologies should be driven by goals that are formulated before monitoring begins (Pollock et al. 2002, Witmer 2005). These goals should specify the purpose of the monitoring program, the parameters of interest such as abundance or occupancy, desired precision levels for population estimates and detectability, and how results will be used. Second, managers should evaluate survey designs, sampling methods, and statistical analyses and select those that account for imperfect detection, provide precise and unbiased estimates, and align with the species' ecology (Pollock et al. 2002, Witmer 2005). Third, a power analysis is needed to evaluate the ability of the chosen protocol and analytical methods to meet the goals of the specific monitoring program (Gibbs et al. 1999). After the monitoring program is underway and data becomes available, additional analyses should be conducted to re-assess the ability of the chosen protocol and analytical method to meet objectives (Gibbs et al. 1999). Fourth, managers should consider the logistical feasibility of the proposed

survey, including budget, time, and personnel constraints. Lastly, the population monitoring program should yield results that are easily interpretable by the intended audience.

No studies have formally evaluated the efficacy of different sampling and analytical methodologies for monitoring Dusky Grouse populations, especially those that account for imperfect detection and aim to produce unbiased estimates of population sizes and trends. To effectively monitor and manage Dusky Grouse populations, reliable species-specific survey methods need to be developed, tested, and implemented. The primary goal of my dissertation research was to inform the development of an effective population monitoring program for Dusky Grouse that met the Montana Department of Fish, Wildlife and Parks' monitoring goal of unbiased and precise (coefficient of variation $\leq 15\%$) annual estimates of abundance. After defining monitoring goals, we evaluated various sampling and analytical methods that may allow precise abundance estimation. First, we created the first species distribution models of Dusky Grouse habitat in Montana, which improved our understanding of Dusky Grouse habitat relationships and helped us select appropriate sampling locations. Second, we evaluated different sampling methods, protocols, and survey conditions to find those that maximized probability of detection for Dusky Grouse. Third, we used simulations to evaluate different protocols (*i.e.*, number of sites and visits) and analytical methods for producing unbiased and precise abundance estimates using different abundance and detection scenarios. Finally, we provide recommendations for the creation of a population monitoring for Dusky Grouse in Montana.

CHAPTER TWO

USING AN ENSEMBLE APPROACH TO PREDICT HABITAT OF DUSKY GROUSE

Contribution of Authors and Co-Authors

Manuscript in Chapter 2

Author: Elizabeth Leipold

Contributions: Conceptualization, data curation, formal analysis, investigation, methodology, validation, and writing

Co-Author: Claire Gower

Contributions: Conceptualization, writing review and editing

Co-Author: Lance B. McNew

Contributions: Conceptualization, methodology, supervision, validation, writing review and editing

Manuscript Information

Elizabeth Leipold, Claire Gower, Lance McNew

Status of Manuscript:
☐ Prepared for submission to a peer-reviewed journal
☒ Officially submitted to a peer-reviewed journal
☐ Accepted by a peer-reviewed journal
☐ Published in a peer-reviewed journal

Avian Conservation and Ecology

Introduction

Dusky Grouse (*Dendragapus obscurus*) are an under-monitored galliform and conifer forest specialist found in the interior mountain ranges of western North America (Aldrich 1963, Zwickel and Bendell 2004). Although presumed to occupy most of their historical distribution (Zwickel and Bendell 2004), basic information on population trends, regional habitat associations, and resolute estimates of species distributions are lacking. Unlike other upland gamebird species, standardized survey protocols are not developed or broadly applied for Dusky Grouse. Common multi-species survey protocols (*e.g.*, the Breeding Bird Survey) are ineffective for monitoring Dusky Grouse populations due to a mismatch between survey locations and remote Dusky Grouse habitats that limit encounter rates (Sauer et al. 2020). The lack of information on population status, distributions, and habitat associations hinders effective population management. Increasing environmental stressors (*e.g.*, wildfire, exurban development, timber harvests, beetle kill, climate change) in Dusky Grouse habitats necessitate the development of targeted and robust population and habitat monitoring protocols (Martinka 1972, Redfield 1973, Chan-McLeod and Bunnell 2003, Youtz et al. 2022).

Accurate species distribution models (SDMs) provide information on distribution and habitat associations that are useful for conservation and management. Species distribution models can be used to direct survey locations towards potential habitat thus increasing the likelihood of species detection, assist with determining conservation status, delineate areas for conservation, and help predict a species response to management actions or climate change (Guisan et al. 2006, Sofaer et al. 2019). Recently the number of techniques available for creating species distribution models has grown, and now includes more classic techniques such as

resource selection functions (RSFs), as well as newer machine learning methods (Elith and Graham 2009, Grenouillet et al. 2011). Each approach has its own limitations, and no one method is universally best for all applications (Araùjo and New 2006, Elith and Graham 2009). In addition, the best technique for predicting habitat suitability may differ within the study area versus outside the study area (Guisan et al. 2017). Unfortunately, the subjective choice of modeling technique can influence the predictions of species occurrence (Araùjo and New 2006, Pearson et al. 2006). Because conservation planning is increasingly reliant upon SDMs (Guisan and Thuiller 2005, Guisan et al. 2013), it is imperative that predictions of species occurrence and distribution are accurate. Recent research has highlighted the benefits of ensemble modeling, where predictions of species distributions are produced with several statistical techniques, which can improve accuracy and reduce uncertainty in SDM predictions (Araújo et al. 2005, Marmion et al. 2009, Grenouillet et al. 2011). In addition, consensus within the suite of models on predicted habitat may increase certainty in the model's accuracy, while variation in predictions across models may serve as an index of uncertainty in species occurrence (Latif et al. 2013).

We used an ensemble modeling approach to understand habitat associations and predict the distribution of Dusky Grouse in Montana, USA. Our specific objectives were to: (1) explore relationships between Dusky Grouse occurrence and landscape-level habitat characteristics, (2) generate and test the accuracy of predictions of dusky habitat using multiple modeling techniques, and (3) evaluate the ability of our state-wide predictions to guide monitoring efforts by being able to predict appropriate population survey sites at scales relevant to management. To address these objectives, we developed and applied two types of species distribution models,

RSFs and randomized classification trees (*e.g.*, Random Forest), and used an ensemble of predictions to identify potential habitat for Dusky Grouse in Montana.

Methods

Study Area

Our study area included the entire state of Montana, USA. State-level wildlife management by the Montana Department of Fish, Wildlife & Parks (MFWP) is divided into 7 administrative regions (Figure 1). Dominant vegetation types, based on vegetation physiognomy in western Montana (Regions 1–3) are mainly conifer forests, intermixed with shrublands and intermountain foothills grasslands (Landfire 2016a). Eastern Montana (Regions 6–7) are dominated by grasslands, shrublands, and cultivated lands, and mountainous Dusky Grouse habitat is less abundant and more isolated (Landfire 2016a). Central Montana (Regions 4–5) transitions from vegetation types found in western Montana to those found in eastern Mountain and is dominated by both mountainous and coniferous forests in the west and grasslands, shrublands, and cultivated lands toward the east (Landfire 2016a). Elevation varies from 550–3897m (United States Geological Survey 2017).

Grouse Observations

We used two independent datasets of Dusky Grouse observations: a dataset with used and pseudo-absent locations for training and testing our models, and an independent dataset with presence-only locations for additional validation tests. For training our SDMs, we obtained Dusky Grouse observation data from the Integrated Monitoring in Bird Conservation Regions program (IMBCR) administrated by the Bird Conservancy of the Rockies. IMBCR survey sites

occur over much of the mid-western and western parts of the United States, with the surveyed land broken up into different strata that are based on land ownership and topographic features (Pavlacky et al. 2017, Hanni et al. 2018, Woiderski et al. 2018). A grid of 1-km^2 cells is generated for each stratum, with 16 sites evenly spaced every 250 m within each cell (Woiderski et al. 2018). Each spring during May–July, a spatially balanced sampling algorithm called generalized random-tessellation stratification (GRTS), is used to randomly select a minimum of 2 sample units (cells) within each stratum, within which observers conduct 6-minute point-counts at each of the 16 sites (Woiderski et al. 2018). We obtained observation data from spring surveys conducted during 2009–2020 for a total of 25,654 surveys conducted across 6,092 sites in Montana. Dusky Grouse were detected (observed ≥ 1 time) at 132 sites and not detected (pseudo-absent) at 5,960 sites (Table 1; Figure 1). Because the detection of grouse is imperfect, the observation data fit a standard used vs available sampling design common to species distribution modeling (Design 1, sampling protocol A; Manly et al. 2002).

Montana Fish, Wildlife & Parks (MFWP) field staff recorded the geographic locations of incidental Dusky Grouse observations observed during unrelated field activities conducted in the springs (April–June) of 2017–2021. During the 4-year period, 194 Dusky Grouse locations were recorded (Figure 1), which we used as an independent dataset to further evaluate the predictive accuracy of our models.

Environmental Predictors

We assumed that all Dusky Grouse observed were located within 250-m of the IMBCR point count location because Dusky Grouse calls are difficult to detect at distances greater than 100 m (Farnsworth 2020). We calculated the mean statistic or proportion of a habitat

characteristic within the 250-m radii circle centered on the survey point using geospatial modeling environment (GME), remotely sensed geospatial datasets, and the spatial analyst tools in ArcGIS Pro (Environmental Systems Research Institute, Redlands, CA; Appendix A; Beyer 2015). Because Dusky Grouse tend to be found at higher elevations, may prefer east to south-facing slopes, and brood-rearing females have been found to prefer more moderate slopes, we extracted average elevation, slope, and proportions of different facing (N, NE, E, etc.) aspects from a digital elevation model (Stauffer and Peterson 1986, U.S Geological Survey 2017, Farnsworth 2020). In addition, we calculated the mean distance to the nearest stream and to the nearest road using spatial analyst tools from ArcGIS pro (Environmental Systems Research Institute, Redlands, CA) and road and stream geospatial data layers (Montana Spatial Data Infrastructure 2017, 2018). As the attribute data for the geospatial road layer was incomplete, we had to group all road types together including highways, secondary roads, and forest service roads with and without seasonal closures. We did not expect this to affect our results. We used the LANDFIRE geospatial data with a 30 × 30 m spatial resolution to describe existing vegetation type (EVT), which is the type of plant community present, projected canopy cover in 1% increments (EVC), and average height of the dominant vegetation given in 1-m increments (EVH; Landfire 2016a, b, c, 2019, 2020). We condensed the 1% increments for the canopy vegetation to 10% increments and the 1-m increments for vegetation height to 5-m increments to reduce the number of variables evaluated. For both EVC and EVH data, there were also several categories of developed habitat or barren habitat that were grouped into two categories: developed and sparse vegetation. In addition, we created a conifer forest layer based on the descriptions for the different LANDFIRE vegetation types. We used this layer to calculate the

average distance to the edge of the conifer forest from within the forest and outside of the forest (Appendix A; LANDFIRE 2016a). We removed variables from consideration if they occurred at less than 1% of the survey sites.

Habitat Associations and Ensemble of Predictions

Resource Selection Functions. We fit RSFs using general linear mixed models (GLMMs) with a logit link function, binomial error distribution, and the "bobyqa" optimizer with a maximum of 100,000 iterations for approximating beta coefficients using the 'lme4' package in program R (Bates et al. 2015, R Core Team 2017). Our GLMMs included the binomial response variable of whether a Dusky Grouse was detected (1) or not detected (0) at each site, combinations of environmental predictors, and a random intercept for unique IMBCR transects to account for dependencies in the observation data due to the survey points being grouped along survey routes (Zurr 2009, Hanni et al. 2018).

Prior to model fitting, we explored possible non-linear responses of Dusky Grouse to habitat variables using univariate generalized additive models (GAMs) and linear equations hypothesized to represent the linear and nonlinear forms such as a quadratic form [$x + x^2$] and pseudolinear threshold ($\ln[x + 0.001]$; Franklin 2000, Guisan and Zimmerman 2000, Guisan et al. 2002, Dugger et al. 2005, McNew et al. 2015). We performed the preliminary screenings of the three functional responses using univariate models built using GLMMs with a logit link function and binomial error distribution, evaluating the model support using Akaike's Information Criterion for small sample size (AIC_c; Burnham and Anderson 2002). We also removed additional variables from consideration if they showed no relationship with use by Dusky Grouse resulting in 90 environmental predictor variables (Appendix A). After preliminary

screenings of the functional responses, we assessed multicollinearity in the remaining habitat predictor variables for all possible pairings using Spearman-rank correlations. We considered variables to be correlated when $|r| > 0.7$. If variables were correlated, we first used knowledge of general Dusky Grouse habitat to evaluate which variable was more biologically relevant to Dusky Grouse. If no previous information about the habitat characteristic was available, using the univariate models with the best performing functional response for the correlated variables we evaluated model support using AIC_c, and whichever correlated variable was least supported was removed from our analysis (Burnham and Anderson 2002, Arnold 2010, Aldridge et al. 2012). If a variable was correlated ($|r| > 0.7$) with more than one variable, we evaluated correlations based upon most correlated to least, removing variables until only one uncorrelated variable remained in the dataset. After assessing for pairwise correlations, we had 66 remaining variables.

We first evaluated predictors in groups based on variable type: aspect, other non-vegetation variables (slope, elevation, distance to variables), conifer vegetation type (divided into two groups that were later combined due to model convergence issues), hardwood vegetation type, grassland vegetation type, shrubland vegetation type, riparian vegetation type, other vegetation type, tree canopy cover, shrub canopy cover, herbaceous vegetation cover (also divided into multiple groups that were later combined due to model convergence issues), other vegetation canopy cover, and vegetation height. Within each group, we used backwards elimination to determine the top performing variables for inclusion in the final candidate model set, with variable removal based on the p-value calculated using the ‘lme4’ package in program R from asymptotic Wald tests, where the variable with the highest p-value > 0.05 was removed

(Hosmer et al. 2013, Bates et al. 2015, Heinze et al. 2018). Backwards selection continued until all variables within the model had p-values < 0.05 (Heinze et al. 2018). The top performing variables from each group were then added to a global model and again evaluated using backwards elimination to determine a final set of variables for predicting Dusky Grouse habitat. We calculated the 95% confidence intervals for the beta coefficients using the Wald method, which estimates the fixed-effects confidence intervals, using the 'lme4' package in program R (Bates et al. 2015, R Core Team 2017). We used the high and low confidence intervals to create two additional maps to examine uncertainty in the predictions (Appendix B).

Random Forest. We developed random forest (RF) models using the *train* and *trainControl* functions and the 'rf' model from the 'caret' package in R (Kuhn 2008, R Core Team 2017). Random forest models are sensitive to datasets where the response variables are imbalanced, such as our IMBCR dataset where the number of pseudo-absent locations greatly outnumbered the used locations (Evans and Cushman 2009, Kuhn and Johnson 2013, Kuhn 2019). To account for our dataset being unbalanced, we used the down-sampling function within the caret package to rarify the random sampling data to a 1:1 ratio with the used locations (Evans et al. 2011, Kuhn and Johnson 2013, Kuhn 2019). We tuned our model by varying the number of trees and the number of variables to possibly split at each node (Kuhn 2008, Kuhn and Johnson 2013, R Core Team 2017). The number of variables to possibly split at each node, "mtry", was tested with the square root of the number of predictors, the square root of the number of predictors divided by 2, and the square root of the number of predictors times 2 (Breiman 2001, Kuhn and Johnson 2013). The number of trees tested were 300, 500, 800, 1000, and 2000. After we tuned the model, we trained it with repeated cross validation, with 5 folds and 500 repeated

k-fold cross validation iterations. We generated variable importance using the 'randomForest' package, which calculates the impact of removing a variable on the model or mean decrease in accuracy (Liaw and Wiener 2002, R Core Team 2017).

Predictions of Dusky Grouse Habitat

We developed separate statewide predictions of relative use from each model. We used a 250-m moving window to create spatial layers for each variable upon which to predict our models. We first used slope coefficients from our top GLMM to fit an RSF (Manly et al. 2002). Second, to evaluate Dusky Grouse occurrence across Montana using the random forest model, we used the predict function in R with our 250-m circular moving window layers to construct a predictive map of potential Dusky Grouse habitat (Kuhn 2008, R Core Team 2017). We then rescaled RSF and random forest predictive maps of potential Dusky Grouse habitat in Montana to be between 0 and 1, so that the two predictive maps were on the same scale.

Model Evaluation

We evaluated the performance of our models in two ways: repeated k-fold cross validation with 5 folds where 80% of the IMBCR data used to train the model and 20% used to test the model, and with an independent dataset. We conducted a simulation with 500 iterations (externally for the RSF and within the model fitting process for the RF) where we used k-fold cross validation and threshold-independent ROC/Area Under Curve (AUC) to evaluate mean model performance with the IMBCR training dataset (Zweig and Campbell 1993, Fielding and Bell 1997). We calculated the average AUC value with a 95% confidence interval. An AUC greater than 0.7 indicates that the model has acceptable predictive power and that the

performance is better than that of pure chance (Fielding and Bell 1997, Boyce et al. 2002, Hosmer et al. 2013, Bohnett et al. 2020).

In addition, we tested model predictions using an independent dataset of incidental grouse observations collected by MFWP and comparing it with the presence locations from the IMBCR dataset. For each MFWP and IMBCR Dusky Grouse observation, we calculated the RSF value and the RF value. For each model type (RSF, RF), we used the IMBCR dataset to categorize the values into 5 quantile bins of equal size (20% of the data in each bin) that represented increasing relative probability of a point being classified as a site used by Dusky Grouse (Boyce et al. 2002, Johnson et al. 2006, McNew et al. 2013). The quantile bins represented low, medium-low, medium, medium-high, and high probability of relative use. We then regressed the observed proportion of grouse locations from the MFWP or test dataset in each quantile bin with the observed proportions of grouse locations in each quantile bin from the IMBCR or training dataset. We used linear regression to compare the training and testing datasets, and we considered a good model fit to have a high R^2 value, a slope of 1, and an intercept of 0 (Johnson et al. 2006, McNew et al. 2013).

Calculating Potential Dusky Grouse Habitat in Montana

We used the quantile bin that correctly predicted 75% of the used points in the training and test datasets as our threshold for delineating habitat and created a binary map of habitat and non-habitat for each model. To evaluate the accuracy of the threshold, we conducted a simulation with 500 iterations, where we calculated the average percent of correctly predicted locations with a 95% confidence interval for a subset (80%) of the MFWP dataset. We conducted this simulation for the state-wide MFWP data and for each MFWP region. Because predictive

accuracies of both models were similar (see Results) we added the binary maps of our two individual models, giving each model equal weight (0.5), to obtain a final map created from the ensembled prediction of potential habitat of Dusky Grouse in Montana (a frequency histogram approach; Araùjo and New 2006, Le Lay et al. 2010, Stohlgren et al. 2010). The ensemble map displayed values ranging from 0–2, where the pixel value was related to the number of models that predicted it to be habitat. A value of 2 indicates that both models predicted that pixel to be habitat, while a value of 1 indicates that only one model predicted that area to be habitat and a value of 0 indicates that both models predicted the area to not be habitat. We considered areas with a value of 2 to be high relative probability of use and areas with a value of 1 to be medium-high relative probability of use.

We calculated the amount of area within each MFWP administrative region and Montana that was predicted to be medium-high and high relative probability of use. We calculated the amount of Dusky Grouse habitat in each category by summing the number of pixels predicted to be within the categories and multiplying by pixel size (0.0009 km^2). The amount of Dusky Grouse habitat in Montana and within each MFWP administrative region was calculated as ranging between the high relative probability of use category and total potential habitat (the sum of both the medium-high and high probability of use categories total habitat.

Results

Location Data

The majority of the used locations for the IMBCR dataset were in MFWP Regions 1 and 2, while the majority of the presence locations for the MFWP dataset were in Regions 3 and 5 (Figure 2). Of the regions with presence locations, the fewest presence locations for both datasets

were in MFWP Region 4 (Figure 2). There were no used points in the IMBCR dataset in Region 5 (Figure 2).

Dusky Grouse Habitat Associations

From the RSF model we found 7 habitat predictors to impact Dusky Grouse occurrence (Table 2). All variables described are not standardized. Two variables had a quadratic relationship with relative probability of use: average distance to nearest stream (β_1= 7.40 ± 2.11SE, β_2 = -7.49 ± -2.70) and proportion of northern rocky mountain foothill conifer wooded steppe (β_1= 216.70 ± 32.83, β_2 = -5557.00 ± 137.60; Table 3, Figure 3). Average slope had a positive linear relationship with relative probability of use (β = 1.03 ± SE 0.26). Proportion of inter-mountain basins montane sagebrush steppe (β = 0.16 ± SE 0.06), and the proportion of trees with a height of 16–20 m (β = 0.32 ± SE 0.08) had positive nonlinear relationships with relative probability of use by Dusky Grouse and the proportion of trees with a height of 1–5 m (β = -0.63 ± SE 0.24) and distance to road (β = -0.31 ± 0.14) had negative nonlinear relationships with relative probability of use (Table 3, Figure 3). Conditional and marginal R^2 values for this model were 0.69 and 0.66, respectively, indicating that most of the variation in the response data from our model is described by the fixed effects, with only an additional 3% associated with our points being clustered along survey routes.

We also examined the variables of importance from the Random Forest model, and the top 10 in decreasing order from most important to least important were: proportion of trees with a height of 16–20 m, average slope, average elevation, proportion of Douglas fir forest and woodland, proportion of trees with a height of 21–25 m, proportion of montane-foothill deciduous shrubland, proportion of montane mixed conifer forest, proportion of area with 30–

39% shrub canopy cover, proportion of trees with a height of 1–5 m, and proportion of area with big sagebrush steppe (Figure 4). We evaluated the marginal impact of a variable on the random forest's predictions using partial dependency plots. Proportion of trees with a height of 16–20 m, slope, elevation, proportion of Douglas fir forest and woodland, proportion of trees with a height of 21–25m, proportion of montane-foothill deciduous shrubland, proportion of montane mixed conifer forest, proportion of 30–39% canopy shrub cover, and proportion of big sagebrush steppe all have positive nonlinear relationships, while proportion of trees with a height of 1–5 m and proportion of 30–39% canopy herb cover have negative nonlinear relationships (Figure 5).

Model Evaluation

The average AUC values for the RSF and RF models were 0.89 (95% CI: 0.85–0.93) and 0.87 (95% CI: 0.83–0.92), respectively (Figure 6). The RSF model correctly classified 150/193 (78%) of the independent grouse locations into the medium-high and high categories of relative probability of use. Linear regression produced an intercept close to zero (95% CI: -0.40–0.18), a slope of 1.55 (95% CI: 0.45, 2.65), and a high R^2 value (0.87), indicating high predictive accuracy (Figure 5). The RF model also had high predictive accuracy, with 181/193 (94%) of the independently detected Dusky Grouse locations correctly classified into the medium-high and high category bins of relative probability of use. Linear regression produced an intercept close to zero (95% CI: -0.30, 0.23), a slope of 1.17 (95% CI: 0.30, 2.06), and a R^2 value of 0.86 (Figure 7). Because both models had similarly high predictive accuracy, we used the 60–80% quantile bin (medium-high relative probability of use) as a threshold to create two binary maps using the frequency histogram method to obtain ensembled estimates of spatially-explicit habitat for Dusky Grouse in Montana. The percent of locations correctly classified as habitat from the

MFWP data was highest in Region 1 for the RSF model, in Regions 1, 2, and 4 for the RF model and ensemble predictions, and was lowest in Region 5 for all three predictions (Table 4).

Calculating Potential Dusky Grouse Habitat in Montana. Slight differences existed in the predicted habitat between the RSF and RF models, with the RSF model having more conservative estimates and the RF model predicting higher amounts of habitat across the majority of the regions (exception is MFWP Region 3; Table 5, Figure 8). Despite the slight differences in the amounts of predicted habitat (a 7% difference in total habitat and non-habitat predicted), there were high amounts of agreement (93%) between the RSF and RF models on whether an area was predicted habitat or non-habitat. Across both models, MFWP regions 1, 2, and 3 had the highest amounts of potential Dusky Grouse habitat (Table 5, Figure 8). Using our ensembled map we predicted 83,160–109,125 km^2 in Montana to be potential Dusky Grouse habitat (Table 5) with the majority of the habitat occurring in MFWP regions 1–5 (Figure 8). Of the predicted habitat for the ensembled map, 76% was predicted to have high relative probability of use and 24% was predicted to have medium-high relative probability of use (Table 5, Figure 8).

Discussion

We used IMBCR's dataset of Dusky Grouse observations and an ensemble modeling approach to evaluate habitat associations and create statewide predictions of Dusky Grouse habitat in Montana. Our RSF and RF models found somewhat different landscape metrics for predicting habitat suitability which resulted in slight differences in predicted habitat. However, both models had high predictive accuracy and predictions of potential Dusky Grouse habitat were generally similar among methods. By using an ensemble of models, created by summing 2

binary maps, we identified some uncertainty (areas of disagreement between models) in our predictions and created a robust prediction of habitat suitability for Dusky Grouse that can be used to inform habitat and population management programs in Montana.

Agreement between our landscape-level evaluation of habitat associations and previously reported field-based habitat associations of Dusky Grouse supports the validity of our predictive habitat suitability models (Johnsgard 2016). Dusky Grouse were strongly associated with coniferous and mountainous forests, and the coverages of forest height classes were important predictors of relative habitat suitability during the breeding season in both models. In addition we found relative habitat suitability increased with the coverage of mid-old growth coniferous forest (tree heights of 16–25 m; Cade and Hoffman 1993). Also consistent with previous field work, our RF model indicated strong positive associations of breeding Dusky Grouse with forests dominated by Douglas fir, lodgepole pine, and ponderosa pine (Marshall 1946, Martinka 1972, Cade and Hoffman 1990). During the reproductive season, Dusky Grouse have also been found to prefer more open forests compared to more closed forests during the winter (Stauffer and Peterson 1986). Support for partial coverages of three vegetation types (foothill conifer wooded steppe, montane foothill deciduous shrubland, and montane sagebrush steppe) suggest the importance of transitional vegetation types as Dusky Grouse migrate from high elevation forested habitat in the winter to open canopy and herbaceous nesting habitats (Mussehl 1960, 1963, Zwickel 1973, Johnsgard 2016).

The RSF and RF models had similar, but subtly different, spatial predictions of potential Dusky Grouse habitat. Generally, the RF model predicted more hectares of habitat than the RSF model. Discrepancies between model predictions (7% of Montana) were largely due to the

difference in the importance of the effect of road proximity, with the largest differences in roadless areas (*e.g.* the Bob Marshall Wilderness). The top RSF model included an estimated negative effect of distance to road on the relative probability of use, whereas this effect was ranked second to last in importance by the RF model resulting in an extremely low impact on the RF's prediction. The supported positive effect of road proximity on Dusky Grouse use is not intuitive but may be the result of other correlated variables in the model or how we treated the road layer that was then used to estimate distance to road. When we created our road layer, we did not differentiate between road types, which included highways, other high-traffic roads, low-traffic forest service roads, and roads with seasonal closures. The substrate of the roads within the road layer also differed and included native material, dirt, gravel, and paved. The majority of used points were closer in proximity to forest service roads, that were made of native material or dirt and may experience seasonal closures that could result in lower intensity of use. There is some support that Dusky Grouse males will display on old logging roads (Martinka 1972), and this behavior with the lack of differentiation between forest service roads and other road types may have resulted in a positive effect of road proximity that may not hold true for higher-trafficked roads with non-native surfaces. Despite the areas of disagreement among models, the two models agreed 93% of the time, and 76% of the predicted habitat in the ensemble map was predicted by both the RSF and RF models, and statewide predictive accuracy of both holdout training and independent Dusky Grouse observations was high.

Transferability of model predictions to unsampled areas outside of Montana are likely limited by regional variation in habitat relationships. For example, the coverage of trees with a height of 16–20 m was an important predictor of relative habitat suitability in Montana where

this tree height corresponded to preferred conifer forests at elevations of 560–3,401 m but may not be a good indicator of selection where this relationship does not occur (Araùjo and Guisan 2006, Randin et al. 2006, Heikkinen et al. 2012). At finer spatial extents (*e.g.*, MFWP administrative regions), heterogeneity in landscape metric relationships may reduce the predictive accuracy of our statewide models in areas where training data sample sizes were small (*i.e.*, where Dusky Grouse observations were few). Though we found the predictive accuracy of our individual models to be high (≥77%) for the state of Montana, predictive performance of our statewide models varied across MFWP administrative regions. For the RSF predictive map, we correctly classified 88% of the independent locations within MFWP regions 1–4, but only 46% were correctly classified for Region 5, an area with no presence locations within the training dataset. We found that despite the lack of observed grouse locations, our RF model had almost twice the predictive accuracy of the RSF model for Region 5 (43% vs 87%). Differences in the predictive performance of RSF and RF models within and outside of (*e.g.*, extrapolated) study areas further justify an ensemble approach to species distribution modeling (Marmion et al. 2009, Duque-Lazo et al. 2016). By combining multiple models, ensemble models improve accuracy and predictive performance over individual models, depending upon the accuracy of the individual models used (Marmion et al. 2009, Stohlgren et al. 2010, Grenouillet et al. 2011). Indeed, predictive accuracy improved to 94% in Region 5 when ensembled predictions of habitat suitability were used, and overall accuracy for the entire state of Montana improved to 97%. Other studies have also found increased robustness and predictive power when using an ensemble of models (Marmion et al. 2009, Stohlgren et al. 2010, Latif et al. 2013, Fuller et al.

2018) and in our case, it did so despite relatively few presence locations in some administrative regions.

Species distribution models are often used to address many conservation and management objectives, including surveillance or monitoring, finding new populations of a species, and designating areas for conservation (Guisan and Thuiller 2005, Williams et al. 2009, Le Lay et al. 2010, Stohlgren et al. 2010, Crall et al. 2013, Guisan et al. 2013, Fuller et al. 2018, Sofaer et al. 2019). For all purposes, it is important that model predictions are accurate and identify areas of predictive uncertainty. By using an ensemble of models, we accurately and confidently predicted areas of habitat versus non-habitat for Dusky Grouse in Montana, even in administrative areas that had few to no presence locations in the training dataset.

Conclusion

Our spatially resolute and statewide predictions of relative habitat suitability derived from observations produced by the rigorous and randomized IMBCR survey program are 1) an advancement on previous *ad hoc* delineations Dusky Grouse distribution based on incidental publicly reported observations, and 2) provide justifiable strata for prioritizing and planning Dusky Grouse population monitoring. By using multiple modeling techniques and an ensemble approach to prediction, we were able to understand relative habitat use and predict potential Dusky Grouse habitat. Our results provide baseline information on Dusky Grouse habitats in Montana that can be used to inform conservation planning and future research. Our results can be used to inform decisions related to management (*e.g.*, timber harvests, energy permitting) in relation to Dusky Grouse. Wildfire and beetle kill are common occurrences in Dusky Grouse habitat and having a greater understanding of habitat selection and a prediction of potential

Dusky Grouse habitat may be useful for future research to guide management and can be used to target areas for conservation efforts. In addition, our predictive map can be used to identify suitable survey areas for long-term population monitoring. Our study represents a first step in developing robust statewide population-level assessments of Dusky Grouse.

Table 1. Summary of location data. For the IMBCR dataset, the number of used and pseudo-absent points in total and per MFWP region. For the MFWP incidental data, the number of Dusky Grouse (DUGR) observations in total and per MFWP region. NAs are the result of points being located either just outside or on the border of Montana.

Region	IMBCR		MFWP
	Used	Pseudo-absent	DUGR
Region 1	41	893	26
Region 2	50	494	22
Region 3	30	815	86
Region 4	11	832	12
Region 5	0	452	47
Region 6	0	1241	0
Region 7	0	1171	0
NA	0	62	1
Total	132	5960	194

Table 2. Definitions for variables in the final RSF habitat model for predicting Dusky Grouse occurrence. We calculated the mean statistic or proportion of a habitat characteristic within a 250-m radii circle centered on the survey point. Relationship form represents the marginal relationship between a variable and probability of occurrence and is evaluated using a univariate model examining potential linear, quadratic, and pseudo-linear threshold relationships using linear equations.

Variable	EVT code	Definition	Vegetation Physiognomy	Relationship Form	Direction
Distance to Road	N/A	Average distance to nearest road (km)	N/A	linear	negative
Slope	N/A	Average slope	N/A	nonlinear: pseudo-linear threshold	positive
Distance to stream	N/A	Average distance to nearest stream (km)	N/A	nonlinear: quadratic	positive, then negative
Foothill Conifer Wooded Steppe	EVT 7165	Proportion of northern rocky mountain foothill conifer wooded steppe	Conifer	nonlinear: quadratic	positive, then negative
Montane Sagebrush Steppe	EVT 7126	Proportion of inter-mountain basins montane sagebrush steppe	Shrubland	nonlinear: pseudo-linear threshold	positive
Tree Height 1–5m	N/A	Proportion of trees with a height of 1–5m	N/A	nonlinear: pseudo-linear threshold	negative
Tree Height 16–20m	N/A	Proportion of trees with a height of 16–20m	N/A	nonlinear: pseudo-linear threshold	positive

Table 3. Slope estimates for all terms in the final RSF habitat model for predicting Dusky Grouse occurrence with 95% confidence intervals.

Variable	Estimated slope (β_i)	Lower 95% Confidence Interval	Upper 95% Confidence Interval
Distance to Road	-0.31	-0.58	-0.03
Distance to Stream	7.40	3.26	11.53
Distance to Stream^2	-7.49	-12.79	-2.19
Foothill Conifer Wooded Steppe	216.70	152.32	281.03
Foothill Conifer Wooded Steppe^2	-5557.00	-5826.86	-5287.36
ln(Slope + 0.001)	1.03	0.52	1.54
ln(Montane Sagebrush Steppe + 0.001)	0.16	0.05	0.27
ln(Tree Height 1–5m + 0.001)	-0.68	-1.14	-0.22
ln(Tree Height 16–20m + 0.001)	0.32	0.15	0.48

Table 4. Percent of simulated data correctly classified for all of Montana and each MFWP region for the independent dataset. Percent correctly classified is calculated with 95% confidence intervals for the three models: resource selection function model (RSF), random forest model (RF), and the ensemble model.

Area	RSF Model	RF Model	Ensemble Model
Montana	77.7 (95% CI: 74.7, 81.2)	93.8 (95% CI: 92.2, 95.5)	96.9 (95% CI: 96.1, 98.1)
Region 1	96.2 (95% CI: 95.0, 100)	100 (95% CI: 100, 100)	100 (95% CI: 100, 100)
Region 2	85.6 (95% CI: 81.3, 93.8)	100 (95% CI: 100, 100)	100 (95% CI: 100, 100)
Region 3	87.2 (95% CI: 83.8, 91.2)	94.3 (95% CI: 92.6, 97.1)	96.5 (95% CI: 95.6, 98.5)
Region 4	83.6 (95% CI: 77.8, 100)	100 (95% CI: 100, 100)	100 (95% CI: 100, 100)
Region 5	45.9 (95% CI: 37.8, 51.4)	87.3 (95% CI: 83.8, 91.9)	93.7 (95% CI: 91.9, 97.3)

Table 5. Estimated area (km^2) of potential Dusky Grouse habitat for Montana FWP administrative regions for the 3 predictive maps. The RSF and RF models are divided into a binary map of habitat and non-habitat based on the 60% quantile, while the ensemble map is based on an ensemble frequency histogram where consensus between the models on predicted habitat resulted in high relative probability of use and areas of unagreed upon predicted habitat between the RSF and RF models resulted in medium-high relative probability of use, and consensus between the models on predicted non-habitat resulted in non-habitat. Total habitat is the sum of the medium high and high relative probability of use categories.

Region	RSF: Non-Habitat:	RSF: Habitat	RF: Non-Habitat	RF: Habitat	E: Non-Habitat	E: Med. High	E: High	E: Total Habitat
Region 1	9489	25045	5402	29133	4714	5463	24357	29821
Region 2	7112	20195	4498	22809	4073	3464	19770	23234
Region 3	22589	27509	22669	27429	19077	7104	23917	31021
Region 4	60602	10725	55435	15892	54751	6535	10041	16576
Region 5	40171	5456	39471	6157	38538	2566	4524	7089
Region 6	71873	581	71590	865	71459	544	451	995
Region 7	78732	351	78944	139	78694	289	100	390
Total	290570	89862	278008	102423	271306	25966	83160	109125

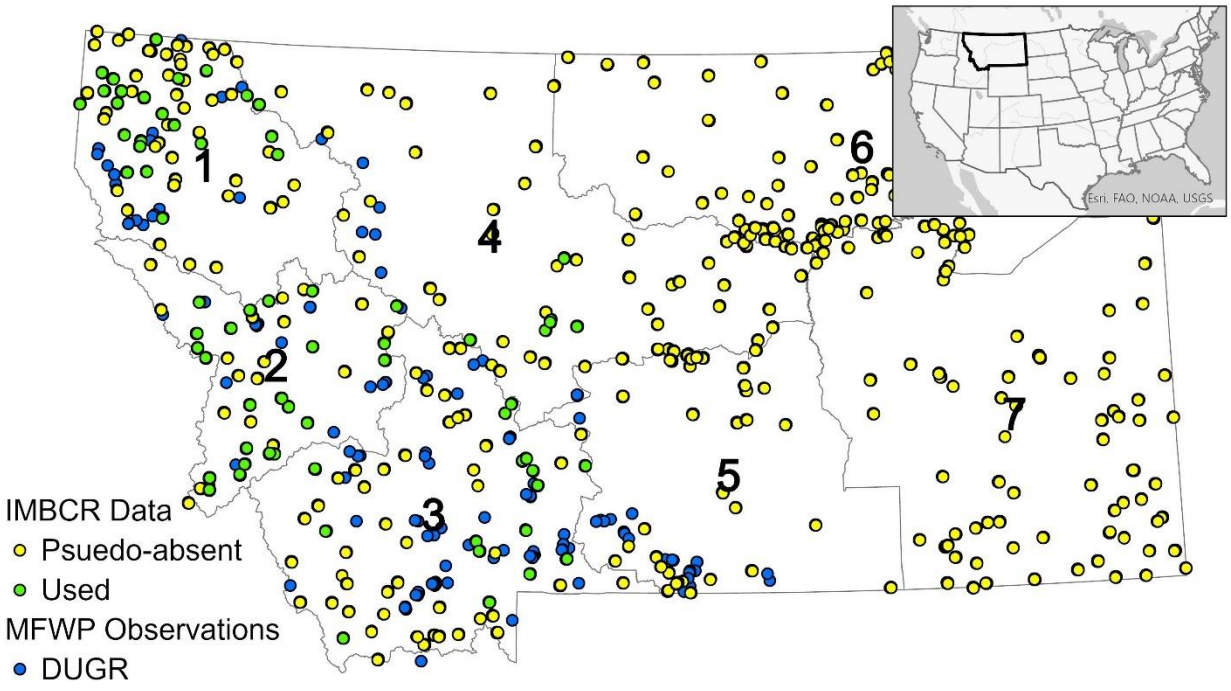

Figure 1. Map of study area with IMBCR survey sites (n = 6,092) and MFWP incidental observations of Dusky Grouse (n = 194). At the IMBCR sites, 132 were classified as used (Dusky Grouse detected) and 5,960 as pseudo absent (Dusky Grouse not detected). Montana Fish Wildlife & Parks divides Montana into seven administrative regions for conservation and management. FWP regions are outlined in gray and labeled by region number (regions 1-3 on the left, 4-5 in the center, and 6-7 on the right).

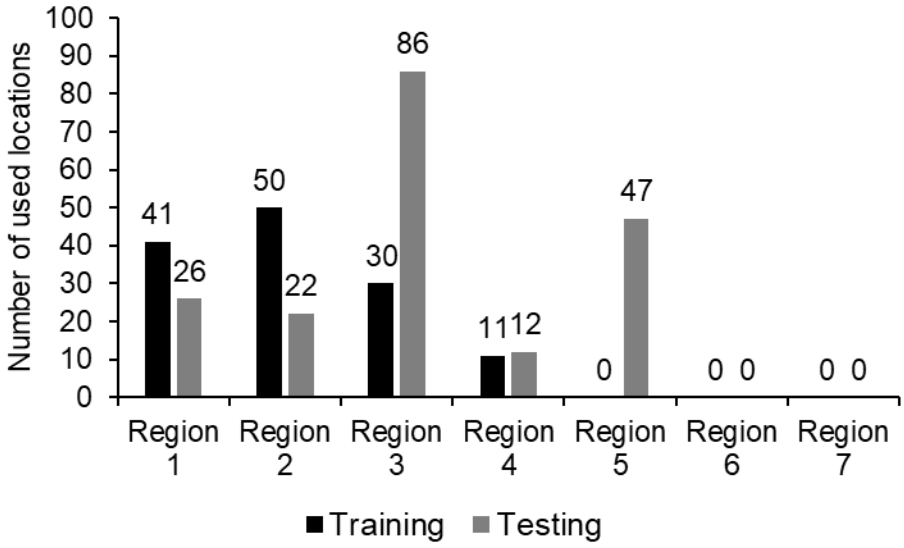

Figure 2. Total number of used (Dusky Grouse detected) locations for the training (IMBCR) and the testing (MFWP) datasets for each MFWP region. No used locations were observed in Regions 6 and 7 for either dataset.

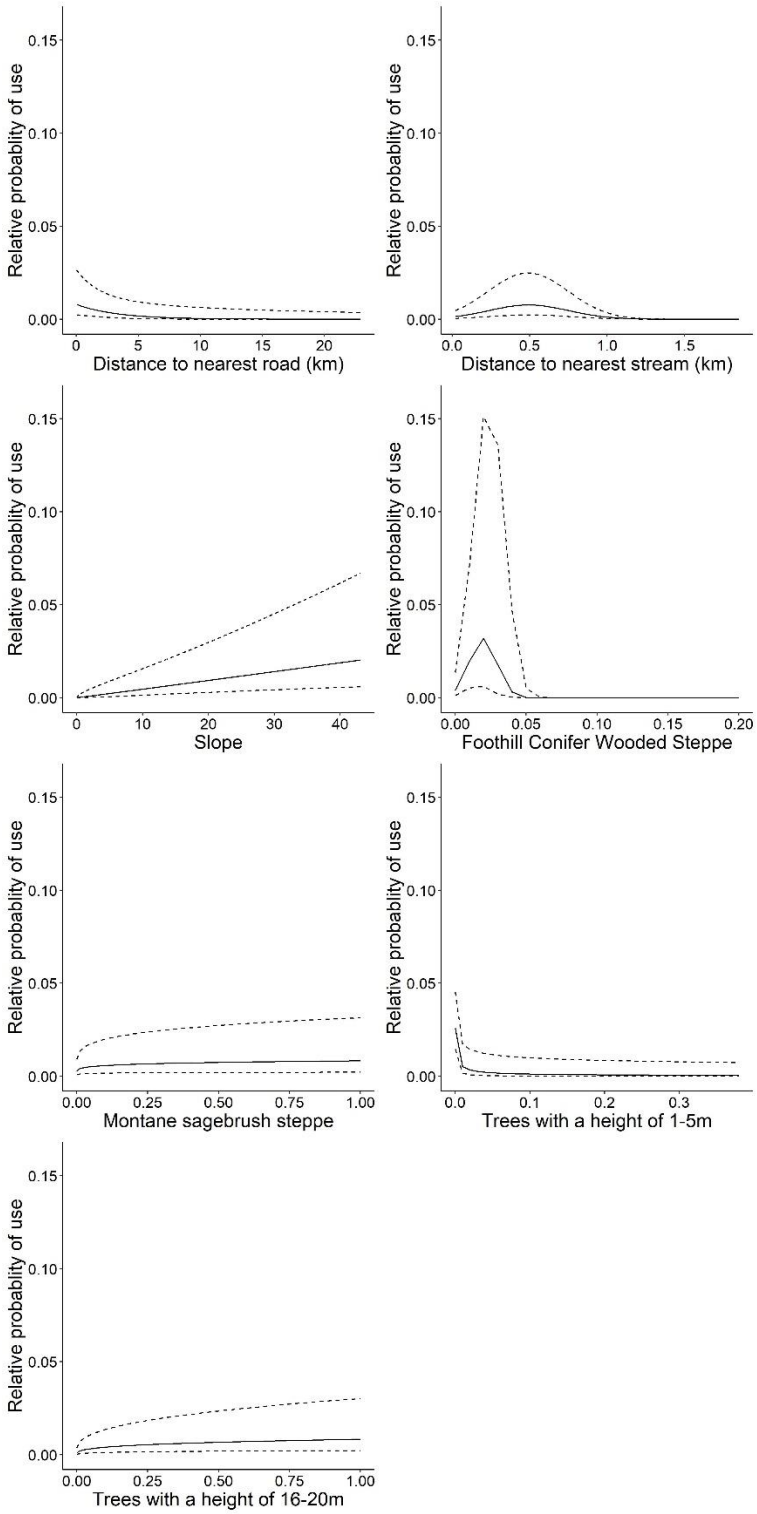

Figure 3. Predicted relative probability of use for covariates in the RSF model with 95% confidence intervals (dashed lines) while all other covariates are held at their average value.

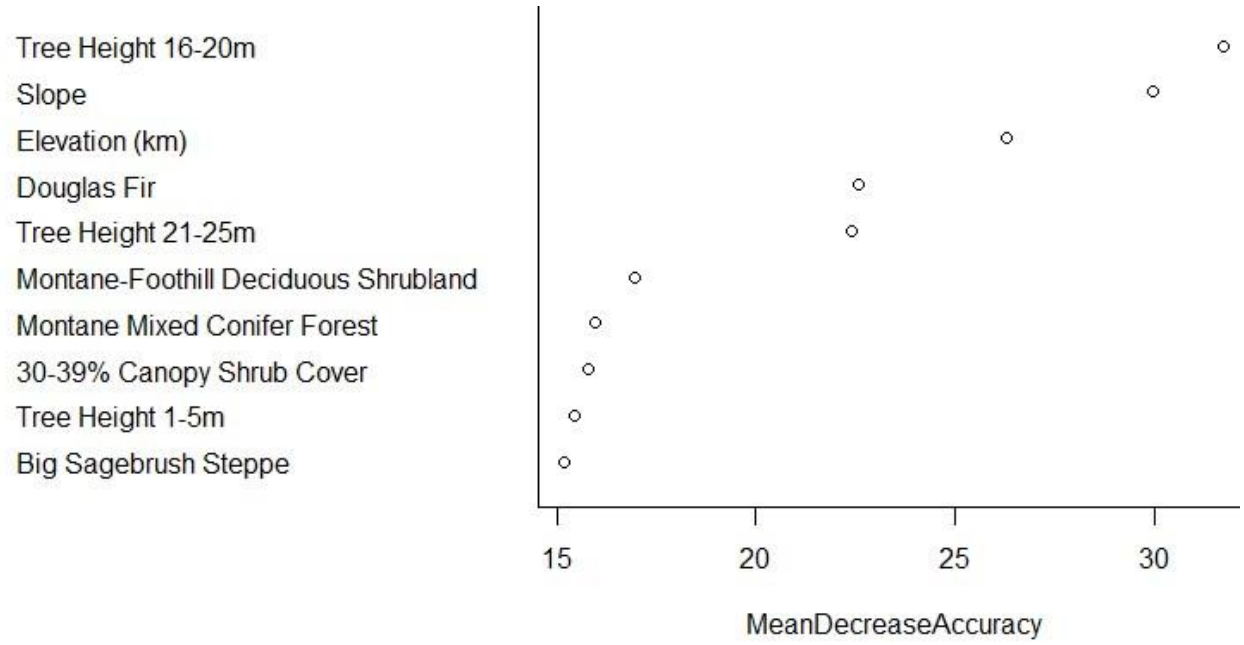

Figure 4. Variable importance plot for the top 10 important variables from the random forest model. Variable importance was calculated as the impact of removing a variable on the model or mean decrease in accuracy.

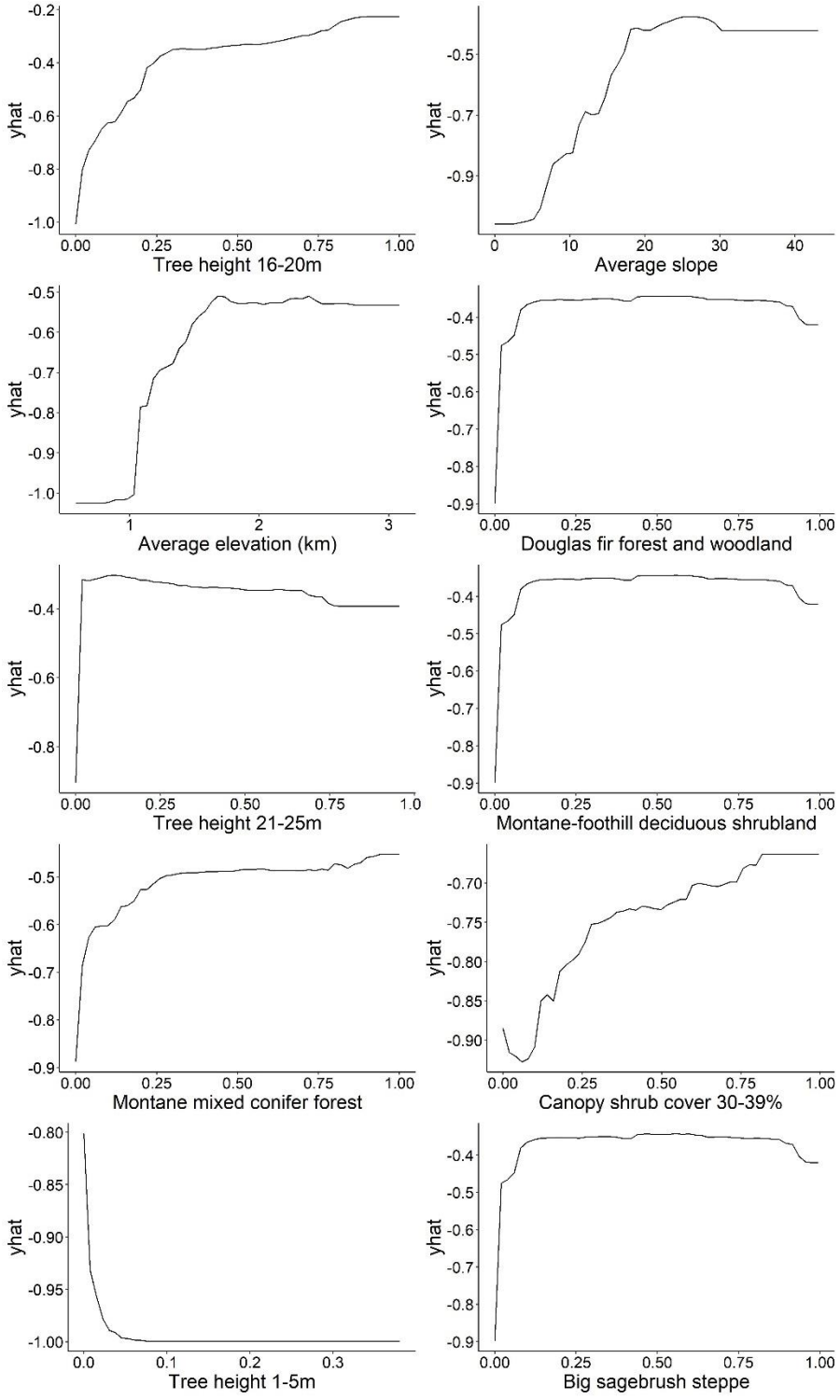

Figure 5. Partial dependency plots for the variables of greatest importance for fitting the random forest model to evaluate the marginal effect of a variable on the random forest's predictions.

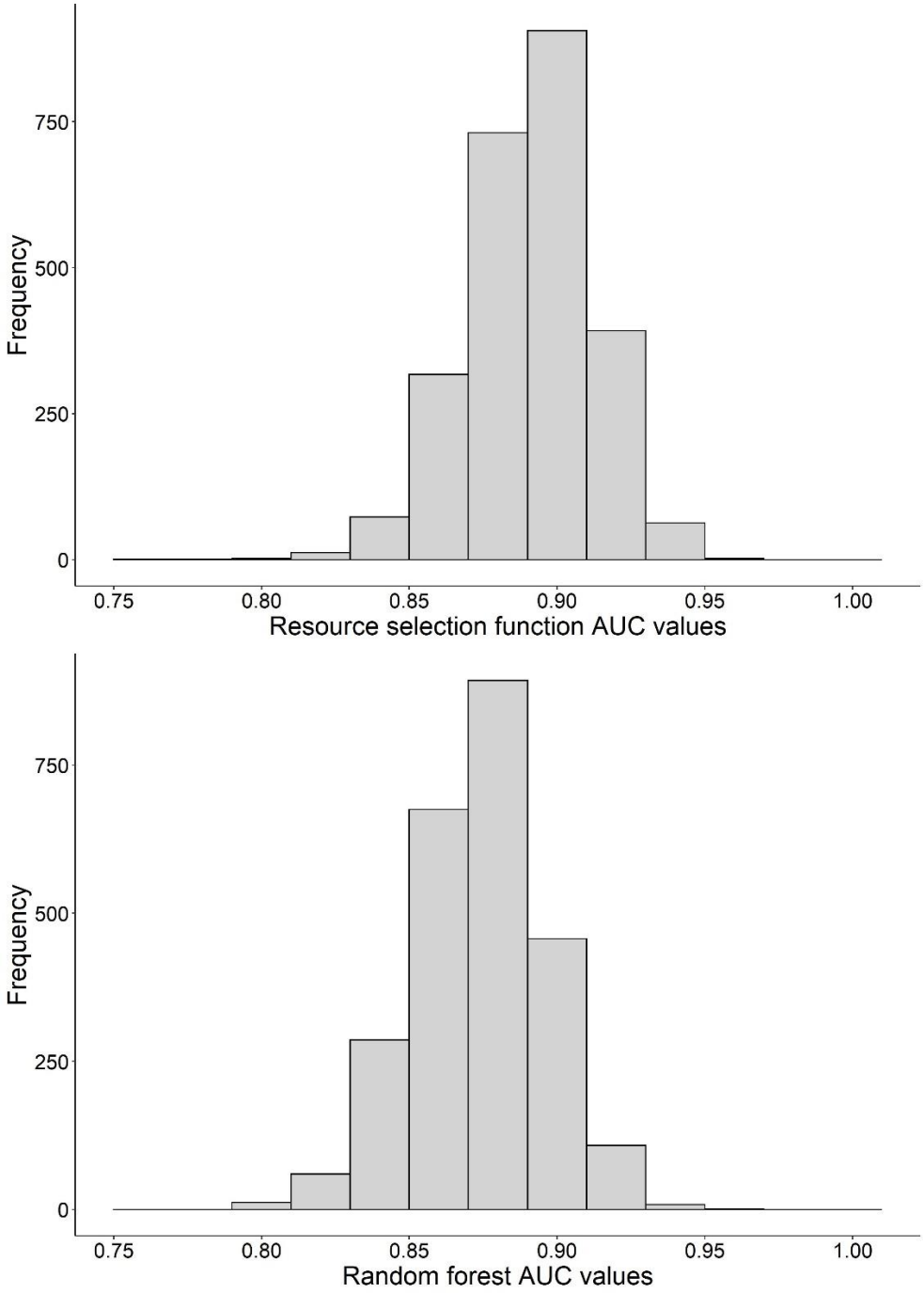

Figure 6. Histogram of the AUC values from the repeated k-fold cross validation for the resource selection model (top) and random forest model (bottom). Average AUC for the RSF model was 0.89 (95% CI: 0.85-0.93) and for the RF model was 0.87 (95% CI: 0.82, 0.92).

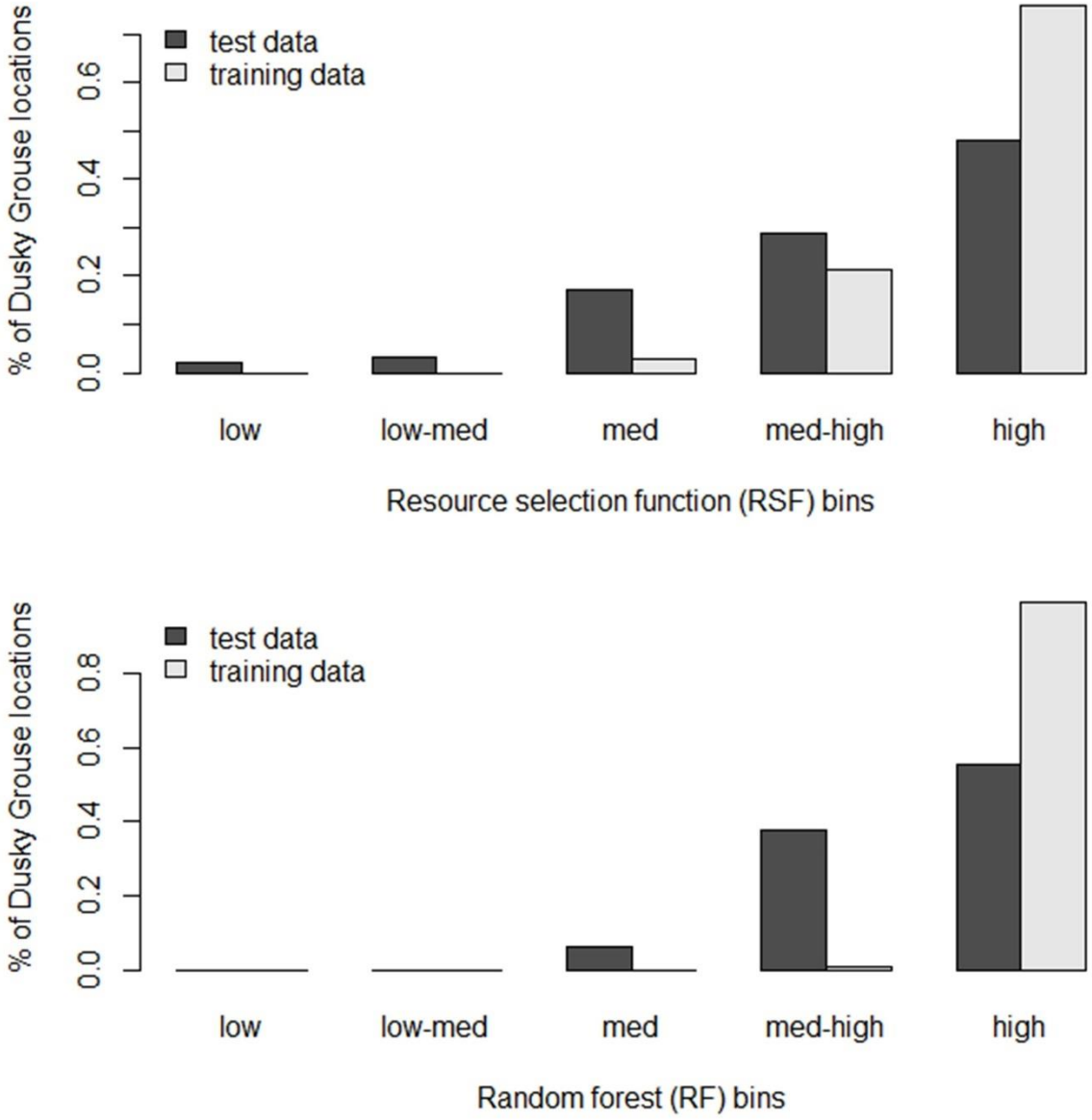

Figure 7. Proportion of Dusky Grouse locations in five bins of increasing relative probability of use values for resource selection function values (top) and random forest model values (bottom) that we used to train (n = 132) and test (n = 193; 1 location was outside MT) the different models of predicted Dusky Grouse habitat. A good predictive model will assign most of the training and test Dusky Grouse locations to medium-high or high categories of predicted use.

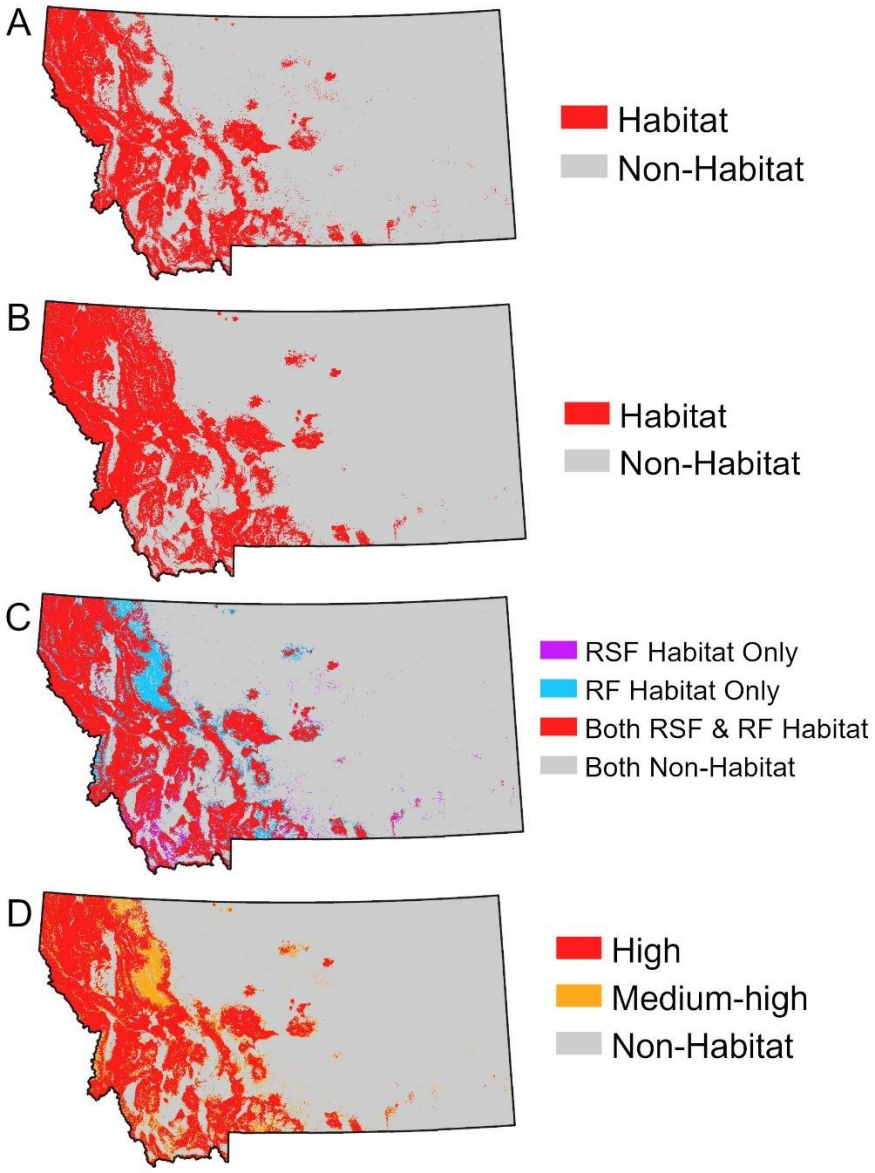

Figure 8. Predicted Dusky Grouse habitat (red) for the resource selection function map (A) and random forest map (B). Areas of consensus and differences (C) in predicted Dusky Grouse habitat between the RSF and RF models, where areas both models predict habitat are red, where only RSF predicted habitat are purple, areas where only RF predicted habitat are blue, and areas where both models predict non-habitat are gray. Predicted Dusky Grouse habitat for the ensemble model (D) where red represents habitat with high probability of use, orange represents habitat with medium-high probability of use, and gray represents non-habitat. MFWP administrative regions are delineated in gray (left top to bottom: Regions 1, 2, 3; center top to bottom: Regions 4, 5; and right top to bottom: 6, 7).

CHAPTER THREE

MAXIMIZING THE PROBABIITY OF DETECTION DUSKY GROUSE IN MONTANA: IMPLICATIONS FOR POPULATION MONITORING

Contribution of Authors and Co-Authors

Manuscript in Chapter 3

Manuscript in Chapter 2

Author: Elizabeth Leipold

Contributions: Conceptualization, data curation, formal analysis, investigation, methodology, validation, and writing

Co-Author: Claire Gower

Contributions: Conceptualization, writing review and editing

Co-Author: Lance B. McNew

Contributions: Conceptualization, methodology, supervision, validation, writing review and editing

Manuscript Information

Elizabeth Leipold, Lance McNew

Status of Manuscript:
☒ Prepared for submission to a peer-reviewed journal
☐ Officially submitted to a peer-reviewed journal
☐ Accepted by a peer-reviewed journal
☐ Published in a peer-reviewed journal

Introduction

Probability of detection plays an important role in the development of field survey protocols and species monitoring. The inability of surveyors to perfectly observe individuals impacts the utility of unadjusted counts for monitoring wildlife populations (Rosenstock et al. 2002). If detection probability is not incorporated into abundance estimates and observation error varies spatially or temporally, then variation in counts may be the result of changes in abundance or changes in detection or both (Rosenstock et al. 2002, Thompson 2002, Farnsworth et al. 2005). Spatial and temporal variability in detection probability can result from survey conditions (*e.g.*, time of day, day of season, weather, habitat) and intrinsic factors (*e.g.*, grouse age, breeding status). The exploration of relationships between probability of detection and spatially and temporally variable sampling conditions (*e.g.*, environmental conditions, survey protocols) can provide insight into advantageous field protocols that maximize the probability of detecting individuals of a target species (Jakob et al. 2010, Fregmen et al. 2016). When species occur at low densities or are difficult to observe, maximizing detection is important for decreasing necessary survey effort for obtaining accurate estimates in occupancy modeling (MacKenzie and Royle 2005), and is a concept that may also hold true for obtaining relatively precise and unbiased population estimates (Chapter 4).

Probability of detection is affected by both availability and perceptibility (Nichols et al. 2009, Amundson et al. 2014). For an individual to be available for detection, it must be present in the survey area, and either be visible or emit an auditory cue (Nichols et al. 2009). Perceptibility is the probability that an observer detects an individual given that it is available for detection (Nichols et al. 2009, Amundson et al. 2014). Availability for detection during a survey

can be affected by a variety of conditions including time of day, seasonality, weather, and breeding stage, while perceptibility can be impacted by observer ability, habitat, or background noise level. Perceptibility can be improved through training and surveying when background noise level is low (Nichols et al. 2009, Amundson et al. 2014). Availability can be improved through field methods such as electronic playback or by surveying during times or conditions in which individuals are more conspicuous.

Despite their status as a game species, Dusky Grouse (*Dendragapus obscurus*) are under-monitored across most of their range. Dusky Grouse habitat is affected by natural and anthropogenic forces such as timber harvest, beetle-kill, wildfire, and climate change (Bendell and Elliot 1967, Martinka 1972, Pelren and Crawford 1999, Chan-McLeod 2003, Youtz et al. 2022). To effectively manage Dusky Grouse habitat and establish appropriate harvest targets, accurate and precise estimates of population size and trends are needed. Endemic to coniferous and mountainous areas of western North America, Dusky Grouse habitat presents notable challenges for managers conducting surveys, especially under spring conditions in years with heavy snowpack. In addition, low population densities and naturally low probability of detection makes precise abundance estimation difficult and hinders development of feasible and rigorous monitoring programs (Aldrich 1963, Rogers 1963, MacKenzie et al. 2005, Zwickel and Bendell 2004). While little can be done to improve habitat accessibility, increasing the probability of detecting a Dusky Grouse when present can decrease the amount of survey effort required while maintaining our ability to obtain precise population estimates (Chapter 4).

Dusky Grouse perform a breeding display during the spring that makes them more conspicuous and thus easier to detect (Blackford 1958, Bendell and Elliott 1967). Males spread

their tail feathers, inflate their air sacs, conduct flutter flights, and make several distinct calls that include a loud hooting and a much softer repetitive hooting which can be heard up to 100 m (Blackford 1958, Mussehl 1963a, Zwickel and Bendell 2004). Females may respond to displaying males with a cackle or whinny (Blackford 1963, Stirling and Bendell 1966). Consequently, spring counts based largely on displaying males is the most common approach used to monitor populations of Dusky Grouse (Zwickel 1990, Sands and Pope 2010), but the consistency and frequency of a male's breeding display may be influenced by time of season and day, weather, and the presence of females (Mussehl 1960, Stirling and Bendell 1966, Archibald 1976, Hannon 1980, Zimmerman and Gutiérrez 2007, Fregmen et al 2016, Farnsworth 2020). Alternately, summer brood surveys, which can also be affected by weather (Dienes 2022) may be useful for indexing both abundance and productivity. However, the cryptic nature of brood-rearing females often leads to low detectability, small sample sizes, and thus imprecise abundance estimates. (Rogers 1963, Sands and Pope 2010, Hansen et al. 2015).

Field methods such as electronic playback can affect the efficacy of spring and brood surveys by affecting probability of detection. Electronic playback of female grouse calls in the spring or chick distress calls in the summer have improved detection of several grouse species, including Dusky Grouse, by eliciting vocal and visual responses (Stirling and Bendell 1966, Harju 1974, Johnson et al. 1981, Bland 2003, Jakob et al. 2010, Roy et al. 2020). Detectability may also be influenced by placement of point or transect survey locations. For ease of accessibility, grouse surveys are often conducted along roadsides or trails, where sound may transmit farther increasing detection (Yip et al. 2017), increased anthropogenic disturbance may alter grouse availability for detection or increased visibility may affect perceptibility. The effects

of placing point or transect surveys along roadsides and trails on probability of detection is often unevaluated for grouse surveys.

Although previous research indicates significant effects of time, weather, and other environmental conditions on avian detection probabilities (Robbins 1981, Zimmerman and Gutiérrez 2007, Conway and Gibbs 2011, Heward et al. 2019, Morelli et al. 2022), few studies have investigated the correlates of detection probability for Dusky Grouse. Moreover, peak breeding activity varies from late-April through May across the species' distribution (Zwickel and Bendell 2004) affecting timing of both spring and brood surveys, so region-specific information is needed for the development of effective monitoring programs. A high response rate to playback could significantly increase the probability of detection during surveys by increasing availability, but the actual consistency of response may still vary with time of season, day, and environmental conditions. Understanding the efficacy of spring and brood counts, the effects of electronic playback, and which environmental factors cause variation in response to playback can help devise monitoring programs that maximize the probability of detection while minimizing survey effort.

Our goal was to investigate what factors influence detectability of Dusky Grouse in order to recommend field-based survey protocols and optimal survey conditions that maximize the probability of detecting Dusky Grouse for the purpose of developing a population monitoring program. Our objectives were to:

1) identify field-based protocols that result in the highest relative probability of detecting Dusky Grouse, specifically evaluating:

a) the relative performance of spring (May–June) surveys of breeding grouse and summer (June–July) brood surveys for monitoring populations,

b) whether the use of electronic playback of grouse calls increased the probability of detecting a grouse, and

c) the impact of survey site placement on probability of detection (*e.g.*, along roads, trails, or off-trail)

2) identify the conditions when probability of detection is highest, specifically evaluating

a) temporal impacts (*e.g.*, time of breeding season and time of day) and

b) different weather conditions (*i.e.*, precipitation, temperature, cloud cover).

Study area

We conducted Dusky Grouse surveys on public lands (*e.g.*, forest service, state, and BLM) across western Montana during spring-summer 2019 and spring 2020–21 within areas identified previously as suitable for Dusky Grouse (Chapter 2). The study area incorporated mountainous and coniferous habitats ranging from the southern border with Idaho and Wyoming to the Canadian border. The Montana Department of Fish Wildlife and Parks (MFWP) divides Montana into 7 administrative regions and surveys occurred in Regions 1–5 (Chapter 2; Figure. 9). Within this broad area, we used an existing habitat suitability model to delineate areas of potential Dusky Grouse habitat and generate survey locations (Chapter 2; Figure 9). Based on five weather stations across western MT in Kalispell, Missoula, Bozeman, Great Falls, and Red Lodge during 201–2021, average April temperature was 5.6 °C, average minimum temperature was -10.2 °C, and average max temperature was 24.3 °C. The average temperature during the month of May was 10.4 °C, average minimum temperature was -3.8 °C, and average maximum

temperature was 27 °C (United States National Weather Service). Precipitation came in the form of rain or snow with average rainfall 4.8 cm in April and 7.1 cm in May (United States National Weather Service). Average snowfall in April was 25.4 cm and 7.9 cm in May (United States National Weather Service).

Methods

Field Methods

We conducted grouse surveys off-trail during 2019 and on roads and trails during 2020 and 2021, with routes consisting of 5-6 points. The first point for each route was randomly generated using ArcMap 10.3.1. During the 2019 pilot season, the first point was placed 300 m from a road or trail to facilitate accessibility, with subsequent sites placed 500 m apart in a pentagon shape (Figure 10), with the same set of potential routes used during both spring and summer. A pentagon shape ensured that the starting point and ending point were relatively close together in order to decrease time spent surveying and was similar to other avian survey protocols (Farnsworth 2020, Swicegood et al. 2023). Protocols changed from the pilot season to later seasons, and during 2020 and 2021, the first point of a route was placed within 150 m of a trailhead or along a road where the observer would park ≥ 100 m away. Along the road or trail, five subsequent points were spaced 400 m apart to ensure independence for a total of 6 points per route (Figure 10). We used the same set of potential routes for both 2020 and 2021. Trained field biologists (MFWP employees) and volunteers selected among the randomly generated potential routes and conducted point-counts for Dusky Grouse from 10 April–21 May and 17 June–31 July in 2019, and 10 April–1 June during 2020 and 2021.

During the 2019 pilot season, we surveyed each point three times on three different mornings within a 2-week period. Surveys consisted of two 4-minute consecutive point-counts, the first without electronic playback and the second with electronic playback played using a portable mp3 player or smart phone with a portable speaker (SanDisk 8 GB Clip Jam Mp3 Player, JBL Charge 3 speaker). During the spring (April–May) we used electronic playback of a female Dusky Grouse call (cantus, cackle, and whinny) to increase the probability of detecting both male and female Dusky Grouse, and in the summer (June–July) we used a chick distress call to elicit responses from females with broods. Playback recordings consisted of 30 seconds of playback, then 30 seconds of silence, repeated for the entire 4-minute period.

During 2020 and 2021, two point-counts were conducted at each point as the observer traveled from the start to the end of the route, which were located along roads and trails, and then two additional point-counts at each point as the observer traveled from the end to the beginning of the route, allowing four point-counts to be conducted during a single morning. A 10-minute break occurred between the last point between the initial and return visits. Each pair of point-counts was conducted consecutively with ≤ 1 minute between them, and each point-count was treated as a replicate survey visit. During 2020 and 2021, all point-counts were conducted in the spring using electronic playback of female cantus and cackle calls.

During all three years, all Dusky Grouse observations, visual or auditory, were recorded. Observers were trained to keep track of individual birds during a single point-count and to not record the same individual twice. Point count surveys were conducted between dawn and 11:00 on days without precipitation and wind speed <19 km hr^{-1}. Total time needed to complete each

route varied between 3–7 hours. If light precipitation began during the survey, surveys were completed.

We recorded day since surveys started, start time of survey (used to calculate minutes since sunrise), background noise level, and weather conditions at each site for each pair of point-counts. Background noise level, including that from road traffic and streams, was categorized as: 0 = no background noise, 1 = slight background noise, but no auditory impairment, 2 = some background noise and some auditory impairment, and 3 = deafening and total auditory impairment. We recorded average temperature and wind speed using a handheld weather meter (Kestrel model 2000, Kestrel Meters, Boothwyn, PA), cloud cover (0–15% , 16–50%, 51–80% , and 81–100%), and precipitation conditions (fog, rain, snow, or none).

Estimating Probability of Detection

Evaluation of Field-based Survey Protocols. To evaluate the effectiveness of spring (10 April–21 May) versus summer (17 June–31 July) surveys, we compared number of surveys completed, probability of detection of Dusky Grouse, and the frequency of surveys across the sampling period using the 2019 surveys. To estimate probability of detection during each sampling period, we evaluated single-season N-mixture models (Royle 2004) using the *pcount* function in the R package ‘unmarked’ (Fisk and Chandler 2011, R Core Team 2017). We parameterized two models for each sampling period with constant probability of detection and abundance: point-counts without electronic playback and point-counts with electronic playback. We compared the estimates of probability of detection between the two models for each sampling period to evaluate the effects of electronic playback on probability of detection.

We evaluated potential overdispersion in our observation data by evaluating and comparing models with different abundance distributions: Poisson, a negative binomial, and a zero-inflated Poisson (Kéry and Schaub 2012, Kéry and Royle 2016). We evaluated and compared support for models using Akaike's Information Criterion (AIC) to identify the statistical distribution with the most support, which we subsequently used for estimating probability of detection (Burnham and Anderson 2002, Kéry and Schaub 2012).

To compare route types, we estimated probability of detection for spring surveys conducted with electronic playback using single season N-mixture models (Fisk and Chandler 2011, R Core Team 2017). We estimated probability of detection for off-trail surveys (2019 data) separately from the road and trail surveys (2020 and 2021 data) due to differences in protocols. We used route type and year as covariates for modeling probability of detection for the road and trail surveys.

Evaluating Effects of Survey Conditions. To evaluate the impacts of survey day, minutes since sunrise, and weather on probability of detection, we used the data from the spring surveys in 2020 and 2021. We evaluated single-season N-mixture models (Royle 2004) using the *pcount* function in the 'unmarked' package in R (Royle 2004, Kery 2008, Fisk and Chandler 2011, Kery and Schaub 2012, R Core Team 2017). We evaluated our N-mixture models using a Poisson distribution for abundance and examined overdispersion ($\widehat{c}$) using the N-mixture goodness of fit test function, *Nmix.gof.test* (Mazerolle 2020).

We standardized our continuous covariates by subtracting the mean and dividing by the standard deviation calculated over all four visits. We evaluated pairwise correlation among covariates using Pearson's correlation coefficients, considering $|r| > 0.70$ to indicate correlation.

Prior to model fitting, we examined the possibility of nonlinear relationships between probability of detection and two covariates: minutes since sunrise and day of sampling period (Bendell and Elliot 1967, Zwickel and Bendell 2004, Farnsworth 2020). We used univariate models to test for linear and nonlinear (quadratic) relationships, evaluating model support using AIC (Burnham and Anderson 2002). We also hypothesized that day may have an interactive relationship with minutes since sunrise and thus evaluated both additive and interactive models. We again evaluated model support using AIC (Burnham and Anderson 2002).

We then evaluated model support for 12 different *a priori* models based on hypotheses about the impacts of day, minutes since sunrise, weather conditions, and noise level on probability of detection, while parameterizing a constant model that estimated an average abundance for all sites. We included background noise level in all but the null model of detection probability. We included a fully parameterized model for probability of detection as well as combinations of different weather conditions with minutes since sunrise, day, and noise level. We evaluated model support using AIC, and then used the top model to predict the effects of survey conditions on probability of detection (Burnham and Anderson 2002). We also calculated the days and minutes since sunrise that fell in the 90^{th} percentile of their respective probability of detection in order to present a range of ideal survey times and dates.

Results

We surveyed 90 and 110 points during the spring and summer, respectively, during the pilot season in 2019. Most (98%) sites during each sampling period were surveyed three times. The majority (95%) of our Dusky Grouse observations during spring 2019 were auditory. Few Dusky Grouse observations occurred during summer 2019. During 2020 and 2021, we conducted

four visits and recorded covariates at a total of 2,286 unique points, with 837 points (37%) visited during both years, with the result of 3,123 point-count sets of four-counts or a total of 12,492 point-counts. During springs 2020 and 2021, 79% of our Dusky Grouse observations were purely auditory with an additional 10% both auditory and visual.

For the 2019 data, a Poisson distribution was most supported, indicating no overdispersion (Appendix C). For the 2020 and 2021 data, the data also did not appear overdispersed ($\hat{c}$ = 1.4), and therefore, we continued to use a Poisson distribution.

Spring v. Summer Sampling

More points were surveyed during the summer sampling period (110) than during the spring sampling period (90) due to increased accessibility and availability of MFWP wildlife biologists. Survey effort during the spring sampling period was concentrated at the end of the sampling period when accessibility was highest versus in summer when sampling was more evenly distributed (Figure 11). Probability of detecting a Dusky Grouse was much lower in the summer (approximately 0) than in the spring (> 0) with or without the use of electronic playback (Table 6).

Effect of Electronic Playback

The estimated probability of detection was greater when using electronic playback during spring surveys (0.28; 95% CI: 0.13, 0.50) versus when not used (0.09; 95% CI: 0.01, 0.48; Table 6, Figure 12). In summer surveys for both point-counts with and without electronic playback, the estimated probability of detection was similar (0.0002; 95% CI: 0,1 for both). The lack of precision in the confidence intervals of the estimates is a result of having few detections. Only 4 grouse were observed during point counts without playback, and 4 during point counts with

playback, suggesting that the use of electronic playback during the summer surveys did not improve the probability of detecting Dusky Grouse (Table 6).

Comparison of Road, Trail, and Off-trail Point-Count Surveys

The probability of detection was not significantly different across years or survey type (off-trail, road, trail; Table 7, Figure 13). Off-trail in 2019, average probability of detection was 0.28 (95% CI: 0.13–0.50). In 2020 and 2021, probability of detection for both road (p = 0.32, 95% CI: 0.27–0.38, p = 0.38, 95% CI: 0.33–0.43 respectively) and trails (p = 0.42, 95% CI: 0.37–0.48, p = 0.36, 95% CI: 0.32–0.41 respectively) was similar.

Effects of Survey Conditions

When evaluating pairwise correlation, we did not find any of our continuous variables to be correlated ($|r| > 0.70$; Appendix D). Because of our strict sampling protocol, variability in precipitation and wind speed was low, with 90% of the precipitation category classified as none and mean wind speed during surveys measured at 1.42 km/hr (SD = 1.95). Estimated cloud cover across surveys was more variable with 44% of cloud cover classified as 0–15%, 11% classified as 16–50%, 11% classified as 51–80%, and 34% classified as 81–100% cloud cover. Temperature varied from -14.1 to 26.1 with average temperature during surveys measured at 6.8°C. The majority of background noise (77%) was ranked at a 0 or 1. Average minutes since sunrise during surveys was 134 (SD = 72). Average survey date was May 14th (SD = 11). We found that an additive model for minutes and day had more support than an interactive model (Table 8). The top model within our candidate set contained minutes since sunrise, day of

sampling period, noise level, cloud cover, and temperature (Table 9). The top model was followed by the fully parameterized model for probability of detection (Table 9).

Except for when it is the variable of interest, we held temperature, minutes since sunrise, and day during the sampling period at average, cloud cover at 0-15%, and background noise level at 0. After accounting for the other variables, temperature had a positive linear relationship with probability of detecting a Dusky Grouse (β= 0.12, 95% CI: -0.02, 0.25), but the confidence intervals for the estimated beta coefficient overlapped zero indicating some uncertainty in this effect (Table 10, Figure 14). We found that probability of detection was highest on clear days when cloud cover was 0–15% and when background noise level was low (Table 10, Figures 15, 16). For cloud cover we found that probability of detection was greater for 0-15% cloud cover, but then once 0-15% was surpassed there was little difference in probability of detection between the categories (Figure 15). We found strong support for a quadratic relationship between probability of detection and minutes since sunrise β_1= 0.43, 95% CI: 0.04, 0.82, β_2 = -0.75, 95% CI: -1.16, -0.34) and between probability of detection and day of sampling period (β_1 = 1.31, 95% CI: 0.58, 2.04, β_2 = -1.28, 95% CI: -1.99, -0.57; Tables 10, 11, 12). Probability of detection was maximized at 86 minutes past sunrise with our predicted optimal window of time from 9–162 minutes post sunrise (Figure 17). For day of sampling period, probability of detection was maximized on day 34 (May 13th; Figure 18). We estimated the optimal sampling period to be between 3 May–23 May (Figure 18).

Discussion

Our study identifies and evaluates the effects of survey methodology and environmental conditions on the detection probability of Dusky Grouse. We found that electronic playback of

female calls during spring substantially increased the probability of detecting Dusky Grouse. We did not find route type to impact probability of detection. In addition, we found that noise level, cloud cover, temperature, day of survey season, and minutes since sunrise also affect the probability of detecting Dusky Grouse in the presence of electronic playback. Precipitation and wind speed were uninformative covariates, likely because they were already controlled for through survey protocol and therefore there was little variation in these variables.

Although spring and summer surveys have previously been used for monitoring populations of grouse (Sands and Pope 2010), we found that our estimates of probability of detection during the summer were uninformative due to large confidence intervals as a result of few grouse detections, thereby limiting the utility of summer surveys for population monitoring. We used the same survey locations for both spring and summer sampling, and this may have resulted in a mismatch between summer survey locations and brood-rearing habitat potentially resulting in the low probability of detection during summer surveys. Nevertheless, efforts to increase detection probability during the summer by using electronic playback were unsuccessful. These results are contrary to studies that found that chick distress calls often elicit an auditory or visual response from a hen with a brood (Stirling and Bendell 1966, Harju 1974). However, electronic playback of female calls substantially increased the probability of detecting grouse during spring surveys by increasing males calling and conducting flutter-flights and females cackling which is consistent with previous work (Stirling and Bendell 1966, Harju 1974, Farnsworth 2020).

Background noise, the majority of which was the result of river noise or anthropogenic noise (roads, planes, trains) had a strong impact on probability of detection and most likely

affected perceptibility as the majority of our observations were auditory. Consistent with our results, background noise is considered to negatively affect the ability of an observer to hear or detect grouse (Roy et al. 2020, Riley et al. 2021).

Other survey conditions may have affected availability. Cloud cover has had mixed effects on other grouse species, with some responding positively to increased cloud cover while others respond negatively (Evans et al. 2007, Farnsworth 2020). Consistent with previous research, we found Dusky Grouse to respond negatively to increasing cloud cover (Farnsworth 2020). The effect of temperature on breeding displays also varies for gallinaceous species. Eurasian woodcock display behavior increases as minimum temperature increases; for ruffed grouse, initial morning temperature has not been shown to be correlated with probability of detection, although change in temperature during the transect survey has been (Zimmerman and Gutiérrez 2007, Heward et al. 2019). We found that the probability of detecting a Dusky Grouse increased slowly as temperatures increased, but the exact impact of temperature on probability of detection is uncertain given that the confidence intervals for the coefficient estimate slightly overlapped zero. Both wind and precipitation were successfully controlled for within the survey protocol.

In addition to weather, we found probability of detection for Dusky Grouse to be strongly related to date (day of period) and time (minutes since sunrise). Peaks in breeding behavior for both time of day and season are expected when electronic playback is not used. Electronic playback helps increase detection and potentially homogenize detectability across surveys (Jakob et al. 2010). When electronic playback was used in Utah, researchers found a slightly positive linear relationship between probability of detection and date when playback was used versus a

quadratic relationship when electronic playback was not used (Farnsworth 2020). Contrary to those results, we found that when electronic playback was used there was still a quadratic relationship between probability of detection and day. Hypothesizing that probability of detection is positively linked with spikes in breeding behavior, such as breeding display or calls (female cackle, male hooting), we would expect that peak detection also aligns with peak copulation and breeding display behavior. Back calculating from peak hatch date, which varies from the end of May to the beginning of July across Nevada, Colorado, Utah, Montana, and British Columbia, peak breeding behavior of Dusky Grouse has historically occurred from the end of April through the middle of May (Zwickel and Bendell 2004). Historic studies (> 50 years ago) in western Montana in the Bitterroot and Bridger mountains found peak hatch to occur in the third week of June, and peak breeding activity between the last week of April and first week of May (Mussehl 1960, 1963b). We found our preferred survey window to be later than those suggested by past studies in Montana, with our highest detection occurring between May 3–May 23, with a peak on May 13th. Differences in peak breeding activity between studies in Montana > 50 years ago and our current study could be the result of changes in climate and vegetation, inaccuracies in the back-calculating from peak hatch dates to peak copulation, or that peak copulation doesn't perfectly align with peak breeding displaying when electronic playback is used.

In other grouse studies, peak detection occurred at sunrise or slightly before sunrise with and without electronic playback (Bendell and Elliot 1967, Fregmen et al 2016, Farnsworth 2020, Roy et al. 2020). Our study found peak detection to occur 86 minutes, or 1.5 hours past sunrise. While it is possible that the later peak in detection is the result of increased perceptibility due to

increased visibility from increased light, most detections during our surveys were auditory, making this unlikely. It may also be that Dusky Grouse are more responsive to playback during the first part of the morning but may not display unprompted as frequently post-sunrise. We found the ideal survey window to occur between 9 and 162 minutes past sunrise, indicating that there is a broad period of time in which playback surveys may be conducted.

Management Recommendations

Understanding factors that impact probability of detection helps managers develop effective survey protocols that are sustainable for long-term monitoring of Dusky Grouse. While survey routes along roads and trails were more logistically feasible compared to off-trail and type of survey route did not affect probability of detection, impacts of roads on trails on abundance should also be explored before definitive recommendations on route type are made. To maximize probability of detection, we recommend surveying in the spring using electronic playback, during periods of peak breeding display behavior or response to playback, which for Dusky Grouse in Montana occur from 3 May–23 May, from sunrise to approximately 2.5–3 hours post sunrise, and on clear, sunny days with low wind and no precipitation. When incorporating probability of detection into abundance estimates, we recommend modeling detection as a function of day during the sampling period, minutes since sunrise, background noise level, cloud cover, and temperature.

Table 6. Probability of detection for spring and summer sampling periods for point counts conducted with and without electronic playback with 95% confidence intervals.

Period Detected	Spring	Summer
Without playback	0.09 (0.01– 0.48)	0.002 (0–1)
With playback	0.28 (0.13– 0.50)	0.002 (0–1)

Table 7. Estimates of probability of detection with 95% confidence intervals for point counts conducted along different transect types: off trail (2019, n = 90), on roads (2020, n = 845; 2021, n = 744), and trails (2020, n = 803; 2021, n = 731).

Route Type	Year	Estimate	SE	95% Confidence Interval
Road	2020	0.32	0.03	0.27–0.38
Road	2021	0.38	0.03	0.33–0.43
Trail	2020	0.42	0.03	0.37–0.48
Trail	2021	0.36	0.02	0.32–0.41
Off-trail	2019	0.28	0.10	0.13–0.50

Table 8. Model support using AIC for evaluating the relationship between additive verse interactive models for minutes since sunrise and day during the sampling period and the probability of detecting Dusky Grouse.

Models	# Parameters	AIC	delta AIC	Model Weight
Minutes + Days	6	5072.47	0.00	0.92
Days x Minutes	10	5077.29	4.82	0.08

Table 9. Model support for hypothesized relationships between detection and survey conditions. All models are evaluated with constant abundance..

Models	# Parameters	AIC	delta AIC	Model Weight
Minutes + Days + Noise Level + Cloud Cover + Temp	13	4954.56	0.00	0.76
Minutes + Days + Noise Level + Cloud Cover + Temp + Precip[a] + Wind	17	4956.90	2.34	0.24
Minutes + Days + Noise Level	9	4984.02	29.46	0.00
Minutes + Noise Level	7	4991.29	36.73	0.00
Cloud Cover + Noise Level	8	4995.87	41.30	0.00
Days + Noise Level	7	5009.01	54.45	0.00
Wind + Noise Level	6	5016.12	61.56	0.00
Noise Level	5	5017.95	63.39	0.00
Precip[a] + Noise Level	8	5019.02	64.45	0.00
Temp + Noise Level	6	5019.26	64.70	0.00
Null	2	5112.63	158.07	0.00

[a]Precipitation

Table 10. Estimates of coefficients and their 95% confidence interval for standardized covariates from the top model, with constant abundance and survey conditions affecting probability of detection. Reference level for noise level is 0 and for cloud cover is 0-15%.

Survey Condition	Estimate	SE	Lower 95% CI	Upper 95% CI
Int	-0.22	0.09	-0.40	-0.03
Minutes	0.43	0.20	0.04	0.82
Minutes Squared	-0.75	0.21	-1.16	-0.34
Days	1.31	0.37	0.58	2.04
Days Squared	-1.28	0.36	-1.99	-0.57
Temperature (°C)	0.12	0.07	-0.02	0.25
Cloud Cover: 16-50	-0.83	0.19	-1.19	-0.46
Cloud Cover: 51-80	-0.84	0.20	-1.23	-0.45
Cloud Cover: 81-100	-0.47	0.14	-0.74	-0.20
Noise Level: 1	-0.39	0.12	-0.62	-0.16
Noise Level: 2	-1.57	0.20	-1.96	-1.18
Noise Level: 3	-3.04	0.63	-4.27	-1.82

Table 11. Model support using AIC for evaluating linear and quadratic relationships between probability of detection of Dusky Grouse and minutes since sunrise.

Models	# Parameters	AIC	delta AIC	Model Weight
Minutes Quadratic	4	5086.50	0.00	0.98
Minutes Linear	3	5094.62	8.12	0.02

Table 12. Model support using AIC for evaluating linear and quadratic relationships between probability of detection of Dusky Grouse and day during the sampling period

Models	# Parameters	AIC	delta AIC	Model Weight
Days Quadratic	4	5096.55	0	0.9988
Days Linear	3	5110.08	13.52	0.0012

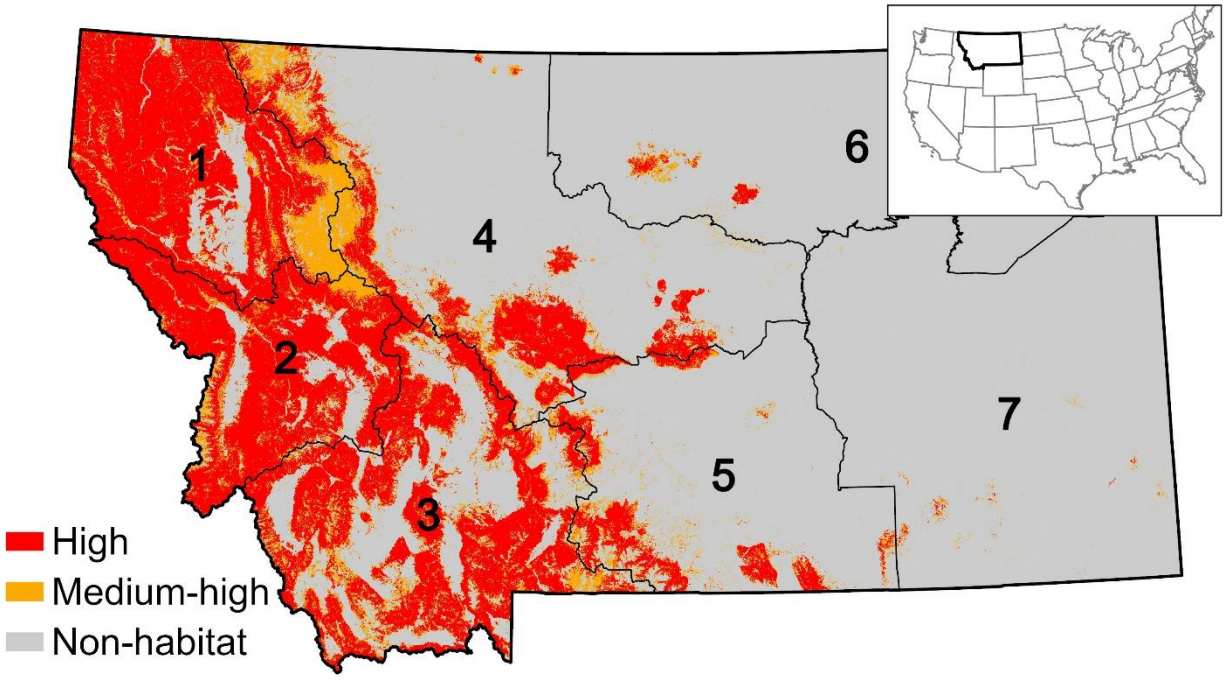

Figure 9. Habitat suitability model for Dusky Grouse habitat in Montana. Areas in orange represent medium-high relative probability of use and areas in red represent high-relative probability of use. Black lines and numbers represent the 7 different MFWP administrative regions.

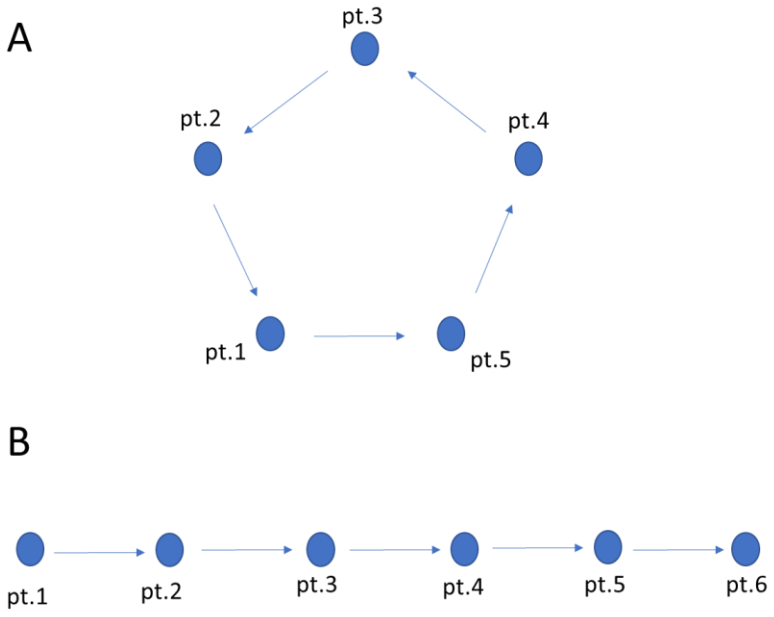

Figure 10. Different route types. (A) pentagon shaped transect used in 2019. (B) line transect with six points used in 2020 and 2021.

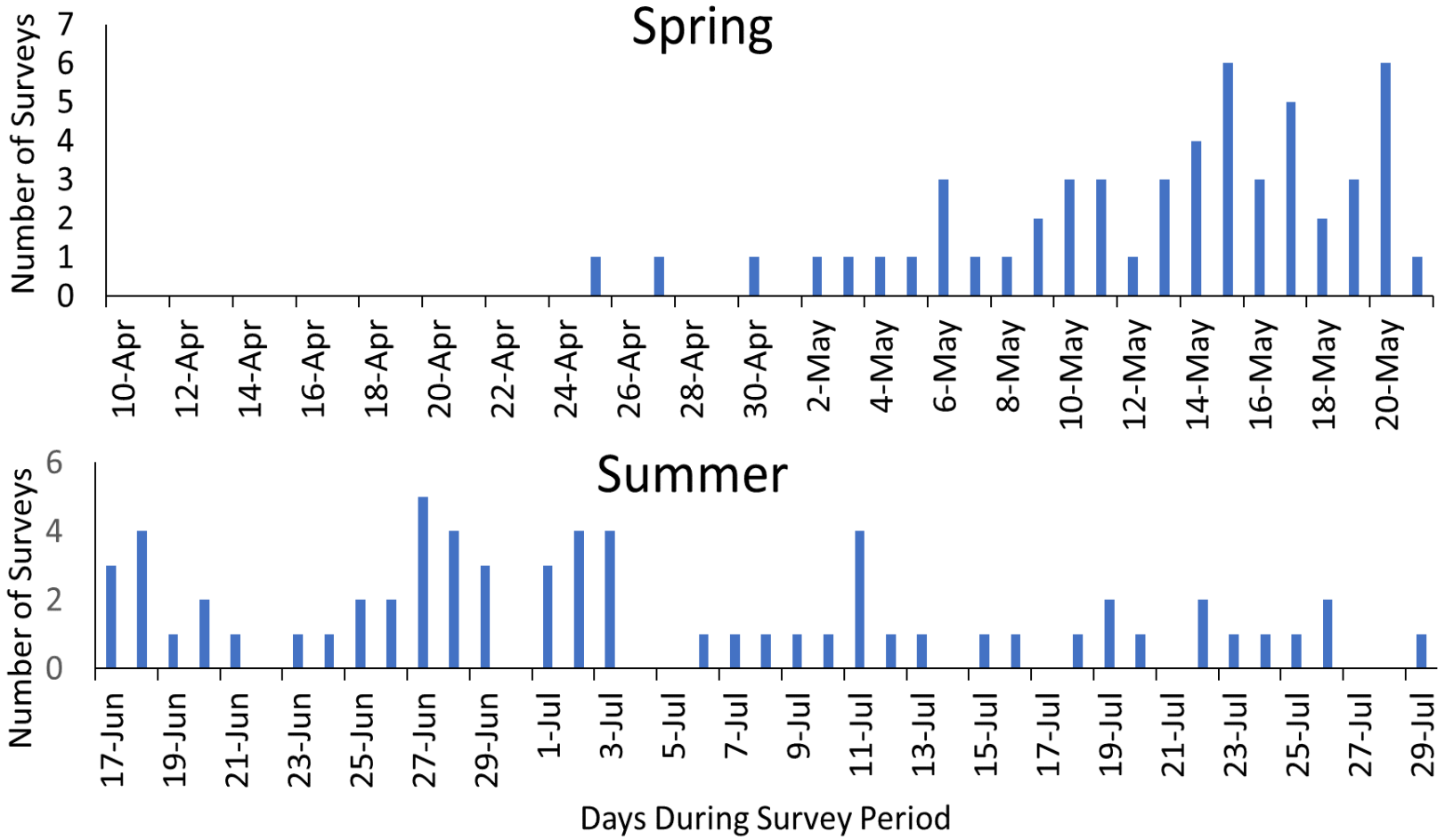

Figure 11. Daily survey effort represented by the number of surveys completed each day for Dusky Grouse surveys conducted in spring and summer 2019.

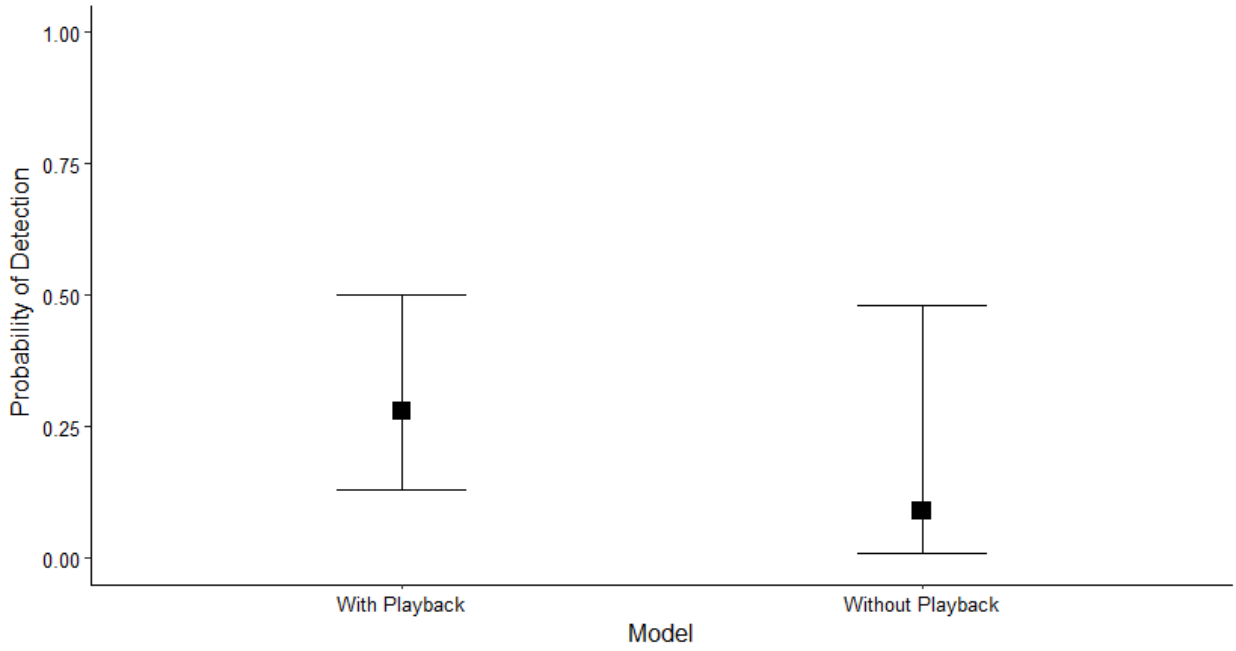

Figure 12. The impacts of electronic playback on probability of detecting a Dusky Grouse with 95% confidence intervals. Data from spring 2019 Dusky Grouse surveys, where female calls were used to elicit male Dusky Grouse responses.

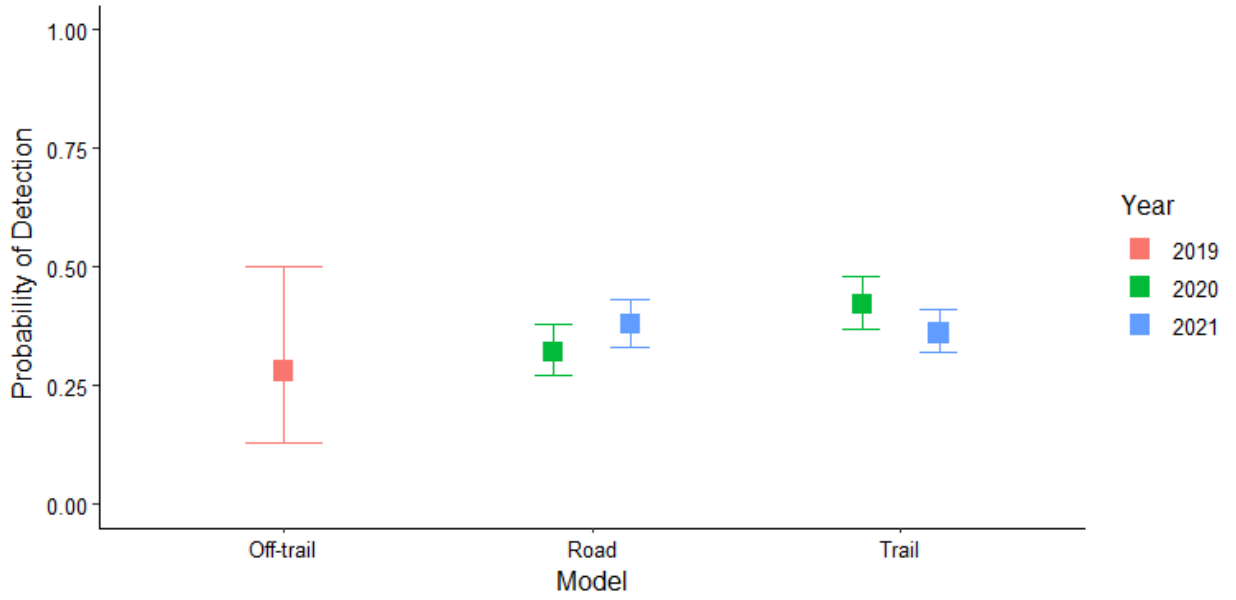

Figure 13. Probability of detection estimates evaluated using single season N-mixture models of Dusky Grouse with 95% confidence intervals for point counts conducted along different route types: off trail (2019, n = 90), on roads (2020, n = 845; 2021, n = 744), and trails (2020, n = 803; 2021, n = 731). Data for the off-trail transects come from the 2019 pilot year surveys conducted

in MFWP region 3. Data for the road and trail transects comes from the 2020 and 2021 surveys conducted across western Montana.

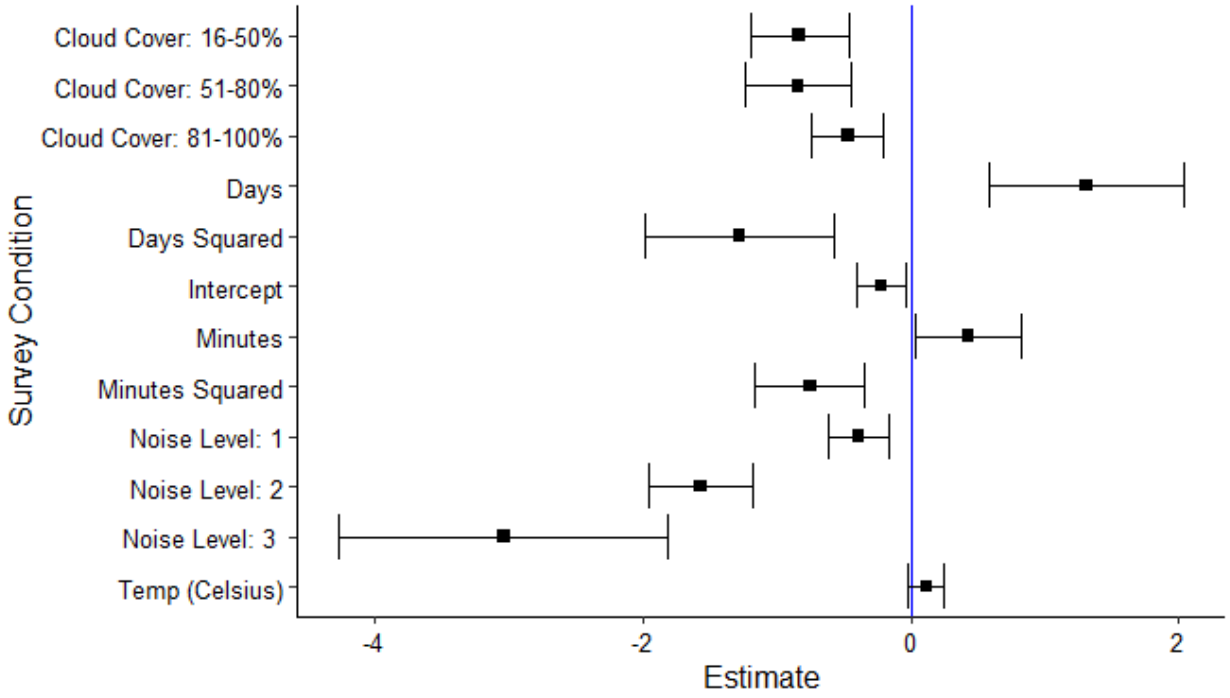

Figure 14. Coefficients of standardized survey conditions with 95% confidence intervals, where survey conditions affected probability of detection and abundance was held constant. Days = day during the sampling period, Minutes = minutes since sunrise. The reference level for cloud cover is 0-15%, and for noise level is 0.

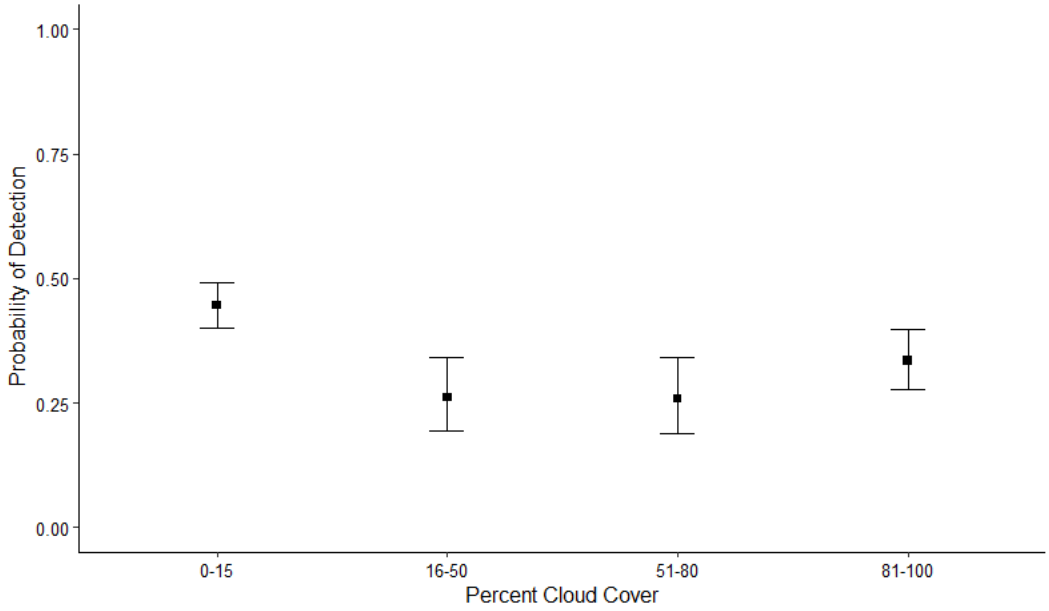

Figure 15. Estimated probability of detection for different cloud cover categories: 0-15% cloud cover, 16-50% cloud cover, 51-80% cloud cover, while minutes since sunrise, day during the sampling period, and temperature were held at average, and background noise was 0.

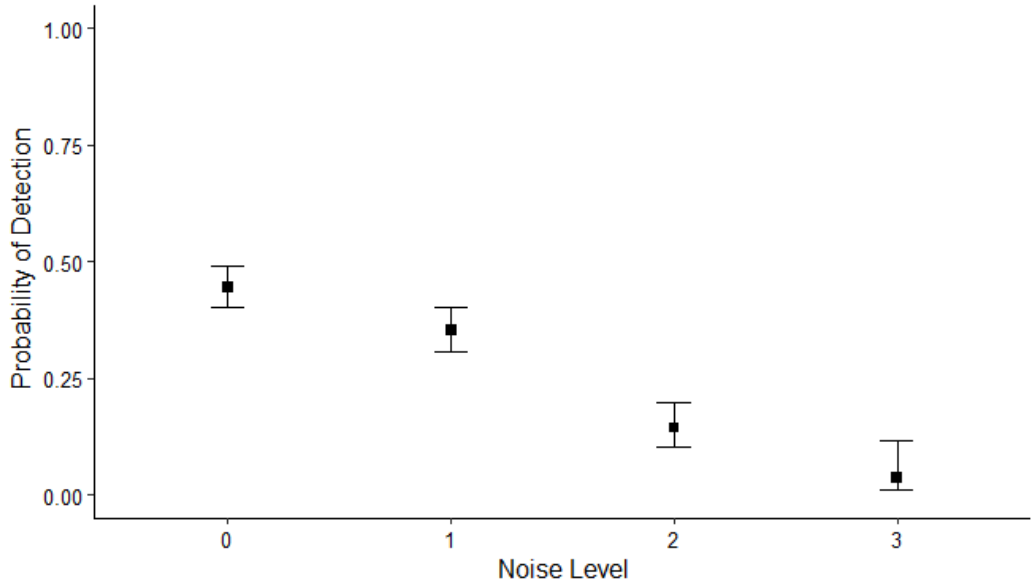

Figure 16. Estimated probability of detection for different noise level categories: 0 = no background noise, 1 = slight background noise, but no auditory impairment, 2 = some background noise and some auditory impairment, and 3 = deafening and total auditory

impairment. Minutes since sunrise, day during the sampling period, temperature were held at average, and cloud cover was held at 0-15%.

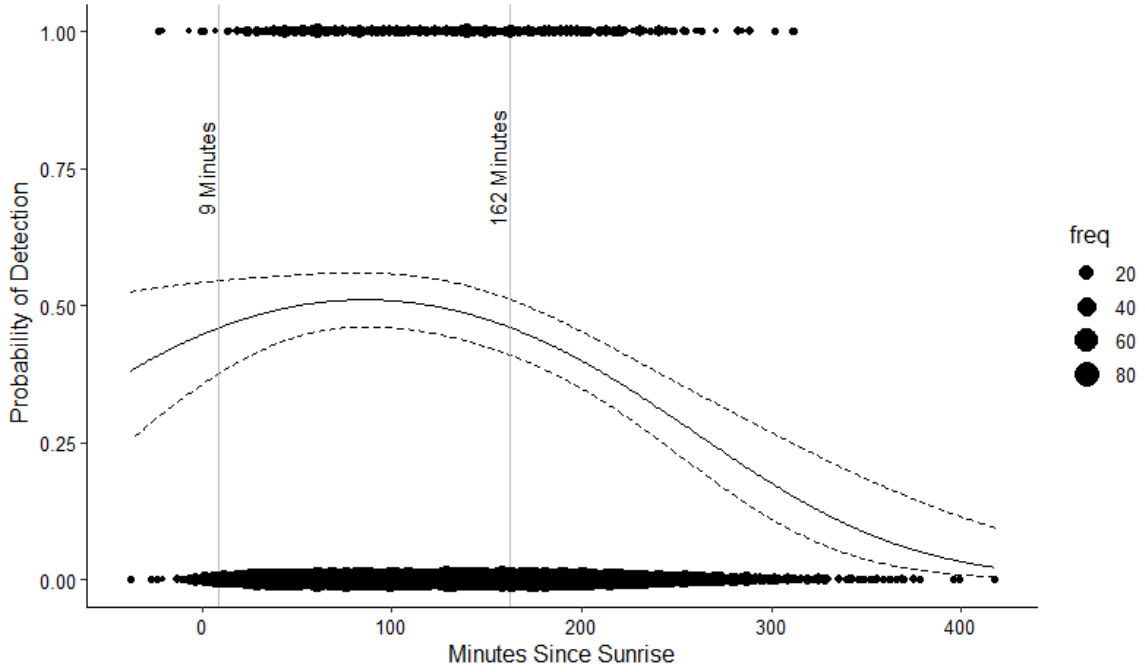

Figure 17. Estimated probability of detection for minutes since sunrise while day during the sampling period and temperature are held at average. Cloud cover is held at 0-15%, and background noise is held at 0.

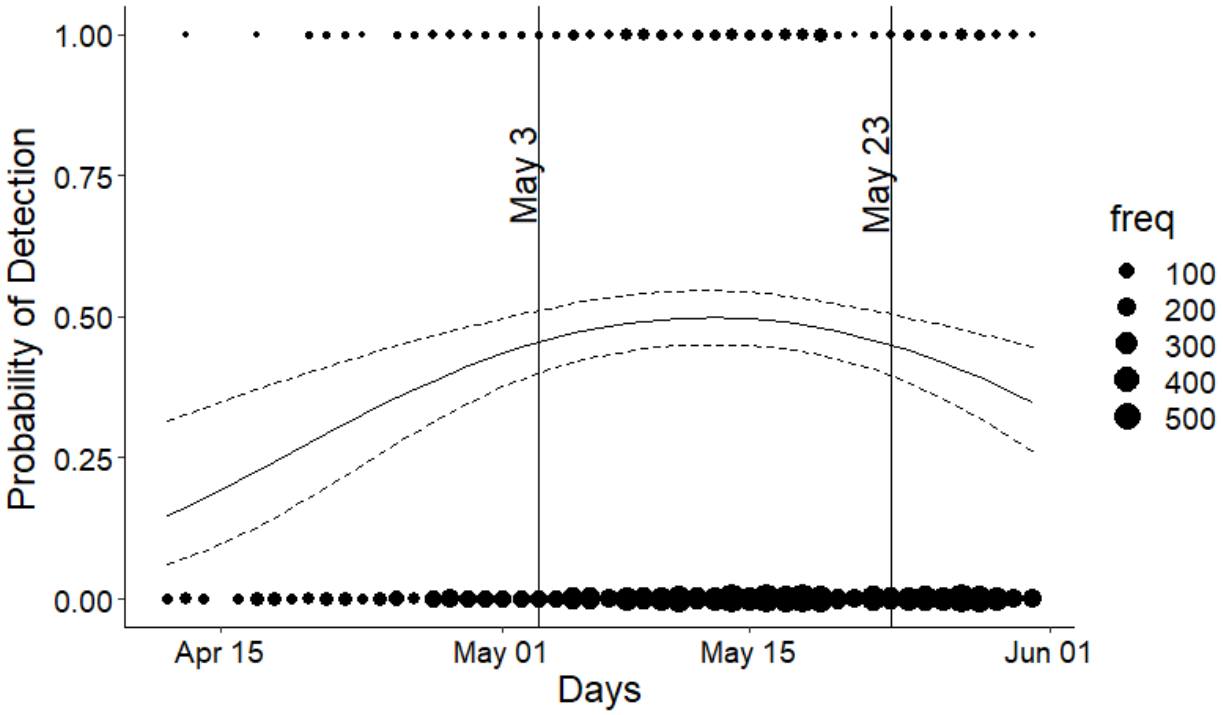

Figure 18. Estimated probability of detection for day during the sampling period while minutes from sunrise, and temperature are held at average. Cloud cover is held at 0-15%, and background noise level is held at 0. Maximum probability of detection is on day May 13th.

CHAPTER FOUR

DEVELOPING A MONITORING PROGRAM FOR DUSKY GROUSE IN MONTANA: EVALUATING METHODS FOR PRODUCING UNBIASED POPULATION INDICES

Contribution of Authors and Co-Authors

Manuscript in Chapter 2

Author: Elizabeth Leipold

Contributions: Conceptualization, data curation, formal analysis, investigation, methodology, validation, and writing

Co-Author: Claire Gower

Contributions: Conceptualization, writing review and editing

Co-Author: Lance B. McNew

Contributions: Conceptualization, methodology, supervision, validation, writing review and editing

Manuscript Information

Elizabeth Leipold, Lance McNew

Status of Manuscript:
☒ Prepared for submission to a peer-reviewed journal
☐ Officially submitted to a peer-reviewed journal
☐ Accepted by a peer-reviewed journal
☐ Published in a peer-reviewed journal

Introduction

Unbiased and precise estimates of abundance are crucial for effective conservation, management, and understanding ecological relationships (Joseph et al. 2009, Weiser et al. 2019, Neubauer and Sikora 2020). Estimates of abundance are used to define conservation priorities, assess whether population objectives are being met and evaluate the impact of management actions (Weist et al. 2019, Doser et al. 2021). Without accurate estimates, limited resources can be used inefficiently, and managers may be unable to identify population declines in a timely manner (Sillett et al. 2012). Population monitoring is especially important for game species where changes in abundance may impact hunting quotas and other aspects of species' management (Jakob et al. 2014). Given high costs and the large amount of effort needed to obtain long-term data on abundance, it is important that monitoring programs are well planned and able to make efficient use of limited resources while still achieving target goals (Weiser et al. 2019, Anderson and Steidl 2019, Kidwai et al. 2019).

Dusky Grouse (*Dendragapus obscurus*) are an under-monitored upland game species found in coniferous and mountainous areas of western North America from New Mexico to central Yukon (Aldrich 1963, Zwickel and Bendell 2004). Despite their status as a game species and concerns over the potential influences of environmental disturbances (*e.g.*, logging, wildfire, beetle infestations) on Dusky Grouse habitat, populations are poorly or inconsistently monitored across their range (Bendell and Elliot 1967, Martinka 1972, Pelren and Crawford 1999, Chan-McLeod 2003, Youtz et al. 2022). Current standardized multispecies avian surveys (*e.g.*, Breeding Bird Survey) are inadequate for monitoring Dusky Grouse because their survey protocols do not yield sufficient Dusky Grouse observations to produce precise and unbiased

estimates of populations trends (Sauer et al. 2020). Dusky Grouse occur in remote and often difficult to access habitats, have low population densities, and low detection rates which has made population monitoring inherently difficult (Rogers 1963) and may limit potential survey and analytical methodologies.

To date, population monitoring of Dusky Grouse has been based on either 1) count-based surveys during the spring breeding season, 2) brood counts during the summer, or 3) reported hunter harvests in the fall (Rogers 1963, Bernales et al. 2017, Espinosa et al. 2018, Gates 2019, New Mexico Department of Game and Fish 2020). Site placement along roads is common for spring and brood counts but may also result in biased estimates due to non-random placement of survey sites, roadside habitat being more representative of edge habitat than interior or non-roadside habitat, and greater anthropogenic disturbance (Rogers 1963, Hanowski and Niemi 1995, Betts et al. 2006, Buckland et al. 2008, Sands and Pope 2010). Recent research has shown that spring surveys using electronic playback to increase detection are most effective for detecting Dusky Grouse (Chapter 3), but quantitative assessments of the performance of survey protocols (route type, number of sites and visits) and analytical approaches for monitoring Dusky Grouse are lacking and are needed to inform best management practices for Dusky Grouse population monitoring.

Count-based surveys of grouse may provide an unbiased index of relative population size across time and space in the presence of random sampling, consistent observation error across time and space, and if counts are positively correlated with abundance. (Pollock et al. 2002, Rosenstock et al. 2002). As it is unlikely that detection error is constant across space or time, it is important to measure this error to adjust estimates of abundance; otherwise observed changes in

counts may be the result of changes in probability of detection, changes in abundance, or both (Rosenstock et al. 2002, Farnsworth et al. 2005). The expansion of analytical models that estimate and incorporate the probability of detection (*p*) into abundance estimation with unmarked animals has advanced population monitoring programs for black grouse (*Lyrurus tetrix*), red grouse (*Lagopus lagopus scoticus*), red-legged partridge (*Alectoris rufa*), rock ptarmigan (*Lagopus muta*), and sage grouse (*Centrocercus urophasianus*; Warren and Baines 2011, Franceschi et al. 2014, Jakob et al. 2014, McCaffery et al. 2016) and shows promise for the monitoring of Dusky Grouse.

Two classes of hierarchical models that can be used to obtain unbiased estimates of abundance of unmarked grouse include, 1) those that estimate detection probabilities through repeated counts during a period of population closure, and 2) those that adjust counts based on estimated distance-decay functions in detection probability (Kéry and Royle 2016). Of the first type, N-mixture models (aka binomial-Poisson mixture models) are a class of hierarchical models that use simple counts replicated spatially and temporally within a period of closure to estimate probability of detection (*p*) and abundance (Royle 2004, Kéry and Royle 2016). The simplicity and relative inexpense of count-based survey protocols needed for this model implies utility over large spatial and temporal scales consistent with statewide and regional application (Kéry and Royle 2016). Additionally, N-mixture models allow for the inclusion of spatial and temporal covariates to evaluate questions related to 1) survey protocol effects on detection probabilities, 2) site-specific effects of habitat conditions or treatments on local abundance, and 3) spatio-temporal effects of climate and management on population size and trajectories (Romano et al. 2017, Katayama et al. 2020, Dinkins et al. 2021) even when data is sparse,

contains many zeros, and when detection probability is low (Yamaura 2013, McCaffery et al. 2016).

Like all statistical models, N-mixture models have critical assumptions that must not be severely violated to ensure the estimator remains unbiased: 1) counts occur within a period of population closure, 2) all observation errors are negative; no false positives, 3) detection probability is constant for all individuals within a site during a survey, 4) individuals are detected independently of other individuals, and 5) the distributions of abundance and detection probability are adequately described by their chosen parametric distribution (Kéry and Schaub 2012, Kéry and Royle 2016). Estimates of abundance can be extremely sensitive to violations of model assumptions (Barker et al. 2018, Duarte et al. 2018, Knape et al. 2018, Link et al. 2018). Nevertheless, N-mixture models yield accurate estimates abundance when assumptions are reasonable (Basile et al. 2016, Kéry 2018, Ficetola et al. 2018, Duarte et al. 2018).

A second class of abundance models uses measured observation distances, rather than repeat surveys, to estimate *p*. Distance sampling models are based on the idea that the probability of detecting an individual decreases with increasing distance from the observer and that the chosen distance-decay detection function can be used to estimate the proportion of individuals unidentified during a survey (Buckland et al. 2001, Rosenstock et al. 2002, Buckland et al. 2015). Recent extensions of the distance sampling model (*e.g.*, hierarchical distance sampling) allow models to incorporate covariates for abundance and detection and accommodate temporary emigration (*e.g.*, availability to be detected; Kéry and Royle 2016). Hierarchical distance sampling (HDS) has been used to estimate density, model relationships between density and habitat associations, and explore relationships between detection and habitat associations and

survey conditions for a variety of species including butterflies, endangered bumblebees, lizards, songbirds, and game birds (Hamm 2013, Furnas et al. 2019, Sullins et al. 2019, McNeil et al. 2019, Reidy et al. 2021, Lewis et al. 2022). Some extensions of hierarchical distance sampling require additional visits for the estimation of availability/temporary emigration, but to incorporate covariates for abundance and detection, only one visit is required (Royle and Kéry 2016). This is an advantage over N-mixture models where multiple visits are needed (Royle and Kéry 2016). On the other hand, the data required for N-mixture models is less intensive as it does not require accurately measuring distances to individuals which can be difficult for auditory signals (Scott et al. 1981, Simons et al. 2007, Buckland et al. 2015). In addition, distance sampling requires that a minimum of 60-100 detections at a variety of distances are obtained for estimating the distance-decay function, which may decrease their utility in the face of low detection or abundance (Buckland et al. 2001, Rosenstock 2002, Rusk et al. 2007, Franceschi et al. 2014).

Distance sampling also produces unbiased estimates if assumptions are reasonable. The assumptions of distance sampling are 1) animals are distributed uniformly in space and independently of the transects or point locations on which the observations are made, 2) probability of detection is a function of distance and detection is perfect at a distance of zero, 3) individuals are detected at their original locations, and 4) distances are measured without error (Buckland et al. 2001, Thomas et al. 2010, Buckland et al. 2015, Kery and Royle 2016).

Expanding on hierarchical distance sampling and time removal is a new model: hierarchical distance sampling with time removal (hereafter time-removal HDS). Time-removal HDS, allows hierarchical distance sampling to incorporate temporary emigration without

needing multiple visits by using time removal to estimate availability. Distance sampling alone without repeated visits is only able to estimate perceptibility (probability of detection given availability). If availability is not estimated, assumptions for distance sampling may be violated, resulting in biased abundance estimates (Amundson et al. 2014). Time removal models by themselves are only able to estimate availability and perceptibility combined and are unable to separate the two processes (Farnsworth et al. 2002, Nichols et al. 2009). Time-removal HDS allows the separate estimation of availability and perceptibility and is able to incorporate covariates for both components of detection, as well as covariates for abundance. Model assumptions include those for distance sampling as well as 1) individuals are identified correctly in reference to species and no double counting, 2) availability and perceptibility are independent, 3) surveys occur within a period of closure, and 4) all individuals within a population are present at a site during the survey so that probability of presence equals 1 (Nichols et al. 2009, Amundson et al. 2014). Similar to the other presented models, time-removal HDS also produces unbiased estimates if assumptions are reasonable.

An effective population monitoring program must 1) have a clear goal and specific objectives, 2) provide precise and unbiased estimates or indices of population size or trends, 3) sufficient statistical power to achieve objectives, 4) be implementable and achievable, and 5) be able to quickly provide clear and understandable results to the intended audience (Gibbs et al. 1999, Pollock et al. 2002, Witmer 2005). A clear objective must encompass the purpose of the monitoring program, how the results will be used, what parameters will be estimated, and the level of accuracy and precision desired (Pollock et al. 2002, Witmer 2005). Survey designs, sampling methods, and statistical analyses need to be evaluated for their ability to work with the

species' ecology, adjust for imperfect detection, account for spatial variation in abundance, and produce unbiased and precise estimates of abundance (Pollock et al. 2002, Witmer 2005). The chosen survey protocol and analytical method should be evaluated using a power analysis and then reevaluated as more data becomes available to ensure that recommended methods are able to meet the objectives (Gibbs et al. 1999). The feasibility of a monitoring program must also be considered with regard to number of personnel, cost, accessibility of survey sites, and survey effort (*i.e.*, number of sites and visits required). The outcome of the monitoring program should be easily interpretable by conservationists and managers.

Based on discussions with wildlife managers at Montana Department of Fish, Wildlife, and Parks, our goal was to design and implement a population monitoring program for Dusky Grouse that yields unbiased and precise estimates of annual abundance with a coefficient of variation (CV) of ≤ 15% and allows wildlife managers to detect biologically meaningful changes in population size over timeframes relative to management. We addressed this goal through the following sequential objectives:

1. Use simulations to identify appropriate field survey protocols (number of sites and visits) for evaluating effects of route type on abundance and obtaining accurate baseline estimates of abundance for Montana,
2. Compare abundance estimates from off-trail, trail, and road-based point counts,
3. Use field survey data and simulations to evaluate the relative performance, measured through bias and precision under varying levels of survey effort, of N-mixture, hierarchical distance sampling, hierarchical distance sampling with time removal and naïve models unadjusted for imperfect detection. We sought to identify the analytical

approach that produced unbiased (*i.e.*, near the truth) and precise (≤15% coefficient of variation) indices of population size with the least amount of required survey effort, and

4. Conduct a power analysis to evaluate whether the final protocol recommended by the simulations was sufficient for accurately estimating population trends in order to identify potential declines in populations of Dusky Grouse.

Our approach was to 1) conduct two initial sets of simulations to identify the most appropriate field survey protocols, 2) compare the impact of placing points off-trail, on trails, or roads on abundance, 3) use field data to provide empirical estimates of abundance and detection that will determine the scenarios under which different protocol simulations would occur, and 4) conduct simulations with multiple statistical estimators under different scenarios to estimate the number of sites and visits needed to obtain unbiased and reasonably precise estimates of abundance.

Study Area

Our study occurred over three years (2019–2021) throughout western Montana in areas predicted to be Dusky Grouse habitat by a habitat suitability model developed based on spring locations (Chapter 2, Figure 9). Predicted Dusky Grouse habitat was dominated by coniferous and mountainous forests in west-central and western portions of the state. The Montana Department of Fish, Wildlife, and Parks (MFWP) divides the state into 7 administrative regions; Regions 1–3 occur in western Montana, Regions 4–5 in central Montana, and Regions 6–7 in eastern Montana (Figure 9). The majority (99%) of Dusky Grouse habitat occurs in MFWP Regions 1–5. During the pilot year (2019), we restricted grouse surveys to MFWP Region 3. In

2020–2021, we expanded the study area to include all Dusky Grouse habitat in MFWP Regions 1–5.

Methods

Field-based Surveys

Field biologists and volunteers specifically trained to conduct Dusky Grouse surveys selected among a randomly generated set of potential line-point transects consisting of 5–6 points based on their accessibility. The first points of the transects were randomly generated using ArcMap 10.3.1 across public land (mainly U.S. Forest Service lands) in areas predicted to be Dusky Grouse habitat (Figure 9). During the 2019 pilot season, surveys consisted of off-trail transects with 5 points placed 500 m apart in a pentagon shape with the first point located 300-m from a road or trail. Surveys in 2020 and 2021 occurred along roads and trails with the first point randomly generated and the subsequent locations placed ≥ 400 m apart (Figure 10). The same set of generated site locations were used in 2020 and 2021. Surveys were conducted during 10 April–21 May in 2019 and 10 April–1 June in 2020 and 2021.

During our pilot season in 2019, we surveyed each site during 3 mornings within a 2-week period. We recorded then number and locations of all Dusky Grouse, ruffed grouse (*Bonasa umbellus*), and spruce grouse (*Canachites canadensis*), collectively referred to as ‘mountain grouse’, while walking between points and during each point-count. Care was taken to not double count grouse. Grouse detected during the line-transect and during a point-count were recorded independently for each method. Point-count surveys consisted of two four-minute point-counts conducted consecutively. The first point-count was conducted without electronic playback of female calls (cantus, whinny, and cackle) and the second point-count was conducted

with playback (SanDisk 8 GB Clip Jam Mp3 Player, JBL Charge 3 speaker). Playback recordings consisted of alternating 30 seconds of calling and 30 seconds of silence until the entire four minutes of the survey had elapsed. For each detection, the distance to each grouse, vocalization, behavior, and sex (if known) was recorded, with distance to grouse measured to the nearest meter with a laser rangefinder. For auditory detections, the location of a grouse was narrowed to a specific area and then distance to that area was measured. To control for measurement error in exact distance for auditory detections, we placed distances into four bins: 0–25 m, 26–50 m, 51–75 m, and 76–100 m. In addition, for use with removal models, for point-counts we also recorded the minute of the survey in which the detection occurred.

In 2020 and 2021, we expanded our survey efforts to all of western Montana (MFWP Regions 1–5), moving transects from off-trail to on roads and trails for logistical reasons. Field biologists and volunteers continued to select survey sites from the randomly generated transects based off accessibility. Surveys were only conducted using electronic playback of the female call edited to only include cantus and cackle. Surveys consisted of a total of four four-minute point-counts at each point located along a transect, each of which was treated as an independent sample and all grouse observed were recorded during each period. Two of the four independent point-counts occurred as the observer traveled from the start to end of the transect, then a 10-minute break occurred, and two additional point-counts occurred as observers traveled from end to the beginning of the transect. Each pair of point-counts was conducted consecutively with ≤ 1 minute between them, yielding a total of four point-counts per point in one morning. Placing repeat visits close in time allowed us to meet the primary assumption of N-mixture models that

surveys are conducted within a period of population closure while allowing transects to only be visited once.

We recorded survey conditions during each point-count including day since the sampling period started, minutes from sunrise, temperature, wind speed, precipitation, cloud cover, and noise level. Day of the season on which surveys occurred was calculated relative to a start day of 10 April (day 1). To determine the time of sunrise, we associated each site with a city within each MFWP Region. We measured temperature (°C) and wind speed (km/hr) using a hand-held weather meter (Kestrel model 2000, Kestrel Meters, Boothwyn, PA). Precipitation, cloud cover and noise level were divided into four categories. Precipitation was classified as none, rain, snow, and fog. Cloud cover was classified as 0–15%, 16–50%, 51–80%, and 81–100% of the sky covered. Noise level was classified as none (0), slight background noise but no hearing impairment (1), moderate background noise and some hearing impairment (2), and deafening background noise and total hearing impairment (3).

Simulations to Inform Field Survey Protocols

2019 Pilot Season Protocols. To evaluate potential protocols for the 2019 pilot season, we conducted a series of 16 simulation scenarios, and analyzed the simulated data using single-season N-mixture models in a Bayesian framework (see Appendix E for a general description of the simulations and model in the BUGS language; Thomas 2006). N-mixture models are composed of two linked sub-models where the variation in local abundance is described with a Poisson distribution (ecological process), and the variation in counts is described by a binomial random process (observation process):

$$N_i \sim Poisson(\lambda) \qquad \text{Equation 1}$$

$$y_{i,j}|N_i \sim Binomial(N_i, p),$$

where N_i is the true abundance at site i, $y_{i,j}$ is the observed count at site i during replicate survey j and p is the probability of detecting a grouse during a survey (Royle 2004, Kéry and Schaub 2012, Kéry and Royle 2016). Priors for the model consisted of standard vague priors: a gamma distribution (0.005, 0.005) for lambda and a uniform distribution (0,1) for probability of detection (Kery and Schaub 2012).

For our simulation scenarios, we varied the number of independent survey sites (50, 100, 200, and 500) and number of visits (2–3), simulating data under two mean local abundance scenarios using a Poisson distribution and a binomial distribution with a constant probability of detection. Our abundance and detection scenarios were informed by preliminary work in northeastern Utah that indicated that average Dusky Grouse abundance in good to excellent habitat in Utah ranged from 0.625 to 1.25 grouse per survey site and that detection probability during a survey was similar across sites and averaged 0.5 (D. Dahlgren, Utah State University, personal communication). We sampled abundance from a Poisson distribution and simulated observations of grouse at each site during each survey by drawing randomly from a binomial distribution, where probability of detection (p) had a mean of 0.5. We used the R2WinBugs package to call WinBugs in R to analyze our simulated datasets and used standard vague priors previously described for all hyper-parameters that provided little or no information about the estimated parameters (Appendix E; Sturtz et al. 2005, Kellner 2019, R Core Team 2017, Kéry and Schaub 2012, Kéry and Royle 2016). We ran three chains of length 40,000 after a burn-in period of 10,000 and thinned the posterior chains by 100 to ensure independence. We assessed convergence visually using traceplots and by using the Gelman-Rubin ($\hat{R}$) statistic, which

examines the variance ratio of the Markov chain Monte Carlo (MCMC) algorithm within and between chains across iterations (Gelman and Rubin 1992). We accepted parameter estimates when they came from Markov chains with $\hat{R}$ between 1.0 and 1.01.

We estimated and quantified bias for mean local abundance (λ), local abundance ($\widehat{N}_i$) per site, total abundance $\widehat{N}$ estimated as $\sum \widehat{N}_i$, and probability of detection (p). To quantify bias for each estimate, we ran 400 iterations of each data simulation and analysis for each survey protocol scenario and calculated the difference between the estimated parameter and true parameter value. We compared the posterior distributions of the mean differences between each estimate and the true values across all 400 simulations and considered an estimate to be clearly biased if the 90% credible interval (CrI) of the differences did not include 0. At each of the iterations we calculated the coefficient of variation $\left(\text{CV} = \frac{estimated\ standard\ deviation}{mean\ parameter\ estimate}\right)$ for total abundance, evaluating the posterior distributions of the 400 derived CV estimates. We estimated the probability that the average coefficient of variation would meet the manager-determined threshold of ≤ 15% by calculating the proportion of the total posterior distribution density greater than 0.15. We considered protocols that resulted in a CV ≤ 15%, 90% of the time to be acceptable for meeting the objective of the monitoring program.

2020 and 2021 Season Protocols. We updated our survey protocols for 2020 and 2021 using empirical estimates of abundance and detection from our 2019 pilot season data for our simulation scenarios. Overall, we conducted a series of 13 simulations analyzed again using single-season N-mixture models in a Bayesian framework using jags (Plummer 2003). Our simulation approach was like that of the previous simulations.

We analyzed data from the point-counts conducted with electronic playback using single-season N-mixture models (*pcount* function, which is the same model structure described above) with the 'unmarked' package in R (Fisk and Chandler 2011, Kery and Royle 2016, R Core Team 2017). We estimated local abundance and probability of detection by specifying a model with constant detection and abundance (Equation 1). We evaluated potential overdispersion in our observation data by evaluating and comparing N-mixture models with different abundance distributions: Poisson, a negative binomial, and a zero-inflated (Kéry and Schaub 2012, Kéry and Royle 2016). We evaluated and compared support for models using Akaike's Information Criterion (AIC) to identify the statistical distribution with the most support, which we subsequently used for estimating local abundance and probability of detection (Burnham and Anderson 2002, Kéry and Schaub 2012).

We evaluated the efficacy of our pilot season survey methods (3 replicated visits at 100 independent survey sites located off trail) using the empirical estimates of abundance (0.36, 95% CI: 0.18, 0.73) and p (0.28, 95% CI: 0.13, 0.50). After examining the results of simulations using the 2019 survey protocol, we evaluated whether estimator precision could be increased by 1) increasing the number of replicate survey visits per point, and 2) increasing numbers of independent survey points. We evaluated simulated datasets based on 100 independent survey points with increasing numbers of replicate visits and then increasing number of survey points with three replicate visits. Next, we kept the number of visits at 4 and varied the number of survey points from 200–360. To examine the feasibility of the potential protocols that yield relatively precise results, we calculated how many survey mornings would be needed if survey transects included 5 or 6 points per transect, and 3 or 4 replicates occurred in one morning.

Effects of Route Type on Abundance

To compare route types (off-trail, trail, and road) for the point-count surveys, we estimated local abundance for spring point-counts conducted using electronic playback using single season N-mixture models evaluated using the pcount function in the R package 'unmarked' (Fisk and Chandler 2011, R Core Team 2017). Given differences in protocol between 2019 and 2020–2021, we estimated abundance for off-trail point counts (equation 1) separately from trail and road point counts (equation 2). We estimated abundance for trail and road point counts by modeling abundance using a log-linear function to account for the effects route type (trail, road) and survey year (2020, 2021):

$$N_i \sim Poisson(\lambda_i) \qquad \text{Equation 2}$$

$$y_{i,j}|N_i \sim Binomial(N_i, p)$$

$$\log(\lambda_i) = \alpha_0 + \alpha_1 * x_{1i} + \alpha_2 * x_{2i}$$

where α_0 is the intercept, α_1 and α_2 correspond to slopes for each covariate (x) , x_{1i} represents route type and x_{2i} represents survey year (Kery and Schaub 2012).

Empirical Estimates of Abundance and Detection to Inform Simulation Scenarios

To evaluate survey effort required to achieve annual estimates of Dusky Grouse abundance with a coefficient of variation of ≤ 15% from point-count and transect survey protocols, we first developed and modeled simulated datasets based on empirical estimates of abundance and detection probabilities from our 2020 and 2021 spring survey effort for N-mixture, hierarchical distance sampling, time-removal HDS, and naïve (raw counts) models. To obtain baseline estimates of local abundance state-wide and within MFWP Regions 1–5, we evaluated the point-count data with single-season N-mixture models (*pcount* function) and HDS

models (*distsamp* function) using the R package 'unmarked' (Fisk and Chandler 2011, Kéry and Schaub 2012, Kéry and Royle 2016). We used a multinomial-Poisson mixture model for the HDS model:

$$N_s \sim Poisson(\lambda_s) \quad \text{Equation 3}$$

$$\log(\lambda_s) = \beta_0 + \beta_1 * x_s$$

$$y_{sh} \sim Multinomial(N_s, \pi_s),$$

where N_s represents the true abundance at site *s*, and a log linear model can be used to model the effect of a covariate (*e.g.* MFWP Region) on expected abundance, λ_s, where β_0 is the intercept, β_1 is the slope, and x_s is the covariate. The observed count of individuals for each site, *s*, in each distance class, *h*, is y_{sh}, and π_{sh} represents the multinomial cell probability for site *s* and distance class *h* (Royle et al. 2004, Kéry and Royle 2016). The multinomial cell probabilities depend on the detection-function parameter sigma, σ, used with the half-normal detection-decay function. We evaluated models where detection was constant and local abundance was constant to obtain average state-wide estimates of abundance. To obtain regional local abundance estimates we evaluated models where detection was constant and abundance varied by MFWP administrative region. To model variation in local abundance, we used a log-linear model for both the N-mixture model (equation 2) and hierarchical distance sampling model (equation 3; Kéry and Royle 2016).

We used a Poisson distribution for our N-mixture models and examined overdisperson ($\widehat{c}$) using the N-mixture goodness of fit test function, *Nmix.gof.test* (Mazerolle 2020). For point-count HDS models, we used the first visit to each site, and then evaluated a constant model with three different detection functions: half-normal, hazard rate, and uniform (Buckland et al. 2001).

We used AIC to rank and select the most appropriate detection function for estimating local abundance (Burnham and Anderson 2002). We then compared regional estimates of local abundance for point counts for the two statistical estimators; estimated local abundance was similar among models (see Results) and we used estimated local abundance and detection probability from the N-mixture model to inform our simulation scenarios (*e.g.*, low abundance, average abundance, and high abundance). For line-transect HDS models we extrapolated the abundance estimate per transect from the point-count abundance estimates from the N-mixture models.

To obtain an average probability of detection we evaluated models with constant probability of detection and constant abundance for all three statistical estimators using the *pcount*, *distsamp*, and *gdistremoval* functions from the *unmarked* package (Fisk and Chandler 2011). The N-mixture (equation 1) and HDS (equation 3) were the same as those described previously except without covariates. We evaluated HDS models for both point-counts and line-transects. We evaluated three different detection functions (half-normal, hazard-rate, and uniform) for line-transect visits 1 and 2, using AIC to select the most appropriate detection function. We used a four-part model hierarchical model as described by Kery and Royle (2016, p. 473-474) and Amundson et al. (2014) for the time-removal HDS model:

$$M_s \sim Poisson\ (\lambda_s) \qquad \text{Equation 4}$$

$$\log(\lambda_s) = \alpha_0 + \alpha_1 * x_s$$

$$N_s \sim Binomial\ (M_s, \phi)$$

$$n_s \sim Binomial(N_s, \bar{p}_s),$$

where $\bar{p}_s$ is made of two components:

$$tint \sim Categorical(\pi_a^c)$$

$$dclass \sim Categorical(\pi_d^c),$$

and M_s represents the local population size at a site (s) is estimated as a Poisson random variable with a mean λ_s (Kery and Royle 2016). The second part of the model represents the number of individuals available to be detected during the distance sampling survey, (N_s), with parameters probability of availability (ϕ) and M_s. The probability of availability (ϕ) describes the probability that an individual is available for detection at all during the survey and is related to the per-interval probability of availability, p_a, where $\phi = 1 - (1 - p_a)^{number\ of\ intervals}$ (Kery and Royle 2016). The number of individuals detected at site s, n_s, is the result of a random binomial draw based on the number available to be detected (N_s) and the net probability of an individual being detected at all in any distance class, $\bar{p}_s$ (Kery and Royle 2016). Last, conditional on n_s, the distributions for two categorical individual covariates for distance class (*dclass*) and time interval (*tint*) are specified (Kery and Royle 2016). Cell probabilities for *dclass* are dependent on the distance-based detection model, while cell probabilities for *tint* are dependent on p_a (Kery and Royle 2016).

Survey protocols often recommend survey conditions under which surveys should or should not be surveyed (*e.g.* not conducting surveys on windy or rainy days), and so we hypothesized that the probability of detecting a Dusky Grouse was impacted by survey conditions. To obtain a high probability of detection, which would represent surveying under recommended survey conditions, we predicted detection probability (p, σ or p_a) under optimal survey conditions: no precipitation, wind, cloud cover or background noise, average temperature, and day of season and minutes from sunrise when peak detection occurs (Chapter 3).

For the N-mixture model and HDS for point-counts p and σ, respectively, were modeled as a function of all survey conditions. Covariates for probability of detection for the N-mixture model were modeled using a logit-link function:

$$N_i \sim Poisson(\lambda) \qquad \text{Equation 5}$$

$$y_{i,j}|N_i \sim Binomial(N_i, p_{i,j})$$

$$\text{logit}(p_{i,j}) = \beta_0 + \beta_1 * x_{1i,j} + \beta_2 * x_{2i,j} + \ldots + \beta_q * x_{q,i,j}$$

where β_0 is the intercept, $\beta_1, \beta_2, \ldots, \beta_q$ represent coefficients, and $x_{1i,j}, x_{2i,j}, \ldots, x_{q,i,j}$ represent different covariates such as precipitation, wind speed, and temperature (Kéry and Schaub 2012). Covariates for the detection function for the hierarchical distance sampling model were modeled using a log-linear function affecting σ:

$$\log(\sigma_s) = \alpha_0 + \alpha_1 * x_{1s} + \alpha_2 * x_{2s} + \ldots + \alpha_q * x_{qs} \qquad \text{Equation 6}$$

where α_0 is the intercept, $\alpha_1, \alpha_2, \ldots \alpha_q$ are the coefficients for the variables, and $x_{1s}, x_{2s}, \ldots x_{qs}$ are different survey conditions (Royle et al. 2004). Probability of detection is broken into two components for time-removal HDS models: availability and perceptibility. We modeled availability (p_a) as a function of precipitation, cloud cover, wind speed, day, and minutes since sunrise, while we modeled perceptibility (σ) as a function of background noise level. Similar to the HDS model, the time-removal HDS model's detection function was also dependent on σ and the effect of background noise was modeled using a log-linear model (equation 6, Amundson et al. 2014, Kéry and Royle 2016). Covariates on availability for the hierarchical distance sampling model were modeled on p_a using a logit-link function (Kery and Royle 2016, Amundson et al. 2014):

$$\text{logit}(p_a) = \beta_0 + \beta_1 * x_{1s} + \beta_2 * x_{2s} + \ldots + \beta_q * x_{qs} \qquad \text{Equation 7}$$

where β_0 is the intercept, $\beta_1, \beta_2, \ldots \beta_q$ are the coefficients for the different covariates, $x_{1s}, \ldots x_{qs}$ such as precipitation and wind speed.

Before fitting models to predict high probability of detection, we first examined the possibility of nonlinear relationships between probability of detection and a survey condition. We hypothesized probability of detection could exhibit nonlinear associations with minutes since sunrise and day during the sampling period due to known temporal display behaviors of grouse (Bendell and Elliot 1967, Zwickel and Bendell 2004, Farnsworth 2020). We explored nonlinear responses by using linear equations to represent our hypothesized relationship. We used $[x + x^2]$ to represent the quadratic form where detection probability may be maximized at some intermediate value of x. We evaluated support for non-linear relationships using AIC to evaluate univariate models for the two different functional responses for the N-mixture, HDS, and time-removal HDS for point-count surveys and HDS for line-transect surveys.

After preliminary screenings of the different potential functional responses, we predicted p, σ, or p_a under optimal survey conditions, which included no wind, cloud cover, precipitation, background noise, optimal estimated minutes from sunrise and day during the sampling period, and average temperature (Chapter 3). The max value of predicted p, σ, or p_a was used as the empirical estimate of 'high' detection probability of a grouse for simulating our datasets. We did not have transect level covariates for survey conditions, so for HDS line-transects we modeled σ as a function of day to obtain our high probability of detection.

We defined average, high, and low abundances (mean local abundance or average abundance per point count) for our simulation scenarios based on empirical estimates of state-wide mean abundance (0.18, 95% CI: 0.17–0.20), the region with the lowest estimated mean

local abundance (0.08, 95% CI: 0.06, 0.11), and the region with the highest estimated mean local abundance (0.31, 95% CI: 0.27–0.37). We defined average detection for each model type, p for N-mixture models (0.37, 95% CI: 0.35, 0.40), σ for HDS point-counts (43, 95% CI: 38–47), σ for HDS line-transects (43, 95% CI: 38–47), σ for time-removal HDS (42, 95% CI: 38–47), and p_a for time-removal HDS (0.23, 95% CI: 0.15–0.34) as the average state-wide constant detection and high p (0.57, 95% CI: 0.52, 0.62), σ for HDS point-counts (58, 95% CI: 38–86), σ for HDS line-transects (51, 95% CI: 38–86), σ for time-removal HDS (48, 95% CI: 41–55), and p_a (0.43, 95% CI: 0.16, 0.69) as the probability of detection under optimal survey conditions. We developed and modeled simulated datasets based on six scenarios:

1. average abundance with average detection,
2. high abundance with average detection,
3. low abundance with average detection,
4. average abundance with high detection,
5. high abundance with high detection, and
6. low abundance with high detection.

Simulations to Evaluate Different Statistical Estimators for Abundance

We simulated data based on empirical estimates of abundance and probability of detection, from the 2020 and 2021 field data and estimated abundance in a Bayesian framework using four methods: single-season N-mixture models (equation 1), HDS (equation 8), time-removal HDS (equation 4), and a naïve model (equation 9). We used a Bayesian framework

because of increased model flexibility and because it allowed us to estimate all the desired parameters ($\lambda, \widehat{N}_i$ per site, $\widehat{N}, p, \sigma, p_a, \phi$) with estimates of uncertainty.

As we are unable to specify a random variable as a multinomial index in BUGS language, to implement HDS models within a Bayesian framework, we needed to use a three-part multinomial, binomial, Poisson mixture model (Kéry and Royle 2016, p. 453) instead of the previously described multinomial-Poisson mixture model:

$$y_s|n_s \sim Multinomial\ (n_s, \pi_s^c) \qquad \text{Equation 8}$$

Where $\pi_k^c = \pi_k/(1-\pi_0)$, with index *k* representing the *k*th element of the vector π_s^c, and $1-\pi_0$ represents total capture probability.

$$n_s|N_s \sim Binomial(N_s, 1-\pi_0)$$

$$N_s \sim Poisson\ (\lambda_s)$$

Within the model, we used a conditional multinomial observation model where we conditioned on the observed data n_s, the number of individuals observed at site *s*, instead of the latent variable, N_s (local abundance; Kéry and Royle 2016). The multinomial distribution in the first part of the model describes the model for the distance class of n_s, the observed individuals which are the result of imperfect detection of N_s as described in the second part of the model (Kéry and Royle 2016). In the third part of the model, similar to the other models we have used, local abundance (N_s) is estimated as a Poisson random variable with a mean λ_s (Kéry and Royle 2016).

The naïve model, evaluated to demonstrate the importance of using an unbiased estimator that incorporates probability of detection, represented a model where detection probability is assumed to be perfect and fitted with a Poisson regression:

$$N_i \sim Poisson(\lambda)$$

We used jags (package *jagsUI*) in R to analyze our simulated datasets and used vague priors for all hyper-parameters that provided little or no information about the estimated parameters: for lambda we used a gamma distribution (0.005, 0.005 or 0.001, 0.001), for probability of detection for the N-mixture model we used a uniform distribution (0,1), for sigma for the HDS model for point-counts and line-transects, and time-removal HDS we used a uniform distribution (0,100), and for probability of availability for time-removal HDS we used a uniform distribution (0,1). (Appendices A–F, Kellner 2019, R Core Team 2021, Kery and Schaub 2012, Kery and Royle 2016). We varied the length of chains, burn-in period, and thinning based on simulation needs for each model type. We assessed convergence using the Gelman-Rubin ($\hat{R}$) statistic and accepted parameter estimates when they came from Markov chains with $\hat{R}$ between 1.0 and 1.1 (Gelman and Rubin 1992).

We quantified bias for the appropriate probability of detection parameters for each model types: probability of detection (p) for the N-mixture model, sigma (σ) for the hierarchical distance sampling models, and availability (ϕ) for the time-removal HDS model. For all models we quantified bias for mean local abundance (λ), estimated local abundance ($\widehat{N}_i$, $\widehat{N}_s$ or $\widehat{M}_i$) per site, and total abundance $\widehat{N}$ estimated as $\sum \widehat{N}_i$ or $\sum \widehat{N}_s$ (or $\widehat{M}$ estimated as $\sum \widehat{M}_i$ for time-removal HDS). To quantify bias, we simulated and evaluated data 500 times for each survey protocol scenario and calculated the difference between the estimated parameter and the true parameter for each iteration. We then compared the posterior distributions of the mean differences between each estimate and the true values across all 500 simulations and considered an estimate to be biased if the 90% credible interval (CrI) of the differences did not include 0. At each of the

iterations we also calculated the coefficient of variation for total abundance ($\widehat{N}$ or $\widehat{M}$) and evaluated the posterior distribution of the 500 derived coefficient of variation estimates in order to determine if the survey protocols resulted in the desired level of precision for total population size. We estimated the probability that the mean coefficient of variation would meet the desired level of precision of a CV of ≤15% by calculating the proportion of the total CV posterior distribution density was > 0.15. We considered a protocol that resulted in a CV ≤ 15%, 90% of the time to be acceptable for the monitoring program.

For the N-mixture, hierarchical distance sampling and time-removal HDS models we evaluated whether estimator precision could be increased by increasing the number of independent survey sites. For our simulated survey protocols for point-counts, we increased the number of sites visited each time by 100 until we achieved unbiased and relatively precise (<15% CV, 90% of the time) estimates of population abundance. We then decreased the number of sites by 20, evaluating the different protocols until the model no longer produced estimates with the desired level of precision, after which we increased the number of sites by 10 to evaluate the midpoint between the thresholds to identify the requisite number of sites. For line transects we started with 100 sites, and then as 100 sites was more than sufficient for reaching our desired level of precision, we decreased the number of sites from 100 by 20 until the coefficient of variation was no longer ≤ 15%, 90% of the time. At that point we then increased the number of sites by 10 and then decreased by 5 to further narrow down the number of sites that need to be visited.

For our N-mixture models (see Appendix E for code) we also varied the number of visits to a site, evaluating survey protocols with 2, 3, or 4 visits. Visiting a site multiple times requires

additional time and survey effort, and so in addition we investigated whether visits could occur back-to-back on or on the same day, which would decrease travel time and make multiple visits more logistically appealing. An implicit assumption of the binomial distribution used in the observation part of the N-mixture model is that events are independent, and this assumption could be violated if back-to-back visits or visits occurring on the same day are correlated. We tested the effects of correlated point-counts on probability of detection and local abundance (Appendix F), with the correlation matrix estimated from the 2020 and 2021 point-count data where back-to-back point counts occurred (Table 18). The correlated data was simulated by summing generated correlated Bernoulli values for each visit, and then using a for loop to filter out datasets that did not yield the desired correlation until a dataset with the desired correlation was produced. The correlations used for the simulations were ± 0.05 of the values in the correlation matrix (Table 18). For the non-correlated simulations, we ran three chains of length 5,000 after a burn-in period of 1,000 and thinned the posterior chains by 1. For the correlated simulations, we ran three chains of 30,000 after a burn-in period of 100 and thinned the posterior chains by 1.

For the hierarchical distance sampling (HDS) models, we evaluated models for both point-counts (Appendix G) and line-transect surveys (Appendix H) using a half-normal detection function determined previously to be appropriate for our data. For the line transect surveys we conducted simulations for transect lengths of 2,681 m (the average transect length) and 5,000 m. For both the line transect and point-count simulations we ran three chains of length 5,000 after a burn-in period of 1,000 and thinned the posterior chains by 1.

For the time-removal HDS model (Appendix I), we evaluated data under two simulation scenarios due to computational constraints and preliminary results indicating the number of point-counts needed (> 6,000) would be logistically unfeasible even for the high abundance, average detection scenarios. We evaluated the model for both high abundance scenarios, and given previous patterns, we assumed the scenarios with high abundance would require the lowest amounts of survey effort. For these simulations we ran three chains of length 20,000 after a burn-in period of 1,000 and thinned the posterior chains by 1.

We evaluated naïve models (Appendix J) for point-counts using the protocols identified to be most effective and logistically feasible. We used only 1 visit and based the number of sites (60, 80, 140, 170, 240, 490) visited on the recommended survey protocol out of the other three model types for the different scenarios. For the simulations, we ran three chains of length 3,000 after a burn-in period of 100 and thinned the posterior chains by 1.

Power Analysis

We generated an initial average local abundance of 0.18 grouse per site for year 0 across 80 sites (recommended protocol based on the average abundance, high detection scenario for the N-mixture model where each site is visited four times), and then to project the population through time, we modeled the persistence of birds at each site using a binomial draw where the probability of persistence was 1 – target annual trend (Steidl et al. 2013, Anderson and Steidl 2019). We examined trends of 1% annual decline, 3% annual decline, 5% annual decline, and 10% annual decline for 3, 5, and 10 years. We simulated counts by randomly drawing from a binomial distribution where $N = N_t$ and p = probability of detection for four visits and used an N-mixture model in *unmarked* to estimate total abundance for each year. We then used the log-

transformed abundance as the response variable and regressed total population across years to get the slope of the population trend for the estimated abundances and true total abundances. We used 90% confidence intervals to determine if the slope of the trend was different than zero for the estimated abundances and ran this simulation 500 times (Gibbs and Melvin 1997, Steidl et al. 2013). The proportion of slopes different from zero represented the power of the protocol, and we considered an acceptable protocol to have a power ≥ 80% (Steidl et al. 2013, Weiser et al. 2019). In addition, we looked at how often the slope was predicted to be negative. We also calculated the mean trend for the estimated abundances and the mean difference between the trends estimated using the estimated abundances and the true abundances, calculating a 95% confidence interval using a quantile of 0.025 and 0.975.

Results

Simulations to Inform Field Survey Protocols

2019 Pilot Season Protocols. Results of our simulations indicated that 3 replicate surveys at each of 100 independent survey sites within a period of closure yielded unbiased and relatively precise (≤15% CV) indices of regional population abundance when the average site-specific abundance was ≥ 0.625 grouse (Appendix K).

2020 and 2021 Season Protocols. A Poisson distribution was most supported for the N-mixture model indicating no overdispersion (Appendix L). We used empirical estimates of abundance, 0.36, and probability of detection, 0.28, when simulating data. Simulations evaluating the efficacy of 2019's survey effort (100 sites visited 3 times) yielded relatively imprecise estimates (CV > 15%; Appendix M). When we kept the number of visits at 3, our simulations indicated that replicate surveys at each of 600 independent sites would be needed

(Appendix M). When only 100 independent sites were surveyed, a minimum of 7 replicate visits was needed to yield unbiased and relatively precise (< 15% CV) indices of regional population abundance (Appendix M).

When we varied the number of sites keeping number of visits at 4, protocols that yielded unbiased and relatively precise (<15% CV) indices of regional population abundance were surveying at 300 and 360 independent survey sites, requiring a respective 50–60, and 60–72 survey mornings (Appendix M). Based on the simulation results, we designed survey protocols for 2020–2021 where at least 360 sites were surveyed 4 times per MFWP region.

Effects of Route Type on Abundance

We surveyed 90 off-trail sites in 2019, 845 and 744 road sites, and 803 and 731 trail sites in 2020 and 2021 respectively. Estimated local abundance was higher for survey points located off-trail (0.36, 95% CI: 0.18–0.73) than those located along trails (0.19, 95% CI: 0.16–0.23 in 2020 and 0.23, 95% CI: 0.20–0.27 in 2021) or roads (0.17, 95% CI: 0.14–0.20 in 2020 and 0.14, 95% CI: 0.12–0.17 in 2021; Table 13, Figure 19).

Empirical Estimates of Abundance and Detection to Inform Simulation Analyses

We conducted 3,292 sets of point-counts (each set varying between 1–4 repeat visits) across 2,372 sites and walked 551 line-transects two times. Due to incomplete data, for the N-mixture model analysis we only used 3,123 sets of point-counts (each with 4 repeat visits), for the HDS point count models we only used data from 3,234 point-counts across 2,349 sites, and for the HDS line-transect models we only used data for 514 transects.

Abundance Estimates. We used a Poisson distribution for the N-mixture models as the data did not appear overdispersed ($\hat{c}$ = 1.4). We found a half-normal detection best fit our data for the HDS models for point-counts (Appendix N). Average estimates of Dusky Grouse abundance for point-counts were 0.18 (95% CI: 0.17, 0.20) Dusky Grouse from the N-mixture model and 0.20 (95% CI: 0.16, 0.24) from the HDS model (Tables 14, 15). Regional local abundance estimates were similar across the N-mixture and point-count distance sampling models (Figure 20). Estimated abundance estimates were lowest for MFWP Region 4, where the N-mixture model estimated a local abundance of 0.08 (95% CI: 0.06, 0.11) and the hierarchical distance sampling model estimated a local abundance of 0.07 (95% CI: 0.04, 0.12; Tables 14, 15). Estimated abundance was greatest in MFWP Region 2, where the N-mixture model estimated a local abundance of 0.31 (95% CI: 0.27, 0.37) and the hierarchical distance sampling model estimated a local abundance of 0.36 (95% CI: 0.27, 0.47; Tables 14, 15). Because, on average, the N-mixture models produced more precise estimates of local abundance, we chose to use estimates from N-mixture models to inform our simulation scenarios; we used a low local abundance of 0.08, an average local abundance of 0.18, and a high local abundance of 0.31 to create simulation scenarios (Table 16).

N-mixture Model Probability of Detection. The average probability of detection was 0.37 (95% CI: 0.35, 0.40). A quadratic relationship between probability of detection and day of survey season and minutes from sunrise was most supported (Chapter 3). Under optimal survey conditions, our high estimate of probability of detection was 0.57 (95% CI: 0.52, 0.62) occurring on May 13th and at 86 minutes post-sunrise (Figure 21, Table 16).

HDS Model Probability of Detection for Point-counts. Average σ for estimating the half-normal detection function was estimated to be 43 (95% CI: 38, 47). While evaluating the effects of survey conditions on σ, unlike with N-mixture models, we only found support for day since sampling period started to have a nonlinear relationship with σ with σ being highest on May 10th (Figure 21, Appendix O). Under optimal conditions, our high estimate for σ for HDS models for point-counts was 58 (95% CI: 38, 86; Table 16).

HDS Model Probability of Detection for Line-transects. When we evaluated the most appropriate detection function for the line-transects for visit 1 both the hazard-rate and half-normal had model support and similar abundance estimates (Appendix N, Figure 22). The half-normal detection function was most supported for visit 2, and the hazard-rate detection function model was unable to converge and produced unrealistically high abundance estimates. As a result, we chose to use a half-normal function to generate our simulated line-transect data and analyze it. Average σ was estimated to be 42 (95% CI: 37, 49; Table 16). We found support for day since the sampling period started to have a nonlinear quadratic relationship with σ, resulting in σ being highest on May 9th with a σ of 51 (95% CI: 42, 61; Figure 21, Table 16, Appendix O).

Time-removal HDS. Average σ (for a half-normal detection function) was estimated to be 42 (95% CI: 38, 47) and availability (ϕ) was calculated to be 0.65 with p_a estimated to be 0.23 (95% CI: 0.15, 0.34; Table 16). We only found support for a quadratic relationship between day since the sampling period started and availability, with availability highest on May 12th (Figure 21, Appendix O). Under ideal survey conditions, our high estimate of probability of

availability (ϕ) was 0.89, p_a was estimated to be 0.43 (95% CI: 0.16, 0.69), and σ for the half-normal detection function was 48 (95% CI: 41, 55; Table 16).

Simulations Evaluating Different Statistical Estimators and Survey Effort

Overall, N-mixture models, HDS for point-counts, and time-removal HDS produced unbiased estimates for both abundance and detection parameters with sufficient survey effort (Figures 23–25). Though protocols for line-transects evaluated using HDS also produced unbiased estimates on average for both abundance and detection parameters, their credible intervals were large indicating that there was high variability in the observed bias of our estimates (Figures 23–25). Protocols for naïve models always produced estimates of mean local abundance that were biased low (Figure 23, Appendix P). The survey protocol that required the fewest total point-counts (number of sites × number of visits) conducted for all scenarios was a protocol for visiting sites 4 times and analyzing the count data using N-mixture models (Figures 26, 27, Table 17). Depending on the scenario the number of sites necessary varied between 60–490.

Generally, estimated precision increased with the number of sites and the number of replicate surveys per site (Appendix Q). For all models, as the probability of detection and/or abundance increased, the number of sites needing to be surveyed and total number of point-count surveys needing to be conducted decreased (Figures 26, 27; See Appendices P-T for all simulation results). The least number of surveys required occurred for scenarios with both high detection and high abundance (Figures 26, 27, Table 17). For example, for point-counts, under simulated conditions of high abundance ($\bar{N}$ = 0.31 grouse per survey point) and average detection ($\bar{p}$ = 0.37, for HDS σ = 43, for time-removal HDS σ = 42, availability = 0.65), 170

survey sites would need to be surveyed 4 times to obtain acceptably precise estimates of population size evaluated using an N-mixture model, 1,090 sites using hierarchical distance sampling and > 6,000 sites for time-removal HDS (Table 17). In contrast, for point-counts, under a high abundance ($\bar{N}$ = 0.31 grouse per survey point) and high detection ($\bar{p}$ = 0.57, for HDS model σ = 58, for time-removal HDS σ = 48, availability = 0.89) only 60 survey sites would need to be surveyed 4 times using an N-mixture model, 800 sites for HDS model for point-counts, and 1,390 sites for time-removal HDS (Table 17).

We found that the counts for the back-to-back point-counts (visits 1 and 2, and 3 and 4), there was evidence of positive correlation ($r = 0.67$, $p < 0.05$), while there was no evidence of correlation between the non-back-to-back visits (visits 1 and 3, 1 and 4, 2 and 3, and 2 and 4; Table 18). Using simulations, we evaluated the effects of correlated counts on abundance estimates produced by N-mixture models and found that when the true probability of detection was ≥ 0.57, the proposed sampling effort and protocol produced unbiased estimates of detection and local abundance (Table 19, Figure 28). We found modest upward bias in detection probability (approximately + 0.10–0.11) and low bias in local abundance (approximately -0.01– -0.04 birds per survey area) when detection rates are ≤ 0.37, our average empirical probability of detection (Table 19, Figure 28).

For line-transects survey protocols, the number of transects that needed to be visited was lower for longer transects (5,000 m) than shorter transects (2,681 m; Figure 29, 30; Appendix S). Under average abundance (5.73 Dusky Grouse per km^2) and high detection probability (σ = 51), for example, only 20 5000-m long transects were required to yield estimates of precision in abundance < 0.15 CV whereas 35 transects were needed when their length was 2,681 m. The

number of required survey transects declined as the probability of detection increased (Figure 29, 30; Appendix S).

When conducting point-count surveys, evaluated using N-mixture models, with six points located along a transect, less transects need to be visited than if conducting line-transect surveys under all high probability of detection scenarios. As an example, under the average abundance, high detection scenario, 14 transects are needed for the point-count protocol, while 35 are needed for transects of 2,681-m in length, and 20 for transects of 5,000-m in length (Table 20). Under average probability of detection scenarios, when conducting point-count surveys with six points located along a transect, the number of transects needing to be visited was lower or equal to that of the line-transect method when line transects were 2,681-m in length, and more than that when line transects were 5,000-m in length. For example, under the average abundance, average detection scenario, 40 transects are needed for the point-counts and transects 2,681-m in length while only 25 are needed for transects 5,000-m in length (Table 20).

Power Analysis

Survey protocols that yielded ≤ 15% CV in annual estimates of abundance did not have power to detect a 1% annual decline in abundance over 10 years but did have power (≥ 80%) to detect a 3% and 5% annual decline (Table 20). Over 5 years, we had power (≥ 80%) to detect a 10% annual decline (Table 20). The average slope was close (within 0.08–1.08) to the target trend for each combination of year and annual decline (Table 21). A negative trend was predicted over 70% of the time for all combinations of 3%, 5%, and 10% annual declines, and after 5 years for a 1% annual decline (Tables 22). On average across the different scenarios the difference

between the annual trends estimated using the estimated abundance and the true abundance was small (Table 23).

Discussion

Through the evaluation of different sampling and analytical methods, we were able to identify survey protocols that are logistically feasible and provide unbiased and precise (CV ≤ 15%) estimates of abundance, providing the necessary information for the development of a monitoring program for Dusky Grouse in Montana. While we found evidence of slightly lower abundance of grouse near roads and trails, the ability of field biologists to conduct surveys is more logistically feasible when these features can be used. Using simulations, we evaluated hundreds of potential protocols under six different realistic scenarios based on empirical estimates of abundance and probability of detection. We found that line-transect surveys evaluated using hierarchical distance sampling, as well as point-count protocols where sites are visited four times and counts are evaluated using N-mixture models yield acceptable accuracy and precision necessary for population monitoring of Dusky Grouse.

Field Sampling

We found that point-count surveys established along roads and trails resulted in reduced abundance (0.13–0.22 grouse per site) than those located away from roads and trails. However, the time and effort needed to access randomly selected off-trail survey locations was prohibitive in the mountainous Dusky Grouse habitats of Montana. Off-trail surveys took up to 8 hours to complete during the spring, whereas surveys conducted along roads and trails were easier to access and completed within a 4-hour period after sunrise when detection probability was

highest. Although surveys located along roads and trails may result in downward biased estimates of abundance, estimates adjusted for spatial and temporal variation in detection probability are useful and unbiased indices of population size. We were unable to evaluate whether local abundance was affected by the type of road or trail (*e.g.*, paved v. unimproved road, non-motorized trails); nevertheless, we limited our subsequent population monitoring recommendations to unimproved roads and trails with low traffic.

Comparison of Statistical Estimators of Abundance

As expected, our analyses of simulated datasets demonstrated that estimated abundance is downward biased when detection probability is ignored (Thompson 2002). Hierarchical abundance models such as N-mixture models, HDS, and time-removal HDS all produced unbiased estimates of abundance regardless of simulated values of detection probability, demonstrating their potential utility in a Dusky Grouse monitoring program. We further examined how precise the estimates of abundance were, which narrowed the field of potential statistical estimators to 1) N-mixture models when survey points are visited four times, and 2) HDS when line-transects are surveyed in the spring for each area of inference (*e.g.*, MFWP administrative region). The exact number of sites and transects required varied based on simulation scenario.

Our results are generally consistent with simulation results of N-mixture models for other species and simulation studies in which increasing the number of plots and visits increased the precision of estimates (McIntyre et al. 2012, Yamuara 2013). As the number of visits increased from 2 to 4, for example, the requisite number of sites required to reach the desired level of precision decreased from 900 to 170 under the high abundance average detection scenario

(Appendix R). Similar to another study, we found that large improvements in estimator precision occurred as probability of detection increased (McIntyre et al 2012). We also found that our models performed well at low local abundances, with estimates more variable under lower local abundance and probability of detection (Yamaura 2013).

The HDS models followed a similar trend to the N-mixture models; the requisite number of sites visited for our desired level of precision decreased as abundance or probability of detection increased. Despite this, even for point-count scenarios with relatively high abundance and detection, the HDS and time-removal HDS models required a prohibitively large number of survey sites that were not logistically feasible. At least 75 grouse observations are needed for accurate estimates of abundance using distance sampling, suggesting limited utility of distance sampling for point-count survey protocols of Dusky Grouse. When mean local abundance was average (*e.g.*, 0.18 Dusky Grouse per point count) and detection was high, the number of sites necessary to obtain the necessary sample size to be able to obtain a precise abundance estimate is prohibitively large (1,360 survey points). Other simulations have shown that the precision for abundance estimates from time-removal HDS is low when probability of availability is low (≤ 0.4; Amundson et al. 2014). While our average probability of availability (0.65) was higher than 0.4, low grouse densities required prohibitively large number of survey points to be visited (> 6,000) to achieve our desired level of precision. In short, our simulation results indicate that distance sampling models applied to grouse counts collected at point-counts will not provide suitably accurate and precise estimates of relative population size for management.

Line transects analyzed using HDS required more achievable survey effort than did point-counts. We examined the utility of transects of two different lengths and found that longer

transects required fewer sites be visited than the shorter transects, assuming Dusky Grouse are distributed randomly in relation to transect length. Nevertheless, longer transects take more time to survey and may have higher likelihood that parts of the transect may be inaccessible, especially early in the season due to snowpack. In comparison to point-counts analyzed using N-mixture models, the shorter line-transects analyzed using HDS required a similar or greater number of transects visited. Due to the large credible intervals when examining bias for the abundance and detection parameters for line-transects analyzed using HDS in addition to needing greater survey effort, we recommend point-counts analyzed using N-mixture models over line-transects analyzed using HDS.

A potential limitation of N-mixture models is that sites must be surveyed multiple times within a period of closure. This repeated survey requirement presents logistical challenges for surveying Dusky Grouse in remote and mountainous habitats. To meet model assumptions of population closure while reducing the time and costs of accessing survey sites, we conducted four replicate visits of a survey site in a single morning. Conducting replicate visits as either consecutive point-counts or within the same morning, may violate an implicit assumption that visits are independent resulting in biased probabilities of detection and abundance. We found that when we evaluated the effect of correlated counts on probability of detection and abundance, that if probability of detection was high (≥ 0.57) then estimates of detection and abundance were still unbiased. Hence, when surveys are conducted under optimal conditions that lead to high probability of detection (Chapter 3), replicate visits can be conducted within a single morning negating logistical constraints that may limit the use of N-mixture models.

Power Analysis

Our recommended protocol derived from the average abundance, high detection scenario (point-counts where 80 sites or 14 transects with 6 points per transect, are visited four times and evaluated using N-mixture models) had high power (≥ 80%) to detect average population declines of 3%, 5%, and 10% over 5–10-year periods, which was lower than expected given precision of annual abundance estimates were < 15%. Nevertheless, we found that the estimated abundance trends were similar to the target trends, and close to the real trends estimated using the true simulated population size, suggesting that while there may be some uncertainty associated with the estimated trends, our protocols may be sufficient for long-term monitoring and able to detect small changes in population size in as little as 3 years. In addition, as the monitoring period increases (> 5 years), the power to detect small changes increases indicating that our protocols are appropriate for long-term monitoring of Dusky Grouse populations.

Conclusions

Precise and unbiased estimates of population size are important for effective conservation and management of Dusky Grouse. We used simulations to evaluate hundreds of potential protocols with different statistical estimators to design a program that produced unbiased and precise estimates of abundance that was logistically feasible for state wildlife agencies with multiple competing priorities. We also evaluated the impact of violating a model assumption that would prevent conducting back-to-back point-count surveys within a single morning, impacting logistic feasibility of survey methods. We recommend conducting spring point-count surveys during periods of high detection with electronic playback (Chapter 3) along low-use or seasonal-use roads and trails, where sites are visited four times within a single morning and counts are

analyzed using N-mixture models. Periods of high detection can be characterized as days with no precipitation, limited cloud cover, no wind, areas with limited background noise, between sunrise and 10:00, and during 3–23 May (Chapter 3). While HDS is commonly used for population monitoring, we found that the number of sites required for point counts was prohibitive. When conducting line-transects, HDS remains a viable option, but still requires more survey effort than the recommended protocol where point-counts are conducted and analyzed using N-mixture models. Our study provides the foundation for a Dusky Grouse monitoring program in Montana and illustrates a process for developing monitoring programs elsewhere for Dusky Grouse and other species.

Table 13. Estimates of local abundance with 95% confidence intervals for point counts conducted along different transect types: off trail (2019, n = 90), on roads (2020, n = 845, 2021, n = 744), and trails (2020, n = 803, 2021, n = 731).

Route Type	Year	Estimate	SE	95% Confidence Interval
Road	2020	0.17	0.02	0.14–0.20
Road	2021	0.14	0.01	0.12–0.17
Trail	2020	0.19	0.16	0.16–0.23
Trail	2021	0.23	0.02	0.20–0.27
Off-trail	2019	0.36	0.13	0.18–0.73

Table 14. Estimates for MFWP regional local abundance (grouse per survey site) evaluated using single season N-mixture models. Average lambda/local abundance was estimated using a model where abundance and detection were both held constant. MFWP regional local abundances were estimated using a model where local abundance was varied by region and detection was held constant.

Parameter	Estimate	SE	95% confidence interval
Region 1 λ	0.13	0.02	0.10–0.17
Region 2 λ	0.31	0.03	0.27–0.37
Region 3 λ	0.19	0.02	0.16–0.23
Region 4 λ	0.08	0.01	0.06–0.11
Region 5 λ	0.21	0.02	0.17–0.26
Average λ	0.18	0.01	0.17–0.20

Table 15. Estimates for MFWP regional local abundance evaluated using hierarchical distance sampling models. Average lambda/local abundance was estimated using a model where abundance and detection were both held constant. MFWP regional local abundances were estimated using a model where local abundance was varied by region and detection was held constant.

Parameter	Estimate	SE	95% confidence interval
Region 1 λ	0.12	0.03	0.08–0.19
Region 2 λ	0.36	0.05	0.27–0.47
Region 3 λ	0.21	0.03	0.15–0.29
Region 4 λ	0.07	0.02	0.04–0.12
Region 5 λ	0.23	0.04	0.16–0.33
Average λ	0.20	0.02	0.16–0.24

Table 16. Parameter estimates used to inform simulation scenarios. Abundance estimates were used to inform scenarios for both single-season N-mixture and hierarchical distance sampling models. σ was used to inform the detection function for all the hierarchical distance sampling models, detection was used to inform the probability of detection for the single-season N-mixture models, and availability was used to inform the probability of availability for the time-removal HDS models. PC = point-count survey, Line = line-transect survey

Model	Survey Type	Parameter	Estimate
All	-	Low λ	0.08
All	-	Average λ	0.18
All	-	High λ	0.31
N-mixture	PC	Average p	0.37
N-mixture	PC	High p	0.57
Hierarchical distance sampling	PC	Average σ	43
Hierarchical distance sampling	PC	High σ	58
Time-removal HDS	PC	Average σ	43
Time-removal HDS	PC	High σ	48
Time-removal HDS	PC	Average ϕ	0.65
Time-removal HDS	PC	High ϕ	0.89
Hierarchical distance sampling	Line	Average σ	42
Hierarchical distance sampling	Line	High σ	51

Table 17. From the simulation results, the number of visits, sites to be surveyed, total number of point counts to be conducted, and the potential number of transects (if there are 6 points on each transect) for providing robust population estimates using N-mixture models (point counts), hierarchical distance sampling (point counts and transects), and time-removal HDS under 6 different scenarios. HA = high abundance, average detection, AA = average abundance, average detection, LA = low abundance, average detection, HH = high abundance, high detection, AH = average abundance, high detection, LH = low abundance, high detection. Simulations were only conducted under 2 scenarios for the time-removal HDS. The transect length evaluated was 2,681m (the average transect length for 2020 and 2021).

Scenario	Model	# of Visits	# of Sites	# of Point Counts	Transect (6pts)
HA	N-mixture point count	4	170	680	29
	HDS point count	1	1,090	1,090	182
	Time-removal HDS point count	1	> 6,000	> 6,000	> 1,000
	HDS transect: 2,681m	1	25	NA	25
	HDS transect: 5,000m	1	15	NA	15
AA	N-mixture point count	4	240	960	40
	HDS point count	1	1870	1870	312
	Time-removal HDS point count	1	NA	NA	NA
	HDS transect: 2,681m	1	40	NA	40
	HDS transect: 5,000m	1	25	NA	25
LA	N-mixture point count	4	490	1960	82
	HDS point count	1	4230	4230	705
	Time-removal HDS point count	1	NA	NA	NA
	HDS transect: 2,681m	1	90	NA	90
	HDS transect: 5,000	1	50	NA	50
HH	N-mixture point count	4	60	240	10
	HDS point count	1	800	800	134
	Time-removal HDS point count	1	1390	1390	232
	HDS transect: 2,681m	1	20	NA	20
	HDS transect: 5,000m	1	15	NA	15
AH	N-mixture point count	4	80	320	14
	HDS point count	1	1360	1360	227
	Time-removal HDS point count	1	NA	NA	NA
	HDS transect: 2,681m	1	35	NA	35
	HDS transect: 5,000m	1	20	NA	20
LH	N-mixture point count	4	140	560	24
	HDS point count	1	3110	3110	519
	Time-removal HDS point count	1	NA	NA	NA
	HDS transect: 2,681m	1	70	NA	70
	HDS transect: 5,000m	1	40	NA	40

Table 18. Correlation matrix for correlation between point counts for combined 2020 and 2021 data. Point counts 1 and 2, and point counts 3 and 4 are conducted back-to-back. All point counts occurred on the same day.

	Point Count 1	Point Count 2	Point Count 3	Point Count 4
Point Count 1	1.00	0.67	0.41	0.44
Point Count 2	-	1.00	0.48	0.47
Point Count 3	-	-	1.00	0.67
Point Count 4	-	-	-	1.00

Table 19. Results of simulations evaluating the effects of correlation between point counts for the recommended protocols for the N-mixture models under 6 different scenarios. Mean (90% credible interval) for bias and coefficient of variation from 500 simulation runs for each suite of parameters. Different scenarios include combinations of high, average, and low abundance paired with either average or high detection. R = number of survey sites, λ = mean abundance per site, σ = mean σ, p.avail = mean probability of availability; CV = coefficient of variation for total population size (Total N) and N.site = estimated number of Dusky Grouse per survey site.

Simulation Parameters				**Bias in λ**	**Bias in *p***	**Bias in Total N**	**Bias in N.site**	**CV Total N**	**Probability CV N.total > 0.15**	**Protocol meets Management equirements**
R	**J**	**λ**	***p***							
170	4	0.31	0.37	-0.04 (-0.11, 0.03)	0.10 (0.05, 0.16)	-6.80 (-13.46, -0.91)	-0.04 (-0.08, -0.01)	0.07 (0.05, 0.09)	0.00	yes
240	4	0.18	0.37	-0.02 (-0.07, 0.02)	0.10 (0.05, 0.15)	-5.69 (-11.41, -0.49)	-0.02 (-0.05, 0.00)	0.07 (0.05, 0.09)	0.00	yes
490	4	0.08	0.37	-0.01 (-0.03, 0.01)	0.11 (0.06, 0.16)	-4.73 (-9.50, -0.05)	-0.01 (-0.02, 0.00)	0.07 (0.05, 0.09)	0.00	yes
60	4	0.31	0.57	0.00 (-0.13, 0.13)	-0.04 (-0.13, 0.04)	0.41 (-2.22, 2.62)	0.01 (-0.04, 0.04)	0.10 (0.06, 0.15)	0.05	yes
80	4	0.18	0.57	0.01 (-0.06, 0.09)	-0.04 (-0.13, 0.03)	0.33 (-1.68, 1.99)	0.00 (-0.02, 0.02)	0.10 (0.07, 0.16)	0.07	yes
140	4	0.08	0.57	0.00 (-0.03, 0.04)	-0.05 (-0.13, 0.02)	0.26 (-1.40, 1.48)	0.00 (-0.01, 0.01)	0.11 (0.07, 0.17)	0.16	yes-ish

Table 20. Predicted power for a protocol where 80 sites are visited 4 times and abundances are estimated using an N-mixture model. Power was examined for a 1, 3, 5, and 10% annual decline over a period of 3, 5, and 10 years. A 10% decline over 10 years was not evaluated as sufficient power was reached after a period of 5 years..

Annual Decline	3 years	5 years	10 years
1%	8.2	14.4	39.2
3%	19	40.6	80.8
5%	26.8	61	94.6
10%	49.6	87.2	NA

Table 21. Mean estimated slopes for predicted annual trend for a protocol where 80 sites are visited 4 times and abundances are estimated using an N-mixture model. Trend were examined for 1, 3, 5, and 10% annual declines over a period of 3, 5, and 10 years. 95% confidence intervals are calculated using a quantile of 0.025 and 0.975. A 10% decline over 10 years was not evaluated.

Annual Decline	3 years	5 years	10 years
1%	-1.13 (-8.29, 5.94)	-1.18 (-6.13, 2.78)	-1.08 (-3.75, 0.84)
3%	-3.58 (-12.82, 4.38)	-3.17 (-9.32, 1.63)	-3.21 (-7.81, -0.1)
5%	-5.3 (-16.25, 3.68)	-5.39 (-13.89, -0.08)	-5.24 (-11.1, -1.16)
10%	-11.08 (-26.6, -0.11)	-10.73 (-21.34, -0.07)	NA

Table 22. Percent of estimated slopes < 0 for predicted annual trend for a protocol where 80 sites are visited 4 times and abundances are estimated using an N-mixture model. Trends were examined for 1, 3, 5, and 10% annual declines over a period of 3, 5, and 10 years. A 10% decline over 10 years was not evaluated.

Annual Decline	3 years	5 years	10 years
1%	60.6	71	80.8
3%	78.8	88.4	97.6
5%	84.4	97.8	99
10%	97.4	98.2	NA

Table 23. Difference between the estimated slopes for predicted annual trend for true abundance and estimated abundances for a protocol where 80 sites are visited 4 times and abundances are estimated using N-mixture model. Trends were examined for 1, 3, 5, and 10% annual declines over a period of 3, 5 and 10 years. A 10% decline over 10 years was not evaluated.

Annual Decline	3 years	5 years	10 years
1%	-0.0005 (-0.0618, 0.0656)	-0.0012 (-0.0406, 0.0358)	-0.0003 (-0.0138, 0.0137)
3%	-0.0030 (-0.0723, 0.0632)	-0.0001 (-0.0399, 0.0350)	0.0007 (-0.0152, 0.0167)
5%	0.0018 (-0.0637, 0.0695)	0.0009 (-0.0343, 0.0.371)	0.0011 (-0.0161, 0.0201)
10%	-0.0007 (-0.0801, 0.0720)	0.0014 (-0.0400, -0.0468)	NA

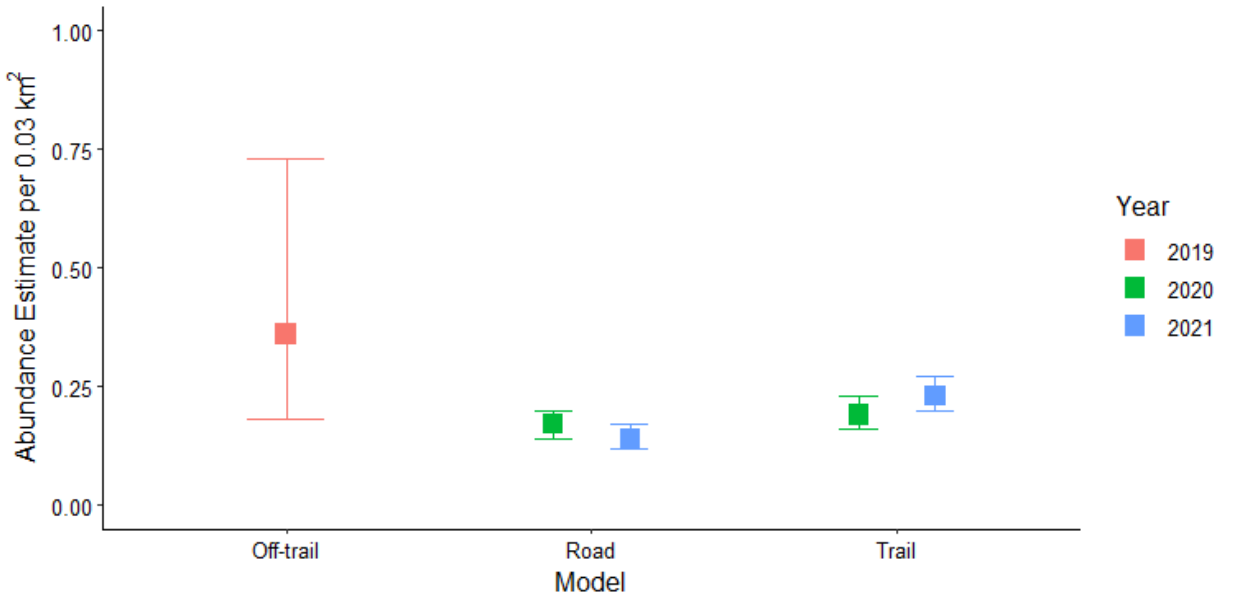

Figure 19. Local abundance estimates evaluated using single season N-mixture models of Dusky Grouse with 95% confidence intervals for point counts conducted along different route types: off-trail, road, and trail. Data for the off-trail transects come from the 2019 pilot year surveys conducted in MFWP region 3. Data for the road and trail transects comes from the 2020 and 2021 surveys conducted across western Montana.

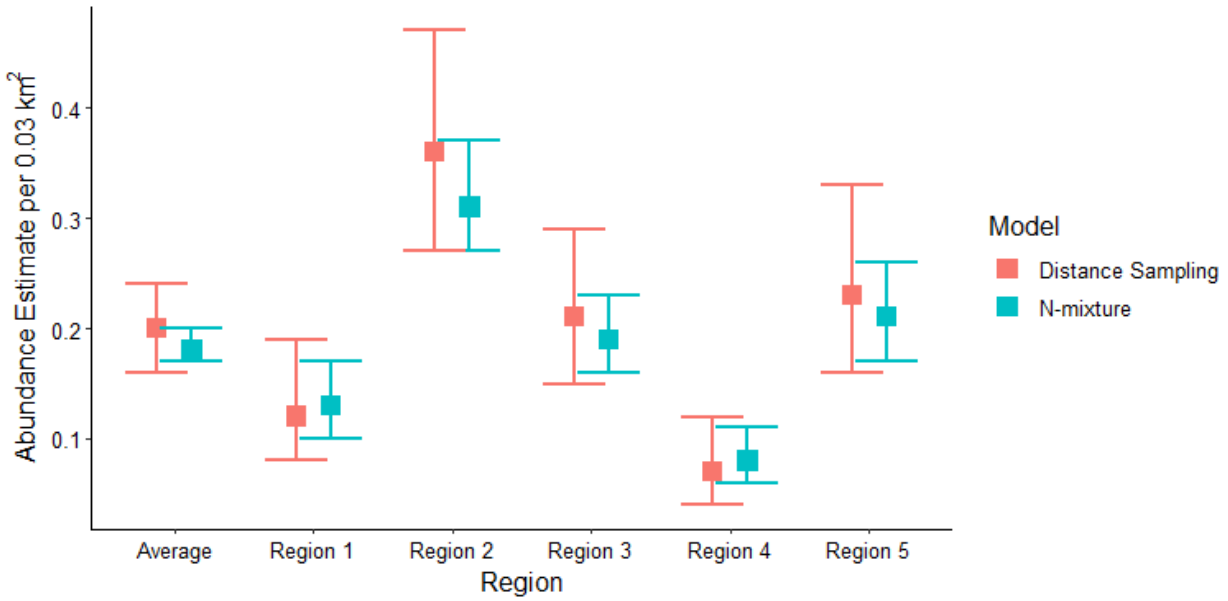

Figure 20. Abundance estimates per point count with 95% confidence intervals across MFWP Regions 1-5 based on N-mixture and hierarchical distance sampling model where detection (p or σ) was held constant and abundance was allowed to vary by region. There is also average abundance from N-mixture and hierarchical distance sampling models where both detection (p or σ) and abundance were held constant.

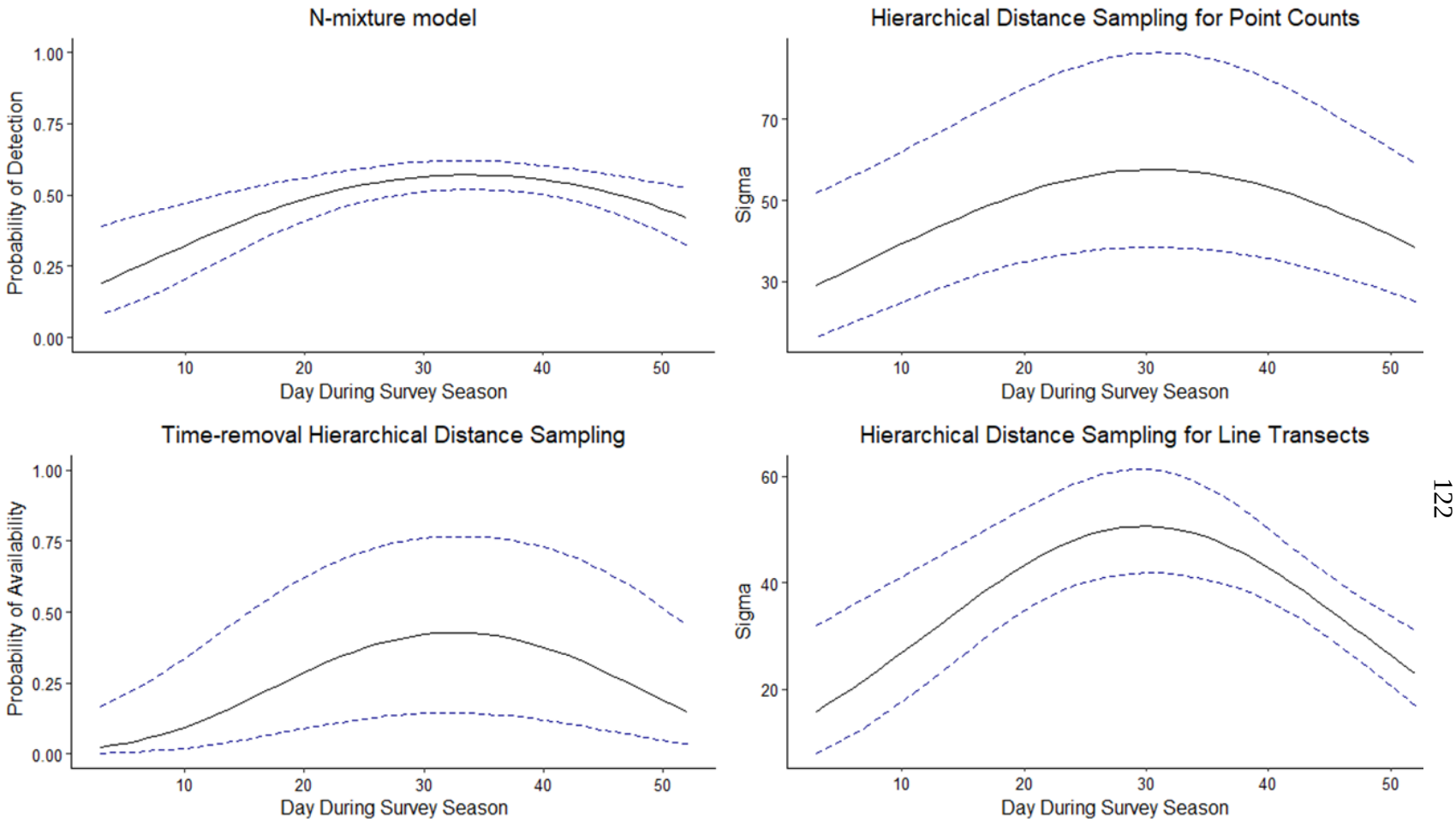

Figure 21. Effect of day during the survey season on probability of detection, σ, or availability for 4 models. 3 models for point counts: N-mixture, hierarchical distance sampling, time-removal HDS, and 1 model for line transects: hierarchical distance sampling. Probability of detection was highest for the N-mixture model on day 34 (May 13th, σ was highest for the hierarchical distance sampling for point counts on day 31 (May 10th), σ was highest for hierarchical distance sampling for line transects on day 30 (May 9th), and availability was highest on day 33 (May 12th) for time-removal HDS models.

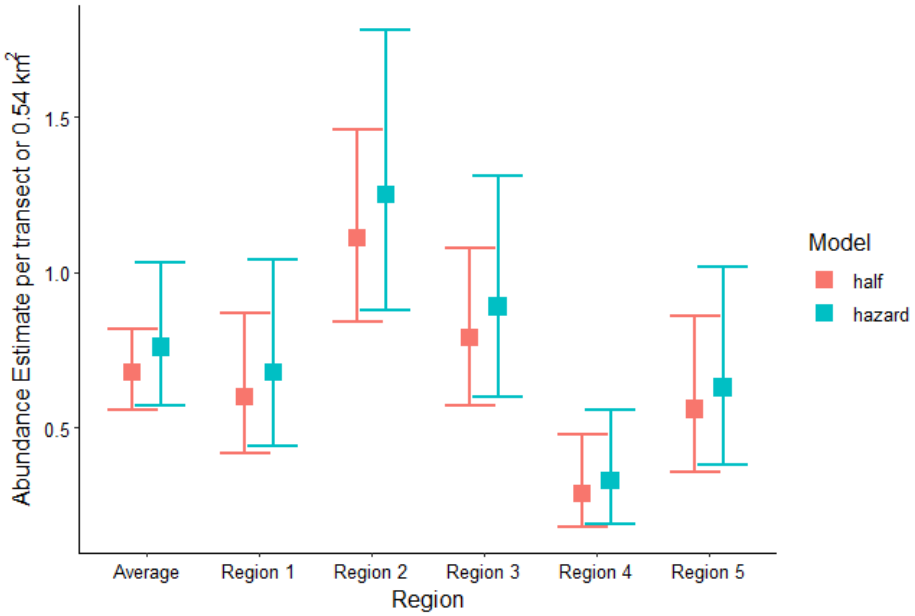

Figure 22. Abundance estimates per point count with 95% confidence intervals across MFWP Regions 1-5 based on hierarchical distance sampling models with a half-normal detection function and a hazard-rate detection function where detection (σ) was held constant and abundance was allowed to vary by region. There is also average abundance from the distance sampling models where both detection (σ) and abundance were held constant.

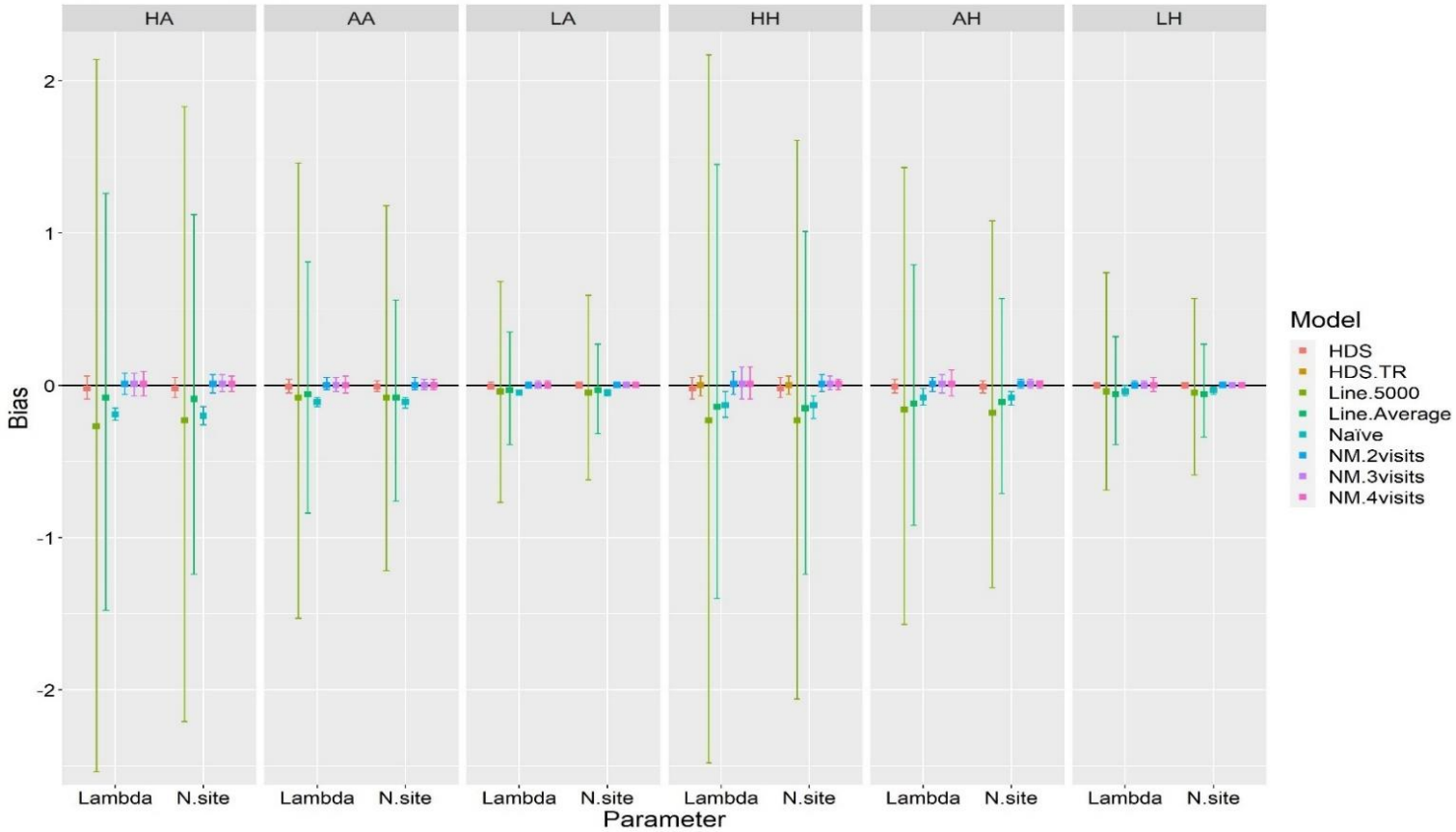

Figure 23. Parameter bias with 90% credible intervals over 500 simulations under 6 scenarios with varying abundance and detection/σ. Parameters are average local/point count abundance (lambda) and abundance at each site (N.site). Scenarios include, HA = high abundance, average detection, AA = average abundance, average detection, LA = low abundance, average detection, HH = high abundance, high detection, AH = average abundance, high detection, and LH = low abundance, high detection. There are 8 models evaluated: HDS = hierarchical distance sampling for point counts, HDS.TR = time-removal HDS, Line.5000 = hierarchical distance sampling for line transects 5000m in length, Line.Average = hierarchical distance sampling for line transects of average (2,681m) length, Naïve = naïve model, and NM with varying visits = N-mixture model with either 2, 3, or 4 visits.

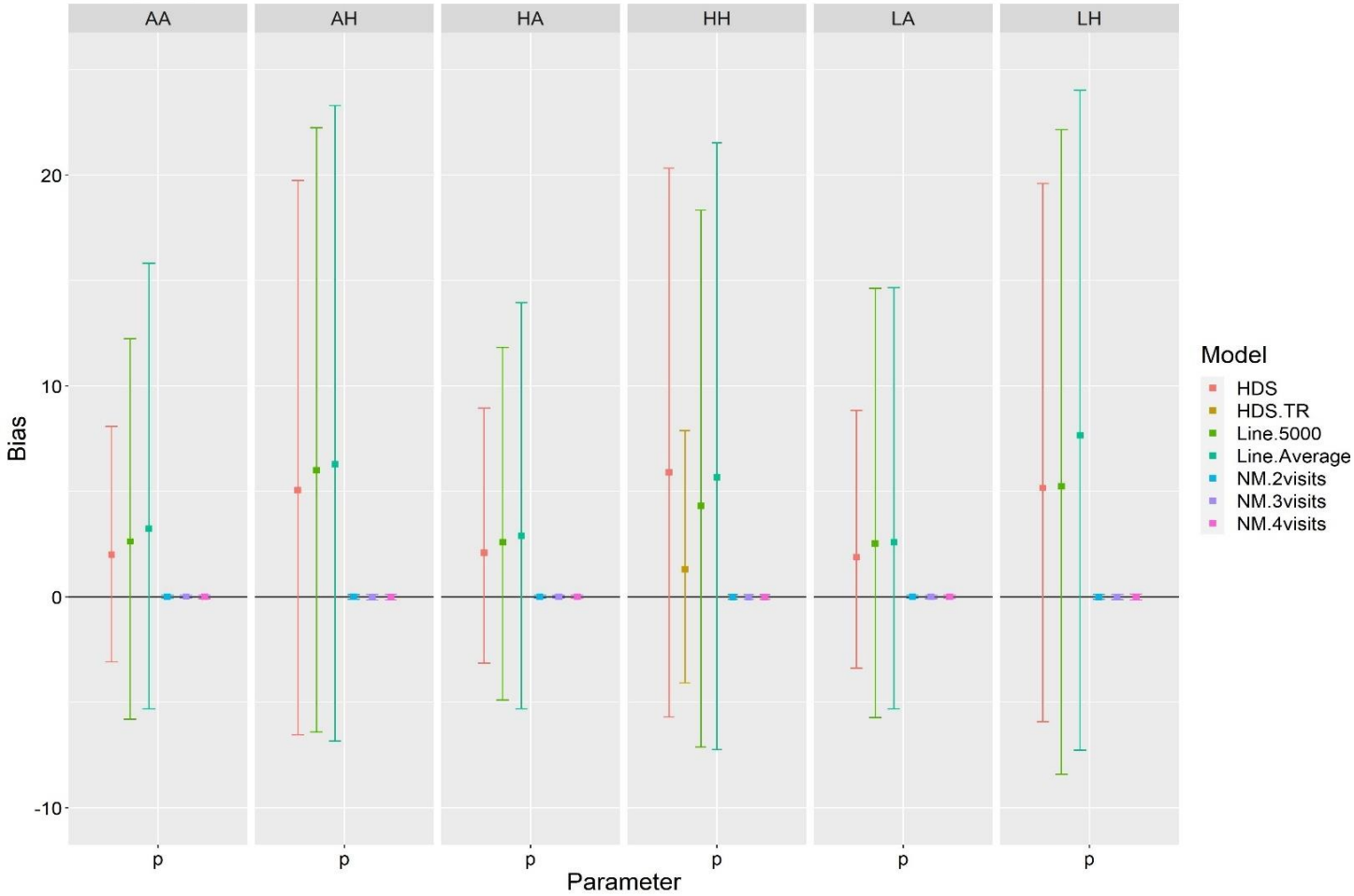

Figure 24. Bias with 90% credible intervals over 500 simulations under 6 scenarios with varying abundance and detection/ σ for probability of detection (N-mixture model) and σ (all hierarchical distance sampling models). Scenarios include, HA = high abundance, average detection, AA = average abundance, average detection, LA = low abundance, average detection, HH = high abundance, high detection, AH = average abundance, high detection, and LH = low abundance, high detection. There 7 models evaluated: HDS = hierarchical distance sampling for point counts, HDS.TR = time-removal HDS, Line.5000 = hierarchical distance sampling for line transects 5000m in length, Line.Average = hierarchical distance sampling for line transects of average (2,681m) length, and NM with varying visits = N-mixture model with either 2, 3, or 4 visits.

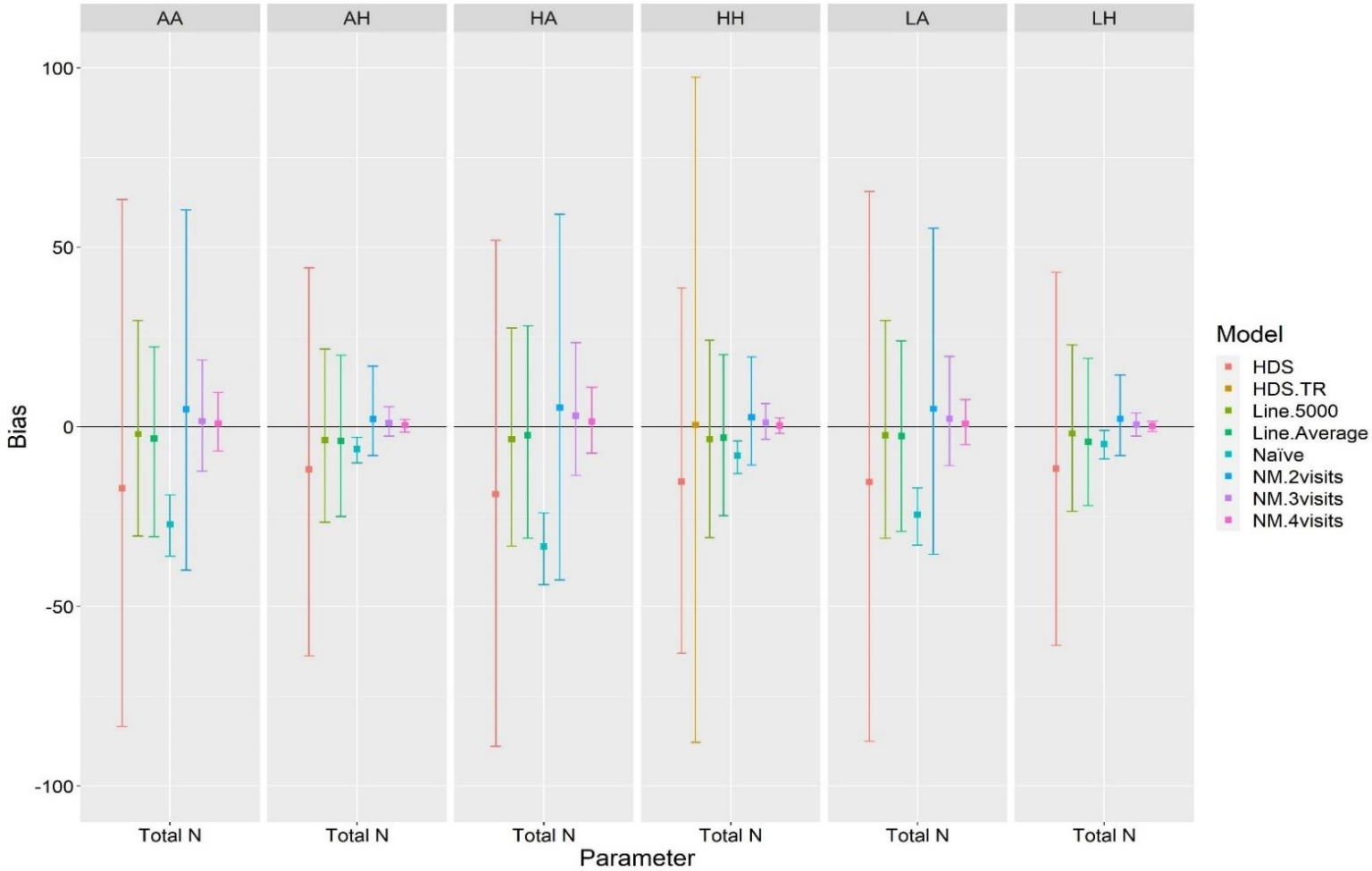

Figure 25. Bias with 90% credible intervals over 500 simulations under 6 scenarios with varying abundance and detection/ σ for total population size (Total N). Scenarios include, HA = high abundance, average detection, AA = average abundance, average detection, LA = low abundance, average detection, HH = high abundance, high detection, AH = average abundance, high detection, and LH = low abundance, high detection. There 7 models evaluated: HDS = hierarchical distance sampling for point counts, HDS.TR = time-removal HDS, Line.5000 = hierarchical distance sampling for line transects 5000m in length, Line.Average = hierarchical distance sampling for line transects of average (2,681m) length, and NM with varying visits = N-mixture model with either 2, 3, or 4 visits.

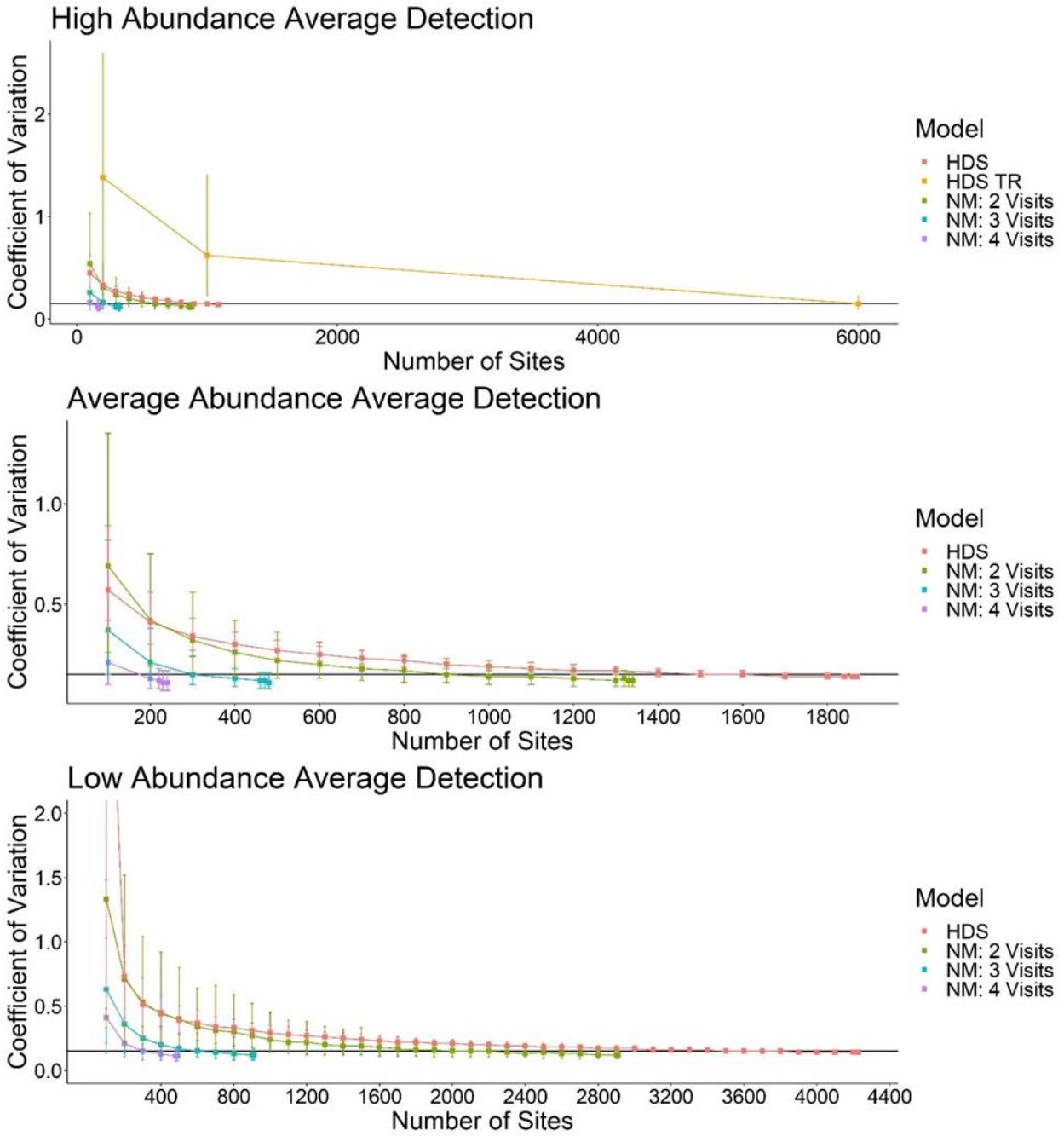

Figure 26. Coefficient of variation with 90% credible intervals for estimates of population size for number of sites visited under different protocols for N-mixture and hierarchical distance sampling models under different scenarios with varying abundance and average detection. For the N-mixture model, protocols with 2, 3, or 4 visits are evaluated. NM = N-mixture model, HDS = hierarchical distance sampling model, HDS TR = time-removal HDS. Horizontal line represents the goal of a coefficient of variation of 0.15 or lower.

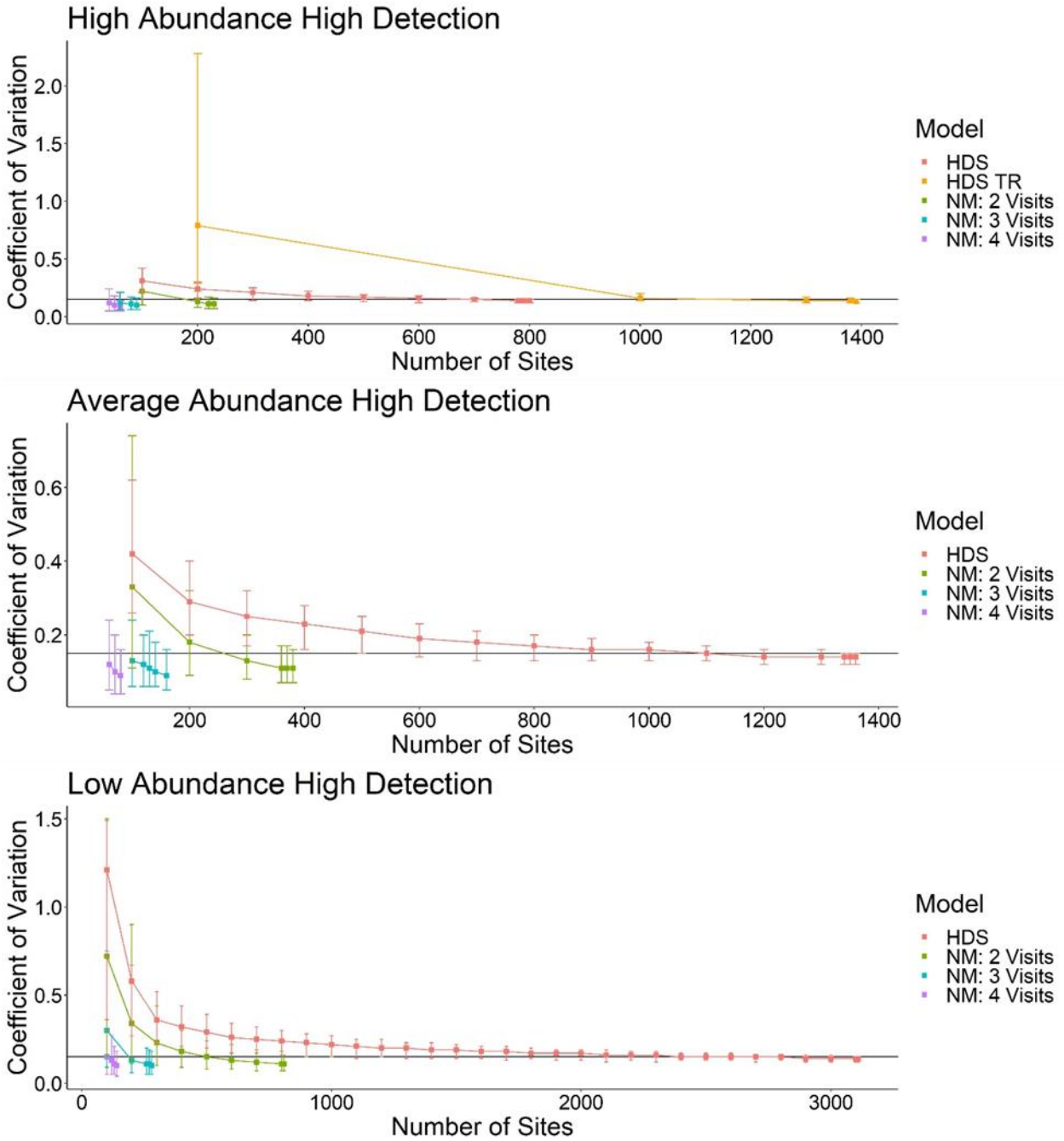

Figure 27. Coefficient of variation with 90% credible intervals for estimates of population size for number of sites visited under different protocols for N-mixture and hierarchical distance sampling models under different scenarios with varying abundance and high detection. For the N-mixture model, protocols with 2, 3, or 4 visits are evaluated. NM = N-mixture model, HDS = hierarchical distance sampling model, HDS TR = time-removal HDS. Horizontal line represents the goal of a coefficient of variation of 0.15 or lower.

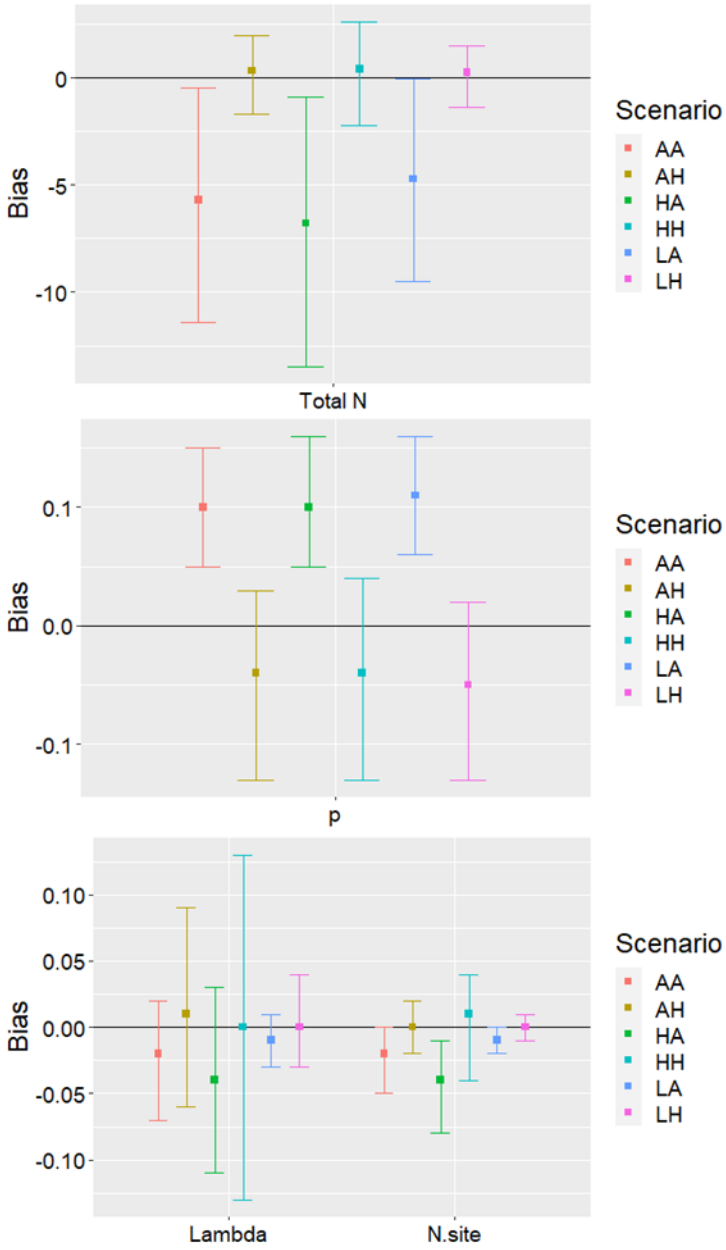

Figure 28. Bias with 90% credible intervals over 500 simulations under 6 scenarios with varying abundance and detection/ σ for total population size (Total N) for N-mixture models with correlated counts. Scenarios are HA = high abundance, average detection, AA = average abundance, average detection, LA = low abundance, average detection, HH = high abundance, high detection, AH = average abundance, high detection, and LH = low abundance, high detection. Models evaluated are the 'best' protocols from the N-mixture models with 4 visits.

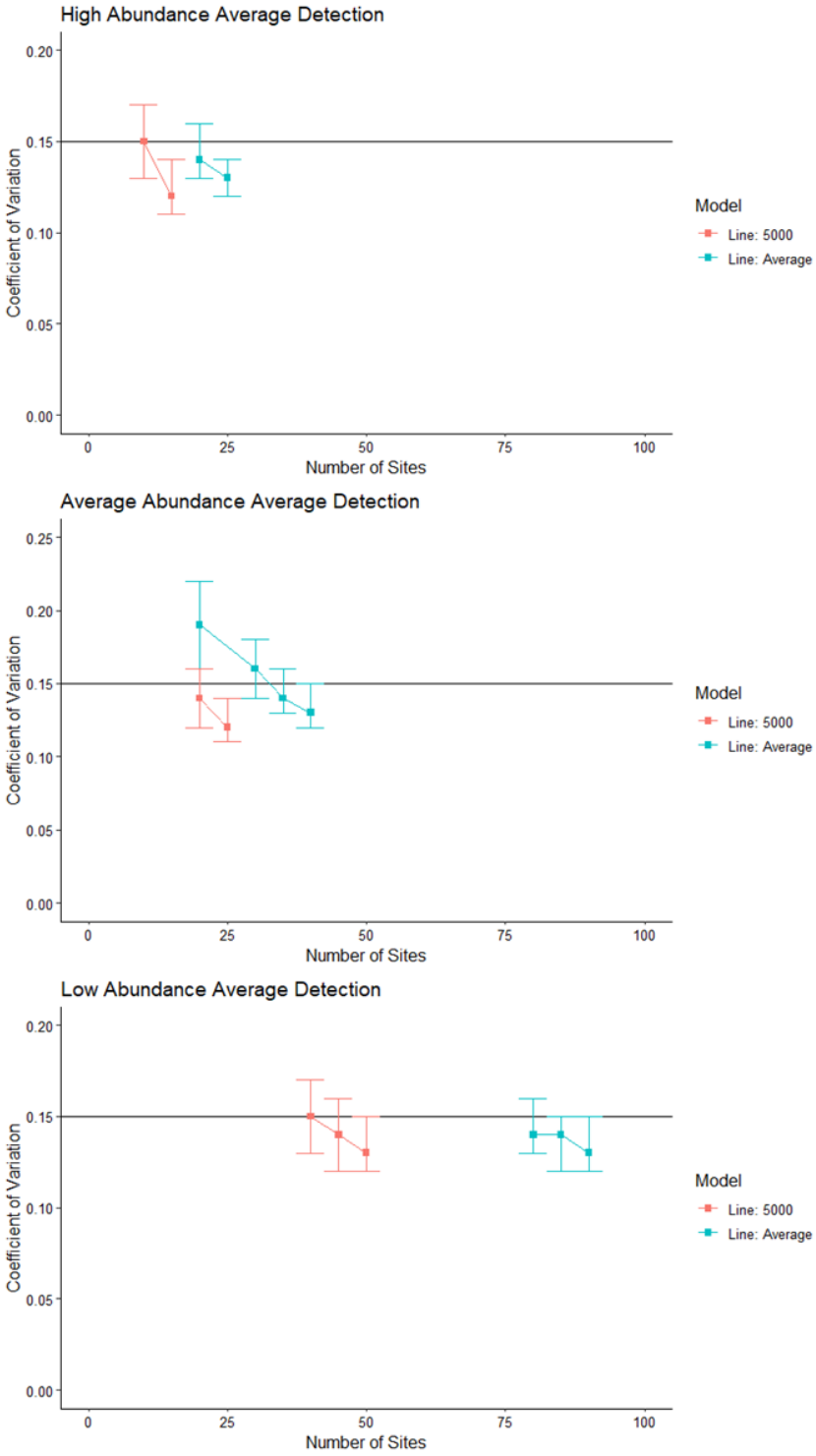

Figure 29. Coefficient of variation with 90% credible intervals for average transect length (2,681m) and 5,000m transect length across differing number of sites visited for three different scenarios where probability of detection was average and abundance varied (high, average, and low).

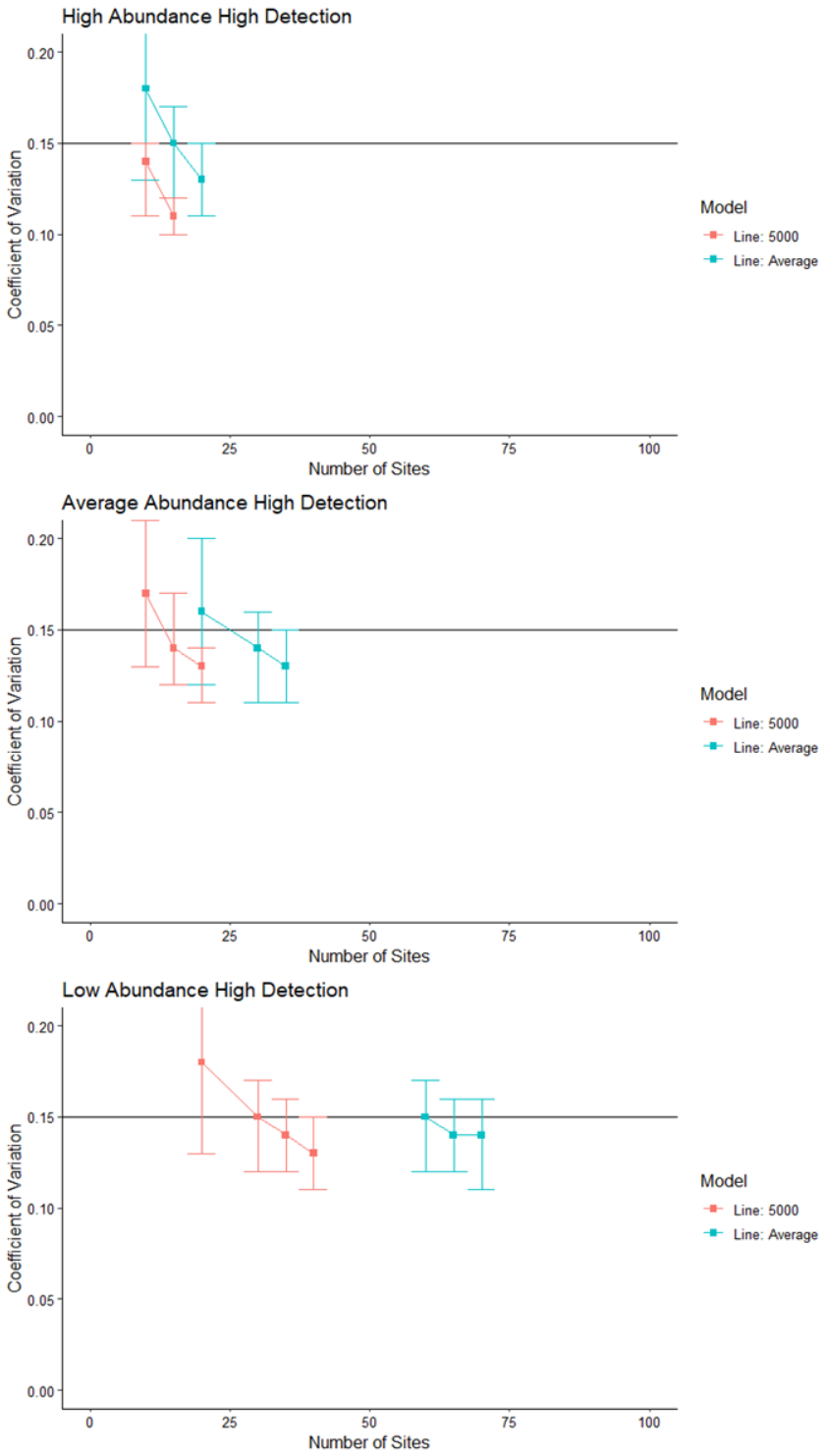

Figure 30. Coefficient of variation with 90% credible intervals for average transect length (2,681m) and 5,000m transect length across differing number of sites visited for three different scenarios where probability of detection was high and abundance varied (high, average, and low).

CONCLUSION

Population monitoring is an important aspect of conservation and management. Without accurate estimates of abundance, trends, and distributions, managers cannot effectively make conservation decisions, understand population trends, or assess changes in a species' range (Guisan et al. 2006, Joseph et al. 2009, Sillett et al. 2012, Sofaer et al. 2019). Understanding the relationship between environmental conditions, management actions and policies, and a species' population trend or distribution allows managers to make appropriate decisions for meeting management goals (Guisan et al. 2006, Sofaer et al. 2019, Doser et al. 2021). Population monitoring of game species is especially important, as information on population status, trends, and distributions affects harvest regulations (Aebischer and Baines 2008, Sands and Pope 2010). Due to limited resources, population monitoring programs must be developed and evaluated so that they provide the desired information while operating within resource constraints (Witmer 2005, Weiser et al. 2019).

Basic information such as population status, trends, habitat associations, and fine-scale distribution is lacking for Dusky Grouse, impeding the ability of managers to effectively make management decisions and designate appropriate hunting regulations. Our goal was to develop and test field methods and analyses for population monitoring of Dusky Grouse in Montana. To be useful for management, a standardized survey protocol must produce an unbiased and precise estimate/index of abundance or density that is relatively easy to describe and implement. Estimates are deemed precise and useful for informing management when they have ≤15% coefficient of variation. To provide recommendations for the creation of a Dusky Grouse population monitoring program in Montana, we 1) developed a species distribution model to

inform survey locations and explore habitat associations for Dusky Grouse, 2) surveyed Dusky Grouse across their range in Montana during different sampling periods using a variety of survey techniques and identified survey conditions and sampling methods that maximized detection, and 3) evaluated the ability of four statistical estimators under different abundance, detection, and survey effort scenarios to produce unbiased and precise estimates of abundance that met monitoring goals.

Using multiple techniques and an ensemble approach, we developed a species distribution model of potential Dusky Grouse habitat that had high predictive accuracy. As expected, we found that the MFWP Regions 1–3 had the most predicted Dusky Grouse habitat, as these areas of Montana are dominated by mountainous and coniferous forests. We also predicted Dusky Grouse habitat in similar areas (*e.g.*, mountainous and coniferous forests) of MFWP Regions 4–5. We found that Dusky Grouse were strongly associated with increased coverage of mid-old growth coniferous forest dominated by Douglas fir, lodgepole pine, and ponderosa pine, which corresponds with previous field-based documentation of Dusky Grouse habitat (Marshall 1946, Martinka 1972, Cade and Hoffman 1990, Cade and Hoffman 1993). The concurrence between previous field-based habitat associations for Dusky Grouse and our model results supported the validity of our predictive model.

We used two techniques when creating our ensemble model for Dusky Grouse distribution: resource selection functions and random forest. While both the random forest model and resource selection function model had high predictive accuracy, predictive accuracy was highest for the ensemble model. Even in MFWP Regions with no training data, such as MFWP Region 5, the models were still able to accurately predict the MFWP dataset of Dusky Grouse

locations as potential habitat. Given the model's high predictive accuracy and similarity in predicted habitat associations to those described in the literature, the model is usable for delineating survey sites for population monitoring. We used this model to determine study sites for evaluating different sampling and analytical methods for estimating Dusky Grouse abundance.

We found that sampling protocol affected the probability of detection for Dusky grouse and that methods traditionally used for grouse population monitoring may not be effective for Dusky Grouse monitoring in Montana. Dusky Grouse detections during the summer were almost non-existent, and spring surveys with electronic playback had much greater numbers of Dusky Grouse observations. Using chick distress calls for summer brood surveys has previously been found to elicit visual and auditory responses from females with broods (Stirling and Bendell 1966), but we did not find this to be the case. In line with previous studies, using female grouse calls (cackle and cantus) during the spring breeding season increased Dusky Grouse responses (Stirling and Bendell 1966, Harju 1974).

Temporal and environmental conditions such as day, minutes post sunrise, noise level, cloud cover, and temperature affected probability of detection of Dusky Grouse. Background noise level likely affected the ability of an observer to detect a grouse, as the majority of our detections were auditory. Most studies reported that, without electronic playback, the probability of detection is expected to peak with breeding behavior during the last week of April and first week of May in Montana, and around sunrise (Mussehl 1960, Mussehl 1963b, Bendell and Elliot 1967, Farnsworth 2020). One study demonstrated that using electronic playback kept the probability of detection consistent (Farnsworth 2020). However, we found that probability of

detection still peaked when electronic playback was used, and that the peaks in detection occurred on 3 May–23 May and 9–162 minutes post-sunrise. Previously studies have found variable associations between cloud cover and probability of detection for grouse (Evans et al. 2007, Farnsworth 2020), and we found that cloud cover negatively impacted Dusky Grouse detection. Detection was highest on clear days and lowest on days that were partly cloudy to fully overcast. We found the effect of temperature to be uncertain. Precipitation and wind speed did not show up in our top model due to being controlled for by the survey protocol and thus not having high variation during surveys. Optimal survey conditions were considered to be clear days with little cloud cover, wind, and no precipitation, during days and times of peak detection (*e.g.* 3 May–23 May and 9–162 minutes post-sunrise).

We identified two survey protocols and analyses that met our goal of producing unbiased estimates of abundance with a coefficient of variation ≤ 15% during periods of optimal survey conditions. The first protocol is a point-count survey protocol with 80 points per region and requires repeated (4) surveys at each point within a short period of time, as well as the use of recordings of female calls (cantus and cackle) to increase and estimate site-specific detection probabilities. This protocol and analysis resulted in precise enough estimates of an annual population index to be useful for monitoring and management. The second survey protocol is based on a line-transect distance sampling approach in which observers walk a 2.6–5 km transect and record the perpendicular distance from the transect to each grouse observation. Both survey protocols resulted in unbiased estimates of population abundance or density. The repeated point count protocol resulted in higher precision than the distance sampling protocol. However,

estimated precision of the distance sampling protocol met our monitoring goals when at least 35 transects of ≥ 2.6 km were surveyed in each area of inference (*e.g.*, MFWP Region).

Management Recommendations

Our habitat model can be used to delineate survey sites for monitoring Dusky Grouse in Montana. To maximize detection and lower the amount of observer effort needed, we recommend conducting surveys during the spring breeding season using female cackle and cantus calls. Surveying under optimal conditions is necessary for maximizing probability of detection, and therefore we recommend surveying between 3 May–23 May, and from sunrise to 2.5–3 hours post-sunrise. Surveys should occur on days with no precipitation and little to no wind. Probability of detection should also be estimated as a function of day, minutes since sunrise, background noise level, cloud cover, and temperature. Compared to line-transects, only a third of the needed transects are required for point-count surveys, and therefore we recommend a protocol of surveying 80 sites 4 times within a single morning, 2 surveys back-to-back on the way down the transect and 2 on the return transect. Counts should be analyzed using N-mixture models.

Population monitoring of Dusky Grouse will allow managers to track abundance and population status at the state level, as well investigate the impacts of management actions (*e.g.*, timber harvest) on Dusky Grouse populations. In addition, the data from population management will allow managers to justify hunting regulations for Dusky Grouse. Based on the results of our study, the Montana Department of Fish, Wildlife and Parks should be able to implement a population monitoring program for Dusky Grouse.

LITERATURE CITED

Aebischer, N. J., and D. Baines. 2008. Monitoring gamebird abundance and productivity in the UK: The GWCT long-term datasets. Revista Catalana d'Ornitologia 24:30-43.

Aldrich, J. W. 1963. Geographic orientation of American tetraonidae. Journal of Wildlife Management 27:528-545.

Aldridge, C. L., D. J. Saher, T. M. Childers, K. E. Stahlnecker, and Z. H. Bowen. 2012. Crucial nesting habitat for gunnison sage-grouse: A spatially explicit hierarchical approach. The Journal of Wildlife Management 76:391-406.

Ammann, G. A., and L. A. Ryel. 1963. Extensive methods of inventorying ruffed grouse in Michigan. Journal of Wildlife Management 27:617-633.

Amundson, C. L., J. A. Royle, C. M. Handel. 2014. A hierarchical model combining distance sampling and time removal to estimate detection probability during avian point counts. The Auk 131(4):476-494.

Anderson, E. M., R. J. Steidl. 2019. Power to detect trends in abundance within a distance sampling framework. Journal of Applied Ecology 57:344-353.

Araùjo, M. B., R. J. Whittaker, R. J. Ladle, and M. Erhard. 2005. Reducing uncertainty in projections of extinction risk from climate change. Global Ecology and Biogeography 14:529-538.

Araùjo, M. B., and New, M. 2006. Ensemble forecasting of species distributions. Trends in Ecology and Evolution. 22:42-47.

Araùjo, M. B., and A. Guisan. 2006. Five (or so) challenges for species distribution modeling. Journal of Biogeography 33:1677-1688.

Archibald, H. L. 1976. Spring drumming patterns of ruffed grouse. The Auk 93(4):808-829.

Arnold, T. W. 2010. Uninformative parameters and model selection using Akaike's information criterion. Journal of Wildlife Management 74:1175-1178.

Atwood, E. L. 1956. Validity of mail survey data on bagged waterfowl. Journal of Wildlife Management 20:1-16.

Barker, R. J., M. R. Schofield, W. A. Link, J. R. Sauer. 2018. On the reliability of N-mixture models for count data. Biometrics 74:369-377.

Barrowclough, G. F., J. G. Groth, L. A. Mertz, R. J. Guterrez. 2004. Phylogeographic structure, gene flow and species status in blue grouse (Dendragapus obscurus). Molecular Ecology 13:1911-1922.

Basile, M., R. Balestrieri, M. Posillico, A. Mancinelli, T. Altea, G. Matteucci. 2016. Measuring bird abundance – A comparison of methodologies between capture/recapture and audio-visual surveys. Avocetta 40:55-61.

Bates, D., M. Machler, B. Bolker, and S. Walker. 2015. Fitting linear mixed-effects models using lme4. Journal of Statistical Software 67:1-48.

Bendell, J. F., P. W. Elliot. 1967. Behavior and the regulation of numbers in blue grouse. Canadian Wildlife Service Report Series: 4, Department of Indian Affairs and Northern Development. Ottawa.

Bernales, H. H., J. D. Robinson, and B. Stringham. 2017. Utah Upland Game Annual Report 2016-17. State of Utah Department of Natural Resources, Division of Wildlife Resources.

Betts, M. G., D. Mitchell, A. W. Diamond, J. Bêty. 2006. Uneven rates of landscape change as a source of bias in roadside wildlife surveys. Journal of Wildlife Management 71(7):2266-2273.

Beyer, H. L. 2015. Geospatial Modeling Environment.Version 0.7.4.0.

Blackford, J. L. 1958. Territoriality and breeding behavior of a population of blue grouse in Montana. The Condor. 60(3):145-158.

Blackford, J. L. 1963. Further observations on the breeding behavior of a blue grouse population in Montana. The Condor. 65(6):485-513.

Bland, J. D. 2003. Estimating the number of territorial males in low-density populations of the sooty grouse. Western Birds 44:279-293.

Bohnett, E., D. Hulse, B. Ahmad, and T. Hoctor. 2020. Multi-level, multi-scale modeling and predictive mapping for jaguars in the Brazilian pantanal. Open Journal of Ecology 10:243-263.

Boyce, M. S., P. R. Vernier, S. E. Nielsen, and F. K. A. Schmiegelow. 2002. Evaluating resource selection functions. Ecological Modelling 157:281-300.

Breiman, L. 2001. Random forests. Machine learning 45:5-32.

Brooks, A. 1929. On *Dendragapus obscurus obscurus*. Auk 46:111-113.

Buckland, S.T., D. R. Anderson, K. P. Burnham, J. L. Laake, D. L. Borchers, and L. Thomas. 2001. Introduction to distance sampling estimating abundance of biological populations. Oxford University Press, Oxford.

Buckland, S. T., E. A. Rexstad, T. A. Marques, and C. S. Oedekoven. 2015. Distance Sampling: Methods and Applications. in A. P. Robinson, S. T. Buckland, P. Reich, and M. McCarthy, editors. Springer International Publishing.

Burnham, K. P., and D. R. Anderson. 2002. Model selection and multimodel inference A practical information-theoretic approach. Second edition. Springer, New York.

Cade, B. S., and R. W. Hoffman. 1990. Winter use of Douglas-Fir forests by blue grouse in Colorado. Journal of Wildlife Management 54:471-479.

Cade, B. S., and R. W. Hoffman. 1993. Differential migration of blue grouse in Colorado. The Auk 110:70-77.

Chan-McLeod, A., and F. L. Bunnell. 2003. Potential approaches to integrating silvicultural control of mountain pine beetle with wildlife and sustainable managment objectives. Pages 267-277 in T. L. Shore, J. E. Brooks, J. E. Stone, editors. Mountain Pine Beetle Symposium: Challenges and Solutions, Keowna, British Columbia, Canada. Natural Resources Canada, Canadian Forest Service, Pacific Forestry Centre, Information Report.

Colorado Parks and Wildlife. 2020. 2019-20 Small Game Harvest Report. Colorado Parks and Wildlife.

Crall, A. W., C. S. Jarnevich, B. Panke, N. Young, M. Renz, and J. Morisette. 2013. Using habitat suitability models to target invasive plant species surveys. Ecological Applications 23:60-72.

Conway, C. J., J. P. Gibbs. 2011. Summary of intrinsic and extrinsic factors affecting detection probablity of marsh birds. Wetlands 31:403-411.

Dahlgren, D. K., E. J. Blomberg, C. A. Hagan, R. D. Elmore. 2021. Upland game bird harvest management. In: K. L. Pope, L. A. Powell (eds) Harvest of fish and wildlife: new paradigms for sustainable management. CRC Press, Boca Raton, FL, USA, pp 307-326.

Dénes, F. V., L. F. Silveira, S. R. Beissinger, and N. Isaac. 2015. Estimating abundance of unmarked animal populations: accounting for imperfect detection and other sources of zero inflation. Methods in Ecology and Evolution 6:543-556.

DeSante, D. F., and T. L. George. 1994. Population trends in the landbirds of western North America. Studies in Avian Biology 15:173-190.

Dienes, Z. R. 2022. Multi-state analysis of August roadside surveys for monitoring ring-necked pheasant and northern bobwhite populations. Thesis. Iowa State University, USA.

Dinkins, J. B., K. J. Lawson, J. L. Beck. 2021. Influence of environmental change, harvest exposure, and human disturbance on population trends of greater sage-grouse. Plos One 16(9).

Doser, J. W., A. S. Weed, E. F. Zipkin, K. M. Miller, A. O. Finley. 2021. Trends in bird abundance differ among protected forests but not bird guilds. Ecological Applications 31(6).

Duarte, A., M. J. Adams, J. T. Peterson. 2018. Fitting N-mixture models to count data with unmodeled heterogeneity: bias, diagnostics, and alternative approaches. Ecological Modeling 374:51-59.

Dugger, K. M., F. Wager, R. G. Anthony, and G. S. Olson. 2005. The relationship between habitat characteristics and demographic performance of northern spotted owls in southern Oregon. The Condor 107:863-878.

Duque-Lazo, J., H. van Gils, T. A. Groen, and R. M. Navarro-Cerrillo. 2015. Transferability of species distribution models: The case of Phytophthora cinnamomi in southwest Spain and southwest Australia. Ecological Modelling 320:62-70.

Elith, J., C. H. Graham. 2009. Do they? How do they? Why do they differ? On finding reasons for differing performances of species distribution models. Ecography 32:66-77.

Espinosa, S. P., M. Scott, T. Donham, and S. Kimble. 2018. Small Game Status: 2018: Harvest Data and Population Status Report. Nevada Department of Wildlife.

Evans, S. A, S. M. Redpath, F. Leckie, and F. Mougeot. 2007. Alternative methods for estimating density in an upland game bird: the red grouse Lagopus lagopus scoticus. Wildlife Biology 13(2):130-139.

Evans, J. S., and S. A. Cushman. 2009. Gradient modeling of conifer species using random forests. Landscape Ecology 24:673-683.

Evans, J. S., M. A. Murphy, Z. A. Holden, and S. A. Cushman. 2011. Modeling species distribution and change using random forest. Pages 139-159 in Predictive species and habitat modeling in landscape ecology. Springer, New York.

Farnsworth, G. L., K. H. Pollock, J. D. Nichols, T. R. Simons, J. E. Hines, J. R. Sauer. 2002. A removal model for estimating detection probabilities from point-count surveys. The Auk 119(2):414-425.

Farnsworth, G. L., J. D. Nichols, J. R. Sauer, S. G. Fancy, K. H. Pollock, S. A. Shriner, T. R. Simons. 2005. Statistical approaches to the analysis of point count data: a little extra information can go a long way. USDA Forest Service Gen. Tech. Rep. PSW-GTR-191.

Farnsworth, Skyler Y. 2020. Forest grouse ecology and management in the Bear River Range northern Utah. Thesis. Utah State University, Logan, Utah.

Fielding, A. H., and J. F. Bell. 1997. A review of methods for the assessment of prediction errors in conservation presence/absence models. Environmental Conservation 24:38-49.

Fisk I., and R. Chandler. 2011. Unmarked: an R package for fitting hierarchical models of wildlife occurrence and abundance. Journal of Statistical Software 43(i10).

Ficetola, G. F., B. Barzaghi, A. Melotto, M. Muraro, E. Lunghi, C. Canedoli, E. L. Parrino, V. Nanni, I. Silva-Rocha, A. Urso, M. A. Carretero, D. Salvi, S. Scali, G. Scari, R. Pennati, F. Andreone, R. Manenti. 2018. N-mixture models reliably estimate the abundance of small vertebrates. Scientific Reports 8:10357.

Flanders-Wanner, B. L., G. C. White, and M. L. L. 2004. Validity of prairie grouse harvest-age ratios as production indices. Journal of Wildlife Management 68:1088-1094.

Franceschi, S., L. Nelli, C. Pisani, A. Franzoi, L. Fattorini, and A. Meriggi. 2014. A monte carlo appraisal of plot and distance sampling for surveys of black grouse and rock ptarmigan populations in alpine protected areas. The Journal of Wildlife Management 78:359-368.

Franklin, A.B., D.R. Anderson, R.J. Gutierrez, and K. P. Burnham. 2000. Climate, habitat quality, and fitness in northern spotted owl populations in northwestern California. Ecological Monographs 70: 539-590.

Fremgen A. L, C. P. Hansen, M. A. Rumble, R. S Gamo, J. J. Millspaugh. 2016. Male greater sage-grouse detectability on leks. The Journal of Wildlife Management. 80(2):266-274.

Fuller, L., M. Shewring, and F. M. Caryl. A novel method for targeting survey effort to identify new bat roosts using habitat suitability modeling. European Journal of Wildlife Research 64:31.

Furnas, B. J., D. S. Newton, G. D. Capehart, C. W. Barrows. 2019. Hierarchical distance sampling to estimate population sizes of common lizards across a desert ecoregion. Ecology and Evolution. 9:3046-3058.

Gates, E. 2019. Annual Report of Small Game, Migratory Birds, Furbearer, Wild Turkey, and Falconry Harvest for the biological year June 1, 2018 – May 31, 2019. Wyoming Game and Fish Deparment.

Gelman, A., and D. B. Rubin. 1992. Inference from iterative simulation using multiple sequences. Statistical Science 7:457-511.

Gibbs, J. P., and S. M. Melvin. 1997. Power to detect trends in waterbird abundance with call-response surveys. The Journal of Wildlife Management 61:1262-1267.

Gibbs, J. P., H. L. Snell, C. E. Causton. 1999. Effective monitoring for adaptive wildlife management: lessons for the Galápagos Islands. The Journal of Wildlife Management 63:1055-1065.

Grenouillet, G., L. Buisson, N. Casajus, and S. Lek. 2011. Ensemble modelling of species distribution: the effects of geographical and environmental ranges. Ecography 34:9-17.

Guisan, A., and N. E. Zimmerman. 2000. Predictive habitat distribution models in ecology. Ecological Modelling 135:147-186.

Guisan, A., T. C. J. Edwards, and T. Hastie. 2002. Generalized linear and generalized additive models in studies of species distributions: setting the scene. Ecological Modelling 157:89-100.

Guisan, A., and W. Thuiller. 2005. Predicting species distribution: offering more than simple habitat models. Ecology Letters 8:993-1009.

Guisan, A., O. Broennimann, R. Engler, M. Vust, N. G. Yoccoz, A. Lehmann, and N. Zimmerman. 2006. Using niche-based models to improve the sampling of rare species. Conservation Biology. 20:501-511.

Guisan, A., R. Tingley, J. B. Baumgartner, I. Naujokaitis-Lewis, P. R. Sutcliffe, A. I. Tulloch, T. J. Regan, L. Brotons, E. McDonald-Madden, C. Mantyka-Pringle, T. G. Martin, J. R. Rhodes, R. Maggini, S. A. Setterfield, J. Elith, M. W. Schwartz, B. A. Wintle, O. Broennimann, M. Austin, S. Ferrier, M. R. Kearney, H. P. Possingham, and Y. M. Buckley. 2013. Predicting species distributions for conservation decisions. Ecology Letters 16:1424-1435.

Guisan, A., W. Thuiller, and N. E. Zimmerman. 2017. Habitat suitability and distribution models, with applications in R. Cambridge University Press, New York, NY.

Hagen, C. A., and T. M. Loughin. 2008. Productivity Estimates From Upland Bird Harvests: Estimating Variance and Necessary Sample Sizes. Journal of Wildlife Management 72:1369-1375.

Hamm, C. A. 2013. Estimating abundance of the federally endangered Mitchell's satyr butterfly using hierarchical distance sampling. Insect Conservation and Diversity. 6:619-626.

Hanni, D. J., C. M. White, N. J. V. Lanen, J. J. Birek, J. M. Berven, and M. F. McLaren. 2018. Integrated monitoring in bird conservation regions (IMBCR): Field protocol for spatially-balanced sampling of land bird populations.

Hannon, S. J. 1980. The cackle call of female blue grouse: does it have a mating or aggressive function? The Auk. 92(2):404-407.

Hanowski, J. M., and G. J. Niemi. 1995. A comparison of on- and off-road bird counts: do you need to go off road to count birds accurately? Journal of Field Ornithology 66(4):469-483.

Hansen, M. C., C. A. Hagen, D. A. Budeau, V. L. Coggins, and B. S. Reishus. 2015. Comparison of 3 surveys for estimating forest grouse population trends. Wildlife Society Bulletin 39:197-202.

Harju, H. J. 1974. An analysis of some aspects of the ecology of dusky grouse. Thesis. University of Wyoming, USA.

Heikkinen, R. K., M. Marmion, and M. Luoto. 2012. Does the interpolation acurracy of species distribution models come at the expense of transferability? Ecography 35:276-288.

Heinze, G., C. Wallisch, and D. Dunkler. 2018. Variable selection – A review and recommendations for the praticing statistician. Biometrical Journal 60:431-449.

Heward, C. J., A. Lowe, G. J. Conway, A. N. Hoodless. 2019. Influence of weather on the Eurasian woodcock's breeding display. Proceedings of the American Woodcock Symposium 11:209-216.

Hosmer, D. W., S. Lemeshow, and R. X. Sturdivant. 2013. Applied logistic regression. Wiley, New York.

Jakob, C., F. Ponce-Boutin, A. Besnard, C. Eraud. 2010. On the efficiency of using song playback during call count survyes of Red-legged partridges (Alectoris rufa). European Journal of Wildlife Research 56:907-913.

Jakob, C., F. Ponce-Boutin, and A. Besnard. 2014. Coping with heterogeneity to detect species on a large scale: N-mixture modeling applied to red-legged partridge abundance. The Journal of Wildlife Management 78:540-549.

Johnsgard, P.A. 2016. The North American grouse: their biology and behavior. Zea Books, Lincoln, NE.Johnson, C. J., S. E. Nielsen, E. H. Merril, T. L. McDonald, and M. S. Boyce. 2006. Resource selection functions based on use-availability data: theoretical motivation and evaluationg methods. Journal of Wildlife Management 70:347-357.

Johnson, R. R., B. T. Brown, L. T. Haight, J. M. Simpson. 1981. Playback recordings as a special avian censusing technique. Studies in Avian Biology 6:68-75.

Johnson, C. J., S. E. Nielsen, E. H. Merril, T. L. McDonald, and M. S. Boyce. 2006. Resource selection functions based on use-availability data: theoretical motivation and evaluationg methods. Journal of Wildlife Management 70:347-357.

Joseph, L. N., C. Elkin, T. G. Martin, H. P. Possingham. 2009. Modeling abundance using N-mixture models: the importance of considering ecological mechanisms. Ecological Applications 19(3):631-642.

Katayama, N., Y. Odaya, T. Amano, H. Yoshida. 2020. Spatial and temporal associations between fallow fields and greater painted snipe density in Japanese rice paddy landscapes. Agriculture, Ecosystems and Environment 295.

Kidwai, Z., J. Jimenez, C. J. Louw, H. P. Nel, J. P. Marshal. 2019. Using N-mixture models to estimate abundance and temporal trends of black rhinoceros (Diceros bicornis L.) populations from aerial counts. Global Ecology and Conservation 19:e00687.

Kellner, K. 2019. jagsUI: A wrapper around 'rjags' to streamline 'Jags' analyses. R package version 1.5.1.

Kéry, M. 2008. Estimating abundance from bird counts: binomial mixture models uncover complex covariate relationships. The Auk 152:336-345.

Kéry, M., J. A. Royle, H. Schmid. 2005. Modeling avian abundance from replicated counts using binomial mixture models. Ecological Applications 15(4):1450-1461.

Kéry, M. 2018. Identifiability in N-mixture models: a large-scale screening test with bird data. Ecology 99(2):281-288.

Kéry, M., and J. A. Royle. 2016. Applied hierarchical modeling in ecology: analysis of distribution, abundance, and species richness in R and BUGS. Academic Press, London, United Kingdom.

Kéry, M., and M. Schaub. 2012. Bayesian Population Analysis Using WinBugs A hiearchical perspective. Elsevier Inc.

Knape, J., D. Arlt, F. Barraquand, Å. Berg, M. Chevalier, T. Pärt, A. Ruete, M. Żmihorski. 2018. Sensitivity of binomial N-mixture models to overdispersion: the importance of assessing model fit. Methods in Ecology and Evolution 9:2102-2114.

Kuhn, M. 2008. Caret package. Journal of Statistical Software 28.

Kuhn, M., and K. Johnson. 2013. Applied Predictive Modeling. Springer.

Kuhn, M. 2019. Building Predictive Models in R Using the caret Package. Journal of Statistical Software 28(5):1-26.

LANDFIREa. 2016. LANDFIRE Existing Vegetation Canopy Layer, LANDFIRE 2016 Remap (LF 2.0.0). U.S. Department of the Interior, Geological Survey. http://landfire.cr.usgs.gov/viewer/. Accessed September 2020.

LANDFIREb. 2016. LANDFIRE Existing Vegetation Height Layer, LANDFIRE 2016 Remap (LF 2.0.0). U.S. Department of the Interior, Geological Survey. http://landfire.cr.usgs.gov/viewer/. Accessed September 2020.

LANDFIREc. 2016. LANDFIRE Existing Vegetation Type Layer, LANDFIRE 2016 Remap (LF 2.0.0). U.S. Department of the Interior, Geological Survey. http://landfire.cr.usgs.gov/viewer/. Accessed September 2020.

LANDFIRE. 2019. LANDFIRE product descriptions with references. U.S. Department of the Interior, Geological Survey.

LANDFIRE. 2020. LANDFIRE 2016 Remap (LF 2.0.0). U.S. Department of the Interior, Geological Survey.

Latif, Q. S., V. A. Saab, J. G. Dudley, and J. P. Hollenbeck. 2013. Ensemble modeling to predict habitat suitability for a large-scale disturbance specialist. Ecology and Evolution 3:4348-4364.

Le Lay, G., R. Engler, E. Franc, and A. Guisan. 2010. Prospective sampling based on model ensembles improves the detection of rare species. Ecography 33:1015-1027.

Lewis, W. B., R. B. Chandler, C. D. Delancey, E. Rushton, G. T. Wann, M. D. McConnell, J. A. Martin. 2022. Abundance and distribution of ruffed grouse Bonasa umbellus at the southern periphery of the range. Wildlife Biology.

Liaw, A., and M. Wiener. 2002. Classification and regression by randomForest. R News 2:18-22.

Link, W. A., M. R. Schofield, R. J. Barker, J. R. Sauer. 2018. On the robustness of N-mixture models. Ecology 99(7):1547-1551.

MacKenzie, D. I., and J. A. Royle. 2005. Designing occupancy studies: General advice and allocating survey effort. Journal of Applied Ecology 42(6):1105-1114.

MacKenzie, D. I., J. D. Nichols, N. Sutton, K. Kawanishi, L. L. Bailey. 2005. Improving inferences in population studies of rare species that are detected imperfectly. Ecology 86(5):1101-1113.

Manly, B. F. J., L. L. McDonald, D. L. Thomas, T. L. McDonald, and W. P. Erickson. 2002. Resource selection by animals statistical design and analysis for field studies. Second edition. Kluwer Academic Publishers, New York.

Marmion, M., M. Parviainen, M. Luoto, R. K. Heikkinen, and W. Thuiller. 2009. Evaluation of consensus methods in predictive species distribution modeling. Diversity and Distributions 15:59-69.

Marshall, W. 1946. Cover preferences, seasonal movements, and food habits of Richardson's grouse and ruffed grouse in southern Idaho. The Wilson Bulletin 1:42-52.

Martinka, R. R. 1972. Structural characteristics of blue grouse territories in southwestern Montana. Journal of Wildlife Management 36:498-510.

McCaffery, R., J. J. Nowak, and P. M. Lukacs. 2016. Improved analysis of lek count data using N-mixture models. The Journal of Wildlife Management 80:1011-1021.

McIntyre, A. P., J. E. Jones, E. M. Lund, F. T. Waterstrat, J. N. Giovanini, S. D. Duke, M. P. Hayes, T. Quinn, A. J. Kroll. 2012. Empirical and simulation evaluations of an abundance estimator using unmarked individuals of cryptic forest-dwelling taxa. Forest Ecology and Management 286:129-136.

McNeil, D. J., C. R V. Otto, E. L. Moser, K. R. Urban-Mead, D. E. King, A. D. Rodewald, J. L. Larkin. 2019. Distance models as a tool for modelling detection probability and density of native bumblebees. Journal of Applied Entomology. 143:225-235.

McNew, L. B., A. J. Gregory, and B. K. Sandercock. 2013. Spatial heterogeneity in habitat selection: Nest site selection by greater prairie-chickens. The Journal of Wildlife Management 77:791-801.

McNew, L. B., D. R. Dwayne Elmore, C. A. Hagan. 2023. Prairie Grouse. In: McNew, L. B., Dahlgren, D. K., Beck, J. L. (eds) Rangeland Wildlife Ecology and Conservation. Spring, Cham.

McNew, L. B., V. L. Winder, J. C. Pitman, and B. K. Sandercock. 2015. Alternative rangeland management strategies and the nesting ecology of greater prairie-chickens. Rangeland Ecology & Management 68:298-304.

Montana Fish, Wildlife and Parks. 2021. Upland Game Bird Annual Harvest Reports. Montana Fish, Wildlife and Parks.

Montana Spatial Data Infrastructure (MSDI). 2017. Transportation Framework. Montana State Library. http://geoinfo.msl.mt.gov/msdi/hydrography Accessed September 2018.

Montana Spatial Data Infrastructure (MSDI). 2018. Hydrography. Montana State Library. http://geoinfo.msl.mt.gov/msdi/transportation/ Accessed September 2018.

Morelli, F., V. Brlik, Y. Benedetti, R. Bussière, L. Moudrá, J. Reif, M. Svitok. 2022. Detection rate of bird species and what it depends on: tips for field surveys. Ecology and Evolution 9.

Mozerolle, M. J. 2020. AICcmodavg: model selection and multimodel inference based on (Q)AIC(c). R package version 2.3-1.

Mussehl, T. W. 1960. Blue grouse production, movements, and populations in the Bridger Mountains, Montana. Journal of Wildlife Management 24:60-68.

Mussehl, T. W. 1963. Blue grouse brood cover selection and land-use implications. Journal of Wildlife Management 27:546-555.

Mussehl, T. W. 1963b. Small Game Research Project, Blue Grouse Population Study Report W-91-R-5. Montana Fish Wildlife and Parks, Montana, USA.

Neubauer G., and A. Sikora. 2020. Abundance estimation from point counts when replication is spatially-intensive but temporally limited: comparing binomial N-mixture and hierarchical distance sampling models. Ornis Fennica 97:131-148.

Newell, J. 2016. Survey and Inventory Protocols in Montana: upland game birds. Montana Department of Fish, Wildlife, and Parks technicial report.

New Mexico Game and Fish. 2020. 2019-20 New Mexico Small Game Voluntary Harvest Reports. New Mexico Game and Fish.

Nichols, J. D., L. Thomas, P. B. Conn. 2009. Inferences about landbird abundance from count data: Recent advances and future directions. In: Thomson, D. L., E. G. Cooch, M. J. Conroy (eds) Environmental and Ecological Statistics volume 3, Modeling demographic processes in marked populations, Environmental and Ecological Statistics 3, Springer, New York.

Oregon Department of Fish & Wildlife. 2023. Ladd Marsh Wildlife Area game bird harvest statistics. Oregon Department of Fish & Wildlife.

Pavlacky, D. C. J., J. A. Lukacs, R. C. Blakesley, D. S. Skokowsky, D. S. Klute, B. A. Hahn, V. J. Dreitz, T. L. George, and D. J. Hanni. 2017. A statistically rigours sampling design to integrate avian monitoring and management within Bird Conservation Regions. PLoS One 12.

Pearson, R. G., W. Thuiller, M. B. Araùjo, E. Martinez-Meyer, L. Brotons, C. McClean, L. Miles, P. Segurado, T. P. Dawson, and D. C. Lees. 2006. Model-based uncertainty in species range prediction. Journal of Biogeography 33:1704-1711.

Pelren, E. C., and J. A. Crawford. 1999. Blue grouse nesting parameters and habitat associations in northeastern Oregon. The Great Basin Naturalist 59:368-373.

Plummer, M. 2003. JAGS: A program for analysis of bayesian graphical models using gibbs sampling. Proceedings of the 3rd International workshop on distributed statistical computing, April 2005, Vienna, Austria.

Pollock, K. H., J. D. Nichols, T. R. Simons, G. L. Farnsworth, L. L. Bailey, J. R. Sauer. 2002. Large scale wildlife monitoring studies: statistical methods for design and analysis. Environmetrics 13:105-119.

Powell, L. A., J. S. Taylor, and T. W. Matthews. 2011. Adaptive Harvest Managment and harvest mortality of Greater Prairie-Chickens. Pages 329-339 in B. K. Sanderock, K. Martin, and G. Segelacher, editors. Ecology, conservation and management of grouse. Studies in Avian Biologty. University of California Press, Berkeley, CA.

R Core Team. 2017. R: A language and environment for statistical computing. R Foundation for Statistical Computing, Vienna, Austria..

Randin, C. F., T. Dirnböck, S. Dullinger, N. E. Zimmerman, M. Zappa, and A. Guisan. 2006. Are niche-based species distribution models transferable in space? Journal of Biogeography. 33:1689-1703.

Redfield, J. A. 1973. Demography and genetics in colonizing populations of blue grouse (Dendragapus obscurus). Evolution 27:576-592.

Reidy, J. L. and F. R. Thompson. 2021. Density and habitat associations of the Woodhouse's scrub-jay in central Texas. The Southwestern Naturalist 66(1):5-12.

Riley, I. P., C. J. Conway, B. S. Stevens, S. B. Roberts. 2021. Aural and visual detection of greater sage-grouse leks: implications for population trend estiamtes. The Journal of Wildlife Management 85(3):508-519.

Robbins, C. 1981. Bird activity levels related to weather. Studies in Avian Biology 6:301-310.

Rogers, G. E. 1963. Blue grouse census and harvest in the United States and Canada. Journal of Wildlife Management 27:579-585.

Romano, A., A. Costa, M. Basile, R. Raimondi, M. Posillico, D. S. Roger, A. Crisci, R. Piraccini, P. Raia, G. Matteucci, B. De Cinti. 2017. Conservation of salamanders in managed forests: Methods and costs of monitoring abundance and habitat selection. Forest Ecology and Management 400:12-18.

Rosenstock, S. S., D. R. Anderson, K. M. Giesen, T. Leukering, and M. F. Carter. 2002. Landbird counting techniques: current practices and an alternative. The Auk 119:46-53.

Roy, C. L., J. H. Giudice, C. Scharenbroich. 2020. Evaluation of cantus-call and pellet surveys for Spruce Grouse (Falicpennis canadensis canace) at the southern extent of their range. Journal of Field Ornithology 91(1):44-63.

Royle, J.A. 2004. N-mixture models for estimating population size from spatially replicated counts. Biometrics 60:108–115.

Royle, J. A., D. K. Dawson, and S. Bates. 2004. Modeling abundance effects in distance sampling. Ecology 85:1591-1997.

Royle, J. A., J. D. Nichols, M. Kery, and E. Ranta. 2005. Modelling Occurrence and Abundance of Species When Detection Is Imperfect. Oikos 110:353-359.

Rusk, J. P., F. Hernández, J. A. Arredondo, F. Hernández, F. C. Bryant, D. G. Hewitt, E. J. Redeker, L. A. Brennan, R. L. Bingham. 2007. An evaluation of survey methods for estimating northern bobwhite abundance in southern Texas. The Journal of Wildlife Management 71(4):1336-1343.

Sands, J. P., and M. D. Pope. 2010. A survey of galliform monitoring programs and methods in the United States and Canada. Wildlife Biology 16:342-356.

Sauer, J. R., W. A. Link, and J. E. Hines. 2020. The North American breeding bird survey, analysis results 1966-2019. in U.S. Geological Survey data release.

Schroeder, M. A. 2006. Blue grouse Dendragapus obscurus are not considered to be two species: dusky grouse Dendragapus obscurus and sooty grouse Dendragapus fuliginosus. Grouse News 32, Newsletter of Grouse Specialist Group.

Schroeder, M. A. 2010. Progress Report: Harvest Management of Forest Grouse in Washington, with a focus in north-central Washington. Washington Department of Fish and Wildlife.

Scott, M. J., F. L. Ramsey, and C. B. Kepler. 1981. Distance estimation as a variable in estimating bird numbers from vocalizations. Studies in Avian Biology 6:334-340.

Sillett, T. S., R. B. Chandler, J. A. Royle, M. Kery, and S. A. Morrison. 2012. Hierarchical distance-sampling models to estimate population size and habitat-specific abundance of an island endemic. Ecological Applications 22:1997-2006.

Simons, T. R., M. W. Alldredge, K. H. Pollock, and J. M. Wettroth. 2007. Experimental analysis of the auditory detection process on avian point counts. The Auk 124:986-999.

Sofaer, H. R., C. S. Jarnevich, I. S. Pearse, R. L. Smyth, S. Auer, G. L. Cook, T. C. Edwards Jr. G. F. Guala, T. G. Howard, J. T. Morisette, and H. Hamilton. 2019. Development and delivery of species distribution models to inform decision-making. BioScience 69:544-557.

Sollman, R., B. Gardner, R. B. Chandler, J. A. Royle, and T. S. Sillet. 2015. An open-population hierarchical distance sampling model. Ecology 96:325-331.

Stauffer, D. F., and S. Peterson, R. 1986. Seasonal microhabitat relationships of blue grouse in southeastern Idaho. The Great Basin Naturalist 46:117-122.

Steidl, R. J., C. J. Conway, A. R. Litt. 2013. Power to detect trends in abundance of secretive marsh birds: effects of species trais and sampling effort. The Journal of Wildlife Management 77(3):445-453.

Stirling, I. and J. F. Bendell. 1966. Census of blue grouse with recorded calls of a female. The Journal of Wildlife Management. 30: 184-187.

Stohlgren, T. J., P. Ma, S. Kumar, M. Rocca, J. T. Morisette, C. S. Jarnevich, and N. Benson. 2010. Ensemble habitat mapping of invasive plant species. Risk Analysis 30:224-235.

Sturtz, S., U. Ligges, A. Gelman. 2005. R2WinBUGS: A package for running WinBUGS from R. Journal of Statistical Software 12(3):1-16.

Sullins, D. S., W. C. Conway, D. A. Haukos, C. E. Comer. 2019. Using pointing dogs and hierarchcial models to evaluate American woodcock winter occupancy and density. Proceedings of the 11th American woodcock symposium 11:154-167.

Thomas, A. 2006. The R Journal: The BUGS language. R News 6(1):17-21.

Thomas, L., S. T. Buckland, E. A. Rexstad, J. L. Laake, S. Strindberg, S. L. Hedley, J. R. Bishop, T. A. Marques, and K. P. Burnham. 2010. Distance software: design and analysis of distance sampling surveys for estimating population size. Journal of Applied Ecology 47:5-14.

Thompson, W. L. 2002. Towards Reliable bird surveys: accounting for individuals present but not detected. The Auk 119:18-25.

U.S. Geological Survey. 2017. The National Map. 3DEP products and services: The National Map, 3D Elevation Program Web page, https://nationalmap.gov/3DEP/3dep_prodserv.html. Accessed September 2018.

United States. National Weather Service. United States, 2023. Web Archive. https://www.weather.gov/wrh/Climate?wfo=mso. Accessed September 2023.

Warren, P., and D. Baines. 2011. Evaluation of the distance sampling technique to survey red grouse Lagopus lagopus scotius on moors in northern England. Wildlife Biology 17:135-142.

Washington Department of Fish and Wildlife. 2022. 2022 Game status and trend report. Wildlife Program, Washington Department of Fish and Wildlife, Olympia, Washington, USA.

Weiser, E. L., J. E. Diffendorfer, L. López-Hoffman, D. Semmens, W. E. Thogmartin. 2019. Consequences of ignoring spatial variation in population trend when conducting a power analysis. Ecography 42:836-844.

Wiest, W. A., M. D. Correll, B. G. Marcot, B. J. Olsen, T. P. Hodgman, G. R. Guntenspergen, W. G. Shriver. 2019. Estimates of tidal-marsh bird densities using Bayesian networks. The Journal of Wildlife Management. 83(1):109-120.

Williams, J. N., C. Seo, J. Thorne, J. K. Nelson, S. Erwin, J. M. O'Brien, and M. W. Schwartz. 2009. Using specie distribution models to predict new occurrences for rare plants. Diversity and Distributions 15:565-576.

Witmer, G. 2005. Wildlife population monitoring: some practical considerations. Wildlife Research. 32:259-263.

Woiderski, B. J., N. E. Drilling, J. M. Timmer, M. F. McLaren, C. M. White, N. J. Van Lanen, D.C. Pavlacky Jr., and R. A. Sparks. 2018. Integrated monitoring in bird conservation

regions (IMBCR): 2017 field season report. Bird Conservancy of the Rockies. Brighton, Colorado, USA.

Yamaura, Y. 2013. Confronting Imperfect Detection: Behavior of Binomial Mixture Models under Varying Circumstances of Visits, Sampling Sites, Detectability, and Abundance, in Small-Sample Situations. Ornithological Science 12:73-88.

Yip, D. A., E. M. Bayne, P. Sólymos, J. Campbell, D. Proppe. 2017. Sound attenuation in forest and roadside environments: Implications for avian point-count surveys. The Condor 119:73-84.

Youtz, Joseph, J. K. Frey, and R. Goljani. 2022. Modeling the impact of climate change and wildfire on the dusky grouse (Dendragapus obscurus) in the American Southwest: implications for conservation. Avian Conservation and Ecology 17(1):35.

Zimmerman, G. S. and R. J. Gutiérrez. 2007. The influence of ecological factors on detecting drumming ruffed grouse. The Journal of Wildlife Management. 71(6): 1765-1772.

Zurr, A. F. 2009. Mixed effects models and extensions in ecology with R. Springer, New York.

Zweig, M. H., and G. Campbell. 1993. Receiver-operating characteristic (ROC) plots: A fundamental evaluation tool in clinical medicine. Clinimal Chemistry 39:567-577.

Zwickel, F. C. 1973. Dispersion of female blue grouse during the brood season. The Condor 75:114-119.

Zwickel, F.C. 1990: Blue grouse—In: Davis, D.E. (Ed.); Handbook ofcensus methods for terrestrial vertebrates. 5th edition. CRC Press, Inc., Boca Raton, Florida, USA, pp. 63-65.

Zwickel, F. C., and J. F. Bendell. 2004. Blue grouse: Their biology and natural history. NRC Research Press, Ottawa, Ontario, Canada.

APPENDICES

APPENDIX A

APPENDIX A: DESCRIPTION OF HABITAT VARIABLES

Table A1. Description of habitat variables (LANDFIRE 2016a, b, c).

Variable	Source	EVT Code (Ecological Systems)	Statistic	Vegetation Physiognomy
North (N) Facing Aspect	DEM	N/A	Proportion	N/A
Northeast (NE) Facing Aspect	DEM	N/A	Proportion	N/A
East (E) Facing Aspect	DEM	N/A	Proportion	N/A
Southeast (SE) Facing Aspect	DEM	N/A	Proportion	N/A
South (S) Facing Aspect	DEM	N/A	Proportion	N/A
Southwest (SW) Facing Aspect	DEM	N/A	Proportion	N/A
West (W) Facing Aspect	DEM	N/A	Proportion	N/A
Northwest (NW) Facing Aspect	DEM	N/A	Proportion	N/A
Flat Aspect	DEM	N/A	Proportion	N/A
Slope	DEM	N/A	mean	N/A
Elevation (km)	DEM	N/A	mean	N/A
Distance (km) to Nearest Road	MSDI	N/A	mean	N/A
Distance (km) to Nearest Stream	MSDI	N/A	mean	N/A
Distance (km) to Forest Edge From Outside of the Forest	EVT	N/A	mean	N/A
Distance (km) to Forest Edge From Inside of the Forest	EVT	N/A	mean	N/A
Northern Rocky Mountain Western Larch Savanna	EVT	7010	Proportion	Conifer
Rocky Mountain Aspen Forest and Woodland	EVT	7011	Proportion	Hardwood
Northern Rocky Mountain Dry-Mesic Montane Mixed Conifer Forest	EVT	7045	Proportion	Conifer
Northern Rocky Mountain Subalpine Woodland and Parkland	EVT	7046	Proportion	Conifer
Northern Rocky Mountain Mesic Montane Mixed Conifer Forest	EVT	7047	Proportion	Conifer
Rocky Mountain Foothill Limber Pine-Juniper Woodland	EVT	7049	Proportion	Conifer
Rocky Mountain Lodgepole Pine Forest	EVT	7050	Proportion	Conifer
Northern Rocky Mountain Ponderosa Pine Woodland and Savanna	EVT	7053	Proportion	Conifer
Rocky Mountain Subalpine Dry-Mesic Spruce-Fir Forest and Woodland	EVT	7055	Proportion	Conifer
Rocky Mountain Subalpine Mesic-Wet Spruce-Fir Forest and Woodland	EVT	7056	Proportion	Conifer
Inter-Mountain Basins Big Sagebrush Shrubland	EVT	7080	Proportion	Shrubland
Northern Rocky Mountain Montane-Foothill Deciduous Shrubland	EVT	7106	Proportion	Shrubland
Inter-Mountain Basins Big Sagebrush Steppe	EVT	7125	Proportion	Shrubland
Inter-Mountain Basins Montane Sagebrush Steppe	EVT	7126	Proportion	Shrubland

Northern Rocky Mountain Lower Montane-Foothill-Valley Grassland	EVT	7139	Proportion	Grassland
Northern Rocky Mountain Subalpine-Upper Montane Grassland	EVT	7140	Proportion	Grassland
Rocky Mountain Subalpine-Montane Mesic Meadow	EVT	7145	Proportion	Grassland
Northern Rocky Mountain Foothill Conifer Wooded Steppe	EVT	7165	Proportion	Conifer
Middle Rocky Mountain Montane Douglas-fir Forest and Woodland	EVT	7166	Proportion	Conifer
Northern Rocky Mountain Subalpine Deciduous Shrubland	EVT	7169	Proportion	Shrubland
Recently Logged-Herb and Grass Cover	EVT	7191	Proportion	Grassland
Recently Logged-Shrub Cover	EVT	7192	Proportion	Shrubland
Recently Logged-Tree Cover	EVT	7193	Proportion	Conifer
Recently Burned-Herb and Grass Cover	EVT	7195	Proportion	Grassland
Recently Burned-Tree Cover	EVT	7197	Proportion	Conifer
Open Water	EVT	7292	Proportion	Open Water
Developed-Roads	EVT	7299	Proportion	Developed-Roads
Western Cool Temperate Pasture and Hayland	EVT	7967	Proportion	Agricultural
Western Cool Temperate Wheat	EVT	7968	Proportion	Agricultural
Northern Rocky Mountain Lower Montane Riparian Woodland	EVT	9012	Proportion	Riparian
Rocky Mountain Alpine-Montane Wet Meadow	EVT	9017	Proportion	Riparian
Rocky Mountain Cliff Canyon and Massive Bedrock	EVT	9018	Proportion	Sparsely Vegetated
Rocky Mountain Subalpine-Montane Riparian Woodland	EVT	9022	Proportion	Riparian
Interior Western North American Temperate Ruderal Shrubland	EVT	9328	Proportion	Exotic Tree-Shrub
Northern Rocky Mountain Lower Montane Riparian Shrubland	EVT	9512	Proportion	Riparian
Interior Western North American Temperate Ruderal Grassland	EVT	9828	Proportion	Exotic Herbaceous
no vegetation present	EVC	N/A	Proportion	N/A
canopy cover from sparse vegetation	EVC	N/A	Proportion	N/A
canopy cover from agricultural crops	EVC	N/A	Proportion	N/A
developed areas	EVC	N/A	Proportion	N/A
Tree Canopy Cover 10-19%	EVC	N/A	Proportion	N/A
Tree Canopy Cover 20-29%	EVC	N/A	Proportion	N/A
Tree Canopy Cover 30-39%	EVC	N/A	Proportion	N/A
Tree Canopy Cover 40-49%	EVC	N/A	Proportion	N/A
Tree Canopy Cover 50-59%	EVC	N/A	Proportion	N/A
Tree Canopy Cover 60-69%	EVC	N/A	Proportion	N/A
Tree Canopy Cover 70-79%	EVC	N/A	Proportion	N/A

Tree Canopy Cover 80-88%	EVC	N/A	Proportion	N/A
Shrub Canopy Cover 10-19%	EVC	N/A	Proportion	N/A
Shrub Canopy Cover 20-29%	EVC	N/A	Proportion	N/A
Shrub Canopy Cover 30-39%	EVC	N/A	Proportion	N/A
Shrub Canopy Cover 40-49%	EVC	N/A	Proportion	N/A
Herb Canopy Cover 10-19%	EVC	N/A	Proportion	N/A
Herb Canopy Cover 20-29%	EVC	N/A	Proportion	N/A
Herb Canopy Cover 30-39%	EVC	N/A	Proportion	N/A
Herb Canopy Cover 40-49%	EVC	N/A	Proportion	N/A
Herb Canopy Cover 50-59%	EVC	N/A	Proportion	N/A
Herb Canopy Cover 60-69%	EVC	N/A	Proportion	N/A
Herb Canopy Cover 70-79%	EVC	N/A	Proportion	N/A
Tree Height 1-5m	EVH	N/A	Proportion	N/A
Tree Height 6-10m	EVH	N/A	Proportion	N/A
Tree Height 11-15m	EVH	N/A	Proportion	N/A
Tree Height 16-20m	EVH	N/A	Proportion	N/A
Tree Height 21-26m	EVH	N/A	Proportion	N/A
Shrub Height 0.1-0.5m	EVH	N/A	Proportion	N/A
Shrub Height shrubs 0.6-1m	EVH	N/A	Proportion	N/A
Shrub Height 1.1-1.5m	EVH	N/A	Proportion	N/A
Shrub Height 1.6-2.0m	EVH	N/A	Proportion	N/A
Herb Height 0.1-0.5m	EVH	N/A	Proportion	N/A
Herb Height 0.6-1m tall	EVH	N/A	Proportion	N/A

Table A2. Description of variables used to create a forest layer for Montana (LANDFIRE 2016a).

EVT code (ecological systems)	Existing Vegetation Type (ecological systems name)	Vegetation Physiognomy	Collapsed Vegetation Type Name
7010	Northern Rocky Mountain Western Larch Savanna	Conifer	Western Larch Forest and Woodland
7045	Northern Rocky Mountain Dry-Mesic Montane Mixed Conifer Forest	Conifer	Douglas-fir-Ponderosa Pine-Lodgepole Pine Forest and Woodland
7046	Northern Rocky Mountain Subalpine Woodland and Parkland	Conifer	Subalpine Woodland and Parkland
7047	Northern Rocky Mountain Mesic Montane Mixed Conifer Forest	Conifer	Douglas-fir-Grand Fir-White Fir Forest and Woodland
7049	Rocky Mountain Foothill Limber Pine-Juniper Woodland	Conifer	Limber Pine Woodland
7050	Rocky Mountain Lodgepole Pine Forest	Conifer	Lodgepole Pine Forest and Woodland
7053	Northern Rocky Mountain Ponderosa Pine Woodland and Savanna	Conifer	Ponderosa Pine Forest, Woodland and Savanna
7055	Rocky Mountain Subalpine Dry-Mesic Spruce-Fir Forest and Woodland	Conifer	Spruce-Fir Forest and Woodland
7056	Rocky Mountain Subalpine Mesic-Wet Spruce-Fir Forest and Woodland	Conifer	Spruce-Fir Forest and Woodland
7057	Rocky Mountain Subalpine-Montane Limber-Bristlecone Pine Woodland	Conifer	Limber Pine Woodland
7062	Inter-Mountain Basins Curl-leaf Mountain Mahogany Woodland	Conifer	Mountain Mahogany Woodland and Shrubland
7165	Northern Rocky Mountain Foothill Conifer Wooded Steppe	Conifer	Douglas-fir Forest and Woodland
7166	Middle Rocky Mountain Montane Douglas-fir Forest and Woodland	Conifer	Douglas-fir Forest and Woodland
7167	Rocky Mountain Poor-Site Lodgepole Pine Forest	Conifer	Lodgepole Pine Forest and Woodland
7179	Northwestern Great Plains-Black Hills Ponderosa Pine Woodland and Savanna	Conifer	Ponderosa Pine Forest, Woodland and Savanna
7193	Recently Logged-Tree Cover	Conifer	Transitional Forest Vegetation
7197	Recently Burned-Tree Cover	Conifer	Transitional Forest Vegetation
7200	Recently Disturbed Other-Tree Cover	Conifer	Transitional Forest Vegetation
7061	Inter-Mountain Basins Aspen-Mixed Conifer Forest and Woodland	Conifer-Hardwood	Aspen-Mixed Conifer Forest and Woodland
7009	Northwestern Great Plains Aspen Forest and Parkland	Hardwood	Aspen Forest, Woodland, and Parkland
7011	Rocky Mountain Aspen Forest and Woodland	Hardwood	Aspen Forest, Woodland, and Parkland
7161	Northern Rocky Mountain Conifer Swamp	Riparian	Spruce-Fir Forest and Woodland
9019	Rocky Mountain Lower Montane-Foothill Riparian Woodland	Riparian	Western Riparian Woodland and Shrubland
9022	Rocky Mountain Subalpine-Montane Riparian Woodland	Riparian	Western Riparian Woodland and Shrubland

APPENDIX B

APPENDIX B: UNCERTAINTY MAPS FOR RSF MODEL

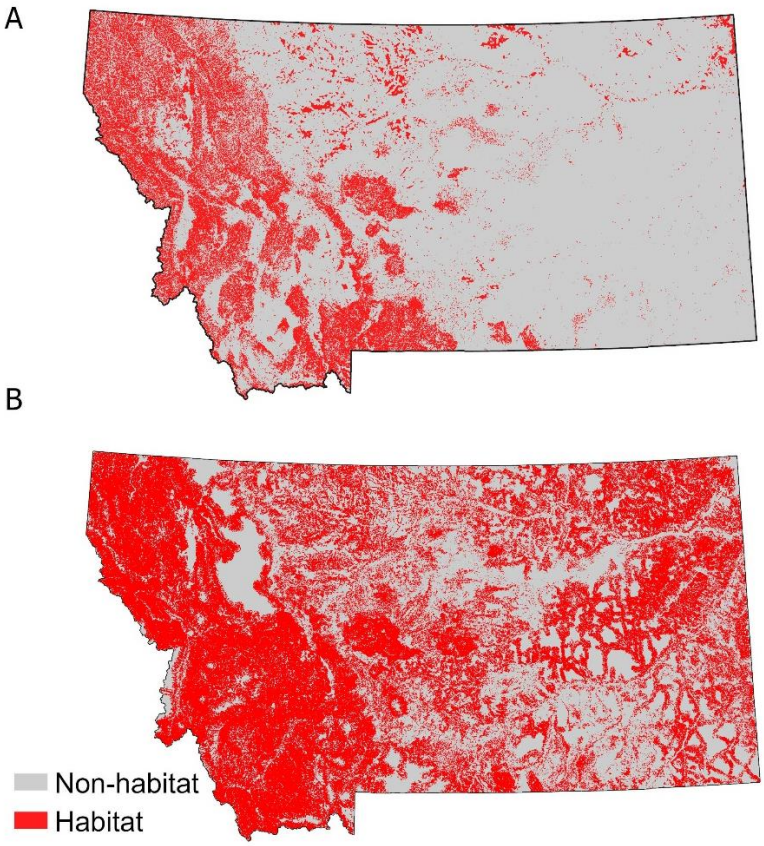

Figure B1. Uncertainty maps for the RSF model. Map A (top) represents a map created using the high confidence intervals for the RSF's beta estimates and then converted to a binary map using the same threshold as used when creating the RSF binary map. Map B represents a map created using the low confidence intervals for the RSF's beta estimates, following the same methodology used to create map A.

APPENDIX C

APPENDIX C: MODEL SUPPORT FOR EVALUATING OVERDISPERSION

Table C1. Support for candidate models predicting abundance and probability of detection estimates using N-mixture models for surveys conducted without electronic playback for spring 2019 pilot season. Three different abundance distributions are examined: Poisson distribution, negative binomial distribution, and zero-inflated Poisson distribution. The number of parameters (K), AIC values, Δ AIC values, and model weights (w_i) are reported.

Model	**K**	**AIC**	**Δ AIC**	w_i
Poisson distribution	2	120.08	0.00	0.47
Zero-inflated Poisson distribution	3	121	0.91	0.3
Negative Binomial distribution	3	121.53	1.45	0.23

Table C2. Support for candidate models predicting abundance and probability of detection estimates using N-mixture models for surveys conducted with electronic playback for spring 2019 pilot season. Three different abundance distributions are examined: Poisson distribution, negative binomial distribution, and zero-inflated Poisson distribution. The number of parameters (K), AIC values, Δ AIC values, and model weights (w_i) are reported.

Model	**K**	**AIC**	**Δ AIC**	w_i
Poisson distribution	2	171.72	0.00	0.47
Zero-inflated Poisson distribution	3	172.59	0.87	0.3
Negative Binomial distribution	3	173.19	1.47	0.23

Table C3. Support for candidate models predicting abundance and probability of detection estimates using N-mixture models for surveys conducted without electronic playback for summer 2019 pilot season. Three different abundance distributions are examined: Poisson distribution, negative binomial distribution, and zero-inflated Poisson distribution. The number of parameters (K), AIC values, Δ AIC values, and model weights (w_i) are reported.

Model	**K**	**AIC**	**Δ AIC**	w_i
Poisson distribution	2	47.18	0.00	0.58
Zero-inflated Poisson distribution	3	49.18	2.00	0.21
Negative Binomial distribution	3	49.18	2.00	0.21

Table C4. Support for candidate models predicting abundance and probability of detection estimates using N-mixture models for surveys conducted with electronic playback for summer 2019 pilot season. Three different abundance distributions are examined: Poisson distribution, negative binomial distribution, and zero-inflated Poisson distribution. The number of parameters (K), AIC values, Δ AIC values, and model weights (w_i) are reported.

Model	**K**	**AIC**	**Δ AIC**	w_i
Poisson distribution	2	47.18	0.00	0.58
Zero-inflated Poisson distribution	3	49.18	2.00	0.21
Negative Binomial distribution	3	49.18	2.00	0.21

APPENDIX D

APPENDIX D: CORRELATION FOR CONTINOUS VARIABLES

Table D1. Correlation matrix between continuous covariates. Minutes = Minutes since sunrise, Day = Day during the sampling period, Temp. = Temperature

	Minutes	Day	Wind	Temp.
Minutes	1.000	-0.034	0.125	0.409
Day	-	1.000	0.004	0.221
Wind	-	-	1.000	0.046
Temp.	-	-	-	1.000

APPENDIX E

APPENDIX E: BAYESIAN MODEL SPECIFICATION AND SIMULATION CODE FOR N-MIXTURE MODELS

Complete Bayesian model specification and simulation code in R language for evaluating Dusky Grouse survey protocols for point counts analyzed using N-mixture models where local abundance and probability of detection were kept constant.

```
# Function for simulating and analyzing data using a N-mixture model for point counts in which average local abundance and probability of detection are kept constant.

# Code adapted from:
#Kery, M. and J. A. Royle. 2016. Applied hierarchical modeling in ecology: analysis of distribution, abundance, and species richness in R and BUGS. Academic Press, London, United Kingdom.
# Kery, M. and M. Schaub. 2012. Bayesian population analysis using WinBUGS. A hierarchical perspective. Elsevier Inc.

# S = number of spatial reps/ number of sites
# V = number of visits at each site (temporal reps)
# lambda = average local abundance
# prob = probability of detection
# num.sim = number of simulations

#Simulate Data - Nmixture model. Parameters estimated: lambda and probability of detection
Sim.Nmix.fn <- function(S=S, V=V, lambda = lambda, prob = prob, num.sim = num.sim) {
  library(jagsUI) # use the JAGS for analyzing data within a Bayesian framework

  #***************
  # Define Bayesian Model
  #***************

  # Specify model in Bugs language
  sink("NMmodel.txt")
  cat("
    model {

    # Priors
      lambda ~ dgamma(0.005, 0.005)      # Standard vague prior for lambda
      p ~ dunif(0, 1) #vague prior for probability of detection

    # Likelihood
      # Biological model for true abundance
        for (i in 1:S) {
          N[i] ~ dpois(lambda) #describes spatial variation in abundance (N)
       # Observation model for replicated counts
          for (j in 1:V) {
            y[i,j] ~ dbin(p, N[i]) #count (observation) for each visit at each site
          } # j
```

```
      } # i

     #Derived parameters
     Ntotal <- sum(N[]) #total of abundance at each site (N)
  }
  ",fill = TRUE)
sink()

#************************************************
# Loop for replicating datasets and assessing bias
#************************************************

num.sim <- num.sim

# Create empty vectors to store results from replicated datasets
m.bias.Nsite <- vector("list",num.sim)  #examine bias in abundance (N) at each site
sd.bias.Nsite <- vector("list",num.sim)
baye.pvalue.Nsite <- vector("list",num.sim)

m.bias.p <- vector("list",num.sim) #bias in probability of detection
sd.bias.p <- vector("list",num.sim)
baye.pvalue.p <- vector("list",num.sim)

m.bias.Ntot <- vector("list",num.sim) #bias in total N
sd.bias.Ntot <- vector("list",num.sim)
baye.pvalue.Ntot <- vector("list",num.sim)

m.bias.lam <- vector("list",num.sim)  #bias in recovered lambda (mean abundance at site)
sd.bias.lam <- vector("list",num.sim)
baye.pvalue.lam <- vector("list",num.sim)


m.CV.lam <- vector("list",num.sim)  #coefficient of variation for lambda (mean abundance at
site)
sd.CV.lam <- vector("list",num.sim)
prop.CV.lam <- vector("list", num.sim)

m.CV.Ntot <- vector("list",num.sim) #coefficient of variation for total N
sd.CV.Ntot <- vector("list",num.sim)
prop.CV.Ntot <- vector("list", num.sim)

#********************
# Start Simulation
#********************
```

```
# Stick simulation in loop and replicate num.sim times
system.time(for (k in 1:num.sim) {  #keep track of how long simulation takes

  #Simulate data
  S = S  # spatial reps
  V = V  # temporal reps
  lambda = lambda # mean abundance at site
  prob = prob # probablity of detection

  # Create structure to contain counts
  y <- array(dim = c(S,V))

  # sample abundance from a Poisson (lambda = 0.3)
  N <- rpois(n=S, lambda=lambda)

  # sample counts from a Binomial distribution (N, prob = 0.3)
  for (j in 1:V){
    y[,j] <- rbinom(n = S, size = N, prob = prob)
  }

  # Bundle data
  win.data <- list(y = y, S = nrow(y), V = ncol(y))

  # initial values
  Nst <- apply(y, 1, max) + 1# This line is vital
  inits <- function() list(N = Nst)

  # Define parameters to be monitored
  params <- c("lambda", "p", "Ntotal", "N")

  # MCMC settings
  ni <- 5000
  nt <- 1
  nb <- 1000
  nc <- 3

  start.time = Sys.time()  #set timer
  # run model
  out <- jags(win.data, inits, params, "NMmodel.txt", n.chains = nc,
              n.thin = nt, n.iter = ni, n.burnin = nb, parallel = TRUE)
  print(out)

  end.time = Sys.time()
```

```
   elapsed.time = round(difftime(end.time, start.time, units = 'mins'), dig = 2)
   cat('sim', k,', Posterior computed in ', elapsed.time, ' minutes\n\n', sep='')

   #***************************************
   #### Evaluate bias ####
   #***************************************
   #Bias in N (site specific abundance)
   bias.Nsite <- out$mean$N - N #calculates bias
   m.bias.Nsite[k] <- mean(bias.Nsite) #averages bias and places within vector
   sd.bias.Nsite[k] <- sd(bias.Nsite) #gets standard deviation of bias places within vector
   baye.pvalue.Nsite[k] <-mean(N > out$mean$N)  #Bayesian P-value (proportion of simulations
where the true abundance was greater than the estimated abundance - values close to 0 or 1
indicate significant bias)

   #Bias in lambda (average local abundance) - descriptions same as above
   bias.lam <- out$mean$lambda - lambda
   m.bias.lam[k] <- mean(bias.lam)
   sd.bias.lam[k] <- sd(bias.lam)
   baye.pvalue.lam[k] <- mean(lambda > out$mean$lambda)

   #Bias in p - descriptions same as above
   bias.p <- out$mean$p - prob
   m.bias.p[k] <- mean(bias.p)
   sd.bias.p[k] <- sd(bias.p)
   baye.pvalue.p[k] <- mean(prob > out$mean$p)

   #Bias in Ntotal (total population size) - descriptions same as above
   bias.Ntot <- out$mean$Ntotal - sum(N)
   m.bias.Ntot[k] <- mean(bias.Ntot)
   sd.bias.Ntot[k] <- sd(bias.Ntot)
   baye.pvalue.Ntot[k] <- mean(sum(N) > out$mean$Ntotal)

   #Coefficient of Variation in Ntotal (total population size) - want to be under 15%
   CV.Ntot <- out$sd$Ntotal/out$mean$Ntotal #standard deviation divided by mean
   m.CV.Ntot[k] <- mean(CV.Ntot)
   sd.CV.Ntot[k] <- sd(CV.Ntot)
   prop.CV.Ntot[k] <- mean(CV.Ntot < 0.15)

   #Coefficient of Variation in local abundance (lambda / average local abundance)
   CV.lam <- out$sd$lambda/out$mean$lambda
   m.CV.lam[k] <- mean(CV.lam)
   sd.CV.lam[k] <- sd(CV.lam)
   prop.CV.lam[k] <- mean(CV.lam < 0.15)
```

```
  }  ) #This will be the end of the simulations

  #********************
  # Summary of Results
  #********************
  results <- c("lambda", "prob", "N.total", "N.site", "N.total.CV", "lambda.CV", "Prob.CV.Ntot",
"Prob.CV.lambda")
  mean.bias <- round(c((mean(unlist(m.bias.lam))), (mean(unlist(m.bias.p))),
(mean(unlist(m.bias.Ntot))), (mean(unlist(m.bias.Nsite))), (mean(unlist(m.CV.Ntot))),
(mean(unlist(m.CV.lam))), NA, NA),2)

  lower.CI <- round(c((quantile(unlist(m.bias.lam), 0.05)), (quantile(unlist(m.bias.p), 0.05)),
(quantile(unlist(m.bias.Ntot), 0.05)), (quantile(unlist(m.bias.Nsite), 0.05)),
(quantile(unlist(m.CV.Ntot), 0.05)), (quantile(unlist(m.CV.lam), 0.05)), NA, NA),2) #lower 90%
credible interval

  upper.CI <- round(c((quantile(unlist(m.bias.lam), 0.95)), (quantile(unlist(m.bias.p), 0.95)),
(quantile(unlist(m.bias.Ntot), 0.95)), (quantile(unlist(m.bias.Nsite), 0.95)),
(quantile(unlist(m.CV.Ntot), 0.95)), (quantile(unlist(m.CV.lam), 0.95)), NA, NA),2) #upper 90%
credible interval

  greater.15.CV <- c(NA, NA, NA, NA, NA, NA, (mean(unlist(m.CV.Ntot) > 0.15)),
(mean(unlist(m.CV.lam) > 0.15))) #percent of CV's greater than 15%

  Baye.pvalue <- round(c((mean(unlist(baye.pvalue.lam))), (mean(unlist(baye.pvalue.p))),
(mean(unlist(baye.pvalue.Ntot))), (mean(unlist(baye.pvalue.Nsite))), NA, NA, NA, NA),2)

  sim.results <- data.frame(results,mean.bias,lower.CI, upper.CI, Baye.pvalue, greater.15.CV)
#creates a table of results
  print(sim.results)

  #*****************
  #Post processing
  #*****************
  # Set plots so that six plots can be created in one image
  par(mfrow = c(6,1), mai=c(0.5,0.2,0.2,0.2), mar=c(1,5,1,2), oma=c(1,1,1,1), las=1)

  # Plots
  (hist(unlist(m.bias.Nsite), xlim=c(-1,1), breaks=120, main="", ylab="N.site"))
  (abline(v=0, col="red", lwd=3))

  (hist(unlist(m.bias.lam), xlim=c(-1,1), main="", ylab="lambda"))
  (abline(v=0, col="red", lwd=3))
```

```
  (hist(unlist(m.bias.p), xlim=c(-0.5,0.5), main="", ylab="Detection prob."))
  (abline(v=0, col="red", lwd=3))

  (hist(unlist(m.bias.Ntot), xlim=c(-100,100), main="", ylab="Total N"))
  (abline(v=0, col="red", lwd=3))

  (hist(unlist(m.CV.Ntot), xlim=c(0,0.5), main="", ylab="CV Ntotal"))
  (abline(v=0.15, col="red", lwd=3))

  (hist(unlist(m.CV.lam), xlim=c(0,0.5), main="", ylab="CV lambda"))
  (abline(v=0.15, col="red", lwd=3))

  return(list(sim.results=sim.results, m.bias.Nsite=unlist(m.bias.Nsite), m.bias.lam =
unlist(m.bias.lam), m.bias.p = unlist(m.bias.p), m.bias.Ntot = unlist(m.bias.Ntot), m.CV.Ntot =
unlist(m.CV.Ntot), m.CV.lam = unlist(m.CV.lam), lambda = lambda, prob = prob, S = S, V = V,
num.sim = num.sim))
}
```

APPENDIX F

APPENDIX F: BAYESIAN MODEL SPECIFICATION AND SIMULATION CODE FOR N-MIXTURE MODELS WHERE POINT COUNT VISITS WERE CORRELATED

Complete Bayesian model specification and simulation code in R language for evaluating Dusky Grouse survey protocols for point counts analyzed using N-mixture models where local abundance and probability of detection were kept constant, and point counts visits were correlated.

```
# Functions for simulating data for four visits per site that are correlated where visits 1 & 2 have a correlation of 0.67, 1 & 3 have a correlation of 0.41, 1 & 4 have a correlation of 0.44, 2 & 3 have a correlation of 0.48, 2 & 4 have a correlation of 0.47, and 3 & 4 have a correlation of 0.67. Correlations are based off point counts from 2020 and 2021 data where all counts occurred on the same day and visits 1 & 2, and visits 3 & 4 were back-to-back. There are two functions: rcorrbinom which simulates the correlated counts and Sim.Nmix.fn which uses rcorrbinom to simulate correlated data and then analyzes the data using an N-mixture model. Average local abundance (lambda) across and probability of detection are kept constant.

# rcorrbinom code adapted from:
#https://stats.stackexchange.com/questions/284996/generating-correlated-binomial-random-variables

# Sim.Nmix.fn code adapted from:
#Kery, M. and J. A. Royle. 2016. Applied hierarchical modeling in ecology: analysis of distribution, abundance, and species richness in R and BUGS. Academic Press, London, United Kingdom.
# Kery, M. and M. Schaub. 2012. Bayesian population analysis using WinBUGS. A hierarchical perspective. Elsevier Inc.

# S = number of spatial reps/ number of sites
# V = number of visits at each site (temporal reps)
# lambda = average local abundance
# prob = probability of detection
# num.sim = number of simulations

# n = number of observations
# size = number of trials
# prob = probability of detection
# corr1 = correlation between visit 1 & visit 2: 0.67
# corr2 = correlation between visit 2 & visit 3: 0.47
# corr3 = correlation between visit 3 & visit 4: 0.67

# Creates data where visit 1 is correlated with visit 2, visit 2 is correlated with visit 3, and visit 3 is correlated with visit 4
# Creates correlated Bernoulli random variables, which frequently resulted in correlation between the binomial values
rcorrbinom <- function(n, size = size, prob, corr1 = corr1, corr2 = corr2, corr3 = corr3) {
  #Check inputs
  if (!is.numeric(n))           { stop('Error: n must be numeric') }
```

```
if (length(n) != 1)            { stop('Error: n must be a single number') }
if (as.integer(n) != n)        { stop('Error: n must be a positive integer') }
if (n < 1)                   { stop('Error: n must be a positive integer') }
if (!is.numeric(size))         { stop('Error: n must be numeric') }
if (length(size) != 1)         { stop('Error: n must be a single number') }
if (as.integer(size) != size)   { stop('Error: n must be a positive integer') }
if (size < 1)                { stop('Error: n must be a positive integer') }
if (!is.numeric(prob))         { stop('Error: prob1 must be numeric') }
if (length(prob) != 1)         { stop('Error: prob1 must be a single number') }
if (prob < 0)                { stop('Error: prob1 must be between 0 and 1') }
if (prob > 1)                { stop('Error: prob1 must be between 0 and 1') }
if (!is.numeric(corr1))          { stop('Error: corr must be numeric') }
if (length(corr1) != 1)          { stop('Error: corr must be a single number') }
if (corr1 < -1)               { stop('Error: corr must be between -1 and 1') }
if (corr1 > 1)               { stop('Error: corr must be between -1 and 1') }
if (!is.numeric(corr2))          { stop('Error: corr must be numeric') }
if (length(corr2) != 1)          { stop('Error: corr must be a single number') }
if (corr2 < -1)               { stop('Error: corr must be between -1 and 1') }
if (corr2 > 1)               { stop('Error: corr must be between -1 and 1') }
if (!is.numeric(corr3))          { stop('Error: corr must be numeric') }
if (length(corr3) != 1)          { stop('Error: corr must be a single number') }
if (corr3 < -1)               { stop('Error: corr must be between -1 and 1') }
if (corr3 > 1)               { stop('Error: corr must be between -1 and 1') }

  #Compute probabilities
#Between visit 1 & visit 2
P00.1   <- (1-prob)*(1-prob) + corr1*sqrt(prob*prob*(1-prob)*(1-prob))
P01.1   <- 1 - prob - P00.1
P10.1   <- 1 - prob - P00.1
P11.1   <- P00.1 + prob + prob - 1
PROBS.1 <- c(P00.1, P01.1, P10.1, P11.1)
if (min(PROBS.1) < 0)       { stop('Error: corr is not in the allowable range') }

#Between visit 2 & visit 3
P00.2   <- (1-prob)*(1-prob) + corr2*sqrt(prob*prob*(1-prob)*(1-prob))
P01.2   <- 1 - prob - P00.2
P10.2   <- 1 - prob - P00.2
P11.2   <- P00.2 + prob + prob - 1
PROBS.2a <- c(P00.2, P01.2) # First one is zero
PROBS.2b <- c(P10.2, P11.2) # First one is not zero
if (min(PROBS.2a) < 0)       { stop('Error: corr is not in the allowable range')}
if (min(PROBS.2b) < 0)       { stop('Error: corr is not in the allowable range')}

#Between visit 3 & visit 4
```

```
  P00.3   <- (1-prob)*(1-prob) + corr3*sqrt(prob*prob*(1-prob)*(1-prob))
  P01.3   <- 1 - prob - P00.3
  P10.3   <- 1 - prob - P00.3
  P11.3   <- P00.3 + prob + prob - 1
  PROBS.3a <- c(P00.3, P01.3) # First one is zero
  PROBS.3b <- c(P10.3, P11.3) # First one is not zero
  if (min(PROBS.3a) < 0)       { stop('Error: corr is not in the allowable range')}
  if (min(PROBS.3b) < 0)       { stop('Error: corr is not in the allowable range')}

  #Generate the output
  # Generates counts for visits 1 & 2
  # sample.int = n (number of items to choose from), size (number of items to choose), replace
(sample with replacement), prob (vector of probability weights for obtaining the elements of the
vector beign sampled)
  RAND.1 <- array(sample.int(4, size = n*size, replace = TRUE, prob = PROBS.1),
                  dim = c(n, size)) #produces count group, 1 = 00, 2 = 01, 3 = 10 4 = 11
  VALS.1 <- array(0, dim = c(2, n, size)) # will hold results of each trial so could have multiple
arrays if size > 1
  OUT.1  <- array(0, dim = c(2, n)) # will hold counts

  for (i in 1:n)    {
    for (j in 1:size) {
      VALS.1[1,i,j] <- (RAND.1[i,j] %in% c(3, 4)) #is Rand.1 in count groups 3 or 4 (counts 10 or
11)
      VALS.1[2,i,j] <- (RAND.1[i,j] %in% c(2, 4)) }  # is Rand.1 in count groups 2 or 4 (counts
01 or 11)
    OUT.1[1, i]   <- sum(VALS.1[1,i,]) #sums number of detections in first visit -> count for visit
1
    OUT.1[2, i]   <- sum(VALS.1[2,i,]) #sums number of detections in second visit -> count for
visit 2
    }

  # Section generates counts for visits 2 & 3, where visit 2 counts are identical to the previous
visit 2 counts
  RAND.2 <- array(0, dim = c(n, n*size)) #creates array filled with zeros
  for (i in 1:n) {
    for (j in 1:size) {
      if (VALS.1[2,i,j] > 0) { #if for visit 2, count is greater than 0
        RAND.2[i,j] <- sample.int(2, size = 1, replace = TRUE, prob = PROBS.2b) #place in count
group
        if (RAND.2[i,j] == 1) {
          RAND.2[i,j] <- 3 #if in group 1, gets placed in overall group 3 (1,0)
        }
        else {
```

```
        RAND.2[i,j] <- 4 #otherwise placed in overall group 4 (1,1)
       }
      }
      else {
       RAND.2[i,j] <- sample.int(2, size = 1, replace = TRUE, prob = PROBS.2a) #place in count
group 1(0,0) or 2(0,1)

      }
    }
  }

  VALS.2 <- array(0, dim = c(2, n, size)) #will hold results of each trial
  OUT.2  <- array(0, dim = c(2, n)) #will hold counts

  for (i in 1:n)    {
    for (j in 1:size) {
      VALS.2[1,i,j] <- (RAND.2[i,j] %in% c(3, 4)) #is Rand.2 in probability groups 3 or 4 (counts
10 or 11)
      VALS.2[2,i,j] <- (RAND.2[i,j] %in% c(2, 4)) } # is Rand.2 in probability groups 2 or 4
(counts 01 or 11)
    OUT.2[1, i]   <- sum(VALS.2[1,i,]) #sums number of detections in second visit
    OUT.2[2, i]   <- sum(VALS.2[2,i,]) #sums number of detections in third visit
  }

  # Section generates counts for visits 3 & 4, where visit 3 counts are identical to the previous
visit 3 counts
  RAND.3 <- array(0, dim = c(n, n*size)) #creates array filled with zeros
  for (i in 1:n) {
    for (j in 1:size) {
      if (VALS.2[2,i,j] > 0) { #if for visit 3, count is greater than 0
       RAND.3[i,j] <- sample.int(2, size = 1, replace = TRUE, prob = PROBS.3b) #place in count
group
        if (RAND.3[i,j] == 1) {
         RAND.3[i,j] <- 3 #if in group 1, gets placed in overall group 3 (1,0)
        }
        else {
         RAND.3[i,j] <- 4 #otherwise placed in overall group 4 (1,1)
        }
      }
      else {
       RAND.3[i,j] <- sample.int(2, size = 1, replace = TRUE, prob = PROBS.3a) #place in count
group 1(0,0) or 2(0,1)

      }
```

```
   }
  }

  VALS.3 <- array(0, dim = c(2, n, size)) #will hold results of each trial
  OUT.3  <- array(0, dim = c(2, n)) #will hold counts

  for (i in 1:n)    {
    for (j in 1:size) {
      VALS.3[1,i,j] <- (RAND.3[i,j] %in% c(3, 4)) #is Rand.3 in probability groups 3 or 4 (counts
10 or 11)
      VALS.3[2,i,j] <- (RAND.3[i,j] %in% c(2, 4)) } # is Rand.3 in probability groups 2 or 4
(counts 01 or 11)
    OUT.3[1, i]   <- sum(VALS.3[1,i,]) #sums number of detections in third visit
    OUT.3[2, i]   <- sum(VALS.3[2,i,]) #sums number of detections in fourth visit
  }

  # Give output- counts per visit per site
  y <- array(dim = c(n,4))
  y[,1] <- OUT.1[1,]
  y[,2] <- OUT.1[2,]
  y[,3] <- OUT.2[2,]
  y[,4] <- OUT.3[2,]
  y
}

# S = number of sites
# V = number of visits
# lambda = mean local abundance
# prob = probability of detection
# num.sim = number of simulations
# The code doesn't work perfectly for outputting correlated counts, so the corr values are the
input to get the correlation we want which is the rho values

#Simulate Data - Nmixture model. Parameters estimated: lambda and probability of detection
# corr1 & corr3 = 0.30, corr2 = -0.20
Sim.Nmix.fn <- function(S=S, V=V, lambda = lambda, prob = prob, num.sim = num.sim, corr1
= corr1, corr2 = corr2, corr3 = corr3, rho1 = rho1, rho2 = rho2, rho3 = rho3) {
  library(jagsUI) # use the JAGS for analyzing data within a Bayesian framework

  #***************
  # Define Bayesian Model
  #***************

  # Specify model in Bugs language
```

```
sink("modelCC.txt")
cat("
  model {

  # Priors
    lambda ~ dgamma(0.005, 0.005)      # Standard vague prior for lambda
    p ~ dunif(0, 1) #vague prior for probability of detection

  # Likelihood
    # Biological model for true abundance
      for (i in 1:S) {
        N[i] ~ dpois(lambda) #describes spatial variation in abundance (N)
     # Observation model for replicated counts
        for (j in 1:V) {
          y[i,j] ~ dbin(p, N[i]) #count (observation) for each visit at each site
        } # j
      } # i

     #Derived parameters
     Ntotal <- sum(N[]) #total of abundance at each site (N)
  }
  ",fill = TRUE)
sink()

#************************************************
# Loop for replicating datasets and assessing bias
#************************************************

num.sim <- num.sim

# Create empty vectors to store results from replicated datasets
m.bias.Nsite <- vector("list",num.sim)  #examine bias in abundance (N) at each site
sd.bias.Nsite <- vector("list",num.sim)
baye.pvalue.Nsite <- vector("list",num.sim)

m.bias.p <- vector("list",num.sim) #bias in probability of detection
sd.bias.p <- vector("list",num.sim)
baye.pvalue.p <- vector("list",num.sim)

m.bias.Ntot <- vector("list",num.sim) #bias in total N
sd.bias.Ntot <- vector("list",num.sim)
baye.pvalue.Ntot <- vector("list",num.sim)

m.bias.lam <- vector("list",num.sim)  #bias in recovered lambda (mean abundance at site)
```

```
  sd.bias.lam <- vector("list",num.sim)
  baye.pvalue.lam <- vector("list",num.sim)

    m.CV.lam <- vector("list",num.sim)  #coefficient of variation for lambda (mean abundance at
site)
  sd.CV.lam <- vector("list",num.sim)
  prop.CV.lam <- vector("list", num.sim)

  m.CV.Ntot <- vector("list",num.sim) #coefficient of variation for total N
  sd.CV.Ntot <- vector("list",num.sim)
  prop.CV.Ntot <- vector("list", num.sim)

  #*********************
  # Start Simulation
  #*********************

  # Stick simulation in loop and replicate num.sim times

    system.time(for (k in 1:num.sim) {  #keep track of how long simulation takes

    #Simulate data
    S = S  # spatial reps
    V = V  # temporal reps
    lambda = lambda # mean abundance at site
    prob = prob # probablity of detection
    rho1 = rho1 # desired correlation
    rho2 = rho2
    rho3 = rho3
    corr1 = corr1 # modified correlation
    corr2 = corr2
    corr3 = corr3

    # Create structure to contain counts
    y <- array(dim = c(S,V))

    for(f in 1:1000){ #if correlated counts fail to be created, then it tries again (prevents simulation
from crashing)
      N <- rpois(n=S, lambda=lambda) # sample abundance from a Poisson distribution
    # sample counts from a Binomial distribution
    for(m in 1:200000) { #tries for creating count from simulated abundance (N)

      my <- array(NA,dim = c(S,4)) #creates empty array for counts
      for (i in 1:S){
        NN <- N[i]
```

```
      if (NN > 0){ #if actual abundance is > 0, sample using the rcorrbinom function to create
counts
        ymy <- rcorrbinom(n = 1, size = NN, prob = prob, corr1 = 0.30, corr2 = -0.20, corr3 =
0.30)
        my[i,] <- ymy
       }
       else { # if actual abundance is 0, then the counts are automatically 0
        my[i,] <- 0
       }
     }

     data.y.cor <- cor(my) # get correlation of count data and make sure that it is within 0.05 of
the desired correlation
     cor1 <- (data.y.cor[1,2] >= (rho1 - 0.05) & data.y.cor[1,2] <= (rho1 + 0.05))
     cor2 <- (data.y.cor[2,3] >= (rho2 - 0.05) & data.y.cor[2,3] <= (rho2 + 0.05))
     cor3 <- (data.y.cor[3,4] >= (rho3 - 0.05) & data.y.cor[3,4] <= (rho3 + 0.05))
     cor13 <- (data.y.cor[1,3] >= (0.41 - 0.05) & data.y.cor[1,3] <= (0.41 + 0.05))
     cor14 <- (data.y.cor[1,4] >= (0.44 - 0.05) & data.y.cor[1,4] <= (0.44 + 0.05))
     cor24 <- (data.y.cor[2,4] >= (0.47 - 0.05) & data.y.cor[2,4] <= (0.47 + 0.05))

     if (cor1 %in% NA){
      cor1 <- FALSE
     }
     if (cor2 %in% NA){
      cor2 <- FALSE
     }
     if (cor3 %in% NA){
      cor3 <- FALSE
     }
     if (cor13 %in% NA){
      cor13 <- FALSE
     }
     if (cor14 %in% NA){
      cor14 <- FALSE
     }
     if (cor24 %in% NA){
      cor24 <- FALSE
     }

     # if count data has the correct correlation then export the count data and break the for loop
     if (cor1 == TRUE & cor2 == TRUE & cor3==TRUE & cor13==TRUE & cor14==TRUE &
cor24==TRUE){
       y <- my
       cat("iteration ", m) #print how many iterations it took get count data
```

```
    break
   }
  }
   cat(" attempt", f ) #print how many times N had to be generated to get count data with correct correlation (created to keep simulation from stopping/crashing)
   if (is.na(mean(y)) == FALSE){
    break #exit for loop with count data
   }
  }

  # Bundle data
  win.data <- list(y = y, S = nrow(y), V = ncol(y))

  # initial values
  Nst <- apply(y, 1, max) + 1# This line is vital
  inits <- function() list(N = Nst)

  # Define parameters to be monitored
  params <- c("lambda", "p", "Ntotal", "N")

  # MCMC settings
  ni <- 30000
  nt <- 1
  nb <- 100
  nc <- 3

  start.time = Sys.time()  #set timer
  # run model
  out <- jags(win.data, inits, params, "modelCC.txt", n.chains = nc,
          n.thin = nt, n.iter = ni, n.burnin = nb, parallel = TRUE)
  print(out)

  end.time = Sys.time()
  elapsed.time = round(difftime(end.time, start.time, units = 'mins'), dig = 2)
  cat('sim', k,', Posterior computed in ', elapsed.time, ' minutes\n\n', sep='')

  #*************************************
  #### Evaluate bias ####
  #*************************************
  ##Bias in N (site specific abundance)
  bias.Nsite <- out$mean$N - N #calculates bias
  m.bias.Nsite[k] <- mean(bias.Nsite) #averages bias and places within vector
  sd.bias.Nsite[k] <- sd(bias.Nsite) #gets standard deviation of bias places within vector
```

```
   baye.pvalue.Nsite[k] <-mean(N > out$mean$N)  #Bayesian P-value (proportion of simulations where the true abundance was greater than the estimated abundance - values close to 0 or 1 indicate significant bias)

   ##Bias in lambda (average local abundance) - descriptions same as above
   bias.lam <- out$mean$lambda - lambda
   m.bias.lam[k] <- mean(bias.lam)
   sd.bias.lam[k] <- sd(bias.lam)
   baye.pvalue.lam[k] <- mean(lambda > out$mean$lambda)

   ##Bias in p - descriptions same as above
   bias.p <- out$mean$p - prob
   m.bias.p[k] <- mean(bias.p)
   sd.bias.p[k] <- sd(bias.p)
   baye.pvalue.p[k] <- mean(prob > out$mean$p)

   ##Bias in Ntotal (total population size) - descriptions same as above
   bias.Ntot <- out$mean$Ntotal - sum(N)
   m.bias.Ntot[k] <- mean(bias.Ntot)
   sd.bias.Ntot[k] <- sd(bias.Ntot)
   baye.pvalue.Ntot[k] <- mean(sum(N) > out$mean$Ntotal)

   ##Coefficient of Variation in Ntotal (total population size) - want to be under 15%
   CV.Ntot <- out$sd$Ntotal/out$mean$Ntotal #standard deviation divided by mean
   m.CV.Ntot[k] <- mean(CV.Ntot)
   sd.CV.Ntot[k] <- sd(CV.Ntot)
   prop.CV.Ntot[k] <- mean(CV.Ntot < 0.15)

   #Coefficient of Variation in local abundance (lambda / average local abundance)
   CV.lam <- out$sd$lambda/out$mean$lambda
   m.CV.lam[k] <- mean(CV.lam)
   sd.CV.lam[k] <- sd(CV.lam)
   prop.CV.lam[k] <- mean(CV.lam < 0.15)

   }  ) #This will be the end of the simulations

  #*********************
  # Summary of Results
  #*********************
  results <- c("lambda", "prob", "N.total", "N.site", "N.total.CV", "lambda.CV", "Prob.CV.Ntot", "Prob.CV.lambda")
  mean.bias <- round(c((mean(unlist(m.bias.lam))), (mean(unlist(m.bias.p))), (mean(unlist(m.bias.Ntot))), (mean(unlist(m.bias.Nsite))), (mean(unlist(m.CV.Ntot))), (mean(unlist(m.CV.lam))), NA, NA),2)
```

```
  lower.CI <- round(c((quantile(unlist(m.bias.lam), 0.05)), (quantile(unlist(m.bias.p), 0.05)),
(quantile(unlist(m.bias.Ntot), 0.05)), (quantile(unlist(m.bias.Nsite), 0.05)),
(quantile(unlist(m.CV.Ntot), 0.05)), (quantile(unlist(m.CV.lam), 0.05)), NA, NA),2) #lower 90%
credible interval

  upper.CI <- round(c((quantile(unlist(m.bias.lam), 0.95)), (quantile(unlist(m.bias.p), 0.95)),
(quantile(unlist(m.bias.Ntot), 0.95)), (quantile(unlist(m.bias.Nsite), 0.95)),
(quantile(unlist(m.CV.Ntot), 0.95)), (quantile(unlist(m.CV.lam), 0.95)), NA, NA),2) #upper 90%
credible interval

  greater.15.CV <- c(NA, NA, NA, NA, NA, NA, (mean(unlist(m.CV.Ntot) > 0.15)),
(mean(unlist(m.CV.lam) > 0.15))) #percent of CV's greater than 15%

  Baye.pvalue <- round(c((mean(unlist(baye.pvalue.lam))), (mean(unlist(baye.pvalue.p))),
(mean(unlist(baye.pvalue.Ntot))), (mean(unlist(baye.pvalue.Nsite))), NA, NA, NA, NA),2)

  sim.results <- data.frame(results,mean.bias,lower.CI, upper.CI, Baye.pvalue, greater.15.CV)
#creates a table of results
  print(sim.results)

  #*****************
  #Post processing
  #*****************
  # Set plots so that six plots can be created in one image
  par(mfrow = c(6,1), mai=c(0.5,0.2,0.2,0.2), mar=c(1,5,1,2), oma=c(1,1,1,1), las=1)

  # Plots
  (hist(unlist(m.bias.Nsite), xlim=c(-5,5), breaks=120, main="", ylab="N.site"))
  (abline(v=0, col="red", lwd=3))

  (hist(unlist(m.bias.lam), xlim=c(-1,1), main="", ylab="lambda"))
  (abline(v=0, col="red", lwd=3))

  (hist(unlist(m.bias.p), xlim=c(-0.5,0.5), main="", ylab="Detection prob."))
  (abline(v=0, col="red", lwd=3))

  (hist(unlist(m.bias.Ntot), xlim=c(-100,100), main="", ylab="Total N"))
  (abline(v=0, col="red", lwd=3))

  (hist(unlist(m.CV.Ntot), xlim=c(0,0.5), main="", ylab="CV Ntotal"))
  (abline(v=0.15, col="red", lwd=3))

  (hist(unlist(m.CV.lam), xlim=c(0,0.5), main="", ylab="CV lambda"))
```

```
  (abline(v=0.15, col="red", lwd=3))

  return(list(sim.results=sim.results, m.bias.Nsite=unlist(m.bias.Nsite), m.bias.lam =
unlist(m.bias.lam), m.bias.p = unlist(m.bias.p), m.bias.Ntot = unlist(m.bias.Ntot), m.CV.Ntot =
unlist(m.CV.Ntot), m.CV.lam = unlist(m.CV.lam), lambda = lambda, prob = prob, S = S, V = V,
num.sim = num.sim))
}
```

APPENDIX G

APPENDIX G: BAYESIAN MODEL SPECIFICATION AND SIMULATION CODE FOR POINT-COUNTS EVALUATED USING HIERARCHICAL DISTANCE SAMPLING

Complete Bayesian model specification and simulation code in R language for evaluating Dusky Grouse survey protocols for point counts analyzed using hierarchical distance sampling where local abundance and probability of detection (sigma) were kept constant.

```
# Function for simulating and analyzing data using a hierarchical distance sampling model for point counts where both abundance and detection is kept constant.
# Data is simulated over a square using average local abundance for the square (lambda) and then truncated into a circle with radius B with an average local abundance equal to the estimated average local abundance of a point count site from the 2020 & 2021 data

# Code adapted from: Kery, M. and J. A. Royle. 2016. Applied hierarchical modeling in ecology: analysis of distribution, abundance, and species richness in R and BUGS. Academic Press, London, United Kingdom

# nsites = number of sites
# lambda = average local abundance per site over a square with area 2B x 2B where B = radius of circle
# lambda1 = average local abundance per point count site (so average local abundance within a circle with a radius of B)
# sigma = sigma for the half-normal detection function
# num.sim = number of simulations

# SET WORKING DIRECTORY
Sim.HDS.point.fn <- function(nsites = nsites, lambda = lambda, sigma = sigma, num.sim = num.sim, lambda1 = lambda1) {
  library(jagsUI) # use the JAGS for analyzing data within a Bayesian framework

  #***************
  # Define Bayesian Model
  #***************

  # Specify model in Bugs language, but going to use JagsUI/jags
  sink("simHDSpointfunction.txt")
  cat("
 model{
  # Priors
  sigma ~ dunif(0,100) #vague prior for sigma
  lambda ~ dgamma(0.001, 0.001) #standard vague prior for lambda
  for(i in 1:nind){
    dclass[i] ~ dcat(fc[site[i],]) # Part 1 of HM - model for distance class of the observed individuals
  }
  for(s in 1:nsites){
    # Construct cell probabilities for nD distance bands
    for(g in 1:nD){              # midpt = mid-point of each band
```

```
    log(p[s,g]) <- -midpt[g] * midpt[g] / (2 * sigma * sigma) # half-normal detection function
    pi[s,g] <- ((2 * midpt[g] ) / (B * B)) * delta # prob. per interval
    f[s,g] <- p[s,g] * pi[s,g]
    fc[s,g] <- f[s,g] / pcap[s]
   }
   pcap[s] <- sum(f[s,])          # Pr(capture): sum of rectangular areas
   ncap[s] ~ dbin(pcap[s], N[s])   # Part 2 of HM - describes imperfect detection leading to count
n[s]
   N[s] ~ dpois(lambda)         # Part 3 of HM - describes spatial variation in local abundance N[s]
 }
 # Derived parameters
 Ntotal <- sum(N[]) #total of abundance at each site (N)
 area <- nsites*3.141*B*B/1000000 #area in meters of the point count area
 D <- Ntotal/area #calculates density
}
  ",fill = TRUE)
 sink()

 #***************************************************
 # Loop for replicating datasets and assessing bias
 #***************************************************

 num.sim <- num.sim

 # Create empty vectors to store results from replicated datasets
 m.bias.Nsite <- vector("list",num.sim)  #examine bias in abundance (N) at each site
 sd.bias.Nsite <- vector("list",num.sim)
 baye.pvalue.Nsite <- vector("list",num.sim)
 m.Ntrue <- vector("list",num.sim)
 m.N <- vector("list",num.sim)

 m.bias.sigma <- vector("list",num.sim) #bias in sigma
 sd.bias.sigma <- vector("list",num.sim)
 baye.pvalue.sigma <- vector("list",num.sim)
 m.sig <- vector("list", num.sim)

 m.bias.Ntot <- vector("list",num.sim) #bias in total N
 sd.bias.Ntot <- vector("list",num.sim)
 baye.pvalue.Ntot <- vector("list",num.sim)
 m.bias.Ntot <- vector("list", num.sim)
 m.Ntot.true <- vector("list", num.sim)
 m.Ntot <- vector("list", num.sim)
```

```
  m.bias.lam <- vector("list",num.sim)  #bias in recovered lambda (mean abundance at point
count site)
  sd.bias.lam <- vector("list",num.sim)
  baye.pvalue.lam <- vector("list",num.sim)
  m.lambda <- vector("list", num.sim)

  m.bias.den <- vector("list", num.sim) # bias in density
  sd.bias.den <- vector("list", num.sim)
  baye.pvalue.den <- vector("list", num.sim)
  m.density <- vector("list", num.sim)
  m.density.true <- vector("list", num.sim)

  m.CV.lam <- vector("list",num.sim)  #coefficient of variation for lambda (mean abundance at
site)
  sd.CV.lam <- vector("list",num.sim)
  prop.CV.lam <- vector("list", num.sim)

  m.CV.Ntot <- vector("list",num.sim) #coefficient of variation for total N
  sd.CV.Ntot <- vector("list",num.sim)
  prop.CV.Ntot <- vector("list", num.sim)

  #*********************
  # Start Simulation
  #*********************

  # Stick simulation in loop and replicate num.sim times
  system.time(for (k in 1:num.sim) {  #keep track of how long simulation takes

    # ***************
    # Simulate Data
    # ***************
    # Simulate abundance model (Poisson GLM for N)
    N <- rpois(nsites, lambda)     # site specific abundance for square
    N.true <- N                  # for point, those individuals located inside circle (radius = B)
    B <- 100 #radius for circle (meters)
    area <- nsites*3.141*B*B/1000000 #area for circle (meters squared)
    den.true <- sum(N.true)/area #density for point count circle

    # Simulate observation model - set up empty dataframe
    data <- NULL

    for(i in 1:nsites){
      if(N[i]==0){ #if abundance at a site is 0
        data <- rbind(data, c(i,NA,NA,NA,NA)) # save site, y=1, u, v, d
```

```
    next
  }

  # Simulation data on a square
  u <- runif(N[i], 0, 2*B)   #x coordinate for distance from middle of square/circle
  v <- runif(N[i], 0, 2*B)   #y coordinate for distance from middle of square/circle
  d <- sqrt((u-B)^2 + (v-B)^2)  #distance
  N.true[i] <- sum(d<= B)    # Population size inside of count circle

  # Can only count individuals in the circle, so set to zero probability of individuals in the
corners
  p <- exp(-d *d / (2 * (sigma^2)))  # Detection probability - half normal detection function
  pp <- ifelse(d <= B, 1, 0) * p    # Inside or outside circle (times "inside" or "outside")
  y <- rbinom(N[i], 1, pp)  # Detection/non-detection of each individual

  # Subset to "captured" individuals only
  u <- u[y==1]
  v <- v[y==1]
  d <- d[y==1]
  y <- y[y==1]

  # Compile things into a matrix and insert NA if no individuals were captured at site i.
Coordinates (u,v) are not used here.
  if(sum(y) > 0)
    data <- rbind(data, cbind(rep(i, sum(y)), y, u, v, d))
  else
    data <- rbind(data, c(i,NA,NA,NA,NA)) # make a row of missing data
 }
 colnames(data) <- c("site", "y", "u", "v", "d") # name 1st column "site"

 # ***************************
 # Prep Data for analysis
 # ***************************
 ncap <- table(data[,1])           # ncap = 1 if no individuals captured
 sites0 <- data[is.na(data[,2]),][,1] # sites where nothing was seen
 ncap[as.character(sites0)] <- 0    # Fill in 0 for sites with no detections
 ncap <- as.vector(ncap)           # Number of individuals detected per site
 site <- data[!is.na(data[,2]),1]   # Site ID of each observation
 delta <- 25                       # Distance bin width for rectangular approximation
 midpt <- seq(delta/2, B, delta)    # Make mid-points and chop up data
 dclass <- data[,5] %/% delta + 1   # Convert distance to distance category
 nD <- length(midpt)               # Number of distance intervals
 dclass <- dclass[!is.na(data[,2])] # Observed categorical observations
 nind <- length(dclass)            # Total number of individuals detected
```

```
   # Bundle data
   win.data <- list(nsites=nsites, nind=nind, B=B, nD=nD, midpt=midpt, delta=delta, ncap=ncap,
dclass=dclass, site=site)

   # initial values
   Nst <- ncap + 1       # This line is vital
   inits <- function() list(N = Nst, sigma = runif(1,30,60))

   # Define parameters to be monitored
   params <- c("lambda", "sigma", "Ntotal", "D", "N")

   # MCMC settings
   ni <- 5000
   nt <- 1
   nb <- 1000
   nc <- 3

   start.time = Sys.time()  #set timer
   # run model
   out <- jags(win.data, inits, params, "simHDSpointfunction.txt", n.chains = nc,
            n.thin = nt, n.iter = ni, n.burnin = nb, parallel = TRUE)
   print(out)

   end.time = Sys.time()
   elapsed.time = round(difftime(end.time, start.time, units = 'mins'), dig = 2)
   cat('sim', k,', Posterior computed in ', elapsed.time, ' minutes\n\n', sep='')

   #**************************************
   #### Evaluate bias ####
   #**************************************
   #Bias in N (site specific abundance)
   bias.Nsite <- out$mean$N - N.true #calculates bias
   m.bias.Nsite[k] <- mean(bias.Nsite) #averages bias and places within vector
   sd.bias.Nsite[k] <- sd(bias.Nsite) #gets standard deviation of bias places within vector
   baye.pvalue.Nsite[k] <-mean(N.true > out$mean$N)  #Bayesian P-value (proportion of
simulations where the true abundance was greater than the estimated abundance - values close to
0 or 1 indicate significant bias)

   #Bias in lambda (average local abundance) - descriptions same as above
   bias.lam <- out$mean$lambda - lambda1 #calculates bias (estimated lambda for circle - true
lambda per circle(lambda1))
   m.bias.lam[k] <- mean(bias.lam)
   sd.bias.lam[k] <- sd(bias.lam)
```

```
  baye.pvalue.lam[k] <- mean(lambda1 > out$mean$lambda)
  m.lambda[k] <- out$mean$lambda

  #Bias in sigma - descriptions same as above
  bias.sigma <- out$mean$sigma - sigma
  m.bias.sigma[k] <- mean(bias.sigma)
  sd.bias.sigma[k] <- sd(bias.sigma)
  baye.pvalue.sigma[k] <- mean(sigma > out$mean$sigma)
  m.sig[k] <- out$mean$sigma

  #Bias in Ntotal (total population size)  - descriptions same as above
  bias.Ntot <- out$mean$Ntotal - sum(N.true)
  m.bias.Ntot[k] <- mean(bias.Ntot)
  sd.bias.Ntot[k] <- sd(bias.Ntot)
  baye.pvalue.Ntot[k] <- mean(sum(N.true) > out$mean$Ntotal)
  m.Ntot.true[k] <- sum(N.true)
  m.Ntot[k] <- out$mean$Ntotal

  # Bias in density - descriptions same as above
  bias.den <- out$mean$D - den.true
  m.bias.den[k] <- mean(bias.den)
  sd.bias.den[k] <- sd(bias.den)
  baye.pvalue.den[k] <- mean(den.true > out$mean$D)
  m.density.true[k] <- mean(den.true)
  m.density[k] <- out$mean$D

  #Coefficient of Variation in Ntotal (total population size) - want to be under 15%
  CV.Ntot <- out$sd$Ntotal/out$mean$Ntotal #standard deviation divided by mean
  m.CV.Ntot[k] <- mean(CV.Ntot)
  sd.CV.Ntot[k] <- sd(CV.Ntot)
  prop.CV.Ntot[k] <- mean(CV.Ntot < 0.15) #percent with CV < 0.15

  #Coefficient of Variation in local abundance (lambda / average local abundance)
  CV.lam <- out$sd$lambda/out$mean$lambda
  m.CV.lam[k] <- mean(CV.lam)
  sd.CV.lam[k] <- sd(CV.lam)
  prop.CV.lam[k] <- mean(CV.lam < 0.15)

}  ) #This will be the end of the simulations

#********************
# Summary of Results
#********************
```

```
  results <- c("lambda", "sigma", "N.total", "N.site", "N.total.CV", "lambda.CV",
"Prob.CV.Ntot", "Prob.CV.lambda")
  mean.bias <- round(c((mean(unlist(m.bias.lam))), (mean(unlist(m.bias.sigma))),
(mean(unlist(m.bias.Ntot))), (mean(unlist(m.bias.Nsite))), (mean(unlist(m.CV.Ntot))),
(mean(unlist(m.CV.lam))), NA, NA),2)

  lower.CI <- round(c((quantile(unlist(m.bias.lam), 0.05)), (quantile(unlist(m.bias.sigma), 0.05)),
(quantile(unlist(m.bias.Ntot), 0.05)), (quantile(unlist(m.bias.Nsite), 0.05)),
(quantile(unlist(m.CV.Ntot), 0.05)), (quantile(unlist(m.CV.lam), 0.05)), NA, NA),2) #lower 90%
credible interval

  upper.CI <- round(c((quantile(unlist(m.bias.lam), 0.95)), (quantile(unlist(m.bias.sigma), 0.95)),
(quantile(unlist(m.bias.Ntot), 0.95)), (quantile(unlist(m.bias.Nsite), 0.95)),
(quantile(unlist(m.CV.Ntot), 0.95)), (quantile(unlist(m.CV.lam), 0.95)), NA, NA),2) #upper 90%
credible interval

  greater.15.CV <- c(NA, NA, NA, NA, NA, NA, (mean(unlist(m.CV.Ntot) > 0.15)),
(mean(unlist(m.CV.lam) > 0.15))) #percent of CV's greater than 15%

  Baye.pvalue <- round(c((mean(unlist(baye.pvalue.lam))), (mean(unlist(baye.pvalue.sigma))),
(mean(unlist(baye.pvalue.Ntot))), (mean(unlist(baye.pvalue.Nsite))), NA, NA, NA, NA),2)

  sim.results <- data.frame(results,mean.bias,lower.CI, upper.CI, Baye.pvalue, greater.15.CV)
#creates a table of results
  print(sim.results)

  #*****************
  #Post processing
  #*****************
  # Set plots so that six plots can be created in one image
  par(mfrow = c(6,1), mai=c(0.5,0.2,0.2,0.2), mar=c(1,5,1,2), oma=c(1,1,1,1), las=1)

  # Plots
  (hist(unlist(m.bias.Nsite), xlim=c(-1,1), main="", ylab="N.site"))
  (abline(v=0, col="red", lwd=3))

  (hist(unlist(m.bias.lam), xlim=c(-1,1), main="", ylab="lambda"))
  (abline(v=0, col="red", lwd=3))

  (hist(unlist(m.bias.sigma), xlim=c(-10,10), main="", ylab="Sigma"))
  (abline(v=0, col="red", lwd=3))

  (hist(unlist(m.bias.Ntot), xlim=c(-200,200), main="", ylab="Total N"))
  (abline(v=0, col="red", lwd=3))
```

```
  (hist(unlist(m.CV.Ntot), xlim=c(0,1), main="", ylab="CV Ntotal"))
  (abline(v=0.15, col="red", lwd=3))

  (hist(unlist(m.CV.lam), xlim=c(0,1), main="", ylab="CV lambda"))
  (abline(v=0.15, col="red", lwd=3))

  return(list(sim.results=sim.results, m.bias.Nsite=unlist(m.bias.Nsite), m.bias.lam =
unlist(m.bias.lam), m.bias.sigma = unlist(m.bias.sigma), m.bias.Ntot = unlist(m.bias.Ntot),
m.CV.Ntot = unlist(m.CV.Ntot), m.CV.lam = unlist(m.CV.lam), lambda = lambda, sigma =
sigma, nsites = nsites, num.sim = num.sim, density.true = unlist(m.density.true), m.density =
unlist(m.density), Ntot.true = unlist(m.Ntot.true), m.Ntot = unlist(m.Ntot), m.sigma =
unlist(m.sig), m.lambda = unlist(m.lambda), out = out))
}
```

APPENDIX H

APPENDIX H: BAYESIAN MODEL SPECIFICATION AND SIMULATION CODE FOR LINE TRANSECTS EVALUATED USING HIERARCHICAL DISTANCE SAMPLING

Complete Bayesian model specification and simulation code in R language for evaluating Dusky Grouse survey protocols for line transects analyzed using hierarchical distance sampling where local abundance and probability of detection (sigma) were kept constant.

```
# Function for simulating and analyzing data using a hierarchical distance sampling model for line transects where both abundance and sigma (detection) are kept constant.

# Code adapted from: Kery, M. and J. A. Royle. 2016. Applied hierarchical modeling in ecology: analysis of distribution, abundance, and species richness in R and BUGS. Academic Press, London, United Kingdom

# nsites = number of sites
# lambda = average local abundance per transect
# sigma = sigma for the half-normal detection function
# num.sim = number of simulations
# L = transect length

Sim.HDS.line.fn <- function(nsites = nsites, lambda = lambda, sigma = sigma, num.sim = num.sim, L = L) {
  library(jagsUI) # use the JAGS for analyzing data within a Bayesian framework

  #***************
  # Define Bayesian Model
  #***************

  # Specify model in Bugs language, but going to use JagsUI/jags
  sink("simHDSlinefunction.txt")
  cat("
 model{
  # Priors
  sigma ~ dunif(0,100) #vague prior for sigma
  lambda ~ dgamma(0.001, 0.001) # vague prior for lambda
  for(i in 1:nind){
   dclass[i] ~ dcat(fc[site[i],]) # Part 1 of HM - model for distance class of the observed individuals
}
  for(s in 1:nsites){
    # Construct cell probabilities for nD distance bands
    for(g in 1:nD){              # midpt = mid-point of each band
      log(p[s,g]) <- -midpt[g] * midpt[g] / (2 * sigma * sigma) # half-normal detection function
      pi[s,g] <- delta/B # prob. per interval
      f[s,g] <- p[s,g] * pi[s,g]
      fc[s,g] <- f[s,g] / pcap[s]
    }
    pcap[s] <- sum(f[s,])          # Pr(capture): sum of rectangular areas
```

```
   ncap[s] ~ dbin(pcap[s], N[s])   # Part 2 of HM - describes imperfect detection leading to count
n[s]
   N[s] ~ dpois(lambda)         # Part 3 of HM - describes spatial variation in local abundance N[s]
  }
  # Derived parameters
  Ntotal <- sum(N[]) #total of abundance at each site (N)
  area <- nsites*L*2*B/1000000 #area of transects
  D <- Ntotal/area #density
}
   ",fill = TRUE)
  sink()


  #************************************************
  # Loop for replicating datasets and assessing bias
  #************************************************

  num.sim <- num.sim

  # Create empty vectors to store results from replicated datasets
  m.bias.Nsite <- vector("list",num.sim)  #examine bias in abundance (N) at each site
  sd.bias.Nsite <- vector("list",num.sim)
  baye.pvalue.Nsite <- vector("list",num.sim)
  m.Ntrue <- vector("list",num.sim)
  m.N <- vector("list",num.sim)

  m.bias.sigma <- vector("list",num.sim) #bias in sigma
  sd.bias.sigma <- vector("list",num.sim)
  baye.pvalue.sigma <- vector("list",num.sim)
  m.sig <- vector("list", num.sim)

  m.bias.Ntot <- vector("list",num.sim) #bias in total N
  sd.bias.Ntot <- vector("list",num.sim)
  baye.pvalue.Ntot <- vector("list",num.sim)
  m.bias.Ntot <- vector("list", num.sim)
  m.Ntot.true <- vector("list", num.sim)
  m.Ntot <- vector("list", num.sim)

  m.bias.lam <- vector("list",num.sim)  #bias in recovered lambda (mean abundance at site)
  sd.bias.lam <- vector("list",num.sim)
  baye.pvalue.lam <- vector("list",num.sim)
  m.lambda <- vector("list", num.sim)

  m.bias.den <- vector("list", num.sim) #bias in density
```

```
  sd.bias.den <- vector("list", num.sim)
  baye.pvalue.den <- vector("list", num.sim)
  m.density <- vector("list", num.sim)
  m.density.true <- vector("list", num.sim)

  m.CV.lam <- vector("list",num.sim)  #coefficient of variation for lambda (mean abundance at
site)
  sd.CV.lam <- vector("list",num.sim)
  prop.CV.lam <- vector("list", num.sim)

  m.CV.Ntot <- vector("list",num.sim) #coefficient of variation for total N
  sd.CV.Ntot <- vector("list",num.sim)
  prop.CV.Ntot <- vector("list", num.sim)

  #*********************
  # Start Simulation
  #*********************

  # Stick simulation in loop and replicate num.sim times
  system.time(for (k in 1:num.sim) {  #keep track of how long simulation takes

    # ***************
    # Simulate Data
    # ***************
    # Simulate abundance model (Poisson GLM for N)
    N <- rpois(nsites, lambda)              # site-specific abundances
    N.true <- N #true abundance at each site, for a transect this is the same as N (differs for point
counts)
    B <- 100 #strip half-width
    L <- L #length of transect
    area <- nsites*L*2*B/1000000 #area meters squared
    den.true <- sum(N)/area # true density

    # Simulate observation model - set up empty dataframe
    data <- NULL

    for(i in 1:nsites){
      if(N[i]==0){ #if abundance at a site is 0
        data <- rbind(data, c(i,NA,NA,NA,NA)) # save site, y=1, u, v, d
        next
      }
      # Simulation of distances, uniformly, for each individual in population
      # note it piles up all N[i] guys on one side of the transect
      d <- runif(N[i], 0, B)
```

```
  p <- exp(-d *d / (2 * (sigma^2))) # half-normal detection function
  # Determine if individuals are captured or not
  y <- rbinom(N[i], 1, p)
  u <- v <- rep(NA, N[i])   # coordinates (u,v)
  # Subset to "captured" individuals only
  d <- d[y==1]
  u <- u[y==1]
  v <- v[y==1]
  y <- y[y==1]


  # Compile things into a matrix and insert NA if no individuals were
  # captured at site i. Coordinates (u,v) are not used here.
  if(sum(y) > 0)
    data <- rbind(data, cbind(rep(i, sum(y)), y, u, v, d))
  else
    data <- rbind(data, c(i,NA,NA,NA,NA)) # make a row of missing data
}
colnames(data) <- c("site", "y", "u", "v", "d") # name 1st col "site"

# ************************
# Prep Data for analysis
# ************************
ncap <- table(data[,1])           # ncap = 1 if no individuals captured
sites0 <- data[is.na(data[,2]),1] # sites where nothing was seen
ncap[as.character(sites0)] <- 0    # Fill in 0 for sites with no detections
ncap <- as.vector(ncap)           # Number of individuals detected per site
site <- data[!is.na(data[,2]),1]   # Site ID of each observation
delta <- 10                       # Distance bin width for rect. approx.
midpt <- seq(delta/2, B, delta)    # Make mid-points and chop up data
dclass <- data[,5] %/% delta + 1   # Convert distance to distance category
nD <- length(midpt)               # Number of distance intervals
dclass <- dclass[!is.na(data[,2])] # Observed categorical observations
nind <- length(dclass)            # Total number of individuals detected

# Bundle data
win.data <- list(nsites=nsites, nind=nind, B=B, nD=nD, midpt=midpt, delta=delta, ncap=ncap,
dclass=dclass, site=site, L=L)

# initial values
Nst <- ncap + 1       # This line is vital
inits <- function() list(N = Nst, sigma = runif(1,30,60))

# Define parameters to be monitored
```

```
params <- c("lambda", "sigma", "Ntotal", "D", "N")

# MCMC settings
ni <- 5000
nt <- 1
nb <- 1000
nc <- 3

start.time = Sys.time()  #set timer
# run model
out <- jags(win.data, inits, params, "simHDSlinefunction.txt", n.chains = nc,
          n.thin = nt, n.iter = ni, n.burnin = nb, parallel = TRUE)
print(out)

end.time = Sys.time()
elapsed.time = round(difftime(end.time, start.time, units = 'mins'), dig = 2)
cat('sim', k,', Posterior computed in ', elapsed.time, ' minutes\n\n', sep='')

#************************************
#### EValuate bias ####
#************************************
#Bias in N (site specific abundance)
bias.Nsite <- out$mean$N - N.true #calculates bias
m.bias.Nsite[k] <- mean(bias.Nsite) #averages bias and places within vector
sd.bias.Nsite[k] <- sd(bias.Nsite) #gets standard deviation of bias places within vector
baye.pvalue.Nsite[k] <-mean(N.true > out$mean$N)  #Bayesian P-value (proportion of
simulations where the true abundance was greater than the estimated abundance - values close to
0 or 1 indicate significant bias)

#Bias in lambda (average local abundance) - descriptions same as above
bias.lam <- out$mean$lambda - lambda
m.bias.lam[k] <- mean(bias.lam)
sd.bias.lam[k] <- sd(bias.lam)
baye.pvalue.lam[k] <- mean(lambda > out$mean$lambda)
m.lambda[k] <- out$mean$lambda

#Bias in sigma - descriptions same as above
bias.sigma <- out$mean$sigma - sigma
m.bias.sigma[k] <- mean(bias.sigma)
sd.bias.sigma[k] <- sd(bias.sigma)
baye.pvalue.sigma[k] <- mean(sigma > out$mean$sigma)
m.sig[k] <- out$mean$sigma

#Bias in Ntotal (total population size)  - descriptions same as above
```

```
   bias.Ntot <- out$mean$Ntotal - sum(N.true)
   m.bias.Ntot[k] <- mean(bias.Ntot)
   sd.bias.Ntot[k] <- sd(bias.Ntot)
   baye.pvalue.Ntot[k] <- mean(sum(N.true) > out$mean$Ntotal)
   m.Ntot.true[k] <- sum(N.true)
   m.Ntot[k] <- out$mean$Ntotal

   #Bias in density - descriptions same as above
   bias.den <- out$mean$D - den.true
   m.bias.den[k] <- mean(bias.den)
   sd.bias.den[k] <- sd(bias.den)
   baye.pvalue.den[k] <- mean(den.true > out$mean$D)
   m.density.true[k] <- mean(den.true)
   m.density[k] <- out$mean$D

   #Coefficient of Variation in Ntotal (total population size) - want to be under 15%
   CV.Ntot <- out$sd$Ntotal/out$mean$Ntotal #standard deviation divided by mean
   m.CV.Ntot[k] <- mean(CV.Ntot)
   sd.CV.Ntot[k] <- sd(CV.Ntot)
   prop.CV.Ntot[k] <- mean(CV.Ntot < 0.15)

   #Coefficient of Variation in local abundance (lambda / average local abundance)
   CV.lam <- out$sd$lambda/out$mean$lambda
   m.CV.lam[k] <- mean(CV.lam)
   sd.CV.lam[k] <- sd(CV.lam)
   prop.CV.lam[k] <- mean(CV.lam < 0.15)

  }  ) #This will be the end of the simulations

  #*********************
  # Summary of Results
  #*********************
  results <- c("lambda", "sigma", "N.total", "N.site", "N.total.CV", "lambda.CV",
"Prob.CV.Ntot", "Prob.CV.lambda")
  mean.bias <- round(c((mean(unlist(m.bias.lam))), (mean(unlist(m.bias.sigma))),
(mean(unlist(m.bias.Ntot))), (mean(unlist(m.bias.Nsite))), (mean(unlist(m.CV.Ntot))),
(mean(unlist(m.CV.lam))), NA, NA),2)

  lower.CI <- round(c((quantile(unlist(m.bias.lam), 0.05)), (quantile(unlist(m.bias.sigma), 0.05)),
(quantile(unlist(m.bias.Ntot), 0.05)), (quantile(unlist(m.bias.Nsite), 0.05)),
(quantile(unlist(m.CV.Ntot), 0.05)), (quantile(unlist(m.CV.lam), 0.05)), NA, NA),2) #lower 90%
credible interval
```

```
  upper.CI <- round(c((quantile(unlist(m.bias.lam), 0.95)), (quantile(unlist(m.bias.sigma), 0.95)),
(quantile(unlist(m.bias.Ntot), 0.95)), (quantile(unlist(m.bias.Nsite), 0.95)),
(quantile(unlist(m.CV.Ntot), 0.95)), (quantile(unlist(m.CV.lam), 0.95)), NA, NA),2) #upper 90%
credible interval

  greater.15.CV <- c(NA, NA, NA, NA, NA, NA, (mean(unlist(m.CV.Ntot) > 0.15)),
(mean(unlist(m.CV.lam) > 0.15))) #percent of CV's greater than 15%

  Baye.pvalue <- round(c((mean(unlist(baye.pvalue.lam))), (mean(unlist(baye.pvalue.sigma))),
(mean(unlist(baye.pvalue.Ntot))), (mean(unlist(baye.pvalue.Nsite))), NA, NA, NA, NA),2)

  sim.results <- data.frame(results,mean.bias,lower.CI, upper.CI, Baye.pvalue, greater.15.CV)
#creates a table of results
  print(sim.results)

  #*****************
  #Post processing
  #*****************
  # Set plots so that six plots can be created in one image
  par(mfrow = c(6,1), mai=c(0.5,0.2,0.2,0.2), mar=c(1,5,1,2), oma=c(1,1,1,1), las=1)

  # Plots
  (hist(unlist(m.bias.Nsite), xlim=c(-10,10), main="", ylab="N.site"))
  (abline(v=0, col="red", lwd=3))

  (hist(unlist(m.bias.lam), xlim=c(-1,1), main="", ylab="lambda"))
  (abline(v=0, col="red", lwd=3))

  (hist(unlist(m.bias.sigma), xlim=c(-10,10), main="", ylab="Sigma"))
  (abline(v=0, col="red", lwd=3))

  (hist(unlist(m.bias.Ntot), xlim=c(-200,200), main="", ylab="Total N"))
  (abline(v=0, col="red", lwd=3))

  (hist(unlist(m.CV.Ntot), xlim=c(0,1), main="", ylab="CV Ntotal"))
  (abline(v=0.15, col="red", lwd=3))

  (hist(unlist(m.CV.lam), xlim=c(0,1), main="", ylab="CV lambda"))
  (abline(v=0.15, col="red", lwd=3))

  return(list(sim.results=sim.results, m.bias.Nsite=unlist(m.bias.Nsite), m.bias.lam =
unlist(m.bias.lam), m.bias.sigma = unlist(m.bias.sigma), m.bias.Ntot = unlist(m.bias.Ntot),
m.CV.Ntot = unlist(m.CV.Ntot), m.CV.lam = unlist(m.CV.lam), lambda = lambda, sigma =
sigma, nsites = nsites, num.sim = num.sim, density.true = unlist(m.density.true), m.density =
```

```
unlist(m.density), Ntot.true = unlist(m.Ntot.true), m.Ntot = unlist(m.Ntot), m.sigma =
unlist(m.sig), m.lambda = unlist(m.lambda), out = out))
}
```

APPENDIX I

APPENDIX I: BAYESIAN MODEL SPECIFICATION AND SIMULATION CODE FOR LINE TRANSECTS EVALUATED USING TIME-REMOVAL HIERARCHICAL DISTANCE SAMPLING

Complete Bayesian model specification and simulation code in R language for evaluating Dusky Grouse survey protocols for point counts analyzed using time-removal HDS where local abundance and probability of detection (sigma) were kept constant.

```
# Function for simulating and analyzing data using a hierarchical distance sampling model and time removal for point counts where both abundance, detection, and availability is kept constant.
# Data is simulated over a square using average local abundance for the square (lambda) and then truncated into a circle with radius B with an average local abundance equal to the estimated average local abundance of a point count site from the 2020 & 2021 data

# Code adapted from:
#Kery, M. and J. A. Royle. 2016. Applied hierarchical modeling in ecology: analysis of distribution, abundance, and species richness in R and BUGS. Academic Press, London, United Kingdom.
#Amundson, C. L., J. A. Royle, C. M. Handel. 2014. A hierarchical model combining distance sampling and time removal to estimate detection probability during avian point counts. The Auk 131(4): 476-494.
#Hostetter, N. J., B. Gardner, T. S. Sillett, K. H. Pollock, T. R. Simmons. 2019. An integrated model decomposing the components of detection probability and abundance in unmarked populations. Ecosphere 10(3)

# nsites = number of sites
# lambda = average local abundance per site over a square with area 2B x 2B where B = radius of circle
# lambda1 = average local abundance per point count site (so average local abundance within a circle with a radius of B)
# sigma = sigma for the half-normal detection function
# num.sim = number of simulations
# p.avail = overall availability probability
# int.avail = time interval-specific availability probability

Sim.HDS.TR.function <- function(nsites = nsites, lambda = lambda, sigma = sigma, num.sim = num.sim, lambda1 = lambda1, p.avail = p.avail) {
  library(jagsUI) # use the JAGS for analyzing data within a Bayesian framework

  #***************
  # Define Model
  #***************

  # Specify model in Bugs language, but going to use JagsUI/jags
  sink("simHDS_TR.txt")
  cat("
model {
  # Prior distributions for basic parameters
```

```
  p.a ~ dunif(0,1) # vague prior for availability (during a)
  sigma ~ dunif(0,100) # vague prior for sigma
  lambda ~ dgamma(0.001, 0.001) # vague prior for abundance

for(s in 1:nsites){

    # Distance sampling detection probability model
    for(b in 1:nD){
      log(g[b,s]) <- -mdpts[b] * mdpts[b] / (2*sigma*sigma)  # Half-normal
      f[b,s] <- (2 * mdpts[b] * delta ) / (B*B) # Radial density function
      pi.pd[b,s] <- g[b,s]*f[b,s]  #  Product Pr(detect)*Pr(distribution)
      pi.pd.c[b,s] <- pi.pd[b,s]/pdet[s]  # Conditional probabilities
    }

    pdet[s] <- sum(pi.pd[,s])  # Probability of detection at all

    # Time-removal probabilities
    for (k in 1:K){
      pi.pa[k,s] <- p.a * pow(1-p.a, (k-1))
      pi.pa.c[k,s] <- pi.pa[k,s]/phi[s] # Conditional probabilities of availability
    }

    phi[s] <- sum(pi.pa[,s]) # Probability of ever available

  }
  # Conditional observation model for categorical covariates
  for(i in 1:nobs){
    dclass[i] ~ dcat(pi.pd.c[,site[i]])
    tint[i] ~ dcat(pi.pa.c[,site[i]])
  }
  # Abundance model
  for(s in 1:nsites){

    n[s] ~ dbin(pdet[s], N[s])    # counts related to probability of detection given availability
    N[s] ~ dbin(phi[s],M[s])      # Number of available individuals
    M[s] ~ dpois(lambda)       # Abundance per survey/site/point

  }

  # Derived quantities
  Mtot <- sum(M[])  # Total population size
  Ntot <- sum(N[])  # Total available population size
  PDETmean <- mean(pdet[]) # Mean perceptibility across sites
  PHImean <- mean(phi[]) # Mean availability across sites
```

```
}
  ",fill = TRUE)
 sink()

 #************************************************
 # Loop for replicating datasets and assessing bias
 #************************************************

 num.sim <- num.sim

 # Create empty vectors to store results from replicated datasets
 m.bias.Msite <- vector("list",num.sim)  #examine bias in abundance (M) at each site
 sd.bias.Msite <- vector("list",num.sim)
 baye.pvalue.Msite <- vector("list",num.sim)
 m.Mtrue <- vector("list",num.sim)
 m.M <- vector("list",num.sim)

 m.bias.sigma <- vector("list",num.sim) #bias in probablity of detection
 sd.bias.sigma <- vector("list",num.sim)
 baye.pvalue.sigma <- vector("list",num.sim)
 m.sig <- vector("list", num.sim)

 m.bias.PHImean <- vector("list",num.sim) #bias in probablity of availability
 sd.bias.PHImean <- vector("list",num.sim)
 baye.pvalue.PHImean <- vector("list",num.sim)
 m.PHImean <- vector("list", num.sim)

 m.bias.Mtot <- vector("list",num.sim) #bias in total M
 sd.bias.Mtot <- vector("list",num.sim)
 baye.pvalue.Mtot <- vector("list",num.sim)
 m.bias.Mtot <- vector("list", num.sim)
 m.Mtot.true <- vector("list", num.sim)
 m.Mtot <- vector("list", num.sim)

 m.bias.lam <- vector("list",num.sim)  #bias in recovered lambda (mean abundance at site)
 sd.bias.lam <- vector("list",num.sim)
 baye.pvalue.lam <- vector("list",num.sim)
 m.lambda <- vector("list", num.sim)

 m.CV.lam <- vector("list",num.sim)  #coefficient of variation for lambda (mean abundance at
site)
 sd.CV.lam <- vector("list",num.sim)
 prop.CV.lam <- vector("list", num.sim)
```

```
m.CV.Mtot <- vector("list",num.sim) #coefficient of variation for total N
sd.CV.Mtot <- vector("list",num.sim)
prop.CV.Mtot <- vector("list", num.sim)

#*********************
# Start Simulation
#*********************

# Stick simulation in loop and replicate num.sim times
system.time(for (k in 1:num.sim) {  #keep track of how long simulation takes

  # ***************
  # Simulate Data
  # ***************
  # Simulate superpopulation abundance model for groups (Poisson GLM for M)
  M <- rpois(nsites, lambda)          # site-specific abundance for square
  M.true <- M                         # for point: inside of circle (radius = B)
  B <- 100 #radius for circle (meters)
  K <- 4 #number of time intervals


  # Simulate observation model - set up empty dataframe
  data <- NULL
  for(i in 1:nsites){
    if(M[i]==0){ #if abundance at a site is 0
      data <- rbind(data,c(i,NA,NA,NA,NA,NA)) # save site, y=1, u, v, d, tint
      next
    }

    # Simulation data on a square
    u <- runif(M[i], 0, 2*B)   #x
    v <- runif(M[i], 0, 2*B)   #y
    d <- sqrt((u-B)^2 + (v-B)^2)  #distance
    M.true[i] <- sum(d<= B)    # Population size inside of count circle

    # Can only count individuals in the circle, so set to zero probability of individuals in the
corners
    p <- ifelse(d <= B, 1, 0) * exp(-d *d / (2 * (sigma^2))) #half-normal detection function

    # Time-removal
    int.avail <- 1 - (1-p.avail)^(1/K) #calculate time-interval specific availability probability
    rem.probs <- c(int.avail, ((1-int.avail)^(1:(K-1)))*int.avail) #calculate probability for each
time interval
```

```
    mn.probs <- c(rem.probs, 1-sum(rem.probs)) #probability for each time interval + probability
not ever available
    aux <- sample(1:(K+1), M[i], replace=TRUE, prob=mn.probs)
    aux[aux==(K+1)] <- 0 #if not capture during intervals 1-K, set to 0

    newp <-  p * as.numeric(aux!=0) #combine probability of detection with availability
    navail <- sum(aux!=0)

    if(navail==0){
      data <- rbind(data,c(i,NA,NA,NA,NA,NA)) # save site, y=1, u, v, d
      next
    }

    # generate count of birds based on combined probability of detection
    y <- rbinom(M[i], 1, newp)
    # Subset to "captured" individuals only
    u <- u[y==1]
    v <- v[y==1]
    d <- d[y==1]
    aux <- aux[y==1]
    y <- y[ y==1]

    # Now compile things into a matrix and insert NA if no individuals were
    # captured at site i. Coordinates (u,v) are not used here.
    if(sum(y)>0){
      data <- rbind(data, cbind(rep(i, sum(y)), y, u, v, d, aux))
    } else {
      data <- rbind(data, c(i,NA,NA,NA,NA,NA)) # make a row of missing data
    }
  } # end of for loop
  colnames(data)[1] <- "site"

  # ************************
  # Prep Data for analysis
  # ************************
  # Create the observed encounter frequencies per site (include the zeros! )
  data <- data[!is.na(data[,2]),]   # Sites where detections did occur
  n <- rep(0,nsites)               # The full site vector
  names(n) <- 1:nsites
  n[names(table(data[,1]))] <- table(data[,1])  # Put in the counts
  site <- data[,1]
  nobs <- nrow(data)

  # Create the distance class data
```

```
nD <- 10            # Number of distance classes
delta <- B/nD       # bin size or width
mdpts <- seq(delta/2,B,delta) # midpoint distance of bins up to max distance
dclass <- data[,"d"] # distance class for each observation
dclass <- dclass%/%delta  +1
tint <- data[,"aux"]

# Bundle data and summarize
win.data<-list(n=n, site=site, dclass=as.numeric(dclass),nsites=nsites,
               nobs=nobs, delta=delta, nD=nD,mdpts=mdpts,B=B, K=K, tint=tint)

Mst <- Nst <- n + 1
inits <- function(){list(M=Mst, N=Nst)}
params <- c("PDETmean", "PHImean", "Mtot", "Ntot", "p.a", "sigma", "lambda", "N", "M")

# MCMC settings
ni <- 20000
nt <- 1
nb <- 1000
nc <- 3

start.time = Sys.time()  #set timer
# run model
out <- jags(win.data, inits, params, "simHDS_TR.txt", n.chains = nc, n.thin = nt, n.iter = ni,
n.burnin = nb, parallel = TRUE)
print(out)

end.time = Sys.time()
elapsed.time = round(difftime(end.time, start.time, units = 'mins'), dig = 2)
cat('sim', k,', Posterior computed in ', elapsed.time, ' minutes\n\n', sep='')

#**************************************
#### Evaluate bias ####
#**************************************
##Bias in N (site specific abundance)
bias.Msite <- out$mean$M - M.true #calculates bias
m.bias.Msite[k] <- mean(bias.Msite) #averages bias and places within vector
sd.bias.Msite[k] <- sd(bias.Msite) #gets standard deviation of bias places within vector
baye.pvalue.Msite[k] <-mean(M.true > out$mean$M)  #Bayesian P-value (proportion of
simulations where the true abundance was greater than the estimated abundance - values close to
0 or 1 indicate significant bias)

##Bias in lambda (average local abundance) - descriptions same as above
```

```
   bias.lam <- out$mean$lambda - lambda1 #calculates bias (estimated lambda for circle - true
lambda per circle(lambda1))
   m.bias.lam[k] <- mean(bias.lam)
   sd.bias.lam[k] <- sd(bias.lam)
   baye.pvalue.lam[k] <- mean(lambda1 > out$mean$lambda)
   m.lambda[k] <- out$mean$lambda

   ##Bias in sigma - descriptions same as above
   bias.sigma <- out$mean$sigma - sigma
   m.bias.sigma[k] <- mean(bias.sigma)
   sd.bias.sigma[k] <- sd(bias.sigma)
   baye.pvalue.sigma[k] <- mean(sigma > out$mean$sigma)
   m.sig[k] <- out$mean$sigma

   ##Bias in availability - descriptions same as above
   bias.PHImean <- out$mean$PHImean - p.avail
   m.bias.PHImean[k] <- mean(bias.PHImean)
   sd.bias.PHImean[k] <- sd(bias.PHImean)
   baye.pvalue.PHImean[k] <- mean(p.avail > out$mean$PHImean)
   m.PHImean[k] <- out$mean$PHImean

   ##Bias in Mtotal (total population size)  - descriptions same as above
   bias.Mtot <- out$mean$Mtot - sum(M.true)
   m.bias.Mtot[k] <- mean(bias.Mtot)
   sd.bias.Mtot[k] <- sd(bias.Mtot)
   baye.pvalue.Mtot[k] <- mean(sum(M.true) > out$mean$Mtot)
   m.Mtot.true[k] <- sum(M.true)
   m.Mtot[k] <- out$mean$Mtot

   ##Coefficient of Variation in Mtotal (total population size) - want to be under 15%
   CV.Mtot <- out$sd$Mtot/out$mean$Mtot #standard deviation divided by mean
   m.CV.Mtot[k] <- mean(CV.Mtot)
   sd.CV.Mtot[k] <- sd(CV.Mtot)
   prop.CV.Mtot[k] <- mean(CV.Mtot < 0.15)

   #Coefficient of Variation in local abundance (lambda / average local abundance)
   CV.lam <- out$sd$lambda/out$mean$lambda
   m.CV.lam[k] <- mean(CV.lam)
   sd.CV.lam[k] <- sd(CV.lam)
   prop.CV.lam[k] <- mean(CV.lam < 0.15)

 }  ) #This will be the end of the simulations

 #********************
```

```
  # Summary of Results
  #*********************
  results <- c("lambda", "sigma", "PHImean", "M.total", "M.site", "N.total.CV", "lambda.CV",
"Prob.CV.Ntot", "Prob.CV.lambda")
  mean.bias <- round(c((mean(unlist(m.bias.lam))), (mean(unlist(m.bias.sigma))),
(mean(unlist(m.bias.PHImean))), (mean(unlist(m.bias.Mtot))), (mean(unlist(m.bias.Msite))),
(mean(unlist(m.CV.Mtot))), (mean(unlist(m.CV.lam))), NA, NA),2)

  lower.CI <- round(c((quantile(unlist(m.bias.lam), 0.05)), (quantile(unlist(m.bias.sigma), 0.05)),
(quantile(unlist(m.bias.PHImean), 0.05)), (quantile(unlist(m.bias.Mtot), 0.05)),
(quantile(unlist(m.bias.Msite), 0.05)), (quantile(unlist(m.CV.Mtot), 0.05)),
(quantile(unlist(m.CV.lam), 0.05)), NA, NA),2) #lower 90% credible interval

  upper.CI <- round(c((quantile(unlist(m.bias.lam), 0.95)), (quantile(unlist(m.bias.sigma), 0.95)),
(quantile(unlist(m.bias.PHImean), 0.95)), (quantile(unlist(m.bias.Mtot), 0.95)),
(quantile(unlist(m.bias.Msite), 0.95)), (quantile(unlist(m.CV.Mtot), 0.95)),
(quantile(unlist(m.CV.lam), 0.95)), NA, NA),2) #upper 90% credible interval

  greater.15.CV <- c(NA, NA, NA, NA, NA, NA, NA, (mean(unlist(m.CV.Mtot) > 0.15)),
(mean(unlist(m.CV.lam) > 0.15))) #percent of CV's greater than 15%

  Baye.pvalue <- round(c((mean(unlist(baye.pvalue.lam))), (mean(unlist(baye.pvalue.sigma))),
(mean(unlist(baye.pvalue.PHImean))), (mean(unlist(baye.pvalue.Mtot))),
(mean(unlist(baye.pvalue.Msite))), NA, NA, NA, NA),2)

  sim.results <- data.frame(results,mean.bias,lower.CI, upper.CI, Baye.pvalue, greater.15.CV)
#creates a table of results
  print(sim.results)

  #*****************
  #Post processing
  #*****************
  # Set plots so that seven plots can be created in one image
  par(mfrow = c(7,1), mai=c(0.5,0.2,0.2,0.2), mar=c(1,5,1,2), oma=c(1,1,1,1), las=1)

  # Plots
  (hist(unlist(m.bias.Msite), xlim=c(-10,10), main="", ylab="M.site"))
  (abline(v=0, col="red", lwd=3))

  (hist(unlist(m.bias.lam), xlim=c(-1,1), main="", ylab="lambda"))
  (abline(v=0, col="red", lwd=3))

  (hist(unlist(m.bias.sigma), xlim=c(-10,10), main="", ylab="Sigma"))
  (abline(v=0, col="red", lwd=3))
```

```
 (hist(unlist(m.bias.PHImean), xlim=c(-10,10), main="", ylab="PHI mean"))
 (abline(v=0, col="red", lwd=3))

 (hist(unlist(m.bias.Mtot), xlim=c(-200,200), main="", ylab="Total M"))
 (abline(v=0, col="red", lwd=3))

 (hist(unlist(m.CV.Mtot), xlim=c(0,1), main="", ylab="CV Mtotal"))
 (abline(v=0.15, col="red", lwd=3))

 (hist(unlist(m.CV.lam), xlim=c(0,1), main="", ylab="CV lambda"))
 (abline(v=0.15, col="red", lwd=3))

 return(list(sim.results=sim.results, m.bias.Msite=unlist(m.bias.Msite), m.bias.lam =
unlist(m.bias.lam), m.bias.sigma = unlist(m.bias.sigma), m.bias.PHImean =
unlist(m.bias.PHImean), m.bias.Mtot = unlist(m.bias.Mtot), m.CV.Mtot = unlist(m.CV.Mtot),
m.CV.lam = unlist(m.CV.lam), lambda = lambda, sigma = sigma, p.avail= p.avail, nsites =
nsites, num.sim = num.sim, Mtot.true = unlist(m.Mtot.true), m.Mtot = unlist(m.Mtot), m.sigma =
unlist(m.sig), m.PHImean = unlist(m.PHImean), m.lambda = unlist(m.lambda), out = out))
}
```

APPENDIX J

BAYESIAN MODEL SPECIFICATION AND SIMULATION CODE FOR NAÏVE MODELS

Complete Bayesian model specification and simulation code in R language for evaluating Dusky Grouse survey protocols for point counts analyzed using naïve models where local abundance and probability of detection were kept constant.

```
# Function for simulating and analyzing data using a naive model where average local abundance is estimated without take probability of detection into account for point counts. Local abundance is kept similar across all sites and probability of detection is kept constant.

# S = number of spatial reps/ number of sites
# V = number of visits at each site (temporal reps) - which was 1 for these simulations
# lambda = average local abundance
# prob = probability of detection
# num.sim = number of simulations

#Simulate Data - Nmixture model. Parameters estimated: lambda and probability of detection
Sim.Naive.fn <- function(S=S, V=V, lambda = lambda, prob = prob, num.sim = num.sim) {
  library(jagsUI)

  #***************
  # Define Model
  #***************

  # Specify model in Bugs language, but going to use JagsUI/jags
  sink("Naive.txt")
  cat("
    model {

    # Priors
      lambda ~ dgamma(0.005, 0.005)      # Standard vague prior for lambda

    # Likelihood
      # Biological model for true abundance
        for (i in 1:S) {
          N[i] ~ dpois(lambda)

        } # i
    #Derived parameters
       Ntotal <- sum(N[])

    }
    ",fill = TRUE)
  sink()

  #************************************************
  # Loop for replicating datasets and assessing bias
```

```
#************************************************

num.sim <- num.sim

m.bias.Nsite <- vector("list",num.sim)  #examine bias in abundance (N) at each site
sd.bias.Nsite <- vector("list",num.sim)
baye.pvalue.Nsite <- vector("list",num.sim)

m.bias.Ntot <- vector("list",num.sim) #bias in total N
sd.bias.Ntot <- vector("list",num.sim)
baye.pvalue.Ntot <- vector("list",num.sim)

m.bias.lam <- vector("list",num.sim)  #bias in recovered lambda (mean abundance at site)
sd.bias.lam <- vector("list",num.sim)
baye.pvalue.lam <- vector("list",num.sim)


m.CV.lam <- vector("list",num.sim)  #coefficient of variation for lambda (mean abundance at
site)
sd.CV.lam <- vector("list",num.sim)
prop.CV.lam <- vector("list", num.sim)

#********************
# Start Simulation
#********************

# Stick simulation in loop and replicate num.sim times
system.time(for (k in 1:num.sim) {  #keep track of how long simulation takes

  #Simulate data
  S = S  # spatial reps
  V = V  # temporal reps
  lambda = lambda # mean abundance at site
  prob = prob # probability of detection

  # Create structure to contain counts
  y <- array(dim = c(S,V))

  # sample abundance from a Poisson distribution
  N <- rpois(n=S, lambda=lambda)

  # sample counts from a Binomial distribution (N, prob)
  for (j in 1:V){
    y[,j] <- rbinom(n = S, size = N, prob = prob)
```

```
}

Count.data <- apply(y,1,max) #max count if more than 1 visit, if 1 visit then counts for that visit

win.data <- list(N = Count.data, S = nrow(y))

# initial values
inits <- function() list(lambda = 1)

# Define parameters to be monitored
params <- c("lambda", "Ntotal", "N")

# MCMC settings
ni <- 3000
nt <- 1
nb <- 100
nc <- 3

start.time = Sys.time()  #set timer
# run model
out <- jags(win.data, inits, params, "Naive.txt", n.chains = nc,
            n.thin = nt, n.iter = ni, n.burnin = nb)
print(out)

end.time = Sys.time()
elapsed.time = round(difftime(end.time, start.time, units = 'mins'), dig = 2)
cat('sim', k,', Posterior computed in ', elapsed.time, ' minutes\n\n', sep='')

#************************************
#### Evaluate bias ####
#************************************
#Bias in N (site specific abundance)
bias.Nsite <- out$mean$N - N #calculates bias
m.bias.Nsite[k] <- mean(bias.Nsite) #averages bias and places within vector
sd.bias.Nsite[k] <- sd(bias.Nsite) #gets standard deviation of bias places within vector
baye.pvalue.Nsite[k] <-mean(N > out$mean$N)  #Bayesian P-value (proportion of simulations where the true abundance was greater than the estimated abundance - values close to 0 or 1 indicate significant bias)

#Bias in lambda (average local abundance) - descriptions same as above
bias.lam <- out$mean$lambda - lambda
m.bias.lam[k] <- mean(bias.lam)
sd.bias.lam[k] <- sd(bias.lam)
```

```
    baye.pvalue.lam[k] <- mean(lambda > out$mean$lambda)

    #Bias in Ntotal (total population size)  - descriptions same as above
    bias.Ntot <- out$mean$Ntotal - sum(N)
    m.bias.Ntot[k] <- mean(bias.Ntot)
    sd.bias.Ntot[k] <- sd(bias.Ntot)
    baye.pvalue.Ntot[k] <- mean(sum(N) > out$mean$Ntotal)

    #Coefficient of Variation in local abundance (lambda / average local abundance)
    CV.lam <- out$sd$lambda/out$mean$lambda #standard deviation divided by mean
    m.CV.lam[k] <- mean(CV.lam)
    sd.CV.lam[k] <- sd(CV.lam)
    prop.CV.lam[k] <- mean(CV.lam < 0.15)

  }  ) #This will be the end of the simulations

  #*********************
  # Summary of Results
  #*********************
  results <- c("lambda", "N.total", "N.site", "lambda.CV", "Prob.CV.lambda")
  mean.bias <- round(c((mean(unlist(m.bias.lam))), (mean(unlist(m.bias.Ntot))),
(mean(unlist(m.bias.Nsite))), (mean(unlist(m.CV.lam))), NA),2)

  lower.CI <- round(c((quantile(unlist(m.bias.lam), 0.05)), (quantile(unlist(m.bias.Ntot), 0.05)),
(quantile(unlist(m.bias.Nsite), 0.05)), (quantile(unlist(m.CV.lam), 0.05)), NA),2) #upper 90%
credible interval

  upper.CI <- round(c((quantile(unlist(m.bias.lam), 0.95)), (quantile(unlist(m.bias.Ntot), 0.95)),
(quantile(unlist(m.bias.Nsite), 0.95)), (quantile(unlist(m.CV.lam), 0.95)), NA),2) #lower 90%
credible interval

  greater.15.CV <- c(NA, NA, NA, NA, (mean(unlist(m.CV.lam) > 0.15)))

  Baye.pvalue <- round(c((mean(unlist(baye.pvalue.lam))), (mean(unlist(baye.pvalue.Ntot))),
(mean(unlist(baye.pvalue.Nsite))), NA, NA),2)

  sim.results <- data.frame(results,mean.bias,lower.CI, upper.CI, Baye.pvalue, greater.15.CV)
#creates a table of results
  print(sim.results)

  #*****************
  #Post processing
  #*****************
  # Set plots so that six plots can be created in one image, which is then saved in a
```

```
  # word document Liz_Sim_Results_Figures
  par(mfrow = c(4,1), mai=c(0.5,0.2,0.2,0.2), mar=c(1,5,1,2), oma=c(1,1,1,1), las=1)

  # Plots
  (hist(unlist(m.bias.Nsite), xlim=c(-5,5), breaks=120, main="", ylab="N.site"))
  (abline(v=0, col="red", lwd=3))

  (hist(unlist(m.bias.lam), xlim=c(-1,1), main="", ylab="lambda"))
  (abline(v=0, col="red", lwd=3))

  (hist(unlist(m.bias.Ntot), xlim=c(-100,100), main="", ylab="Total N"))
  (abline(v=0, col="red", lwd=3))

  (hist(unlist(m.CV.lam), xlim=c(0,0.5), main="", ylab="CV lambda"))
  (abline(v=0.15, col="red", lwd=3))

  return(list(sim.results=sim.results, m.bias.Nsite=unlist(m.bias.Nsite), m.bias.lam =
unlist(m.bias.lam), m.bias.Ntot = unlist(m.bias.Ntot), m.CV.lam = unlist(m.CV.lam), lambda =
lambda, prob = prob, S = S, V = V, num.sim = num.sim))
}
```

APPENDIX K

APPENDIX K: BAYESIAN MODEL SPECIFICATION AND SIMULATION CODE FOR NAÏVE MODELS

Table K1. Results of simulations for developing 2019 pilot season protocols. Estimates of mean abundance per site and probability of detection are from Utah-based researched. Mean (90% credible interval) for bias and coefficient of variation from 400 simulation runs for each suite of parameters. R = number of sites, J = number of replicate visits, λ = mean abundance per site, p = mean detection probability, CV = coefficient of variation for total population size (Total N), and N.site = estimated number of Dusky Grouse per survey site. Yes/No = whether the protocol meets management requirements.

Simulation Parameters				Bias in λ	Bias in *p*	Bias in Total N	Bias in N.site	CV Total N	Prob. CV N.total > 0.15	Yes/ No
R	J	λ	*p*							
50	3	1.25	0.5	0.08 (-0.28 – 0.51)	-0.01 (-0.14 – 0.11)	4.0 (-8.9 – 21.8)	0.08 (-0.17 – 0.43)	0.16 (0.09 – 0.27)	0.48	No
100	3	1.25	0.5	0.05 (-0.21 – 0.36)	-0.01 (-0.09 – 0.08)	4.8 (-14.3 – 25.7)	0.05 (-0.14 – 0.26)	0.09 (0.06 – 0.14)	0.02	Yes
200	3	1.25	0.5	0.01 (-0.18 – 0.20)	-0.004 (-0.06 – 0.05)	4.0 (-18.1 – 31.4)	0.02 (-0.09 – 0.15)	0.06 (0.05 – 0.08)	0.00	Yes
500	3	1.25	0.5	0.008 (-0.11 – 0.11)	-0.002 (-0.04 – 0.04)	5.0 (-35.2 – 46.3)	0.01 (-0.07 – 0.09)	0.04 (0.03 – 0.05)	0.00	Yes
50	2	1.25	0.5	0.35 (-0.30 – 1.87)	-0.02 (-0.22 – 0.13)	17.2 (-12.5 – 90.1)	0.34 (-0.25 – 1.80)	0.39 (0.15 – 0.92)	0.94	No
100	2	1.25	0.5	0.11 (-0.26 – 0.59)	-0.01 (-0.14 – 0.10)	12.8 (-18.0 – 57.3)	0.13 (-0.18 – 0.57)	0.19 (0.11 – 0.34)	0.70	No
200	2	1.25	0.5	0.06 (-0.19 – 0.31)	-0.01 (-0.09 – 0.08)	12.3 (-31.5 – 61.7)	0.06 (-0.16 – 0.31)	0.11 (0.08 – 0.16)	0.14	Yes-ish
500	2	1.25	0.5	0.02 (-0.12 – 0.21)	-0.003 (-0.06 – 0.05)	10.0 (-53.1 – 88.9)	0.02 (-0.11 – 0.18)	0.07 (0.05 – 008)	0.00	Yes
50	3	0.625	0.5	0.07 (-0.19 – 0.39)	-0.02 (-0.16 – 0.11)	3.1 (-4.5 – 15.3)	0.06 (-0.09 – 0.31)	0.19 (0.09 – 0.39)	0.59	No
100	3	0.625	0.5	0.02 (-0.13 – 0.19)	-0.01 (-0.11 – 0.08)	2.3 (-6.1 – 13.7)	0.02 (-0.06 – 0.14)	0.13 (0.07 – 0.16)	0.09	Yes-ish
200	3	0.625	0.5	0.008 (-0.11 – 0.14)	-0.004 (-0.08 – 0.06)	2.3 (-10.4 – 17.8)	0.01 (-0.05 – 0.09)	0.07 (0.05 – 0.09)	0.00	Yes
500	3	0.625	0.5	0.008 (-0.08 – 0.10)	-0.003 (-0.07 – 0.06)	5.1 (-29.7 – 48.5)	0.01 (-0.06 – 0.09)	0.08 (0.06 – 0.10)	0.00	Yes
50	2	0.625	0.5	0.24 (-0.17 – 1.02)	-0.03 (-0.25 – 0.17)	11.9 (-6.5 – 53.4)	0.24 (-0.13 – 1.06)	0.51 (0.16 – 1.10)	0.96	No
100	2	0.625	0.5	0.09 (-0.15 – 0.47)	-0.02 (-0.19 – 0.12)	9.1 (-10.9 – 45.4)	0.09 (-0.11 –0.45)	0.25 (0.11 – 0.47)	0.81	No
200	2	0.625	0.5	0.04 (-0.12 – 0.23)	-0.01 (-0.13 – 0.09)	8.2 (-17.9 – 44.3)	0.04 (-0.09 – 0.22)	0.14 (0.09 – 0.23)	0.34	No
500	2	0.625	0.5	0.02 (-0.08 – 0.12)	-0.008 (-0.07 – 0.06)	8.5 (-31.5 – 49.1	0.02 (-0.06 – 0.10)	0.08 (006 – 0.10)	0.00	Yes

APPENDIX L

APPENDIX L: BAYESIAN MODEL SPECIFICATION AND SIMULATION CODE FOR NAÏVE MODELS

Table L1. Support for candidate models predicting abundance and probability of detection estimates using N-mixture models for surveys conducted with electronic playback for spring 2019 pilot season. Three different abundance distributions are examined: Poisson distribution, negative binomial distribution, and zero-inflated Poisson distribution. The number of parameters (K), AIC values, Δ AIC values, and model weights (w_i) are reported.

Model	**K**	**AIC**	**Δ AIC**	w_i
Poisson distribution	2	171.72	0.00	0.47
Zero-inflated Poisson distribution	3	172.59	0.87	0.3
Negative Binomial distribution	3	173.19	1.47	0.23

APPENDIX M

APPENDIX M: BAYESIAN MODEL SPECIFICATION AND SIMULATION CODE FOR NAÏVE MODELS

Table M1. Results of simulations evaluating the efficacy of survey protocols using parameters estimated from the 2019 spring pilot study. Mean (90% credible interval) for bias and coefficient of variation from 400 simulation runs for each suite of parameters. Simulations evaluated survey protocols with an estimate of abundance and probability of detection from spring 2019 surveys using electronic playback. R = number of survey sites, J = number of replicate visits, λ = mean abundance per site, p = mean detection probability; CV = coefficient of variation for total population size (Total N) and N.site = estimated number of Dusky Grouse per survey site. Yes/No = whether the protocol meets management requirements.

Simulation Parameters				**Bias in λ**	**Bias in *p***	**Bias in Total N**	**Bias in N.site**	**CV Total N**	**Prob. CV N.total > 0.15**	**Yes/ No**
R	**J**	**λ**	***p***							
100	3	0.36	0.28	0.09 (-0.13, 0.45)	0.01 (-0.13, 0.14)	9.13 (-10.30, 45.70)	0.09 (-0.10, 0.46)	0.41 (0.19, 0.77)	1.00	no
200	3	0.36	0.28	0.03 (-0.10, 0.23)	0.01 (-0.09, 0.10)	6.85 (-16.26, 41.21)	0.03 (-0.08, 0.21)	0.24 (0.15, 0.38)	0.93	no
300	3	0.36	0.28	0.02 (-0.09, 0.17)	0.01 (-0.07, 0.09)	5.07 (-22.22, 46.44)	0.02 (-0.07, 0.15)	0.18 (0.12, 0.26)	0.72	no
400	3	0.36	0.28	0.01 (-0.08, 0.12)	0.01 (-0.06, 0.08)	3.29 (-26.64, 38.29)	0.01 (-0.07, 0.10)	0.15 (0.11, 0.20)	0.46	no
500	3	0.36	0.28	0.01 (-0.07, 0.11)	0.00 (-0.06, 0.07)	4.68 (-27.85, 50.47)	0.01 (-0.06, 0.10)	0.13 (0.10, 0.18)	0.21	no
600	3	0.36	0.28	0.01 (-0.07, 0.10)	0.00 (-0.06, 0.06)	3.46 (-37.49, 51.37)	0.01 (-0.06, 0.09)	0.12 (0.09, 0.16)	0.08	yes
100	4	0.36	0.28	0.04 (-0.11, 0.22)	0.00 (-0.10, 0.11)	3.46 (-8.24, 20.94)	0.03 (-0.08, 0.21)	0.25 (0.14, 0.46)	0.90	no
100	5	0.36	0.28	0.02 (-0.11, 0.17)	0.00 (-0.08, 0.09)	1.76 (-6.40, 12.54)	0.02 (-0.06, 0.13)	0.18 (0.11, 0.29)	0.65	no
100	6	0.36	0.28	0.01 (-0.10, 0.15)	0.00 (-0.07, 0.08)	1.34 (-5.58, 10.51)	0.01 (-0.06, 0.11)	0.14 (0.09, 0.20)	0.28	no
100	7	0.36	0.28	0.01 (-0.11, 0.14)	0.00 (-0.07, 0.07)	1.04 (-4.84, 7.61)	0.01 (-0.05, 0.08)	0.11 (0.07, 0.16)	0.09	no
200	4	0.36	0.28	0.01 (-0.09, 0.15)	0.00 (-0.08, 0.07)	2.69 (-12.39, 25.35)	0.01 (-0.06, 0.13)	0.15 (0.11, 0.22)	0.44	no
300	4	0.36	0.28	0.01 (-0.08, 0.10)	0.00 (-0.06, 0.06)	2.20 (-16.33, 22.77)	0.01 (-0.05, 0.08)	0.12 (0.09, 0.16)	0.09	yes-ish
360	4	0.36	0.28	0.00 (-0.07, 0.10)	0.00 (-0.05, 0.05)	1.70 (-16.96, 26.32)	0.00 (-0.05, 0.07)	0.11 (0.08, 0.14)	0.02	yes

APPENDIX N

APPENDIX N: EXAMINING THREE DIFFERENT DETECTION FUNCTIONS FOR HIERARCHICAL DISTANCE SAMPLING MODELS

Support for candidate models examining three different detection functions, half-normal, hazard-rate, and uniform for hierarchical distance sampling transects for point counts.

Table N1. Support for candidate models examining three different detection functions for hierarchical distance sampling models for point counts fitted with constant probability of detection and local density/abundance.

Model	**K**	**AICc**	**Δ AICc**	w_i
Null model, Half-normal detection function	2	2226.8	0.0	1.00
Null model, Uniform detection function	1	2332.4	105.7	0.00
Null model, Hazard-rate detection function	3	2334.4	107.7	0.00

Table N2. Support for candidate models examining three different detection functions for hierarchical distance sampling models for transects for visit 1 fitted with constant probability of detection and local density/abundance.

Model	K	AICc	Δ AICc	w_i
Null model, Hazard-rate detection function	3	1211.34	0.00	0.82
Null model, Half-normal detection function	2	1214.43	3.09	0.18
Null model, Uniform detection function	1	1286.29	74.95	0.00

Table N3. Support for candidate models examining two different detection functions, half-normal and uniform, for hierarchical distance sampling models for transects for visit 2 fitted with constant probability of detection and local density/abundance. The model fitted with the hazard-rate function did not converge and therefore is not included.

Model	K	AICc	Δ AICc	w_i
Null model, Half-normal detection function	2	743.96	0.00	0.99
Null model, Uniform detection function	1	753.55	9.59	0.01

APPENDIX O

APPENDIX O: EVALUATION LINEAR AND NON-LINEAR RELATIONSHIPS FOR BETWEEN DETECTION PARAMETERS AND SURVEY CONDITIONS

Table O1. Model support for candidate models evaluating linear and nonlinear relationships between sigma for the half-normal detection function and day during the survey season, and minute since sunrise evaluated using HDS models for point counts.

Model	# Parameters	AIC	Delta AIC	Model Weight
Day^2	4	2219.5	0.0	0.99
Day	3	2228.8	9.3	0.01
Minutes	3	2228.1	0.0	0.62
$Minutes^2$	4	2229.1	1.0	0.38

Table O3. Model support for candidate models evaluating linear and nonlinear relationships between availability and day during the survey season, and minute since sunrise evaluated using time-removal HDS models.

Model	# Parameters	AIC	Delta AIC	Model Weight
Day^2	4	2784.25	0.0	1.00
Day	3	2797.80	13.55	0.00
$Minutes^2$	4	2797.02	0.0	0.56
Minutes	3	2797.50	0.48	0.44

Table O4. Model support for candidate models evaluating linear and nonlinear relationships between sigma and day during the survey season using HDS for line-transects.

Model	# Parameters	AIC	Delta AIC	Model Weight
Day^2	4	1201.94	0.0	1.00
Day	3	1214.62	12.68	0.00

APPENDIX P

APPENDIX P: SIMULATION RESULTS FOR NAÏVE MODELS

Table P1. Results of simulations evaluating the efficacy of survey protocols using parameters estimated from the 2020 and 2021 spring Dusky Grouse surveys analyzed using naïve model where imperfect detection is not taken into account. Scenarios are based off the "best" protocols for the N-mixture models with four visits. Mean (90% credible interval) for bias and coefficient of variation from 500 simulation runs for each suite of parameters. Simulations evaluated survey protocols with an estimate of abundance and probability of detection from spring 2019 surveys using electronic playback. R = number of survey sites, J = number of replicate visits, λ = mean abundance per site, p = mean detection probability; CV = coefficient of variation for total population size (Total N) and N.site = estimated number of Dusky Grouse per survey site.

Simulation Parameters				**Bias in λ**	**Bias in Total N**	**Bias in N.site**	**CV lambda**	**Prob. CV lambda > 0.15**	**Protocol meets Management Requirements**
R	**J**	**λ**	***p***						
170	1	0.31	0.37	-0.19 (-0.23, -0.15)	-33.32 (-44.00, -24.00)	-0.20 (-0.26, -0.14)	0.23 (0.19, 0.28)	1.00	no
240	1	0.18	0.37	-0.11 (-0.14, -0.08)	-27.15 (-36.00, -19.00)	-0.11 (-0.15, -0.08)	0.26 (0.21, 0.32)	1.00	no
490	1	0.08	0.37	-0.05 (-0.06, -0.04)	-24.44 (-33.00, -17.00)	-0.05 (-0.07, -0.03)	0.27 (0.22, 0.34)	1.00	no
50	1	0.31	0.59	-0.13 (-0.21, -0.04)	-7.98 (-13.00, -4.00)	-0.13 (-0.22, -0.07)	0.31 (0.25, 0.41)	1.00	no
70	1	0.18	0.59	-0.08 (-0.13, -0.02)	-6.20 (-10.05, -2.95)	-0.08 (-0.13, -0.04)	0.38 (0.28, 0.51)	1.00	no
140	1	0.08	0.59	-0.04 (-0.07, 0.00)	-4.79 (-9.00, -1.00)	-0.03 (-0.06, '-0.01)	0.43 (0.30, 0.69)	1.00	no

APPENDIX Q

APPENDIX Q: SIMULATION RESULTS FOR N-MIXTURE MODELS

Table Q1. Results of simulations evaluating the efficacy of survey protocols using parameters from the 2020 and 2021 spring survey data analyzed using single season N-mixture models. Mean (90% credible interval) for bias and coefficient of variation from 500 simulation runs for each suite of parameters. Different scenarios include combinations of high, average, and low abundance paired with either average or high detection. R = number of survey sites, J = number of replicate visits, λ = mean abundance per site, p = mean detection probability; CV = coefficient of variation for total population size (Total N) and N.site = estimated number of Dusky Grouse per survey site. Yes/No = whether the protocol meets management requirements.

Simulation Parameters				**Bias in λ**	**Bias in *p***	**Bias in Total N**	**Bias in N.site**	**CV Total N**	**Prob. CV Total N > 0.15**	**Yes/ No**
R	**J**	**λ**	***p***							
High abundance, Average detection										
100	4	0.31	0.37	0.02, (-0.10, 0.15)	0.00, (-0.12, 0.10)	1.88, (-5.03, 11.22)	0.02, (-0.05, 0.11)	0.16, (0.09, 0.27)	0.51	no
160	4	0.31	0.37	0.02, (-0.07, 0.13)	-0.01, (-0.09, 0.08)	2.16, (-6.31, 13.34)	0.01, (-0.04, 0.08)	0.12, (0.08, 0.18)	0.15	no
170	4	0.31	0.37	0.01, (-0.07, 0.09)	0.00, (-0.08, 0.08)	1.42, (-7.40, 11.02)	0.01, (-0.04, 0.06)	0.11, (0.08, 0.16)	0.08	yes
180	4	0.31	0.37	0.00, (-0.07, 0.10)	0.00, (-0.08, 0.07)	1.06, (-8.16, 11.67)	0.01, (-0.05, 0.06)	0.11, (0.08, 0.15)	0.07	yes
200	4	0.31	0.37	0.01, (-0.07, 0.10)	0.00, (-0.07, 0.07)	1.26, (-8.35, 12.68)	0.01, (-0.04, 0.06)	0.10, (0.07, 0.14)	0.02	yes
100	3	0.31	0.37	0.04, (-0.10, 0.20)	0.00, (-0.12, 0.12)	3.53, (-6.05, 17.46)	0.04, (-0.06, 0.17)	0.26, (0.14, 0.45)	0.90	no
200	3	0.31	0.37	0.02, (-0.07, 0.14)	0.00, (-0.10, 0.10)	3.35, (-9.88, 20.19)	0.02, (-0.05, 0.10)	0.16, (0.10, 0.24)	0.50	no
300	3	0.31	0.37	0.01, (-0.06, 0.10)	0.00, (-0.07, 0.08)	2.29, (-12.37, 21.36)	0.01, (-0.04, 0.07)	0.12, (0.09, 0.16)	0.11	no
320	3	0.31	0.37	0.01, (-0.07, 0.09)	0.00, (-0.08, 0.08)	2.75, (-16.97, 25.09)	0.01, (-0.05, 0.08)	0.12, (0.08, 0.16)	0.11	no
330	3	0.31	0.37	0.01, (-0.07, 0.08)	0.00, (-0.07, 0.07)	3.13, (-13.59, 23.44)	0.01, (-0.04, 0.07)	0.12, (0.08, 0.16)	0.07	yes
340	3	0.31	0.37	0.00, (-0.06, 0.08)	0.00, (-0.08, 0.08)	2.75, (-14.55, 22.55)	0.01, (-0.04, 0.07)	0.11, (0.08, 0.15)	0.07	yes
360	3	0.31	0.37	0.00, (-0.06, 0.09)	0.00, (-0.07, 0.07)	1.33, (-16.21, 22.25)	0.00, (-0.05, 0.06)	0.11, (0.08, 0.14)	0.03	yes
380	3	0.31	0.37	0.01, (-0.06, 0.08)	0.00, (-0.07, 0.08)	2.01, (-17.62, 22.76)	0.01, (-0.05, 0.06)	0.10, (0.08, 0.14)	0.02	yes
400	3	0.31	0.37	0.01, (-0.06, 0.09)	0.00, (-0.07, 0.07)	2.95, (-15.44, 27.48)	0.01, (-0.04, 0.07)	0.10, (0.08, 0.14)	0.02	yes
100	2	0.31	0.37	0.12, (-0.11, 0.54)	0.00, (-0.18, 0.18)	11.37, (-9.03, 52.50)	0.11, (-0.09, 0.53)	0.54, (0.22, 1.03)	1.00	no
200	2	0.31	0.37	0.04, (-0.11, 0.25)	0.01, (-0.14, 0.16)	8.57, (-17.49, 47.24)	0.04, (-0.09, 0.24)	0.31, (0.16, 0.57)	0.96	no
300	2	0.31	0.37	0.03, (-0.09, 0.20)	0.00, (-0.13, 0.13)	9.45, (-20.66, 58.09)	0.03, (-0.07, 0.19)	0.24, (0.14, 0.40)	0.91	no
400	2	0.31	0.37	0.02, (-0.07, 0.16)	0.00, (-0.11, 0.12)	7.60, (-25.18, 54.73)	0.02, (-0.06, 0.14)	0.20, (0.12, 0.31)	0.82	no
500	2	0.31	0.37	0.01, (-0.07, 0.11)	0.00, (-0.10, 0.10)	5.90, (-29.56, 47.75)	0.01, (-0.06, 0.10)	0.17, (0.12, 0.26)	0.67	no
600	2	0.31	0.37	0.00, (-0.07, 0.09)	0.01, (-0.08, 0.10)	2.89, (-36.00, 50.37)	0.00, (-0.06, 0.08)	0.15, (0.10, 0.21)	0.42	no
700	2	0.31	0.37	0.01, (-0.07, 0.10)	0.01, (-0.08, 0.09)	4.77, (-38.69, 61.93)	0.01, (-0.06, 0.09)	0.14, (0.10, 0.19)	0.28	no

800	2	0.31	0.37	0.01, (-0.06, 0.09)	0.01, (-0.08, 0.09)	5.10, (-41.06, 66.28)	0.01, (-0.05, 0.08)	0.13, (0.09, 0.17)	0.15	no
860	2	0.31	0.37	0.01, (-0.05, 0.09)	0.00, (-0.07, 0.08)	5.46, (-41.03, 64.88)	0.01, (-0.05, 0.08)	0.12, (0.09, 0.16)	0.11	no
870	2	0.31	0.37	0.01, (-0.05, 0.09)	0.00, (-0.08, 0.08)	7.37, (-44.62, 75.69)	0.01, (-0.05, 0.09)	0.12, (0.09, 0.16)	0.13	no
880	2	0.31	0.37	0.01, (-0.06, 0.08)	0.00, (-0.07, 0.08)	5.38, (-42.59, 59.15)	0.01, (-0.05, 0.07)	0.12, (0.09, 0.16)	0.10	yes
890	2	0.31	0.37	0.00, (-0.06, 0.08)	0.01, (-0.08, 0.08)	4.27, (-45.13, 69.79)	0.00, (-0.05, 0.08)	0.12, (0.09, 0.16)	0.10	yes
900	2	0.31	0.37	0.01, (-0.06, 0.08)	0.01, (-0.07, 0.09)	2.69, (-49.32, 65.74)	0.00, (-0.05, 0.07)	0.12, (0.09, 0.16)	0.08	yes
Low abundance, Average detection										
100	4	0.08	0.37	0.02, (-0.03, 0.10)	0.00, (-0.17, 0.19)	1.58, (-2.01, 7.60)	0.02, (-0.02, 0.08)	0.41, (0.13, 1.03)	0.90	no
200	4	0.08	0.37	0.01, (-0.03, 0.06)	0.00, (-0.13, 0.13)	1.31, (-3.15, 7.74)	0.01, (-0.02, 0.04)	0.21, (0.10, 0.41)	0.68	no
300	4	0.08	0.37	0.00, (-0.03, 0.04)	0.00, (-0.10, 0.11)	0.88, (-4.64, 6.58)	0.00, (-0.02, 0.02)	0.15, (0.08, 0.26)	0.42	no
400	4	0.08	0.37	0.00, (-0.02, 0.04)	0.00, (-0.10, 0.09)	1.34, (-4.70, 8.78)	0.00, (-0.01, 0.02)	0.13, (0.08, 0.20)	0.22	no
480	4	0.08	0.37	0.00, (-0.02, 0.03)	0.00, (-0.09, 0.08)	1.01, (-4.93, 7.82)	0.00, (-0.01, 0.02)	0.11, (0.07, 0.17)	0.11	no
490	4	0.08	0.37	0.00, (-0.02, 0.03)	0.00, (-0.08, 0.08)	0.81, (-5.01, 7.52)	0.00, (-0.01, 0.02)	0.11, (0.07, 0.16)	0.08	yes
500	4	0.08	0.37	0.00, (-0.02, 0.03)	0.00, (-0.09, 0.08)	1.15, (-5.55, 9.20)	0.00, (-0.01, 0.02)	0.11, (0.07, 0.17)	0.10	yes
100	3	0.08	0.37	0.03, (-0.04, 0.16)	0.01, (-0.19, 0.22)	3.15, (-2.93, 15.56)	0.03, (-0.03, 0.16)	0.63, (0.21, 1.48)	0.99	no
200	3	0.08	0.37	0.01, (-0.04, 0.08)	0.01, (-0.16, 0.19)	2.72, (-3.90, 14.95)	0.01, (-0.02, 0.07)	0.36, (0.13, 0.84)	0.92	no
300	3	0.08	0.37	0.01, (-0.03, 0.06)	0.00, (-0.15, 0.14)	2.45, (-6.08, 15.59)	0.01, (-0.02, 0.05)	0.25, (0.13, 0.51)	0.85	no
400	3	0.08	0.37	0.01, (-0.02, 0.05)	0.00, (-0.12, 0.13)	2.45, (-6.62, 15.33)	0.01, (-0.02, 0.04)	0.20, (0.11, 0.34)	0.73	no
500	3	0.08	0.37	0.00, (-0.03, 0.04)	0.00, (-0.11, 0.12)	2.38, (-7.97, 16.00)	0.00, (-0.02, 0.03)	0.17, (0.10, 0.28)	0.62	no
600	3	0.08	0.37	0.00, (-0.02, 0.04)	0.00, (-0.10, 0.11)	2.07, (-8.32, 16.37)	0.00, (-0.01, 0.03)	0.15, (0.10, 0.23)	0.44	no
700	3	0.08	0.37	0.00, (-0.02, 0.03)	0.00, (-0.08, 0.09)	1.97, (-8.20, 13.22)	0.00, (-0.01, 0.02)	0.14, (0.09, 0.21)	0.29	no
800	3	0.08	0.37	0.00, (-0.02, 0.03)	0.00, (-0.09, 0.11)	1.71, (-10.78, 18.78)	0.00, (-0.01, 0.02)	0.13, (0.08, 0.19)	0.22	no
900	3	0.08	0.37	0.00, (-0.02, 0.03)	0.00, (-0.09, 0.08)	2.03, (-10.17, 16.32)	0.00, (-0.01, 0.02)	0.12, (0.08, 0.18)	0.13	no
910	3	0.08	0.37	0.00, (-0.02, 0.03)	0.00, (-0.09, 0.09)	2.24, (-10.80, 19.64)	0.00, (-0.01, 0.02)	0.12, (0.08, 0.17)	0.12	no
920	3	0.08	0.37	0.00, (-0.02, 0.02)	0.00, (-0.08, 0.08)	1.46, (-10.82, 17.11)	0.00, (-0.01, 0.02)	0.12, (0.08, 0.17)	0.10	yes
940	3	0.08	0.37	0.00, (-0.02, 0.03)	0.00, (-0.07, 0.09)	1.94, (-11.25, 16.90)	0.00, (-0.01, 0.02)	0.11, (0.08, 0.16)	0.08	yes
960	3	0.08	0.37	0.00, (-0.02, 0.02)	0.00, (-0.08, 0.08)	2.13, (-10.50, 16.33)	0.00, (-0.01, 0.02)	0.12, (0.08, 0.16)	0.09	yes
980	3	0.08	0.37	0.00, (-0.02, 0.02)	0.00, (-0.08, 0.08)	1.97, (-11.36, 17.12)	0.00, (-0.01, 0.02)	0.11, (0.08, 0.16)	0.08	yes
1000	3	0.08	0.37	0.00, (-0.02, 0.02)	0.00, (-0.08, 0.08)	2.27, (-10.53, 17.82)	0.00, (-0.01, 0.02)	0.11, (0.08, 0.16)	0.07	yes
100	2	0.08	0.37	0.06, (-0.05, 0.24)	0.04, (-0.16, 0.31)	5.56, (-3.76, 21.43)	0.06, (-0.04, 0.21)	1.33, (0.33, 2.23)	1.00	no
200	2	0.08	0.37	0.04, (-0.04, 0.17)	0.02, (-0.18, 0.26)	7.00, (-5.71, 32.15)	0.04, (-0.03, 0.16)	0.71, (0.23, 1.52)	0.99	no

300	2	0.08	0.37	0.03, (-0.03, 0.12)	0.02, (-0.17, 0.21)	7.42, (-7.29, 39.62)	0.02, (-0.02, 0.13)	0.53, (0.20, 1.04)	0.99	no
400	2	0.08	0.37	0.02, (-0.03, 0.11)	0.01, (-0.18, 0.19)	8.36, (-9.54, 43.31)	0.02, (-0.02, 0.11)	0.44, (0.19, 0.92)	0.99	no
500	2	0.08	0.37	0.02, (-0.03, 0.08)	0.00, (-0.17, 0.16)	9.59, (-10.82, 44.49)	0.02, (-0.02, 0.09)	0.40, (0.19, 0.80)	0.99	no
600	2	0.08	0.37	0.02, (-0.03, 0.08)	0.00, (-0.16, 0.15)	9.36, (-12.34, 46.55)	0.02, (-0.02, 0.08)	0.34, (0.17, 0.64)	0.98	no
700	2	0.08	0.37	0.01, (-0.02, 0.07)	0.01, (-0.14, 0.16)	7.69, (-12.79, 46.84)	0.01, (-0.02, 0.07)	0.31, (0.15, 0.66)	0.95	no
800	2	0.08	0.37	0.01, (-0.02, 0.06)	0.00, (-0.15, 0.14)	9.14, (-16.62, 48.21)	0.01, (-0.02, 0.06)	0.30, (0.15, 0.59)	0.95	no
900	2	0.08	0.37	0.01, (-0.02, 0.05)	0.01, (-0.12, 0.15)	7.25, (-17.19, 40.63)	0.01, (-0.02, 0.05)	0.27, (0.13, 0.52)	0.91	no
1000	2	0.08	0.37	0.01, (-0.02, 0.04)	0.00, (-0.12, 0.12)	7.82, (-18.24, 41.21)	0.01, (-0.02, 0.04)	0.24, (0.14, 0.45)	0.89	no
1100	2	0.08	0.37	0.01, (-0.02, 0.04)	0.01, (-0.11, 0.13)	5.25, (-19.37, 41.46)	0.00, (-0.02, 0.04)	0.22, (0.13, 0.39)	0.85	no
1200	2	0.08	0.37	0.00, (-0.02, 0.04)	0.00, (-0.11, 0.12)	6.14, (-20.92, 48.08)	0.01, (-0.02, 0.04)	0.22, (0.12, 0.38)	0.83	no
1300	2	0.08	0.37	0.01, (-0.02, 0.04)	0.01, (-0.11, 0.12)	6.49, (-22.34, 48.53)	0.00, (-0.02, 0.04)	0.20, (0.12, 0.34)	0.74	no
1400	2	0.08	0.37	0.00, (-0.02, 0.03)	0.00, (-0.11, 0.11)	6.12, (-21.42, 45.54)	0.00, (-0.02, 0.03)	0.19, (0.12, 0.32)	0.74	no
1500	2	0.08	0.37	0.01, (-0.02, 0.03)	0.00, (-0.10, 0.10)	8.10, (-22.94, 50.46)	0.01, (-0.02, 0.03)	0.19, (0.12, 0.33)	0.71	no
1600	2	0.08	0.37	0.00, (-0.02, 0.03)	0.00, (-0.10, 0.10)	7.07, (-24.16, 51.10)	0.00, (-0.02, 0.03)	0.18, (0.11, 0.27)	0.66	no
1700	2	0.08	0.37	0.00, (-0.02, 0.03)	0.01, (-0.09, 0.10)	4.55, (-26.91, 47.20)	0.00, (-0.02, 0.03)	0.17, (0.11, 0.26)	0.55	no
1800	2	0.08	0.37	0.00, (-0.02, 0.03)	0.01, (-0.10, 0.11)	5.79, (-28.18, 50.65)	0.00, (-0.02, 0.03)	0.16, (0.11, 0.24)	0.52	no
1900	2	0.08	0.37	0.00, (-0.02, 0.03)	0.00, (-0.09, 0.10)	6.06, (-29.78, 51.22)	0.00, (-0.02, 0.03)	0.16, (0.10, 0.23)	0.49	no
2000	2	0.08	0.37	0.00, (-0.02, 0.03)	0.00, (-0.09, 0.10)	6.81, (-26.32, 52.48)	0.00, (-0.01, 0.03)	0.15, (0.10, 0.23)	0.43	no
2100	2	0.08	0.37	0.00, (-0.02, 0.03)	0.00, (-0.08, 0.10)	4.50, (-32.48, 48.72)	0.00, (-0.02, 0.02)	0.15, (0.10, 0.21)	0.39	no
2200	2	0.08	0.37	0.00, (-0.01, 0.03)	0.00, (-0.09, 0.09)	6.71, (-29.46, 55.89)	0.00, (-0.01, 0.03)	0.15, (0.10, 0.22)	0.33	no
2300	2	0.08	0.37	0.00, (-0.02, 0.02)	0.01, (-0.09, 0.09)	4.95, (-29.89, 51.25)	0.00, (-0.01, 0.02)	0.14, (0.10, 0.20)	0.27	no
2400	2	0.08	0.37	0.00, (-0.02, 0.02)	0.01, (-0.08, 0.09)	4.08, (-35.24, 50.71)	0.00, (-0.01, 0.02)	0.13, (0.10, 0.20)	0.23	no
2500	2	0.08	0.37	0.00, (-0.02, 0.02)	0.01, (-0.08, 0.09)	5.56, (-35.94, 53.71)	0.00, (-0.01, 0.02)	0.14, (0.09, 0.20)	0.24	no
2600	2	0.08	0.37	0.00, (-0.02, 0.02)	0.00, (-0.08, 0.09)	4.58, (-34.24, 53.14)	0.00, (-0.01, 0.02)	0.13, (0.09, 0.19)	0.18	no
2700	2	0.08	0.37	0.00, (-0.02, 0.02)	0.00, (-0.08, 0.09)	6.38, (-34.09, 54.91)	0.00, (-0.01, 0.02)	0.13, (0.09, 0.19)	0.18	no
2800	2	0.08	0.37	0.00, (-0.01, 0.02)	0.01, (-0.07, 0.08)	3.69, (-36.63, 57.70)	0.00, (-0.01, 0.02)	0.12, (0.09, 0.17)	0.11	no
2900	2	0.08	0.37	0.00, (-0.01, 0.02)	0.01, (-0.07, 0.08)	3.57, (-37.58, 51.97)	0.00, (-0.01, 0.02)	0.12, (0.09, 0.17)	0.12	no
2910	2	0.08	0.37	0.00, (-0.02, 0.02)	0.00, (-0.07, 0.08)	5.02, (-35.49, 55.29)	0.00, (-0.01, 0.02)	0.12, (0.09, 0.15)	0.08	yes
2920	2	0.08	0.37	0.00, (-0.02, 0.02)	0.01, (-0.06, 0.08)	2.61, (-34.79, 51.97)	0.00, (-0.01, 0.02)	0.12, (0.09, 0.15)	0.06	yes
2940	2	0.08	0.37	0.00, (-0.02, 0.02)	0.00, (-0.08, 0.08)	4.05, (-35.93, 60.19)	0.00, (-0.01, 0.02)	0.12, (0.09, 0.16)	0.08	yes
2960	2	0.08	0.37	0.00, (-0.01, 0.02)	0.00, (-0.07, 0.08)	4.75, (-36.66, 57.51)	0.00, (-0.01, 0.02)	0.12, (0.09, 0.15)	0.07	yes
2980	2	0.08	0.37	0.00, (-0.02, 0.02)	0.01, (-0.07, 0.08)	3.26, (-36.81, 58.49)	0.00, (-0.01, 0.02)	0.12, (0.09, 0.15)	0.05	yes

3000	2	0.08	0.37	0.00, (-0.02, 0.02)	0.00, (-0.07, 0.08)	5.78, (-37.41, 53.92)	0.00, (-0.01, 0.02)	0.12, (0.09, 0.15)	0.07	yes
Average abundance, Average detection										
100	4	0.18	0.37	0.01, (-0.07, 0.11)	0.01, (-0.12, 0.14)	1.11, (-3.95, 7.48)	0.01, (-0.04, 0.07)	0.21, (0.10, 0.42)	0.69	no
200	4	0.18	0.37	0.01, (-0.04, 0.07)	0.00, (-0.08, 0.09)	1.36, (-4.86, 8.47)	0.01, (-0.02, 0.04)	0.13, (0.08, 0.19)	0.20	no
220	4	0.18	0.37	0.01, (-0.05, 0.07)	0.00, (-0.09, 0.09)	1.25, (-6.32, 9.73)	0.01, (-0.03, 0.04)	0.12, (0.08, 0.18)	0.18	no
230	4	0.18	0.37	0.01, (-0.05, 0.07)	0.00, (-0.08, 0.09)	1.28, (-5.73, 9.49)	0.01, (-0.02, 0.04)	0.11, (0.07, 0.17)	0.11	no
240	4	0.18	0.37	0.00, (-0.05, 0.06)	0.00, (-0.09, 0.09)	0.89, (-6.76, 9.53)	0.00, (-0.03, 0.04)	0.11, (0.07, 0.17)	0.09	yes
260	4	0.18	0.37	0.01, (-0.04, 0.06)	0.00, (-0.09, 0.08)	1.37, (-6.84, 10.57)	0.01, (-0.03, 0.04)	0.11, (0.07, 0.16)	0.08	yes
280	4	0.18	0.37	0.00, (-0.04, 0.06)	0.00, (-0.08, 0.07)	1.33, (-5.95, 9.43)	0.00, (-0.02, 0.03)	0.10, (0.07, 0.15)	0.04	yes
300	4	0.18	0.37	0.00, (-0.05, 0.06)	0.00, (-0.07, 0.07)	1.00, (-7.05, 9.48)	0.00, (-0.02, 0.03)	0.10, (0.07, 0.14)	0.03	yes
100	3	0.18	0.37	0.03, (-0.08, 0.21)	0.00, (-0.17, 0.16)	3.44, (-4.89, 16.05)	0.03, (-0.05, 0.16)	0.37, (0.15, 0.82)	0.95	no
200	3	0.18	0.37	0.02, (-0.06, 0.11)	0.00, (-0.13, 0.11)	3.41, (-7.04, 19.31)	0.02, (-0.04, 0.10)	0.21, (0.12, 0.38)	0.76	no
300	3	0.18	0.37	0.01, (-0.04, 0.07)	0.00, (-0.11, 0.11)	2.63, (-8.97, 17.91)	0.01, (-0.03, 0.06)	0.15, (0.10, 0.24)	0.44	no
400	3	0.18	0.37	0.01, (-0.04, 0.07)	0.00, (-0.09, 0.09)	2.39, (-10.22, 18.97)	0.01, (-0.03, 0.05)	0.13, (0.09, 0.18)	0.20	no
460	3	0.18	0.37	0.01, (-0.04, 0.06)	0.00, (-0.09, 0.08)	2.49, (-11.72, 21.05)	0.01, (-0.03, 0.05)	0.12, (0.08, 0.16)	0.11	no
470	3	0.18	0.37	0.00, (-0.04, 0.05)	0.00, (-0.09, 0.08)	2.17, (-13.10, 20.65)	0.00, (-0.03, 0.04)	0.12, (0.08, 0.16)	0.12	no
480	3	0.18	0.37	0.00, (-0.04, 0.05)	0.01, (-0.07, 0.08)	1.54, (-12.38, 18.62)	0.00, (-0.03, 0.04)	0.11, (0.08, 0.16)	0.07	yes
500	3	0.18	0.37	0.01, (-0.04, 0.06)	0.00, (-0.09, 0.08)	1.90, (-14.07, 21.18)	0.00, (-0.03, 0.04)	0.11, (0.08, 0.15)	0.07	yes
100	2	0.18	0.37	0.09, (-0.08, 0.39)	0.02, (-0.18, 0.25)	8.78, (-6.90, 35.60)	0.09, (-0.07, 0.36)	0.69, (0.26, 1.35)	0.99	no
200	2	0.18	0.37	0.05, (-0.07, 0.25)	0.01, (-0.18, 0.19)	9.48, (-10.33, 46.88)	0.05, (-0.05, 0.23)	0.42, (0.19, 0.75)	0.99	no
300	2	0.18	0.37	0.03, (-0.06, 0.16)	0.00, (-0.15, 0.15)	8.66, (-13.87, 46.58)	0.03, (-0.05, 0.16)	0.32, (0.16, 0.56)	0.98	no
400	2	0.18	0.37	0.02, (-0.05, 0.12)	0.00, (-0.14, 0.14)	7.97, (-13.87, 46.58)	0.02, (-0.04, 0.12)	0.26, (0.14, 0.42)	0.93	no
500	2	0.18	0.37	0.01, (-0.05, 0.10)	0.00, (-0.12, 0.13)	6.41, (-21.90, 44.79)	0.01, (-0.04, 0.09)	0.22, (0.13, 0.36)	0.89	no
600	2	0.18	0.37	0.01, (-0.04, 0.09)	0.00, (-0.11, 0.11)	7.27, (-21.72, 53.29)	0.01, (-0.04, 0.09)	0.20, (0.13, 0.31)	0.82	no
700	2	0.18	0.37	0.01, (-0.04, 0.08)	0.01, (-0.10, 0.10)	6.19, (-24.29, 51.59)	0.01, (-0.03, 0.07)	0.18, (0.12, 0.17)	0.72	no
800	2	0.18	0.37	0.01, (-0.04, 0.08)	0.01, (-0.10, 0.10)	8.45, (-25.50, 56.03)	0.01, (-0.03, 0.07)	0.17, (0.11, 0.24)	0.64	no
900	2	0.18	0.37	0.01, (-0.04, 0.07)	0.01, (-0.09, 0.09)	5.08, (-31.26, 52.11)	0.01, (-0.03, 0.06)	0.15, (0.11, 0.21)	0.49	no
1000	2	0.18	0.37	0.01, (-0.04, 0.05)	0.01, (-0.08, 0.10)	3.42, (-32.63, 49.22)	0.00, (-0.03, 0.05)	0.14, (0.10, 0.20)	0.38	no
1100	2	0.18	0.37	0.01, (-0.03, 0.06)	0.00, (-0.08, 0.08)	6.42, (-31.86, 58.32)	0.01, (-0.03, 0.05)	0.14, (0.10, 0.19)	0.28	no
1200	2	0.18	0.37	0.01, (-0.04, 0.05)	0.01, (-0.07, 0.09)	3.69, (-36.53, 52.85)	0.00, (-0.03, 0.04)	0.13, (0.09, 0.17)	0.16	no
1300	2	0.18	0.37	0.01, (-0.04, 0.05)	0.01, (-0.07, 0.09)	2.23, (-38.73, 53.64)	0.00, (-0.03, 0.04)	0.12, (0.09, 0.16)	0.11	no

1320	2	0.18	0.37	0.00, (-0.03, 0.05)	0.00, (-0.08, 0.07)	6.10, (-35.34, 59.26)	0.00, (-0.03, 0.04)	0.13, (0.09, 0.17)	0.14	no
1330	2	0.18	0.37	0.00, (-0.04, 0.05)	0.00, (-0.09, 0.08)	4.99, (-41.55, 65.46)	0.00, (-0.03, 0.05)	0.12, (0.09, 0.16)	0.11	no
1340	2	0.18	0.37	0.00, (-0.03, 0.05)	0.00, (-0.08, 0.08)	4.90, (-39.91, 60.40)	0.00, (-0.03, 0.05)	0.12, (0.09, 0.16)	0.10	yes
1360	2	0.18	0.37	0.00, (-0.03, 0.04)	0.01, (-0.06, 0.08)	1.61, (-39.08, 49.20)	0.00, (-0.03, 0.04)	0.12, (0.09, 0.15)	0.06	yes
1380	2	0.18	0.37	0.00, (-0.04, 0.05)	0.00, (-0.08, 0.08)	3.96, (-40.50, 61.42)	0.00, (-0.03, 0.04)	0.12, (0.09, 0.16)	0.09	yes
1400	2	0.18	0.37	0.00, (-0.03, 0.04)	0.01, (-0.07, 0.08)	2.88, (-41.57, 55.45)	0.00, (-0.03, 0.04)	0.12, (0.09, 0.16)	0.07	yes
High abundance, High detection										
40	4	0.31	0.57	0.02, (-0.13, 0.20)	-0.01, (-0.15, 0.12)	0.52, (-1.46, 2.65)	0.01, (-0.04, 0.07)	0.12, (0.05, 0.24)	0.21	no
50	4	0.31	0.57	0.01, (-0.12, 0.15)	-0.01, (-0.14, 0.11)	0.46, (-1.75, 2.79)	0.01, (-0.03, 0.06)	0.10, (0.05, 0.18)	0.11	no
60	4	0.31	0.57	0.01, (-0.11, 0.14)	-0.01, (-0.12, 0.10)	0.34, (-1.86, 2.51)	0.01, (-0.03, 0.04)	0.08, (0.05, 0.14)	0.04	yes
80	4	0.31	0.57	0.01, (-0.10, 0.12)	-0.01, (-0.12, 0.09)	0.54, (-2.26, 3.09)	0.01, (-0.03, 0.04)	0.07, (0.04, 0.11)	0.01	yes
100	4	0.31	0.57	0.00, (-0.09, 0.10)	-0.01, (-0.09, 0.08)	0.46, (-2.30, 3.21)	0.00, (-0.02, 0.03)	0.06, (0.04, 0.09)	0.00	yes
80	3	0.31	0.57	0.01, (-0.09, 0.15)	-0.02, (-0.15, 0.10)	1.04, (-3.19, 5.81)	0.01, (-0.04, 0.07)	0.12, (0.06, 0.21)	0.20	no
90	3	0.31	0.57	0.01, (-0.09, 0.14)	-0.01, (-0.14, 0.09)	1.17, (-2.98, 6.04)	0.01, (-0.03, 0.07)	0.11, (0.06, 0.17)	0.11	no
100	3	0.31	0.57	0.01, (-0.09, 0.12)	-0.02, (-0.13, 0.10)	1.17, (-3.50, 6.48)	0.01, (-0.03, 0.06)	0.10, (0.06, 0.16)	0.07	yes
100	2	0.31	0.57	0.03, (-0.10, 0.20)	-0.01, (-0.18, 0.14)	3.10, (-5.43, 15.37)	0.03, (-0.05, 0.15)	0.22, (0.10, 0.42)	0.71	no
200	2	0.31	0.57	0.01, (-0.07, 0.12)	-0.01, (-0.15, 0.11)	3.09, (-8.55, 18.66)	0.02, (-0.04, 0.09)	0.13, (0.08, 0.22)	0.27	no
260	2	0.31	0.57	0.01, (-0.06, 0.10)	-0.02, (-0.13, 0.09)	3.93, (-8.86, 19.64)	0.02, (-0.03, 0.08)	0.11, (0.07, 0.17)	0.11	no
270	2	0.31	0.57	0.01, (-0.06, 0.09)	-0.01, (-0.12, 0.10)	2.65, (-10.68, 19.44)	0.01, (-0.04, 0.07)	0.11, (0.07, 0.16)	0.10	yes
280	2	0.31	0.57	0.01, (-0.06, 0.09)	-0.01, (-0.12, 0.10)	2.89, (-11.67, 18.31)	0.01, (-0.04, 0.07)	0.10, (0.07, 0.16)	0.06	yes
300	2	0.31	0.57	0.01, (-0.06, 0.08)	0.00, (-0.12, 0.11)	2.38, (-11.06, 17.92)	0.01, (-0.04, 0.06)	0.10, (0.06, 0.14)	0.05	yes
Average abundance, High detection										
60	4	0.18	0.57	0.01, (-0.08, 0.12)	-0.01, (-0.16, 0.11)	0.40, (-1.35, 1.93)	0.01, (-0.02, 0.03)	0.12, (0.05, 0.24)	0.19	no
70	4	0.18	0.57	0.00, (-0.08, 0.09)	-0.01, (-0.16, 0.13)	0.40, (-1.40, 2.08)	0.01, (-0.02, 0.03)	0.10, (0.04, 0.20)	0.13	no
80	4	0.18	0.57	0.01, (-0.07, 0.10)	-0.01, (-0.15, 0.11)	0.44, (-1.53, 2.09)	0.01, (-0.02, 0.03)	0.09, (0.04, 0.16)	0.08	yes
100	4	0.18	0.57	0.00, (-0.06, 0.07)	-0.01, (-0.11, 0.10)	0.38, (-1.78, 2.14)	0.00, (-0.02, 0.02)	0.08, (0.04, 0.12)	0.02	yes
100	3	0.18	0.57	0.01, (-0.06, 0.09)	-0.02, (-0.16, 0.11)	0.92, (-2.17, 4.61)	0.01, (-0.02, 0.05)	0.13, (0.06, 0.24)	0.29	no
120	3	0.18	0.57	0.01, (-0.06, 0.08)	-0.01, (-0.15, 0.11)	0.90, (-2.83, 5.00)	0.01, (-0.02, 0.04)	0.12, (0.06, 0.20)	0.20	no
130	3	0.18	0.57	0.01, (-0.05, 0.08)	-0.02, (-0.16, 0.10)	0.94, (-2.47, 5.02)	0.01, (-0.02, 0.04)	0.11, (0.06, 0.21)	0.14	no
140	3	0.18	0.57	0.01, (-0.05, 0.07)	-0.01, (-0.15, 0.11)	1.04, (-2.65, 5.62)	0.01, (-0.02, 0.04)	0.10, (0.06, 0.18)	0.10	yes

160	3	0.18	0.57	0.01, (-0.06, 0.07)	-0.01, (-0.13, 0.10)	0.81, (-3.10, 5.26)	0.01, (-0.02, 0.03)	0.09, (0.05, 0.16)	0.06	yes
180	3	0.18	0.57	0.00, (-0.05, 0.07)	-0.01, (-0.12, 0.09)	0.75, (-3.39, 5.10)	0.00, (-0.02, 0.03)	0.09, (0.05, 0.14)	0.03	yes
200	3	0.18	0.57	0.00, (-0.05, 0.05)	0.00, (-0.10, 0.09)	0.37, (-4.24, 4.27)	0.00, (-0.02, 0.02)	0.08, (0.05, 0.12)	0.01	yes
100	2	0.18	0.57	0.04, (-0.06, 0.17)	-0.03, (-0.25, 0.17)	3.64, (-4.01, 14.15)	0.04, (-0.04, 0.14)	0.33, (0.11, 0.74)	0.87	no
200	2	0.18	0.57	0.02, (-0.04, 0.09)	-0.02, (-0.18, 0.12)	2.95, (-5.82, 15.54)	0.01, (-0.03, 0.08)	0.18, (0.09, 0.32)	0.60	no
300	2	0.18	0.57	0.01, (-0.04, 0.06)	-0.01, (-0.14, 0.11)	2.68, (-7.26, 14.43)	0.01, (-0.02, 0.05)	0.13, (0.08, 0.20)	0.26	no
360	2	0.18	0.57	0.01, (-0.04, 0.06)	0.00, (-0.11, 0.11)	2.08, (-8.82, 14.99)	0.01, (-0.02, 0.04)	0.11, (0.07, 0.17)	0.12	no
370	2	0.18	0.57	0.01, (-0.04, 0.06)	0.00, (-0.13, 0.10)	2.10, (-8.79, 17.11)	0.01, (-0.02, 0.05)	0.11, (0.07, 0.17)	0.12	no
380	2	0.18	0.57	0.01, (-0.04, 0.05)	0.00, (-0.12, 0.10)	2.16, (-8.01, 16.90)	0.01, (-0.02, 0.04)	0.11, (0.07, 0.16)	0.09	yes
400	2	0.18	0.57	0.00, (-0.04, 0.05)	-0.01, (-0.12, 0.09)	2.35, (-8.74, 15.74)	0.01, (-0.02, 0.04)	0.11, (0.07, 0.16)	0.08	yes
Low abundance, High detection										
100	4	0.08	0.57	0.00, (-0.04, 0.06)	-0.01, (-0.17, 0.14)	0.32, (-0.94, 1.51)	0.00, (-0.01, 0.02)	0.15, (0.05, 0.30)	0.27	no
120	4	0.08	0.57	0.00, (-0.04, 0.05)	-0.02, (-0.18, 0.13)	0.34, (-0.93, 1.65)	0.00, (-0.01, 0.01)	0.13, (0.05, 0.27)	0.20	no
130	4	0.08	0.57	0.00, (-0.04, 0.04)	-0.01, (-0.16, 0.12)	0.33, (-1.29, 1.86)	0.00, (-0.01, 0.01)	0.11, (0.05, 0.21)	0.15	no
140	4	0.08	0.57	0.00, (-0.04, 0.05)	-0.01, (-0.15, 0.13)	0.25, (-1.34, 1.57)	0.00, (-0.01, 0.01)	0.10, (0.04, 0.18)	0.10	yes
160	4	0.08	0.57	0.00, (-0.03, 0.04)	-0.01, (-0.16, 0.11)	0.36, (-1.20, 1.78)	0.00, (-0.01, 0.01)	0.09, (0.04, 0.18)	0.10	yes
180	4	0.08	0.57	0.00, (-0.03, 0.04)	-0.02, (-0.14, 0.10)	0.40, (-1.27, 1.87)	0.00, (-0.01, 0.01)	0.08, (0.04, 0.15)	0.05	yes
200	4	0.08	0.57	0.00, (-0.03, 0.03)	-0.01, (-0.14, 0.11)	0.32, (-1.51, 1.95)	0.00, (-0.01, 0.01)	0.07, (0.04, 0.14)	0.04	yes
100	3	0.08	0.57	0.01, (-0.04, 0.06)	-0.03, (-0.25, 0.16)	1.07, (-1.30, 4.70)	0.01, (-0.01, 0.05)	0.30, (0.09, 0.75)	0.71	no
200	3	0.08	0.57	0.01, (-0.03, 0.05)	-0.01, (-0.17, 0.13)	0.83, (-2.19, 3.84)	0.00, (-0.01, 0.02)	0.13, (0.06, 0.27)	0.28	no
260	3	0.08	0.57	0.00, (-0.03, 0.04)	-0.01, (-0.15, 0.11)	0.64, (-2.90, 4.18)	0.00, (-0.01, 0.02)	0.11, (0.05, 0.20)	0.14	no
270	3	0.08	0.57	0.00, (-0.03, 0.03)	-0.01, (-0.15, 0.12)	0.80, (-2.34, 4.55)	0.00, (-0.01, 0.02)	0.11, (0.05, 0.19)	0.14	no
280	3	0.08	0.57	0.00, (-0.02, 0.03)	-0.01, (-0.14, 0.12)	0.65, (-2.59, 3.81)	0.00, (-0.01, 0.01)	0.10, (0.05, 0.18)	0.10	yes
300	3	0.08	0.57	0.00, (-0.02, 0.04)	-0.01, (-0.12, 0.11)	0.60, (-2.60, 4.04)	0.00, (-0.01, 0.01)	0.09, (0.05, 0.16)	0.06	yes
100	2	0.08	0.57	0.03, (-0.04, 0.17)	-0.04, (-0.31, 0.20)	3.48, (-1.87, 17.18)	0.03, (-0.02, 0.17)	0.72, (0.16, 1.50)	0.96	no
200	2	0.08	0.57	0.02, (-0.03, 0.08)	-0.03, (-0.27, 0.18)	3.35, (-3.14, 16.23)	0.02, (-0.02, 0.08)	0.34, (0.11, 0.90)	0.85	no
300	2	0.08	0.57	0.01, (-0.03, 0.05)	-0.02, (-0.21, 0.14)	2.51, (-4.26, 12.63)	0.01, (-0.01, 0.04)	0.23, (0.10, 0.44)	0.74	no
400	2	0.08	0.57	0.01, (-0.02, 0.04)	-0.01, (-0.16, 0.14)	2.33, (-5.14, 13.15)	0.01, (-0.01, 0.03)	0.18, (0.09, 0.30)	0.56	no
500	2	0.08	0.57	0.00, (-0.02, 0.03)	0.00, (-0.15, 0.12)	1.73, (-6.34, 13.81)	0.00, (-0.01, 0.03)	0.15, (0.08, 0.24)	0.38	no
600	2	0.08	0.57	0.00, (-0.02, 0.03)	-0.01, (-0.15, 0.11)	2.12, (-6.84, 14.17)	0.00, (-0.01, 0.02)	0.13, (0.08, 0.22)	0.26	no
700	2	0.08	0.57	0.00, (-0.02, 0.03)	-0.01, (-0.13, 0.10)	2.05, (-7.04, 12.92)	0.00, (-0.01, 0.02)	0.12, (0.07, 0.19)	0.18	no

800	2	0.08	0.57	0.00, (-0.02, 0.02)	-0.01, (-0.14, 0.10)	2.55, (-8.43, 14.68)	0.00, (-0.01, 0.02)	0.11, (0.07, 0.18)	0.12	no
810	2	0.08	0.57	0.00, (-0.02, 0.03)	-0.01, (-0.12, 0.11)	2.21, (-8.07, 14.45)	0.00, (-0.01, 0.02)	0.11, (0.07, 0.16)	0.09	yes
820	2	0.08	0.57	0.00, (-0.02, 0.03)	-0.01, (-0.12, 0.11)	2.34, (-8.14, 15.44)	0.00, (-0.01, 0.02)	0.11, (0.06, 0.16)	0.09	yes
840	2	0.08	0.57	0.00, (-0.02, 0.03)	-0.01, (-0.12, 0.10)	2.03, (-7.51, 13.65)	0.00, (-0.01, 0.02)	0.11, (0.07, 0.16)	0.07	yes
860	2	0.08	0.57	0.00, (-0.02, 0.03)	-0.01, (-0.13, 0.09)	2.71, (-8.18, 16.54)	0.00, (-0.01, 0.02)	0.11, (0.07, 0.16)	0.09	yes
880	2	0.08	0.57	0.00, (-0.02, 0.02)	-0.01, (-0.13, 0.09)	2.42, (-8.03, 16.64)	0.00, (-0.01, 0.02)	0.10, (0.07, 0.16)	0.07	yes
900	2	0.08	0.57	0.00, (-0.02, 0.02)	-0.01, (-0.11, 0.09)	1.90, (-8.58, 13.68)	0.00, (-0.01, 0.02)	0.10, (0.07, 0.15)	0.05	yes

APPENDIX R

APPENDIX R: SIMULATION RESULTS FOR HIERARCHICAL DISTANCE SAMPLING MODELS FOR POINT-COUNTS

Table R1. Results of simulations evaluating the efficacy of survey protocols using parameters from the 2020 and 2021 spring survey data analyzed hierarchical distance sampling models for point-counts. Mean (90% credible interval) for bias and coefficient of variation from 500 simulation runs for each suite of parameters. Different scenarios include combinations of high, average, and low abundance paired with either average or high detection. R = number of survey sites, λ = mean abundance per site, sigma = sigma for calculating the half-normal detection function; CV = coefficient of variation for total population size (Total N) and N.site = estimated number of Dusky Grouse per survey site. Yes/No = whether the protocol meets management requirements.

Simulation Parameters			**Bias in λ**	**Bias in *sigma***	**Bias in Total N**	**Bias in N.site**	**CV Total N**	**Prob. CV Total N > 0.15**	**Yes /No**
R	**λ**	***sigma***							
High abundance, Average detection									
100	0.31	43	-0.03, (-0.18, 0.25)	12.49, (-8.02, 31.07)	-2.69 (-18.05, 23.53)	-0.03, (-0.18, 0.24)	0.45 (0.31, 0.62)	1.00	no
200	0.31	43	-0.04, (-0.16, 0.15)	9.33, (-6.36, 27.07)	-5.86 (-29.45, 26.54)	-0.03, (-0.15, 0.13)	0.33 (0.27, 0.41)	1.00	no
300	0.31	43	-0.03, (-0.15, 0.12)	6.76, (-6.15, 24.38)	-6.83 (-37.74, 34.02)	-0.02, (-0.13, 0.11)	0.27 (0.23, 0.32)	1.00	no
400	0.31	43	-0.03, (-0.13, 0.10)	5.06, (-4.71, 20.20)	-8.67 (-51.63, 37.50)	-0.02, (-0.13, 0.09)	0.24 (0.20, 0.27)	1.00	no
500	0.31	43	-0.02, (-0.13, 0.09)	4.09, (-5.55, 18.37)	-10.39 (-58.87, 46.26)	-0.02, (-0.12, 0.09)	0.21 (0.18, 0.24)	1.00	no
600	0.31	43	-0.02, (-0.11, 0.09)	3.20, (-4.32, 13.62)	-9.94 (-62.57, 46.39)	-0.02, (-0.10, 0.08)	0.19 (0.17, 0.22)	1.00	no
700	0.31	43	-0.02, (-0.11, 0.07)	2.80, (-4.63, 12.15)	-13.90 (-69.13, 40.18)	-0.02, (-0.10, 0.06)	0.18 (0.16, 0.20)	0.99	no
800	0.31	43	-0.02, (-0.10, 0.07)	2.41, (-4.33, 10.63)	-12.23 (-76.15, 54.38)	-0.02, (-0.10, 0.07)	0.16 (0.14, 0.18)	0.85	no
900	0.31	43	-0.02, (-0.10, 0.06)	2.38, (-3.72, 11.16)	-14.95 (-79.90, 56.56)	-0.02, (-0.09, 0.06)	0.15 (0.14, 0.17)	0.62	no
1000	0.31	43	-0.02, (-0.09, 0.05)	1.86, (-3.68, 9.58)	-15.56 (-86.52, 58.16)	-0.02, (-0.09, 0.06)	0.15 (0.13, 0.16)	0.30	no
1080	0.31	43	-0.02, (-0.09, 0.06)	1.93, (-3.45, 9.13)	-17.44 (-89.20, 60.15)	-0.02, (-0.08, 0.06)	0.14 (0.13, 0.15)	0.11	no
1090	0.31	43	-0.02, (-0.09, 0.06)	2.10, (-3.15, 8.94)	-18.79 (-88.97, 51.88)	-0.02, (-0.08, 0.05)	0.14 (0.13, 0.15)	0.09	yes
1100	0.31	43	-0.02, (-0.09, 0.06)	1.96, (-3.74, 8.62)	-18.82 (-88.62, 61.83)	-0.02, (-0.08, 0.06)	0.14 (0.13, 0.15)	0.09	yes
Low abundance, Average detection									
100	0.08	43	-0.01, (-0.08, 0.14)	14.28, (-8.12, 29.67)	1.51 (-6.81, 13.36)	-0.02, (-0.07, 0.13)	4.13 (0.48, 32.36)	1.00	no
200	0.08	43	0.00, (-0.06, 0.10)	14.16, (-8.22, 31.40)	0.24 (-10.30, 17.32)	-0.00, (-0.05, 0.09)	0.73 (0.37, 0.97)	1.00	no
300	0.08	43	-0.01, (-0.05, 0.06)	13.25, (-7.69, 30.94)	-1.77 (-14.30, 16.92)	-0.01, (-0.05, 0.06)	0.51 (0.34, 0.72)	1.00	no
400	0.08	43	-0.01, (-0.05, 0.06)	11.85, (-8.94, 29.75)	-2.12 (-18.13, 22.77)	-0.01, (-0.05, 0.06)	0.45 (0.32, 0.58)	1.00	no
500	0.08	43	-0.01, (-0.05, 0.06)	11.98, (-8.15, 32.05)	-3.51 (-21.65, 25.54)	-0.01, (-0.04, 0.05)	0.39 (0.29, 0.50)	1.00	no
600	0.08	43	-0.01, (-0.05, 0.05)	10.85, (-7.17, 28.07)	-4.69 (-25.74, 23.21)	-0.01, (-0.04, 0.04)	0.37 (0.29, 0.47)	1.00	no
700	0.08	43	-0.01, (-0.04, 0.04)	9.18, (-7.45, 28.12)	-3.42 (-27.03, 28.64)	-0.00, (-0.04, 0.04)	0.34 (0.27, 0.42)	1.00	no
800	0.08	43	-0.01, (-0.04, 0.04)	9.77, (-5.85, 28.00)	-7.49 (-30.99, 25.53)	-0.01, (-0.04, 0.03)	0.33 (0.26, 0.40)	1.00	no

900	0.08	43	-0.01, (-0.04, 0.03)	9.45, (-5.57, 27.95)	-8.05 (-36.32, 26.72)	-0.01, (-0.04, 0.03)	0.31 (0.25, 0.37)	1.00	no
1000	0.08	43	-0.01, (-0.04, 0.03)	8.49, (-5.67, 27.47)	-7.70 (-36.40, 29.51)	-0.01, (-0.04, 0.03)	0.29 (0.24, 0.35)	1.00	no
1100	0.08	43	-0.01, (-0.04, 0.03)	7.01, (-5.92, 24.80)	-7.10 (-38.17, 31.39)	-0.01, (-0.03, 0.03)	0.28 (0.24, 0.34)	1.00	no
1200	0.08	43	-0.01, (-0.04, 0.03)	7.12, (-6.04, 25.24)	-8.17 (-42.23, 33.67)	-0.01, (-0.04, 0.03)	0.27 (0.22, 0.31)	1.00	no
1300	0.08	43	-0.01, (-0.04, 0.03)	6.33, (-5.33, 23.55)	-8.84 (-47.22, 37.38)	-0.01, (-0.04, 0.03)	0.26 (0.22, 0.30)	1.00	no
1400	0.08	43	-0.01, (-0.04, 0.02)	5.88, (-5.18, 21.26)	-9.01 (-47.30, 31.65)	-0.01, (-0.03, 0.02)	0.25 (0.22, 0.29)	1.00	no
1500	0.08	43	-0.01, (-0.04, 0.03)	5.93, (-5.74, 23.13)	-10.50 (-49.78, 38.86)	-0.01, (-0.03, 0.03)	0.24 (0.21, 0.28)	1.00	no
1600	0.08	43	-0.01, (-0.03, 0.03)	4.62, (-5.59, 20.75)	-7.98 (-51.29, 40.44)	-0.00, (-0.03, 0.03)	0.23 (0.20, 0.27)	1.00	no
1700	0.08	43	-0.01, (-0.03, 0.02)	4.70, (-4.88, 17.78)	-9.67 (-53.32, 36.98)	-0.01, (-0.03, 0.02)	0.22 (0.19, 0.26)	1.00	no
1800	0.08	43	-0.01, (-0.03, 0.02)	5.36, (-4.89, 20.75)	-12.04 (-55.40, 39.73)	-0.01, (-0.03, 0.02)	0.22 (0.19, 0.25)	1.00	no
1900	0.08	43	-0.01, (-0.03, 0.02)	4.19, (-4.65, 19.10)	-9.98 (-55.93, 40.14)	-0.01, (-0.03, 0.02)	0.21 (0.19, 0.24)	1.00	no
2000	0.08	43	-0.01, (-0.03, 0.02)	3.86, (-4.76, 16.80)	-10.47 (-58.77, 40.46)	-0.01, (-0.03, 0.02)	0.21 (0.18, 0.24)	1.00	no
2100	0.08	43	-0.01, (-0.03, 0.02)	4.34, (-4.39, 17.04)	-14.75 (-61.60, 37.68)	-0.01, (-0.03, 0.02)	0.20 (0.18, 0.23)	1.00	no
2200	0.08	43	-0.01, (-0.03, 0.02)	3.81, (-4.39, 15.32)	-10.29 (-60.64, 47.19)	-0.00, (-0.03, 0.02)	0.20 (0.17, 0.22)	1.00	no
2300	0.08	43	-0.01, (-0.03, 0.02)	3.97, (-3.96, 15.66)	-13.67 (-66.91, 39.67)	-0.01, (-0.03, 0.02)	0.19 (0.17, 0.22)	1.00	no
2400	0.08	43	-0.01, (-0.03, 0.02)	3.57, (-4.75, 14.64)	-11.85 (-64.28, 46.87)	-0.00, (-0.03, 0.02)	0.19 (0.17, 0.21)	1.00	no
2500	0.08	43	-0.01, (-0.03, 0.02)	2.97, (-4.48, 13.56)	-11.60 (-67.65, 46.84)	-0.00, (-0.03, 0.02)	0.18 (0.16, 0.21)	1.00	no
2600	0.08	43	-0.01, (-0.03, 0.02)	3.48, (-3.70, 12.30)	-15.97 (-66.83, 44.16)	-0.01, (-0.03, 0.02)	0.18 (0.16, 0.21)	1.00	no
2700	0.08	43	-0.00, (-0.03, 0.02)	2.58, (-5.09, 12.59)	-8.92 (-65.01, 55.51)	-0.00, (-0.02, 0.02)	0.18 (0.16, 0.20)	0.99	no
2800	0.08	43	-0.01, (-0.03, 0.02)	3.19, (-4.47, 14.46)	-14.18 (-70.89, 48.19)	-0.01, (-0.03, 0.02)	0.17 (0.15, 0.19)	0.98	no
2900	0.08	43	-0.01, (-0.03, 0.02)	2.82, (-4.05, 11.38)	-13.56 (-70.86, 46.23)	-0.00, (-0.02, 0.02)	0.17 (0.15, 0.19)	0.96	no
3000	0.08	43	-0.01, (-0.03, 0.02)	2.59, (-3.95, 11.75)	-12.63 (-77.32, 55.70)	-0.00, (-0.04, 0.02)	0.17 (0.15, 0.19)	0.91	no
3100	0.08	43	-0.01, (-0.03, 0.02)	2.67, (-4.22, 11.36)	-13.99 (-74.71, 50.46)	-0.00, (-0.02, 0.02)	0.16 (0.15, 0.18)	0.91	no
3200	0.08	43	-0.01, (-0.03, 0.02)	2.42, (-3.86, 11.09)	-12.78 (-72.98, 48.70)	-0.00, (-0.02, 0.02)	0.16 (0.14, 0.18)	0.84	no
3300	0.08	43	-0.01, (-0.03, 0.01)	2.75, (-3.53, 11.68)	-17.05 (-76.50, 47.78)	-0.01, (-0.02, 0.01)	0.16 (0.14, 0.18)	0.79	no
3400	0.08	43	-0.01, (-0.03, 0.01)	2.29, (-3.60, 10.31)	-14.90 (-75.36, 53.96)	-0.00, (-0.02, 0.01)	0.16 (0.14, 0.17)	0.71	no
3500	0.08	43	-0.01, (-0.03, 0.01)	2.55, (-4.12, 11.03)	-18.15 (-78.58, 51.00)	-0.01, (-0.02, 0.01)	0.15 (0.14, 0.17)	0.63	no
3600	0.08	43	-0.01, (-0.03, 0.02)	2.33, (-3.43, 10.19)	-16.56 (-80.80, 57.00)	-0.00, (-0.02, 0.02)	0.15 (0.14, 0.17)	0.54	no
3700	0.08	43	-0.00, (-0.02, 0.02)	2.14, (-3.73, 9.85)	-14.32 (-81.42, 55.24)	-0.00, (-0.02, 0.01)	0.15 (0.13, 0.16)	0.42	no
3800	0.08	43	-0.01, (-0.02, 0.01)	2.10, (-3.73, 9.33)	-15.58 (-79.81, 52.56)	-0.00, (-0.02, 0.01)	0.15 (0.13, 0.16)	0.33	no
3900	0.08	43	-0.01, (-0.02, 0.01)	1.94, (-4.04, 8.77)	-14.41 (-80.78, 54.87)	-0.00, (-0.02, 0.01)	0.14 (0.13, 0.16)	0.25	no
4000	0.08	43	-0.01, (-0.03, 0.01)	2.39, (-3.36, 9.73)	-19.42 (-87.05, 50.46)	-0.00, (-0.02, 0.01)	0.14 (0.13, 0.16)	0.22	no
4100	0.08	43	-0.01, (-0.02, 0.01)	1.91, (-3.33, 8.78)	-16.27 (-84.71, 56.91)	-0.00, (-0.02, 0.01)	0.14 (0.13, 0.16)	0.17	no
4200	0.08	43	-0.01, (-0.02, 0.01)	2.05, (-3.31, 9.73)	-18.75 (-93.80, 54.63)	-0.00, (-0.02, 0.01)	0.14 (0.13, 0.15)	0.13	no
4220	0.08	43	-0.01, (-0.02, 0.01)	1.83, (-3.33, 8.36)	-16.98 (-82.82, 57.28)	0.00, (-0.02, 0.01)	0.14 (0.13, 0.15)	0.11	no
4230	0.08	43	-0.01, (-0.02, 0.02)	1.88, (-3.38, 8.84)	-15.39 (-87.53, 65.58)	0.00, (-0.02, 0.02)	0.14 (0.13, 0.15)	0.08	yes
4240	0.08	43	-0.01, (-0.02, 0.01)	2.29, (-3.36, 8.51)	-21.31 (-92.40, 52.07)	-0.01, (-0.02, 0.01)	0.14 (0.13, 0.15)	0.08	yes
4260	0.08	43	0.00, (-0.02, 0.02)	1.67, (-3.96, 8.20)	-15.67 (-85.26, 62.21)	0.00, (-0.02, 0.01)	0.14 (0.13, 0.15)	0.10	yes

4280	0.08	43	-0.01, (-0.02, 0.01)	2.06, (-2.99, 9.06)	-20.57 (-89.29, 51.27)	0.00, (-0.02, 0.01)	0.14 (0.13, 0.15)	0.07	yes
4300	0.08	43	-0.01, (-0.02, 0.01)	1.72, (-3.70, 7.72)	-15.77 (-88.18, 56.97)	-0.00, (-0.02, 0.01)	0.14 (0.13, 0.15)	0.08	yes
Average abundance, Average detection									
100	0.18	43	-0.00, (-0.12, 0.17)	15.49, (-7.38, 31.57)	0.13 (-11.95, 16.33)	0.00, (-0.12, 0.16)	0.57 (0.36, 0.89)	1.00	no
200	0.18	43	-0.00, (-0.11, 0.13)	12.14, (-7.20, 29.91)	-3.59 (-21.45, 26.09)	-0.02, (-0.11, 0.13)	0.41 (0.30, 0.56)	1.00	no
300	0.18	43	-0.01, (-0.09, 0.10)	9.61, (-7.65, 28.24)	-3.79 (-26.80, 29.27)	-0.01, (-0.09, 0.10)	0.34 (0.27, 0.43)	1.00	no
400	0.18	43	-0.01, (-0.09, 0.09)	7.97, (-6.91, 26.01)	-5.38 (-33.14, 30.68)	-0.01, (-0.08, 0.08)	0.30 (0.25, 0.36)	1.00	no
500	0.18	43	-0.02, (-0.08, 0.07)	7.65, (-5.88, 25.75)	-9.19 (-43.12, 31.31)	-0.02, (-0.09, 0.06)	0.27 (0.23, 0.32)	1.00	no
600	0.18	43	-0.02, (-0.08, 0.07)	6.20, (-6.02, 23.24)	-9.85 (-46.30, 36.80)	-0.02, (-0.08, 0.06)	0.25 (0.22, 0.29)	1.00	no
700	0.18	43	-0.02, (-0.08, 0.05)	5.83, (-5.39, 22.42)	-11.67 (-55.37, 34.89)	-0.02, (-0.08, 0.05)	0.23 (0.20, 0.27)	1.00	no
800	0.18	43	-0.01, (-0.07, 0.05)	4.98, (-4.78, 18.80)	-11.43 (-57.57, 38.71)	-0.01, (-0.07, 0.05)	0.22 (0.19, 0.25)	1.00	no
900	0.18	43	-0.01, (-0.07, 0.05)	4.13, (-4.87, 17.00)	-11.08 (-66.05, 43.72)	-0.01, (-0.07, 0.05)	0.20 (0.18, 0.23)	1.00	no
1000	0.18	43	-0.01, (-0.06, 0.05)	3.60, (-4.64, 14.11)	-11.68 (-62.54, 44.27)	-0.01, (-0.06, 0.04)	0.19 (0.17, 0.22)	1.00	no
1100	0.18	43	-0.01, (-0.06, 0.04)	3.30, (-3.83, 13.09)	-13.53 (-67.11, 40.76)	-0.01, (-0.06, 0.04)	0.18 (0.16, 0.21)	1.00	no
1200	0.18	43	-0.01, (-0.06, 0.05)	3.03, (-4.29, 12.80)	-12.82 (-66.73, 51.98)	-0.01, (-0.06, 0.04)	0.17 (0.15, 0.20)	0.98	no
1300	0.18	43	-0.01, (-0.06, 0.04)	3.07, (-3.36, 11.84)	-17.82 (-76.43, 44.09)	-0.01, (-0.06, 0.03)	0.17 (0.15, 0.19)	0.95	no
1400	0.18	43	-0.01, (-0.06, 0.05)	2.50, (-3.88, 10.64)	-15.13 (-74.78, 57.71)	-0.01, (-0.05, 0.04)	0.16 (0.14, 0.18)	0.84	no
1500	0.18	43	-0.01, (-0.05, 0.04)	2.21, (-3.47, 8.91)	-14.60 (-75.93, 54.73)	-0.01, (-0.05, 0.04)	0.15 (0.14, 0.17)	0.67	no
1600	0.18	43	-0.01, (-0.05, 0.04)	2.18, (-3.71, 9.73)	-16.56 (-83.86, 54.38)	-0.01, (-0.05, 0.03)	0.15 (0.14, 0.17)	0.46	no
1700	0.18	43	-0.01, (-0.05, 0.04)	2.32, (-3.26, 9.01)	-18.61 (-84.83, 56.63)	-0.01, (-0.05, 0.03)	0.14 (0.13, 0.16)	0.28	no
1800	0.18	43	-0.01, (-0.05, 0.03)	2.03, (-3.37, 8.46)	-18.09 (-92.63, 56.68)	-0.01, (-0.05, 0.03)	0.14 (0.13, 0.16)	0.13	no
1860	0.18	43	-0.01, (-0.05, 0.04)	1.82, (-3.30, 8.48)	-17.80 (-90.37, 60.18)	-0.01, (-0.05, 0.03)	0.14 (0.13, 0.15)	0.11	no
1870	0.18	43	-0.01, (-0.05, 0.04)	1.99, (-3.09, 8.08)	-17.12 (-83.53, 63.25)	-0.01, (-0.04, 0.03)	0.14 (0.13, 0.15)	0.06	yes
1880	0.18	43	-0.01, (-0.05, 0.03)	1.85, (-3.38, 8.26)	-17.15 (-86.41, 52.00)	-0.01, (-0.05, 0.03)	0.14 (0.13, 0.15)	0.06	yes
1900	0.18	43	-0.01, (-0.05, 0.04)	1.86, (-3.59, 7.59)	-18.32 (-85.32, 60.60)	-0.01, (-0.04, 0.03)	0.14 (0.12, 0.15)	0.06	yes
High abundance, High detection									
100	0.31	58	-0.02, (-0.14, 0.14)	10.09, (-8.59, 22.55)	-1.09 (-11.26, 12.84)	-0.01, (-0.11, 0.13)	0.31 (0.21, 0.42)	1.00	no
200	0.31	58	-0.02, (-0.11, 0.12)	9.78, (-7.40, 24.12)	-3.68 (-19.30, 21.72)	-0.02, (-0.10, 0.11)	0.24 (0.16, 0.30)	0.97	no
300	0.31	58	-0.02, (-0.11, 0.11)	8.14, (-8.13, 23.82)	-4.21 (-27.23, 30.31)	-0.01, (-0.09, 0.10)	0.21 (0.14, 0.25)	0.93	no
400	0.31	58	-0.02, (-0.11, 0.09)	7.40, (-7.80, 23.03)	-5.78 (-34.83, 35.01)	-0.01, (-0.09, 0.09)	0.18 (0.14, 0.22)	0.90	no
500	0.31	58	-0.02, (-0.09, 0.08)	6.68, (-6.91, 21.36)	-7.48 (-39.28, 37.20)	-0.01, (-0.08, 0.07)	0.17 (0.13, 0.19)	0.87	no
600	0.31	58	-0.02, (-0.10, 0.06)	6.90, (-7.22, 22.48)	-11.47 (-51.76, 38.69)	-0.02, (-0.09, 0.06)	0.16 (0.12, 0.18)	0.75	no
700	0.31	58	-0.02, (-0.09, 0.06)	6.03, (-6.39, 19.76)	-12.12 (-54.45, 42.24)	-0.02, (-0.08, 0.06)	0.15 (0.13, 0.16)	0.41	no
780	0.31	58	-0.02, (-0.09, 0.06)	6.15, (-6.42, 21.11)	-14.02 (-61.94, 47.12)	-0.02, (-0.08, 0.06)	0.14 (0.12, 0.15)	0.13	no
790	0.31	58	-0.02, (-0.08, 0.06)	5.72, (-5.60, 18.78)	-13.11 (-58.29, 40.61)	-0.02, (-0.07, 0.05)	0.14 (0.12, 0.15)	0.11	no
800	0.31	58	-0.02, (-0.09, 0.05)	5.90, (-5.70, 20.32)	-15.31 (-63.06, 38.67)	-0.02, (-0.08, 0.05)	0.14 (0.12, 0.15)	0.07	yes

Average abundance, High detection									
100	0.18	58	0.00, (-0.10, 0.15)	7.71, (-13.26, 21.42)	0.83 (-7.59, 13.95)	0.01, (-0.08, 0.14)	0.42 (0.26, 0.62)	1.00	no
200	0.18	58	-0.01, (-0.08, 0.09)	10.25, (-8.05, 22.96)	-2.08 (-13.86, 14.53)	-0.01, (-0.07, 0.07)	0.29 (0.20, 0.40)	1.00	no
300	0.18	58	-0.01, (-0.07, 0.09)	9.23, (-10.02, 24.04)	-2.12 (-18.90, 23.19)	-0.01, (-0.06, 0.08)	0.25 (0.17, 0.32)	0.98	no
400	0.18	58	-0.01, (-0.06, 0.08)	8.15, (-9.92, 23.51)	-2.03 (-23.80, 28.60)	-0.01, (-0.06, 0.07)	0.23 (0.16, 0.28)	0.97	no
500	0.18	58	-0.01, (-0.06, 0.06)	7.94, (-7.61, 22.71)	-4.11 (-27.47, 27.83)	-0.01, (-0.05, 0.06)	0.21 (0.15, 0.25)	0.95	no
600	0.18	58	-0.01, (-0.06, 0.06)	7.92, (-9.48, 22.36)	-6.11 (-33.32, 34.50)	-0.01, (-0.06, 0.06)	0.19 (0.14, 0.23)	0.93	no
700	0.18	58	-0.01, (-0.06, 0.06)	7.28, (-7.67, 23.09)	-6.49 (-35.11, 34.33)	-0.01, (-0.05, 0.05)	0.18 (0.13, 0.21)	0.89	no
800	0.18	58	-0.01, (-0.06, 0.06)	7.65, (-9.07, 23.18)	-7.84 (-42.33, 39.52)	-0.01, (-0.05, 0.05)	0.17 (0.13, 0.20)	0.83	no
900	0.18	58	-0.01, (-0.05, 0.05)	6.39, (-8.22, 22.16)	-7.78 (-43.56, 44.66)	-0.01, (-0.05, 0.05)	0.16 (0.13, 0.19)	0.85	no
1000	0.18	58	-0.01, (-0.05, 0.04)	6.83, (-6.72, 21.75)	-10.79 (-49.12, 38.50)	-0.01, (-0.05, 0.04)	0.16 (0.13, 0.18)	0.75	no
1100	0.18	58	-0.01, (-0.05, 0.05)	6.13, (-7.44, 20.08)	-10.78 (-49.51, 43.62)	-0.01, (-0.05, 0.04)	0.15 (0.13, 0.17)	0.61	no
1200	0.18	58	-0.01, (-0.05, 0.04)	6.50, (-5.82, 20.76)	-12.26 (-53.03, 37.08)	-0.01, (-0.04, 0.03)	0.14 (0.12, 0.16)	0.36	no
1300	0.18	58	-0.01, (-0.05, 0.04)	5.12, (-6.20, 19.93)	-10.41 (-61.06, 45.39)	-0.01, (-0.05, 0.03)	0.14 (0.12, 0.16)	0.17	no
1340	0.18	58	-0.01, (-0.05, 0.03)	4.95, (-6.75, 18.81)	-10.71 (-57.01, 38.66)	-0.01, (-0.04, 0.03)	0.14 (0.12, 0.15)	0.11	no
1350	0.18	58	-0.01, (-0.05, 0.04)	5.38, (-6.36, 19.01)	-12.58 (-58.27, 40.85)	-0.01, (-0.04, 0.03)	0.14 (0.12, 0.15)	0.12	no
1360	0.18	58	-0.01, (-0.05, 0.04)	5.05, (-6.55, 19.75)	-11.90 (-63.80, 44.26)	-0.01, (-0.05, 0.03)	0.14 (0.12, 0.15)	0.08	yes
1380	0.18	58	-0.01, (-0.05, 0.03)	5.15, (-6.16, 19.62)	-13.08 (-61.06, 41.45)	-0.01, (-0.04, 0.03)	0.14 (0.12, 0.15)	0.07	yes
1400	0.18	58	-0.01, (-0.05, 0.04)	4.36, (-7.56, 18.45)	-9.17 (-58.23, 50.97)	-0.01, (-0.04, 0.04)	0.14 (0.12, 0.15)	0.06	yes
Low abundance, high detection									
100	0.08	58	0.02, (-0.05, 0.13)	5.48, (-20.85, 19.54)	2.59 (-4.04, 12.89)	0.03, (-0.04, 0.13)	1.21 (0.36, 1.49)	1.00	no
200	0.08	58	0.00, (-0.04, 0.07)	7.98, (-13.24, 21.30)	0.72 (-7.48, 13.90)	0.00, (-0.04, 0.07)	0.58 (0.27, 0.67)	1.00	no
300	0.08	58	0.00, (-0.04, 0.06)	8.30, (-11.25, 21.53)	0.71 (-9.00, 15.79)	0.00, (-0.03, 0.05)	0.36 (0.23, 0.52)	1.00	no
400	0.08	58	0.00, (-0.04, 0.05)	8.19, (-11.23, 22.25)	0.00 (-11.74, 17.47)	0.00, (-0.03, 0.04)	0.32 (0.21, 0.44)	1.00	no
500	0.08	58	0.00, (-0.03, 0.04)	8.66, (-10.65, 22.78)	-0.33 (-11.98, 19.26)	0.00, (-0.02, 0.04)	0.29 (0.20, 0.39)	1.00	no
600	0.08	58	0.00, (-0.03, 0.03)	9.75, (-8.83, 23.85)	-2.22 (-15.78, 19.92)	0.00, (-0.03, 0.03)	0.26 (0.17, 0.34)	0.99	no
700	0.08	58	-0.01, (-0.03, 0.03)	9.31, (-8.07, 23.65)	-2.32 (-16.86, 18.75)	0.00, (-0.02, 0.03)	0.25 (0.17, 0.32)	0.99	no
800	0.08	58	0.00, (-0.03, 0.03)	8.95, (-7.86, 23.35)	-2.93 (-20.13, 21.50)	0.00, (-0.03, 0.03)	0.24 (0.16, 0.30)	0.97	no
900	0.08	58	0.00, (-0.03, 0.03)	8.83, (-7.93, 24.28)	-3.17 (-23.30, 23.45)	0.00, (-0.03, 0.03)	0.23 (0.15, 0.28)	0.95	no
1000	0.08	58	-0.01, (-0.03, 0.02)	9.43, (-7.93, 23.04)	-5.59 (-25.15, 25.45)	-0.01, (-0.03, 0.03)	0.22 (0.15, 0.27)	0.95	no
1100	0.08	58	-0.01, (-0.03, 0.03)	8.64, (-8.63, 24.51)	-4.62 (-26.64, 23.74)	0.00, (-0.02, 0.02)	0.21 (0.14, 0.25)	0.93	no
1200	0.08	58	0.00, (-0.03, 0.03)	7.57, (-9.11, 22.10)	-4.06 (-27.77, 28.33)	0.00, (-0.02, 0.02)	0.20 (0.15, 0.25)	0.95	no
1300	0.08	58	0.00, (-0.03, 0.02)	7.59, (-8.74, 23.67)	-4.74 (-30.13, 28.41)	0.00, (-0.02, 0.02)	0.20 (0.14, 0.23)	0.92	no
1400	0.08	58	-0.01, (-0.03, 0.02)	7.48, (-8.38, 22.72)	-5.41 (-30.14, 29.74)	0.00, (-0.02, 0.02)	0.19 (0.14, 0.23)	0.93	no
1500	0.08	58	-0.01, (-0.03, 0.02)	7.60, (-7.38, 21.62)	-6.25 (-32.28, 27.84)	0.00, (-0.02, 0.02)	0.19 (0.14, 0.22)	0.92	no
1600	0.08	58	-0.01, (-0.03, 0.02)	7.30, (-8.74, 23.07)	-5.39 (-35.20, 37.24)	0.00, (-0.02, 0.02)	0.18 (0.14, 0.21)	0.91	no

1700	0.08	58	-0.01, (-0.03, 0.02)	8.12, (-6.56, 23.34)	-9.18 (-38.67, 30.63)	-0.01, (-0.02, 0.02)	0.18 (0.13, 0.21)	0.86	no
1800	0.08	58	-0.01, (-0.03, 0.02)	7.10, (-7.04, 21.88)	-7.74 (-37.97, 32.14)	0.00, (-0.02, 0.02)	0.17 (0.14, 0.20)	0.89	no
1900	0.08	58	-0.01, (-0.03, 0.02)	7.06, (-7.84, 22.71)	-7.80 (-42.93, 36.47)	0.00, (-0.02, 0.02)	0.17 (0.13, 0.19)	0.84	no
2000	0.08	58	-0.01, (-0.03, 0.02)	7.16, (-7.82, 21.61)	-8.67 (-42.97, 35.06)	0.00, (-0.02, 0.02)	0.17 (0.13, 0.19)	0.83	no
2100	0.08	58	-0.01, (-0.03, 0.02)	7.29, (-6.62, 23.00)	-10.84 (-45.52, 35.68)	-0.01, (-0.02, 0.02)	0.16 (0.12, 0.19)	0.81	no
2200	0.08	58	-0.01, (-0.02, 0.02)	6.36, (-8.34, 22.27)	-8.32 (-46.97, 38.45)	0.00, (-0.02, 0.02)	0.16 (0.13, 0.18)	0.80	no
2300	0.08	58	-0.01, (-0.03, 0.02)	7.07, (-6.73, 23.50)	-11.29 (-51.19, 40.76)	0.00, (-0.02, 0.02)	0.16 (0.12, 0.18)	0.75	no
2400	0.08	58	-0.01, (-0.02, 0.02)	5.93, (-7.91, 20.79)	-8.74 (-51.42, 42.91)	0.00, (-0.02, 0.02)	0.15 (0.13, 0.17)	0.72	no
2500	0.08	58	-0.01, (-0.03, 0.02)	6.02, (-6.98, 21.08)	-10.76 (-51.31, 42.65)	0.00, (-0.02, 0.02)	0.15 (0.13, 0.17)	0.65	no
2600	0.08	58	-0.01, (-0.02, 0.02)	6.11, (-6.88, 20.47)	-12.31 (-53.13, 36.12)	0.00, (-0.02, 0.01)	0.15 (0.13, 0.17)	0.56	no
2700	0.08	58	-0.01, (-0.02, 0.01)	6.55, (-6.84, 22.10)	-13.41 (-56.32, 40.97)	0.00, (-0.02, 0.02)	0.15 (0.12, 0.16)	0.45	no
2800	0.08	58	-0.01, (-0.02, 0.02)	5.48, (-6.41, 18.93)	-10.59 (-52.51, 43.38)	0.00, (-0.02, 0.02)	0.15 (0.13, 0.16)	0.32	no
2900	0.08	58	-0.01, (-0.02, 0.01)	5.76, (-6.24, 21.57)	-12.78 (-58.46, 41.17)	0.00, (-0.02, 0.01)	0.14 (0.12, 0.16)	0.23	no
3000	0.08	58	-0.01, (-0.02, 0.02)	5.47, (-6.33, 18.87)	-12.03 (-57.94, 42.01)	0.00, (-0.02, 0.01)	0.14 (0.12, 0.16)	0.20	no
3100	0.08	58	-0.01, (-0.02, 0.01)	5.73, (-4.96, 19.82)	-14.70 (-62.94, 39.28)	0.00, (-0.02, 0.01)	0.14 (0.12, 0.15)	0.11	no
3110	0.08	58	0.00, (-0.02, 0.01)	5.16, (-5.92, 19.60)	-11.62 (-60.84, 43.04)	0.00, (-0.02, 0.01)	0.14 (0.12, 0.15)	0.09	yes
3120	0.08	58	-0.01, (-0.02, 0.01)	5.25, (-6.20, 21.17)	-11.99 (-61.64, 39.36)	0.00, (-0.02, 0.01)	0.14 (0.12, 0.15)	0.10	yes
3140	0.08	58	-0.01, (-0.02, 0.01)	5.28, (-6.70, 19.55)	-13.07 (-59.33, 46.66)	0.00, (-0.02, 0.01)	0.14 (0.12, 0.15)	0.08	yes
3160	0.08	58	-0.01, (-0.02, 0.01)	5.08, (-6.43, 20.59)	-11.48 (-61.55, 50.74)	0.00, (-0.02, 0.02)	0.14 (0.12, 0.15)	0.08	yes
3180	0.08	58	-0.01, (-0.02, 0.01)	5.39, (-6.59, 20.17)	-12.14 (-58.57, 48.50)	0.00, (-0.02, 0.02)	0.14 (0.12, 0.15)	0.07	yes
3200	0.08	58	-0.01, (-0.02, 0.02)	5.33, (-6.77, 20.70)	-13.21 (-65.15, 49.01)	0.00, (-0.02, 0.02)	0.14 (0.12, 0.15)	0.07	yes

APPENDIX S

APPENDIX S: SIMULATION RESULTS FOR HIERARCHICAL DISTANCE SAMPLING MODELS FOR LINE-TRANSECTS

Table S1. Results of simulations evaluating the efficacy of survey protocols using parameters from the 2020 and 2021 spring survey data analyzed hierarchical distance sampling models for line-transects with a length of 2,681 m (average transect length from 2020 and 2021 surveys). Mean (90% credible interval) for bias and coefficient of variation from 500 simulation runs for each suite of parameters. Different scenarios include combinations of high, average, and low abundance paired with either average or high detection. R = number of survey sites, λ = mean abundance per site, sigma = sigma for calculating the half-normal detection function; CV = coefficient of variation for total population size (Total N) and N.site = estimated number of Dusky Grouse per survey site. Yes/No = whether the protocol meets management requirements.

Simulation Parameters			**Bias in λ**	**Bias in *sigma***	**Bias in Total N**	**Bias in N.site**	**CV Total N**	**Prob. CV Total N > 0.15**	**Yes /No**
R	**λ**	***sigma***							
High abundance, Average detection									
20	5.54	42	-0.09 (-1.65, 1.58)	3.59 (-6.06, 17.96)	-2.54 (-29.47, 28.67)	-0.13 (-1.47, 1.43)	0.14 (0.13, 0.16)	0.27	no
25	5.54	42	-0.08 (-1.48, 1.26)	2.90 (-5.32, 13.94)	-2.34 (-31.01, 28.10)	-0.09 (-1.24, 1.12)	0.13 (0.12, 0.14)	0.01	yes
30	5.54	42	-0.05 (-1.27, 1.28)	1.43 (-5.66, 9.53)	-1.79 (-31.05, 28.58)	-0.06 (-1.03, 0.95)	0.12 (0.11, 0.13)	0.00	yes
40	5.54	42	-0.06 (-1.16, 1.14)	1.25 (-5.16, 8.51)	-2.89 (-36.80, 37.46)	-0.07 (-0.92, 0.94)	0.10 (0.09, 0.11)	0.00	yes
60	5.54	42	-0.08 (-0.85, 0.80)	1.16 (-3.70, 6.31)	-4.37 (-45.46, 42.31)	-0.07 (-0.76, 0.71)	0.08 (0.08, 0.09)	0.00	yes
80	5.54	42	-0.04 (-0.77, 0.73)	0.65 (-3.53, 5.19)	-2.71 (-57.15, 49.50)	-0.03 (-0.71, 0.62)	0.07 (0.07, 0.07)	0.00	yes
100	5.54	42	-0.01 (-0.66, 0.67)	0.55 (-2.85, 4.62)	-1.94 (-55.14, 59.02)	-0.02 (-0.55, 0.59)	0.06 (0.06, 0.07)	0.00	yes
Average abundance, Average detection									
20	3.22	42	-0.10 (-1.15, 1.24)	6.16 (-6.66, 23.52)	-2.16 (-19.42, 18.89)	-0.11 (-0.97, 0.94)	0.19 (0.16, 0.22)	0.99	no
30	3.22	42	-0.11 (-1.01, 0.98)	4.26 (-6.44, 19.45)	-2.64 (-25.97, 21.85)	-0.09 (-0.87, 0.73)	0.16 (0.14, 0.18)	0.71	no
35	3.22	42	-0.07 (-0.86, 0.85)	3.29 (-5.27, 15.88)	-2.67 (-26.82, 23.36)	-0.08 (-0.77, 0.67)	0.14 (0.13, 0.16)	0.29	no
40	3.22	42	-0.06 (-0.84, 0.81)	3.23 (-5.31, 15.81)	-3.31 (-30.55, 22.27)	-0.08 (-0.76, 0.56)	0.13 (0.12, 0.15)	0.04	yes
60	3.22	42	-0.04 (-0.72, 0.65)	1.63 (-4.63, 9.25)	-2.69 (-35.61, 33.99)	-0.04 (-0.59, 0.57)	0.11 (0.10, 0.12)	0.00	yes
80	3.22	42	-0.05 (-0.62, 0.53)	1.45 (-4.31, 8.60)	-3.22 (-40.71, 38.56)	-0.04 (-0.51, 0.48)	0.09 (0.09, 0.10)	0.00	yes
100	3.22	42	-0.03 (-0.51, 0.46)	1.01 (-3.88, 6.17)	-3.13 (-42.30, 40.99)	-0.03 (-0.42, 0.41)	0.08 (0.08, 0.09)	0.00	yes
Low abundance, Average detection									
100	1.43	42	-0.01 (-0.35, 0.34)	2.60 (-5.83, 12.97)	-1.81 (-32.22, 30.12)	-0.02 (-0.32, 0.30)	0.13 (0.12, 0.14)	0.01	yes
80	1.43	42	-0.03 (-0.41, 0.39)	3.41 (-6.44, 16.49)	-2.76 (-30.47, 24.64)	-0.03 (-0.38, 0.31)	0.14 (0.13, 0.16)	0.24	no
90	1.43	42	-0.03 (-0.39, 0.35)	2.58 (-5.32, 14.65)	-2.58 (-29.13, 23.93)	-0.03 (-0.32, 0.27)	0.13 (0.12, 0.15)	0.06	yes
85	1.43	42	-0.03 (-0.36, 0.38)	2.92 (-5.81, 13.87)	-2.62 (-26.72, 23.79)	-0.03 (-0.31, 0.28)	0.14 (0.12, 0.15)	0.11	no
High abundance, High detection									

10	5.54	51	-0.25 (-1.97, 1.78)	9.19 (-8.45, 26.34)	-2.64 (-15.51, 14.34)	-0.26 (-1.55, 1.43)	0.18 (0.13, 0.22)	0.84	no
15	5.54	51	-0.10 (-1.56, 1.83)	6.81 (-9.23, 23.51)	-1.79 (-19.00, 21.42)	-0.12 (-1.27, 1.43)	0.15 (0.12, 0.17)	0.45	no
20	5.54	51	-0.14 (-1.40, 1.45)	5.67 (-7.24, 21.52)	-3.04 (-24.75, 20.15)	-0.15 (-1.24, 1.01)	0.13 (0.11, 0.15)	0.04	yes
40	5.54	51	-0.13 (-1.23, 0.95)	3.45 (-5.73, 15.85)	-4.63 (-39.53, 29.92)	-0.12 (-0.99, 0.75)	0.09 (0.09, 0.10)	0.00	yes
60	5.54	51	-0.07 (-0.85, 0.81)	1.93 (-5.28, 10.23)	-4.25 (-48.17, 41.12)	-0.07 (-0.80, 0.69)	0.08 (0.07, 0.08)	0.00	yes
80	5.54	51	-0.05 (-0.71, 0.65)	1.03 (-4.26, 7.88)	-3.45 (-47.22, 37.54)	-0.04 (-0.59, 0.47)	0.07 (0.06, 0.07)	0.00	yes
100	5.54	51	-0.01 (-0.65, 0.71)	0.96 (-4.28, 6.81)	-2.32 (-52.68, 47.03)	-0.02 (-0.53, 0.47)	0.06 (0.06, 0.06)	0.00	yes
Average abundance, High detection									
20	3.22	51	-0.14 (-1.08, 1.04)	9.42 (-8.57, 26.65)	-3.06 (-18.03, 16.03)	-0.15 (-0.90, 0.80)	0.16 (0.12, 0.20)	0.73	no
30	3.22	51	-0.15 (-0.93, 0.72)	7.63 (-5.95, 24.20)	-4.65 (-22.60, 18.41)	-0.15 (-0.75, 0.61)	0.14 (0.11, 0.16)	0.20	no
35	3.22	51	-0.12 (-0.92, 0.79)	6.28 (-6.85, 23.29)	-3.94 (-24.98, 19.96)	-0.11 (-0.71, 0.57)	0.13 (0.11, 0.15)	0.02	yes
40	3.22	51	-0.10 (-0.85, 0.73)	5.18 (-7.40, 21.19)	-4.05 (-27.98, 23.58)	-0.10 (-0.70, 0.59)	0.12 (0.11, 0.14)	0.00	yes
60	3.22	51	-0.07 (-0.76, 0.61)	3.47 (-6.39, 16.87)	-3.40 (-35.24, 28.49)	-0.06 (-0.59, 0.47)	0.10 (0.0, 0.11)	0.00	yes
80	3.22	51	-0.06 (-0.62, 0.52)	2.52 (-5.84, 13.79)	-4.22 (-39.76, 32.49)	-0.05 (-0.50, 0.41)	0.09 (0.08, 0.09)	0.00	yes
100	3.22	51	-0.04 (-0.56, 0.46)	2.12 (-5.06, 11.52)	-4.91 (-45.84, 37.84)	-0.05 (-0.46, 0.38)	0.08 (0.07, 0.08)	0.00	yes
Low abundance, High detection									
60	1.43	51	-0.07 (-0.44, 0.42)	7.36 (-7.83, 24.88)	-3.36 (-21.23, 19.94)	-0.06 (-0.35, 0.33)	0.15 (0.12, 0.17)	0.45	no
65	1.43	51	-0.03 (-0.41, 0.42)	6.42 (-7.71, 22.17)	-1.66 (-20.76, 21.16)	-0.03 (-0.32, 0.33)	0.14 (0.12, 0.16)	0.25	no
70	1.43	51	-0.06 (-0.39, 0.32)	7.66 (-7.27, 24.01)	-4.18 (-21.92, 18.97)	-0.06 (-0.34, 0.27)	0.14 (0.11, 0.16)	0.10	yes
80	1.43	51	-0.04 (-0.37, 0.40)	6.17 (-7.75, 20.89)	-3.14 (-23.48, 23.70)	-0.04 (-0.29, 0.30)	0.13 (0.11, 0.14)	0.01	yes
100	1.43	51	-0.03 (-0.36, 0.32)	4.63 (-7.44, 20.77)	-3.65 (-30.02, 27.41)	-0.04 (-0.30, 0.27)	0.12 (0.10, 0.13)	0.00	yes

Table S2. Results of simulations evaluating the efficacy of survey protocols using parameters from the 2020 and 2021 spring survey data analyzed hierarchical distance sampling models for line-transects with a length of 5,000m. Mean (90% credible interval) for bias and coefficient of variation from 500 simulation runs for each suite of parameters. Different scenarios include combinations of high, average, and low abundance paired with either average or high detection. R = number of survey sites, λ = mean abundance per site, sigma = sigma for calculating the half-normal detection function; CV = coefficient of variation for total population size (Total N) and N.site = estimated number of Dusky Grouse per survey site. Yes/No = whether the protocol meets management requirements.

Simulation Parameters			**Bias in λ**	**Bias in *sigma***	**Bias in Total N**	**Bias in N.site**	**CV Total N**	**Prob. CV Total N > 0.15**	**Yes /No**
R	**λ**	***sigma***							
High abundance, Average detection									
10	10.33	42	-0.36 (-3.42, 2.95)	4.59 (-5.73, 19.76)	-3.08 (-29.41, 24.03)	-0.31 (-2.94, 2.40)	0.15 (0.13, 0.17)	0.47	no

15	10.33	42	-0.27 (-2.54, 2.14)	2.58 (-4.90, 11.82)	-3.47 (-33.21, 27.46)	-0.23 (-2.21, 1.83)	0.12 (0.11, 0.14)	0.00	yes
20	10.33	42	-0.13 (-2.33, 2.03)	1.78 (-5.26, 9.68)	-2.99 (-40.46, 37.18)	-0.15 (-2.02, 1.86)	0.10 (0.10, 0.12)	0.00	yes
40	10.33	42	-0.05 (-1.51, 1.48)	0.74 (-3.61, 5.70)	-1.29 (-51.31, 44.90)	-0.03 (-1.28, 1.12)	0.07 (0.07, 0.08)	0.00	yes
60	10.33	42	-0.09 (-1.27, 1.20)	0.67 (-2.43, 4.70)	-5.92 (-69.32, 56.28)	-0.10 (-1.16, 0.94)	0.06 (0.06, 0.06)	0.00	yes
80	10.33	42	-0.04 (-1.05, 1.04)	0.47 (-2.39, 3.98)	-4.56 (-73.02, 62.47)	-0.06 (-0.91, 0.78)	0.05 (0.05, 0.05)	0.00	yes
100	10.33	42	-0.08 (-1.01, 0.99)	0.40 (-2.34, 3.01)	-8.19 (-84.39, 69.41)	-0.08 (-0.84, 0.69)	0.05 (0.04, 0.05)	0.00	yes
Average abundance, Average detection									
20	6	42	-0.10 (-1.72, 1.56)	3.06 (-5.41, 15.58)	-2.51 (-28.58, 25.43)	-0.13 (-1.43, 1.27)	0.14 (0.12, 0.16)	0.14	no
25	6	42	-0.08 (-1.53, 1.46)	2.62 (-5.81, 12.23)	-2.01 (-30.41, 29.61)	-0.08 (-1.22, 1.18)	0.12 (0.11, 0.14)	0.00	yes
30	6	42	-0.05 (-1.42, 1.33)	2.00 (-4.49, 11.27)	-2.08 (-36.65, 30.71)	-0.07 (-1.22, 1.02)	0.11 (0.10, 0.12)	0.00	yes
40	6	42	-0.04 (-1.04, 1.13)	1.19 (-4.56, 7.65)	-1.72 (-37.93, 34.09)	-0.04 (-0.95, 0.85)	0.10 (0.09, 0.10)	0.00	yes
60	6	42	-0.05 (-1.08, 0.78)	0.99 (-3.25, 6.33)	-3.26 (-51.41, 43.90)	-0.05 (-0.86, 0.73)	0.08 (0.07, 0.08)	0.00	yes
80	6	42	-0.02 (-0.79, 0.80)	0.51 (-3.34, 4.95)	-0.82 (-51.25, 48.55)	-0.01 (-0.64, 0.61)	0.07 (0.06, 0.07)	0.00	yes
100	6	42	-0.04 (-0.79, 0.70)	0.54 (-2.81, 4.36)	-4.23 (-62.13, 52.88)	-0.04 (-0.62, 0.53)	0.06 (0.06, 0.06)	0.00	yes
Low abundance, Average detection									
40	2.67	42	-0.08 (-0.84, 0.73)	3.86 (-5.99, 16.94)	-3.09 (-27.32, 23.42)	-0.08 (-0.68, 0.59)	0.15 (0.13, 0.17)	0.42	no
45	2.67	42	-0.08 (-0.76, 0.67)	3.68 (-4.89, 15.58)	-3.60 (-28.97, 25.27)	-0.08 (-0.64, 0.56)	0.14 (0.12, 0.16)	0.14	no
50	2.67	42	-0.04 (-0.77, 0.68)	2.52 (-5.73, 14.62)	-2.34 (-31.02, 29.58)	-0.05 (-0.62, 0.59)	0.13 (0.12, 0.15)	0.05	yes
60	2.67	42	-0.06 (-0.65, 0.60)	2.17 (-5.55, 12.34)	-3.22 (-35.98, 29.53)	-0.05 (-0.60, 0.49)	0.12 (0.11, 0.13)	0.00	yes
80	2.67	42	-0.05 (-0.59, 0.55)	1.95 (-4.65, 9.91)	-3.37 (-37.17, 35.92)	-0.04 (-0.46, 0.45)	0.10 (0.09, 0.11)	0.00	yes
100	2.67	42	-0.01 (-0.47, 0.46)	1.14 (-4.19, 6.95)	-1.38 (-36.59, 37.71)	-0.01 (-0.37, 0.38)	0.09 (0.09, 0.10)	0.00	yes
High abundance, High detection									
10	10.33	51	-0.37 (-2.89, 2.60)	6.23 (-7.93, 22.81)	-2.88 (-23.44, 22.58)	-0.29 (-2.34, 2.26)	0.14 (0.11, 0.15)	0.11	yes-ish
15	10.33	51	-0.23 (-2.48, 2.17)	4.32 (-7.13, 18.33)	-3.40 (-30.83, 24.10)	-0.23 (-2.06, 1.61)	0.11 (0.10, 0.12)	0.00	yes
20	10.33	51	-0.19 (-2.25, 1.91)	2.98 (-6.97, 16.01)	-2.94 (-37.56, 32.09)	-0.15 (-1.88, 1.60)	0.10 (0.09, 0.11)	0.00	yes
40	10.33	51	-0.18 (-1.49, 1.19)	1.66 (-4.07, 9.92)	-7.09 (-50.55, 39.84)	-0.18 (-1.26, 1.00)	0.07 (0.06, 0.07)	0.00	yes
60	10.33	51	-0.04 (-1.25, 1.07)	0.73 (-3.92, 6.40)	-2.17 (-61.66, 56.14)	-0.04 (-1.03, 0.94)	0.06 (0.05, 0.06)	0.00	yes
80	10.33	51	-0.07 (-1.10, 0.93)	1.02 (-3.48, 6.07)	-6.89 (-76.07, 53.61)	-0.09 (-0.95, 0.67)	0.05 (0.05, 0.05)	0.00	yes

100	10.33	51	-0.04 (-0.99, 0.85)	0.60 (-3.08, 5.30)	-2.65 (-77.98, 72.19)	-0.03 (-0.78, 0.72)	0.04 (0.04, 0.04)	0.00	yes
Average abundance, High detection									
10	6	51	-0.24 (-2.08, 1.90)	9.10 (-8.94, 26.79)	-2.25 (-16.35, 16.15)	-0.22 (-1.63, 1.61)	0.17 (0.13, 0.21)	0.81	no
15	6	51	-0.22 (-1.77, 1.44)	7.12 (-7.50, 24.09)	-3.36 (-21.34, 17.06)	-0.22 (-1.42, 1.14)	0.14 (0.12, 0.17)	0.34	no
20	6	51	-0.16 (-1.57, 1.43)	6.00 (-6.41, 22.23)	-3.68 (-26.62, 21.67)	-0.18 (-1.33, 1.08)	0.13 (0.11, 0.14)	0.01	yes
40	6	51	-0.06 (-1.15, 1.17)	2.34 (-6.25, 13.91)	-2.44 (-39.09, 34.63)	-0.06 (-0.98, 0.87)	0.09 (0.08, 0.10)	0.00	yes
60	6	51	-0.07 (-0.94, 0.79)	1.90 (-4.58, 10.08)	-5.19 (-49.50, 38.98)	-0.09 (-0.82, 0.65)	0.07 (0.07, 0.08)	0.00	yes
80	6	51	-0.04 (-0.78, 0.80)	1.09 (-4.84, 7.94)	-1.46 (-54.12, 49.80)	-0.02 (-0.68, 0.62)	0.06 (0.06, 0.07)	0.00	yes
100	6	51	-0.06 (-0.72, 0.57)	0.98 (-4.15, 6.88)	-3.24 (-56.26, 51.08)	-0.03 (-0.56, 0.51)	0.06 (0.05, 0.06)	0.00	yes
Low abundance, High detection									
20	2.67	51	-0.12 (-0.99, 0.93)	9.29 (-8.90, 26.61)	-2.43 (-14.89, 14.82)	-0.12 (-0.74, 0.74)	0.18 (0.13, 0.22)	0.84	no
30	2.67	51	-0.07 (-0.78, 0.86)	7.28 (-9.63, 24.44)	-2.46 (-20.13, 20.37)	-0.08 (-0.67, 0.68)	0.15 (0.12, 0.17)	0.54	no
35	2.67	51	-0.08 (-0.78, 0.75)	6.12 (-8.26, 22.59)	-2.56 (-22.43, 20.67)	-0.07 (-0.64, 0.59)	0.14 (0.12, 0.16)	0.23	no
40	2.67	51	-0.04 (-0.69, 0.74)	5.24 (-8.42, 22.15)	-1.84 (-23.56, 22.83)	-0.05 (-0.59, 0.57)	0.13 (0.11, 0.15)	0.07	yes
60	2.67	51	-0.05 (-0.58, 0.53)	4.27 (-6.23, 18.55)	-2.89 (-28.54, 25.77)	-0.05 (-0.48, 0.43)	0.11 (0.10, 0.12)	0.00	yes
80	2.67	51	-0.03 (-0.52, 0.50)	2.86 (-5.52, 15.18)	-3.57 (-35.98, 30.26)	-0.04 (-0.45, 0.38)	0.10 (0.09, 0.10)	0.00	yes
100	2.67	51	-0.04 (-0.48, 0.47)	2.78 (-5.09, 13.67)	-4.16 (-39.69, 33.94)	-0.04 (-0.40, 0.34)	0.09 (0.08, 0.09)	0.00	yes

APPENDIX T

APPENDIX T: SIMULATION RESULTS FOR TIME-REMOVAL HIERARCHICAL DISTANCDE SAMPLING

Table T1. Results of simulations evaluating the efficacy of survey protocols using parameters from the 2020 and 2021 spring survey data analyzed using time-removal HDS models. Mean (90% credible interval) for bias and coefficient of variation from 500 simulation runs for each suite of parameters. Different scenarios include combinations of high, average, and low abundance paired with either average or high detection. R = number of survey sites, λ = mean abundance per site, sigma = mean sigma, p.avail = mean probability of overall availability; CV = coefficient of variation for total population size (Total M) and M.site = estimated number of Dusky Grouse per survey site.

Simulation Parameters				**Bias in λ**	**Bias in *sigma***	**p.avail**	**Bias in Total M**	**Bias in M.site**	**CV Total M**	**Prob. CV M.total > 0.15**	**Yes /No**
R	**λ**	***sigma***	***p.avail***								
High abundance, average detection											
200	0.31	43	0.65	0.32 (-0.15, 1.27)	11.04 (-7.40, 30.23)	-0.03 (-0.27, 0.24)	64.52 (-29.02, 256.44)	0.32 (-0.15, 1.28)	1.38 (0.54, 2.59)	1.00	no
1000	0.31	43	0.65	0.17 (-0.10, 0.65)	2.26 (-4.49, 11.99)	-0.04 (-0.29, 0.18)	175.90 (-99.60, 658.26)	0.18 (-0.10, 0.66)	0.62 (0.23, 1.40)	1.00	no
6000	0.31	43	0.65	0.01 (-0.06, 0.09)	0.44, (-2.33 3.35)	-0.01 (-0.12, 0.09)	63.86 (-313.64, 563.16)	0.01 (-0.05, 0.09)	0.15 (0.10, 0.22)	0.33	no
High abundance, high detection											
200	0.31	48	0.89	0.15 (-0.13, 0.55)	10.90 (-6.77, 26.49)	-0.08 (-0.32, 0.07)	30.64 (-22.93, 115.62)	0.15 (-0.11, 0.58)	0.79 (0.29, 2.28)	1.00	no
1000	0.31	48	0.89	0.00 (-0.08, 0.09)	2.49 (-4.59, 12.39)	-0.02 (-0.10, 0.05)	1.32 (-70.19, 86.43)	0.00 (-0.07, 0.09)	0.16 (0.14, 0.20)	0.78	no
1300	0.31	48	0.89	0.00 (-0.09, 0.07)	1.83 (-4.18, 10.15)	-0.01 (-0.09, 0.04)	0.20 (-88.30, 82.51)	0.00 (-0.07, 0.06)	0.14 (0.12, 0.17)	0.18	no
1380	0.31	48	0.89	0.00 (-0.07, 0.07)	1.49 (-4.37, 9.16)	-0.02 (-0.09, 0.04)	4.77 (-80.91, 95.09)	0.00 (-0.06, 0.07)	0.14 (0.12, 0.16)	0.11	no
1390	0.31	48	0.89	-0.01 (-0.07, 0.06)	1.88 (-4.21, 8.61)	-0.01 (-0.08, 0.04)	-5.11 (-92.07, 91.14)	0.00 (-0.07, 0.07)	0.13 (0.12, 0.15)	0.09	yes
1400	0.31	48	0.89	0.00 (-0.07, 0.08)	1.47 (-4.37, 8.64)	-0.01 (-0.07, 0.04)	2.80 (-87.32, 106.15)	0.00 (-0.06, 0.08)	0.13 (0.12, 0.15)	0.06	yes
1500	0.31	48	0.89	0.00 (-0.07, 0.06)	1.31 (-4.08, 7.88)	-0.01 (-0.09, 0.04)	0.52 (-87.88, 97.36)	0.00 (-0.06, 0.06)	0.13 (0.12, 0.15)	0.04	yes